

TECHNISCHE UNIVERSITÄT MÜNCHEN

TUM School of Engineering and Design

Augmented Reality Pilot Assistance System for Helicopter Shipboard Operations

Tim Oliver Mehling

Vollständiger Abdruck der von der TUM School of Engineering and Design der Technischen Universität München zur Erlangung des akademischen Grades eines Doktors der Ingenieurwissenschaften genehmigten Dissertation.

Vorsitz:

Prof. Dr.-Ing. Florian Holzapfel

Prüfer*innen der Dissertation:

1. Prof. Dr.-Ing. Manfred Hajek
2. Prof. Dr. phil. Klaus Bengler

Die Dissertation wurde am 19.04.2022 bei der Technischen Universität München eingereicht und durch die TUM School of Engineering and Design am 18.09.2022 angenommen.

Abstract

Visual and control augmentation methods have the potential to support helicopter pilot's direct perception during critical helicopter shipboard operations in a highly demanding and harsh maritime environment including degraded visual environments and varying ship states. The present work investigates in a helicopter-ship approach and landing visual augmentation concept with scene-linked visual augmentation modes designed for an HMD with see-through capabilities to enhance pilot's situational awareness. Additional advanced flight control modes, optimized in corporation with maritime test pilots, focus on rendering pilots' control inputs more precise, while simultaneously decreasing subjective workload statistically significant. For evaluation, two simulator flight test campaigns together with ten maritime test and fleet pilots from the armed forces, industry, and public authorities were conducted completing a total of over 200 helicopter ship missions in a safe environment. Two main scenarios were considered: a helicopter ship approach scenario within degraded visibility conditions down to 200 m, and a final recovery task within demanding and varying ship motions. The results indicate that subjective workload and the corresponding handling qualities remained at constant level 1 with visual and control augmentation being enabled while DVE conditions and ship motions increased. Flight data analysis as well as subjective ratings showed that all pilots preferred higher degrees of helicopter stabilization harmonized with the HMD visual augmentation in the near ship environment. However, the hover-over-deck scenario demonstrated limitations of the HMD technology due to the available limited field-of-view.

Keywords:

Augmented Reality, Helicopter Shipboard Operations, Helmet-Mounted Display, Human-Machine Interface, Pilot Assistance System, Pilot-in-the-Loop, Handling Qualities Model, Visual Augmentation.

Zusammenfassung

Methoden der visuellen Erweiterung bei gleichzeitig höheren Stabilisierungsgraden haben das Potenzial, die direkte Wahrnehmung des Hubschrauberpiloten während kritischer Hubschrauber-Manöver in Schiffsnähe in einer anspruchsvollen und rauen maritimen Umgebung zu unterstützen, einschließlich bei schlechten Sichtbedingungen und dynamischen Schiffsbewegungen. Die vorliegende Arbeit untersucht Konzepte der visuellen Augmentierung mit szenengebundenen Modi, die für ein Helmsichtsystem entwickelt wurden, um das Situationsbewusstsein des Piloten während dem Anflug und der Landung auf ein Schiff zu verbessern. Zusätzliche Flugregler, die gemeinsam mit Testpiloten der Marine optimiert wurden, konzentrieren sich darauf, die Steuereingaben der Piloten präziser zu adressieren und gleichzeitig die subjektive Arbeitsbelastung signifikant zu senken. Zur Evaluierung des Konzeptes wurden zwei Flugtestkampagnen in einem Simulator mit zehn Test- und Flottenpiloten der Marine, Industrie und Behörden durchgeführt, die insgesamt über 200 Missionen in einer sicheren Umgebung flogen. Dazu wurden zwei Hauptuntersuchungspunkte betrachtet: ein Schiffanflug Szenario unter eingeschränkten Sichtverhältnissen bis zu einer Sichtweite von 200m und eine Endanflug Mission bis zur Landung unter anspruchsvollen, variierenden Schiffsbewegungen. Die Ergebnisse zeigen, dass die subjektive Arbeitsbelastung und Bewertung der Flugführung bei aktivierter visueller Augmentierung und zugeschalteten höheren Kontrollmodi konstant niedrig auf Level 1 bleiben, selbst während die Sichtweite rapide abnimmt und die Schiffsbewegungen stark zunehmen. Die Flugdatenanalyse sowie weitere subjektive Bewertungen offenbarten, dass alle Piloten höhere Stabilisierungsgrade des Hubschraubers bei einer gleichzeitigen visuellen Augmentierung auf dem HMD in der schiffsnahen Umgebung bevorzugten. Die finalen Schwebeflüge über Deck demonstrierten jedoch auch die Grenzen der HMD-Technologie aufgrund ihres begrenzten dargestellten Sichtfeldes.

Schlüsselwörter:

Erweiterte Realität, Maritime Hubschrauber Operationen, Helmsichtsystem, Mensch-Maschine-Interaktion, Pilotenassistenzsystem, Pilotenmodell, Visuelle Erweiterung.

Dedicated to my family.
For you, my beloved daughter Valentina Daniela Ilonka.

Acknowledgments

I would like to express my deepest gratitude to my doctor father Prof. Dr.-Ing. Manfred Hajek who made it possible for me to accomplish research in a field where my profession meets my passion. The discussions on the technical details as well as the strategical orientation of my research work at the Institute of Helicopter Technology at the TUM Technical University of Munich inspired me within my career path in the industry. I would also like to thank my second assessor Prof. Dr. phil. Klaus Bengler for introducing me to the world of ergonomics during several impressive discussions and workshops on the human machine interface. I would like to thank the chairing professor of the rigorosum of my dissertation for the arrangement in a festive environment. Finally, I would like to express my thoughts in remembrance on my mentor Prof. Dr.-Ing. Matthias Heller who passed away during the manufacturing of this work. He gave me important thoughts to my nature and research work in the flight test environment.

My beloved wife M.Sc. Isabella Mehling encourages, supports, and shares my passion of aviation. Isabella, you took me by the hand when unforeseeable challenges raised offside this work. I thank you from the bottom of my heart for your power and endless affection. As my mom, Ilonka Mehling, passed away during the fabrication of this work, I am very grateful to my family and best friends.

As I got the great chance to work together with Prof. Dr. Sc. Milan Vrdojak and Dr.-Ing. Omkar Halbe, our common research and friendship fascinated me from the beginning, and I am looking forward to continuing our journey in the world of rotorcraft systems. It had always been and is a great privilege for me to share and discuss my thoughts together with experts, colleagues, and friends from the institute.

Moreover, a great thanks goes to all the pilots who participated, supported, enriched, and challenged my work. It is a pleasure for me to discuss and fly with you. Thank you, M.Sc. Christoph Jaksch giving me valuable feedback as a colleague and friend. Finally, i would also like to express my gratitude to Martina Thieme, the good soul of the institute making me feel homelike.

Prior journal publications

Further results have been published in the following international journals:

Mehling, T., Halbe, O., Vrdoljak, M., Hajek, M., “Visual and Control Augmentation Techniques for Pilot Assistance during Helicopter Shipboard Recovery,” published in Journal of AHS American Helicopter Society, April 2022. DOI: 10.4050/JAHS.67.042004

Halbe, O., Mehling, T., Vrdoljak, M., Hajek, M., “Synthesis and Piloted Evaluation of Advanced Rotorcraft Response-Types Using Robust Sliding Mode Control,” published in Journal of AHS American Helicopter Society, July 2021. DOI: 10.4050/JAHS.66.032008

Vrdoljak, M., Halbe, O., Mehling, T., Hajek, M., “Flight Guidance Concepts To Mitigate Flight Control System Degradation in Urban Air Mobility Scenarios,” published in IEEE Aerospace and Electronic Systems Magazine 2022, August 2022. DOI: 10.1109/MAES.2022.3200933

Prior publications

Further results have been published at the following international conferences:

Mehling, T., Viertler, F., and Paul, T., “Potential of the Unmanned Wingman in Manned-Unmanned Teaming Tested in Flight,” Deutscher Luft- und Raumfahrtkongress 2019, Darmstadt, Germany, October 2019. DOI: 10.25967/490010.

Vrdoljak, M., Halbe, O., Mehling, T., Hajek, M., “Simulator Experiments for Modeling Helicopter Pilot in Roll Tracking Task,” AIAA Science and Technology Forum 2020, Miami, USA, January 2020. DOI: 10.2514/6.2020-2269.

Vrdoljak, M., Mehling, T., Halbe, O., Heller, M., Hajek, M., “Analysis of Manual Control for Personal Aerial Vehicle with Flight Control System Degradation,” 5th International Conference on Smart and Sustainable Technologies, Split, Croatia, September 2020. DOI: 10.23919/SpliTech49282.2020.9243762.

Mehling, T., Halbe, O., Vrdoljak, M., Heller, M., Hajek, M., “Visual Augmentation for Personal Air Vehicles during Flight Control System Degradation,” American Helicopter Society 76th Annual Forum, [Virtual] Virginia Beach, Virginia, USA, October 2020. [Link]

Banas, J., Mehling, T., Paul, T., Cords, A., “Manned-Unmanned Teaming Challenges in the Maritime Environment,” American Helicopter Society 76th Annual Forum, [Virtual] Virginia Beach, Virginia, USA, October 2020. [Link]

Mehling, T., Halbe, O., Gasparac, T., Vrdoljak, M., Hajek, M., “Piloted Simulation of Helicopter Shipboard Recovery with Visual and Control Augmentation,” AIAA Science and Technology Forum 2021, [Virtual] Nashville, USA, January 2021. DOI: 10.2514/6.2021-1136.

Banas, J., Mehling, T., Vyshnevskyy M., Paul, T., Cords, A., “Onboard Safety Systems for Tactical VTOL UAV Operations,” American Helicopter Society 77th Annual Forum, West Palm Beach, Florida, USA, June 2021. [Link]

Halbe, O., Mehling, T., Vrdoljak, M., Hajek, M., “Synthesis and Piloted Evaluation of Advanced Rotorcraft Response-Types Using Robust Sliding Mode Control,” American Helicopter Society 77th Annual Forum, [Virtual] West Palm Beach, Florida, USA, June 2021. [Link]

Mehling, T., Eichhorn, Ch., Yixuan, L., Klinker, G., Hajek, M., “Ship Detection and Visual Augmentation during Helicopter Ship Deck Operations,” AIAA Aviation Forum 2021, [Virtual] Washington, D.C., USA, August 2021. DOI: 10.2514/6.2021-2994

Mehling, T., Werhahn M., Hajek, M., “Enhanced Visual Augmentation during Simulated Helicopter Ship Operations,” Driver Simulation Conference DSC 2021 Europe, Munich, Germany, September 2021.

Mehling, T., Halbe, O., Vrdoljak, M., Hajek, M., “Evaluation of a Pilot Assistance System during Simulated Helicopter Shipboard Operations in DVE conditions,” AIAA Science and Technology Forum 2022, [Virtual] San Diego, USA, January 2022. DOI: 10.2514/6.2022-0513

Kuen, N., Bludau, J., Reiser, A., Mehling, T., Gümmer, V., Hajek, M., “Hardware-in-the-Loop Evaluation of a Quick-Start System for Helicopter Gas Turbine OEI Operations tested in simulated flights,” 48th European Rotorcraft Forum, Winterthur, Suisse, September 2022.

Prior projects within the institute

Further collaboration work has been established:

Mehling, T., Halbe, O., Vrdoljak, M., Hajek, M., “HELIOP – Helicopter Ship Deck Operations,” TUM Technical University of Munich, Institute of Helicopter Technology, Munich, Germany together with the University of Zagreb, Faculty of Mechanical Engineering and Naval Architecture, Zagreb, Croatia. [Link]

In addition, the following student theses and student assistances have been supervised by the author at the Technical University of Munich within the scope of this work:

Gasparac, T., “Assessment of the Pilot Workload during the Helicopter Ship Deck Landing Scenario,” Master Thesis in cooperation with the Faculty of Mechanical Engineering and Naval Architecture, University of Zagreb, Garching, May 2019.

Werhahn, M., “Integration of Visualization Methods to Rotorcraft Simulation Environment ROSIE,” Student Assistance, Garching, July 2019.

Liu, Y., “Augmentation Concept Design for Helicopter Ship Deck Operations at Rotorcraft Simulation Environment ROSIE,” Bachelor Thesis in cooperation with the Faculty of Games Engineering, Garching, August 2019.

Rodriguez Palafox, P., “Leveraging Direct Image Alignment for Local Tracking and Map Updating in a Direct SLAM System,” Master Thesis in cooperation with the Faculty of Computer Vision Group, Garching, August 2019.

Löwenhauser, M., “Capabilities of a Future Primary Flight Display Instrumentation for Helicopter in Flight Tasks,” Term Project, Garching, December 2019.

Haoran, Ch., “Visual Augmentation in Rotorcraft Simulation Environment - A Novel Guidance Approach towards moving Platforms,” Bachelor Thesis in cooperation with the Faculty of Computer Vision Group, Garching, January 2020.

Haoran, Ch., “Simulated IR view within a Maritime Helicopter Ship Interface visualized on a Helmet-Mounted Display,” Student Assistance, Garching, July 2020.

Reyad, A., "Effects of Visual Augmentation and Optical Flow in flight in the Maritime Environment," Bachelor Thesis in cooperation with the Faculty of Computer Vision Group, Garching, September 2020.

Kozica, L., "Flight Test Data Design and Evaluation for the Helicopter-Ship Interface," Bachelor Thesis, Garching, September 2020.

Schmitt, St., "Analyse von Versuchsdaten eines Pilotassistenzsystems für maritime Hubschrauber," Master Thesis, Garching, October 2020.

Corbell, M., "Experimental Test Data Analysis and Evaluation of Simulator Flight Test Scenarios," Bachelor Thesis, Garching, October 2020.

Haoran, Ch., "Proof of Concept Design for a Future Rotorcraft Simulation Environment Architecture," Student Assistance, Garching, April 2021.

Zhihao, L., "Enhanced Visual Augmentation using a Virtual Glide Path Terrain Grid," Bachelor Thesis in cooperation with the Faculty of Computer Vision Group, Garching, May 2021.

Esser, A., "Trend Analysis of Flight Parameters of a Pilot Assistance System for Maritime Helicopters," Bachelor Thesis, Garching, July 2021.

Kozica, L., "Evaluation of a Pilot Workload Model for Helicopter Near Ship Operations," Semester Thesis, Garching, July 2021.

Banon, A., "Extended Workload Analysis for Helicopter Near Shipboard Operations," Semester Thesis in cooperation with the ISAE - Institut Supérieur de l'Aéronautique et de l'Espace, Garching, May 2021.

Fischer, J., "Physics-Based Infrared Sensor Simulation and Visualization on a Helmet-Mounted Display," Master Thesis in cooperation with the Faculty of Computer Vision Group, Garching, February 2022.

Table of Contents

List of Figures	xi
List of Tables	xv
Nomenclature	xvi
Subscripts.....	xvi
Abbreviations.....	xvii
1 Introduction.....	1
1.1 Motivation and Objectives.....	1
1.2 Setting of Dissertation.....	2
2 State-of-the-Art Technologies and Human Visual Perception.....	7
2.1 Helicopter Ship Deck Operations Landing Aids.....	7
2.2 Human Information Processing.....	17
3 Concept of Design for the Visual Augmentation Scheme	25
3.1 Process of Integration and Validation.....	25
3.2 Phases of Flight during a Helicopter Near-Ship Mission	25
3.3 Requirements for a Visual Augmented Helicopter Shipboard Approach.....	29
4 Functions for a Pilot Assistance System during Near-Ship Operations	37
4.1 Image based Ship Detection.....	37
4.2 HMD Visual Augmentation Modes	39
4.3 Control Augmentation Modes	47
5 Helicopter Shipboard Operations Environment	51
5.1 ROSIE Helicopter Ship Interface.....	51
5.2 Visualization of the Maritime Environment	54
5.3 Simulation of a Dynamic Generic Combatant Ship.....	58
5.4 Ship Motion based Data for Pilot-in-the-Loop Simulations	60
5.5 HMD Visual Augmentation in DVE.....	63
6 Experimental Setup for Simulated Flights	66
6.1 Flight Test Campaign Environment.....	66
6.2 Experimental Simulation Methodology	73
6.3 Helicopter Shipboard Operations.....	77

7	Results and Discussion of the Simulator Flight Tests	94
7.1	Handling Qualities during Training Phase	94
7.2	Pilot Workload during Helicopter Ship Approaches using a PAS.....	101
7.3	Flight Envelopes during Helicopter Shipboard Operations	120
7.4	Predictive Handling Qualities Model	142
7.5	Ship Tracking Model Observations	146
8	Conclusions and Recommendations.....	150
	References	157
	Appendix.....	173

List of Figures

Figure 1-1: Brightnite - Fused image visualized to the pilot's HMD [33].....	3
Figure 2-1: Helicopter during final approach over ship landing deck	7
Figure 2-2: Dynamic interface simulation environment [13].....	8
Figure 2-3: SHOLDS GUI [122] (left) and typical SHOL diagram [35] (right)	9
Figure 2-4: DGSi [19] (upper images), HAPS [87] and HRB [19] (lower images)	9
Figure 2-5: 2D and 3D symbology on HDD (left) [25] and on HMD (right) [103]	10
Figure 2-6: 3D symbology (upper image) and seen through HMD (lower image) [27]	11
Figure 2-7: HUD presented tunnel in the sky (left) and cueing set (right)	12
Figure 2-8: HMD symbology during approach (left) and before touchdown (right) [102] .	12
Figure 2-9: Striker Colour helmet (left) and display system (right) [68]	13
Figure 2-10: TopOwl helmet (left) [82] and display system (right) [139].....	14
Figure 2-11: Jedeye helmet (left) and display system (right) [34]	14
Figure 2-12: DLR helicopter ship interface (right) and see-through HMD view [26]	16
Figure 2-13: Virtual conformal landing display [119].....	16
Figure 2-14: The 4-D multiple resource model [152]	18
Figure 2-15: Computed displacements of three ships landing spots [121].....	20
Figure 2-16: Pilot ratings for hover over deck task [121]	21
Figure 2-17: Pilots control activities during hover task over landing spot [121].....	21
Figure 2-18: SferiAssist at two points along an approach to a fixed landing point [161]..	22
Figure 2-19: Optical flows of pilots' view [23].....	23
Figure 3-1: Standard SCA approach chart [105]	26
Figure 3-2: HOSTAC shipboard landing - lateral approach [105].....	27
Figure 3-3: Overview of approach parameters [140]	28
Figure 3-4: Final stages of the recovery of a helicopter to a ship deck [109]	29
Figure 3-5: Side and top view of the approach trajectory, figure not to scale.....	31
Figure 3-6: Side and top view of the landing trajectory, figure not to scale	32
Figure 3-7: Pilot cognition of surface-level interview [97].....	33
Figure 3-8: PAS including main systems (orange) and subsystems (green).....	35
Figure 4-1: Viewing transformations from local space to screen space	38
Figure 4-2: Ship detection in DVEs with ground truth (blue) and prediction (red)	38
Figure 4-3: HMD view during approach (upper row) and landing (lower row)	39
Figure 4-4: HMD Head Fixed Symbology	41
Figure 4-5: HMD Helicopter Fixed Symbology	41
Figure 4-6: HMD SAS (left) and ESAS (right) as seen through HMD during approach ...	42
Figure 4-7: In-flight HMD tunnel view after missed approach	43
Figure 4-8: HMD SLS (left) and ESLS (right) as seen through HMD during landing	44

Figure 4-9: HMD entire moving landing symbology	45
Figure 4-10: PAS ESAS (upper row) and ESLS (lower row) declutter modes.....	46
Figure 4-11: Closed-loop flight control and simulation setup	48
Figure 5-1: Outside view of ROSIE during pilot-in-the-loop flight.....	51
Figure 5-2: ROSIE HDD instrumentation modes	52
Figure 5-3: Drift indicator (left) and deviation indicator (right)	53
Figure 5-4: Sky Map with ship alignment line, figure to scale	53
Figure 5-5: H135 cockpit flight instrumentation during ship approach	54
Figure 5-6: Low (left), medium (middle), high (right) numbers of waves [137]	56
Figure 5-7: Simulated wave surface without (top) and strong (down) chops [137].....	56
Figure 5-8: Animated waves in low (left), moderate (middle), high (right) sea states [17]	57
Figure 5-9: Schematic diagram of stern wake’s field angle [89].....	57
Figure 5-10: Simulated open sea environment (left) and ship wake (right).....	58
Figure 5-11: Cockpit view - Ship operating in low (left) and high (right) sea states	58
Figure 5-12: DDG-90 ship deck in ROSIE (left) and in real environment (right) [1].....	59
Figure 5-13: Calculation of translations from local to world space coordinates.....	59
Figure 5-14: ROSIE cockpit view (right) during ship approach	60
Figure 5-15: Roll (upper) and heave (lower) intensity levels within SCONE	61
Figure 5-16: SCONE mean maxima roll and heave level values	63
Figure 5-17: Side view of pilot using see-through HMD (left) and close-up (right)	64
Figure 5-18: HMD symbology as seen from MAP (left) and behind the deck (right)	65
Figure 6-1: Simulation environments Tegernsee (left) and North Sea (right).....	66
Figure 6-2: Test setup cockpit configuration during experiments.....	68
Figure 6-3: Test setup display configuration during experiments.....	69
Figure 6-4: Top view of suggested course for hover mission task element [1].....	80
Figure 6-5: Two example runs of the hover MTE	80
Figure 6-6: Top view of suggested course for sidestep MTE [1].....	81
Figure 6-7: Two example runs of the sidestep MTE	81
Figure 6-8: Basic display modes for ship approach (left) and landing (right)	82
Figure 6-9: Side view of eight example runs of the approach scenario.....	87
Figure 6-10: Side view of four example runs of the final approach scenario.....	92
Figure 7-1: Views during MTE hover in the Tegernsee environment	95
Figure 7-2: MTEs Hover and Sidestep – pilot ratings, $N=10$	96
Figure 7-3: MTE Hover – top views flight paths.....	97
Figure 7-4: MTE Hover – deviations from ideal flight paths	97
Figure 7-5: Views during MTE sidestep in the Tegernsee environment.....	98
Figure 7-6: MTE Sidestep – top view flight paths	99

Figure 7-7: MTE Sidestep – deviations from ideal flight paths	100
Figure 7-8: Bedford ratings of helicopter ship approach and landing, $N=8$	103
Figure 7-9: Cooper-Harper ratings of helicopter ship approach and landing, $N=8$	105
Figure 7-10: DIPES ratings of helicopter ship approach and landing, $N=8$	106
Figure 7-11: VCR ratings of helicopter ship approach and landing, $N=8$	107
Figure 7-12: Medians of all VCR ratings, $N=8$	108
Figure 7-13: Pilot evaluations of the 3D-conformal approach symbology, $N=8$	109
Figure 7-14: Pilot evaluations of the 3D-conformal landing symbology, $N=8$	110
Figure 7-15: Pilot evaluations of the 2D-flight parameters, $N=8$	111
Figure 7-16: Pilot evaluations of the HMD color concept, $N=8$	111
Figure 7-17: Bedford and Cooper-Harper ratings of helicopter ship final recovery	113
Figure 7-18: NASA-TLX weightings of helicopter ship final recovery – Level 1.....	115
Figure 7-19: NASA-TLX weightings of helicopter ship final recovery – Level 3.....	116
Figure 7-20: Pilot evaluations of the basic 3D-conformal landing symbology	118
Figure 7-21: Side view of helicopter ship approaches in degrading visibility conditions	121
Figure 7-22: Side view of helicopter ship approaches in harsh DVE condition, $N=8$	123
Figure 7-23: Mean deviations from the ideal flight path, $N=8$	124
Figure 7-24: Pilots cyclic inputs during flights, $N=8$	126
Figure 7-25: Pilots collective inputs during flights, $N=8$	126
Figure 7-26: Control inputs analysis of average peaks and average duty cycle, $N=8$...	127
Figure 7-27: Average power per input frequency of pilots' cyclic inputs, $N=8$	129
Figure 7-28: PID5 Test pilot cyclic control roll axis scalograms during DVE flights.....	130
Figure 7-29: PID6 Fleet pilot cyclic control roll axis scalograms during DVE flights.....	131
Figure 7-30: PID5 Test pilot cyclic control roll axis scalograms during DVE flights.....	132
Figure 7-31: PID6 Fleet pilot cyclic control roll axis scalograms during DVE flights.....	132
Figure 7-32: Pilots head motions during flights, $N=8$	133
Figure 7-33: Average power per input frequency of pilots' head motions, $N=8$	134
Figure 7-34: PID2 helicopter flight paths during the final approach	136
Figure 7-35: PID2 helicopter CG positions from behind during the final approach.....	137
Figure 7-36: PID2 helicopter flight paths last 40 sec in different ship motions	138
Figure 7-37: Cyclic and collective control activity during a final approach	140
Figure 7-38: Pilot's head motions during low & high (upper & lower row) ship motions	141
Figure 7-39: Schematic illustration of the HQM model	143
Figure 7-40: MTE Hover - flight path performance of human pilots and pilot model	144
Figure 7-41: MTE Sidestep - flight path performance of human pilots and pilot model .	144
Figure 7-42: MTE Hover - altitude performance of human pilots and pilot model	145
Figure 7-43: MTE Sidestep - altitude performance of human pilots and pilot model	145

Figure 7-44: MTE Sidestep - yaw angle performance of human pilots and pilot model.	146
Figure 7-45: Testing accuracy during pre-training	148
Figure 7-46: Comparison of testing accuracy using SGD and Adam	149

List of Tables

Table 2-1: Key parameters of HMDs.....	15
Table 3-1: Combined phase model for helicopter ship deck approach	29
Table 3-2: PAS SysReqM connected to PAS SysSpec	36
Table 4-1: Available visual and control augmentation modes.....	50
Table 5-1: Ocean waves scaling within ROSIE	57
Table 5-2: SCONE roll and heave levels.....	62
Table 5-3: Resolution and FoV of HMD LCD29.....	64
Table 5-4: IFR categories and visibility limits within ROSIE.....	65
Table 6-1: Visibility limits during experiments.....	69
Table 6-2: Ship motions during experiments	70
Table 6-3: Subjective pilot evaluations of the maritime simulation visualization (N=10)..	71
Table 6-4: Subjective pilot evaluations of the ship simulation visualization (N=10).....	72
Table 6-5: Subjective pilot evaluations of ROSIE (N=10)	72
Table 6-6: Evaluation pilots for pilot-in-the-loop experiments	74
Table 6-7: Simulator flight test program	76
Table 6-8: Simulator flight test points – training phase	79
Table 6-9: Research questions and hypotheses	83
Table 6-10: MTEs – operational block 1.....	85
Table 6-11: Simulator flight test points – operational block 1.....	86
Table 6-12: Group of dependent variables of the operational block 1.....	88
Table 6-13: MTEs – operational block 2.....	90
Table 6-14: Simulator flight test points – operational block 2.....	91
Table 6-15: Group of dependent variables of the operational block 2.....	93
Table 7-1: HELIOP test procedures and modes.....	102
Table 7-2: Purposes of datasets for ship detection	147
Table 7-3: Training settings on four datasets for ship detection	147
Table 7-4: Evaluation of trained models validating all datasets using three metrics	148

Nomenclature

A, B	State and control matrices in the linear state space model
$\mathbf{D}=[D_\theta D_\alpha D_\beta D_\delta]^\top$	Trim displacement of collective, lateral and longitudinal cyclic, and pedals, %
k	Pilot command shaping gains
S	Sliding mode design matrix
$\mathbf{V}=[V_h V_l V_z]^\top$	Forward, lateral, and vertical velocity components in local frame, ms^{-1}
\mathbf{V}_r	Right eigenvectors matrix
V	Lyapunov candidate function
$\mathbf{V}_b=[uvw]^\top$	velocity vector in body-frame, ms^{-1}
$\beta_0, \beta_{1c}, \beta_{1s}$	Blade collective, longitudinal and lateral flapping angles, rad
ε	Size of sliding mode boundary layer
ζ	Damping ratio
$\zeta_0, \zeta_{1c}, \zeta_{1s}$	Blade collective, longitudinal and lateral lead-lagging angles, rad
$\boldsymbol{\theta}=[\varphi \theta \psi]^\top$	Euler angles with respect to north-east-down frame, rad
λ	Inverse time period, s^{-1}
$\rho, \boldsymbol{\rho}$	Sliding mode control gains
$\sigma, \boldsymbol{\sigma}, \boldsymbol{\mu}$	Sliding variables
$\boldsymbol{\omega}=[p q r]^\top$	Angular velocity vector in body frame, $rads^{-1}$
ω	Natural frequency, s^{-1}

Subscripts

bw	Bandwidth
c	Command
cl	Closed loop
e	Error
o	Outer loop

Abbreviations

ACAH	Acceleration Command Acceleration Hold
ACT/FHS	Advanced control technology/flying helicopter simulator
ACVH	Acceleration Command Velocity Hold
Adam	Adaptive Moment Estimation
AFCS	Automatic Flight Control System
AGI	Aeronautical & General Instruments Limited
APV	Approach with Vertical Guidance
AR	Augmented Reality
BOSS	Brownout Symbology System
CAA	Civil Aviation Authority
CAT	Category
CDI	Course Deviation Indicator
CFIO	Controlled Flight Into Objects
CFIT	Controlled Flight Into Terrain
CIGI	Common Image Generator Interface
CoG	Centre of Gravity
CPU	Central Processing Unit
DESC	Descent
DGSI	Digital Glide Slope Indicator
DH	Decision Height
DLR	Deutsches Zentrum für Luft- und Raumfahrt
DO	Design Order (DO-178C, DO-254)
DOF	Degree-Of-Freedom
DVE	Degraded Visual Environment
EASA	European Union Aviation Safety Agency
ESAS	Enhanced Ship Deck Approach Symbology
ESLS	Enhanced Ship Deck Landing Symbology
FAA	Federal Aviation Administration
FAF	Final Approach Fix
FFT	Fast Fourier Transformation
FLIR	Forward Looking Infrared
FP	Forward Perpendicular
FoR	Field of Regard
FoV	Field of View

FP	Fleet Pilot
FTR	Force-Trim Release
GNSS	Global Navigation Satellite System
GVE	Good Visual Environment
HAPS	Hover and Approach Positioning System
HDD	Head-Down Display
HEDELA	Helicopter Deck Landing Assistance
HELIOP	Helicopter Ship Deck Operations
HELI-X	HELicopter Situation Awareness für eXtreme Missionsanforderungen
HELMA	Helicopter Flight Safety in Maritime Operations
HMD	Helmet-Mounted Display
HMI	Human-Machine-Interface
HMSD	Helmet Mounted Sight and Display
HOSTAC	Helicopter Operations from Ships other than Aircraft Carriers
HRB	Horizon Reference Bar
HQM0	Handling Qualities Model
HQR	Handling Qualities Rating
HUD	Heads Up Display
IAF	Initial Approach Fix
ICAO	International Civil Aviation Organization
ID	Identification Number
IFR	Instrument Flight Rules
IG	Image Generator
IIT	Image Intensifier Tubes
IMC	Instrument Meteorological Conditions
IoU	Intersection over Union
LAMP	Non-Linear Seakeeping Prediction Code
LAND	Landing
LiDAR	Light detection and ranging
LoD	Level of Detail
LOS	Line of Sight
MAP	Missed Approach Point
MDA	Minimum Descent Altitude
MDR	Minimum Decision Range
MUS	Must
NATO	North Atlantic Treaty Organization

NAV	Navigation
NVG	Night-Vision Goggles
ONR	Office of Naval Research (U.S. Navy)
OSG	OpenSceneGraph
PAS	Pilot Assistance System
PFD	Primary Flight Display
PID	Pilot Identification Number
PIO	Pilot Induced Oscillation
PnP	Perspective-n-Point
RANSAC	Random Sample Consensus
RCDH	Rate Command Direction Hold
RCHH	Rate Command Height Hold
ROSIE	Rotorcraft Simulation Environment
RVR	Runway Visual Range
SA	Situational Awareness
SAS	Ship Deck Approach Symbology
SBAS	Satellite Based Augmentation System
SCA	Ship-Controlled Approach
SCONE	Systematic Characterization of the Naval Environment
SGD	Stochastic Gradient Descent
SHA	Shall
SHO	Should
SHOLDS	Ships Helicopter Operational Limit Display System
SHOLs	Ship Helicopter Operational Limitations
SLS	Ship Deck Landing Symbology
SMC	Sliding Mode Control
SOAP	SBAS Offshore Approach Procedure (SOAP)
SSQ	Simulator Sickness Questionnaire
SysReqM	Systems Requirements Matrix
SysSpec	System Specification
STANAG	Standardization Agreement (NATO)
TP	Test Pilot
TRC	Translational Rate Command
TRL	Technology Readiness Level
UCE	Usable Cue Environment
VCR	Visual Cue Rating

VFR	Visual Flight Rules
WMO	World Meteorological Organization
WTD61	Wehrtechnische Dienststelle der Luftwaffe 61 (Technical Center for Aircraft and Aeronautical Equipment)
2D	Two Dimensional
3D	Three Dimensional

1 Introduction

Helicopter flights are particularly exposed to safety hazards when entering conditions associated within a “Degraded Visual Environment” (DVE) [134]. Here, low visibility conditions play an important role [32] when rotorcraft are involved to different weather and mission conditions during flight. To increase situational awareness (SA) and decrease pilot workload at same time, helicopter crews challenge with available usable visual cues to pilot the rotorcraft safe during all phases of flight. Especially when it comes to helicopter maneuvers like low-level flight, approach, hover and landing, the rotorcraft must ensure to not hit obstructions within the flight path [96].

The present work describes how flight simulation is used to investigate in offshore helicopter recovery maneuvers, named as helicopter shipboard operations [150] in adverse weather conditions. Moreover, the study goes into helicopter proceedings in a highly dynamic environment caused by different sea states and corresponding ship motions. In parallel, the ship and its moving landing deck is surrounded by obstructions such as the rear deck wall of the ship to face the pilot in sum with three different challenges during flight:

- Demanding adverse weather conditions (DVEs),
- a highly dynamic landing place with a restricted size, and
- obstacles in the close range of the landing point.

For this purpose, pilots may benefit from a pilot assistance system (PAS) to approach and land the helicopter safely on the ship deck. The PAS designed and investigated within this work is supposed to enhance SA and decrease pilot workload at same time, prevent collision of the rotor blades with the deck wall by increasing obstacle awareness, and improve flight precision performance while operating independent from any weather condition.

1.1 Motivation and Objectives

Extended visual cues and handling qualities (HQs) of rotorcraft will allow a variety of mission sets, enlarging the current naval helicopters reach to establish safe operations such as helicopter shipboard approaches and landings in a harsh environment. To enable safe operations in DVEs, the aircraft may be equipped with pilot assistance systems that address extended visibility to provide real-time 360° SA. Visual displays and head worn displays, such as helmet-mounted displays (HMDs), coupled to onboard sensors support a representation of the threat space in 360°. However, due to their limited filed-of-view (FoV), multimodal cueing [96] is raising to extend limitations of helicopter operations within DVEs. The present work discusses the development and evaluation of a helicopter independent visual and control augmentation concept for helicopter shipboard operations facing DVE

conditions. Implemented real-time ship detection algorithms offer a platform independent landing zone detection and tracking during operation. The “360° SA” is visualized on a low-cost binocular fully colored stereoscopic HMD. Enhanced visual augmentation is coupled to advanced flight control modes, mainly used during approach and landing maneuvers. To ensure a safe and representative test environment, the development and integration of a highly realistic maritime environment to a fixed based helicopter simulator is established. The determination of the visual and control augmentation schema is designed and evaluated together with maritime test and fleet pilots. The purpose of the helicopter ship deck operations (HELIOOP) studies was to evaluate the PAS as a transfer of concepts used for onshore helicopter operations.

The PAS consists of the following main components: Image-based ship detection algorithms creating needed data for a human-centered guidance and obstacle avoidance display concept. Coupling of the scene-linked HMD visual augmentation with corresponding modes of advanced flight control modes for precise operation.

1.2 Setting of Dissertation

This section specifies the problem statement for helicopter offshore operations within the helicopter ship interface. Modus operandi of system development is established with a focus on the integration and test process for aerospace applications. Next, needed assumptions for development, validation, and verification are given. Finally, demands and functions of a PAS for near-ship operations are introduced.

1.2.1 Problem Statement

The demand for helicopters with the capacity to operate in DVEs is substantial: The lack of suitable technologies is apparent because pilot assistance systems for offshore operations are not as available compared to what had been developed for onshore helicopter missions. Operating these aircrafts from sea-based platforms is a challenging endeavor due to multiple factors:

- During the approach, a naval helicopter pilot performs high-workload tasks of switching between instrument information and the outside scenery, often in DVE conditions within a harsh maritime environment.
- To localize the restricted landing area and land safe, pilots must compensate ship motions of the landing area as well. Therefore, a precise maneuvering and stabilization of the rotorcraft to avoid nearby structures of the ship further increases pilot workload.

The domain of these pilot assistance systems for helicopter operations focuses on lowering SA and enhancing cognitive workload by “pilot-in-the-loop” aids:

- First, SA is aimed to be distributed across multiple aids within the cockpit because not all information has to be held in the working memory of the pilot, rather the optimal interaction of both the pilot and on-board technologies.
- Second focus is on cognitive workload. Helicopter pilot's reliance on important visual cues becomes challenging during flight in DVEs when such cues are obscured. When operating the helicopter in DVEs, cognitive demand now greatly increases due to merge information presented in the cockpit (head-down use case) to missing outside scenery visualization (head-up use case).

To increase SA and decrease workload are main goals of future cockpit technologies as developed within this work, especially those focusing on operating in DVEs. The visualization of information on HMDs combines head-up and head-down use cases to eyes-out-of-the-cockpit flying. The pilots do not have to divert visual attention and cognitive resources into the cockpit, such as required within traditional head-down displays (HDDs). This reduces the need to direct view and attention away from external events and primary flight references, potentially increasing SA and reducing workload. Hence, HMDs typically visualize flight parameters, 2D and 3D (conformal) outside scenery synthetic visual cues, as seen in Figure 1-1. Moreover, HMDs offer the opportunity to see-through the overlaid external view and look-through the airframe to use synthetic visual cues in flight.

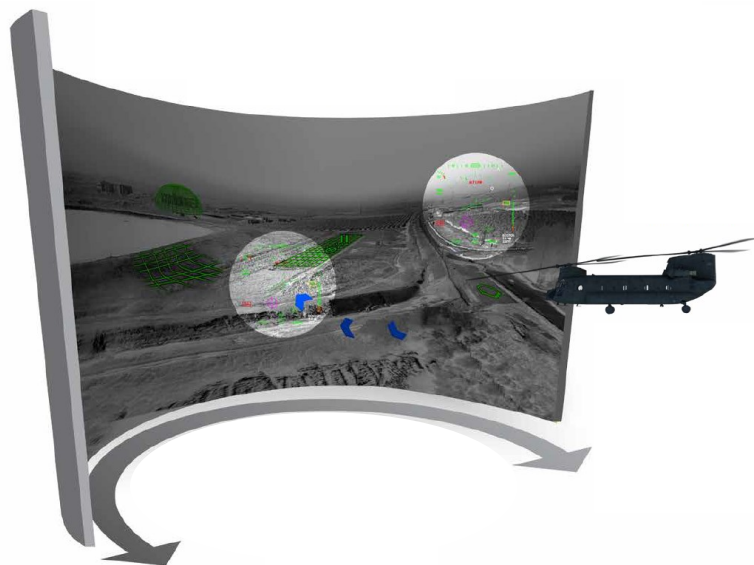


Figure 1-1: Brightnite - Fused image visualized to the pilot's HMD [33]

Beside the heads-up visualization of flight parameters, the representation of a safe flight path free of obstacles, often termed as “a highway in the sky”, gives valuable indications for flight guidance, especially in DVE conditions. The primary objective of the highway is to relieve the tasks of flying and navigation in all weather conditions. Within this work focusing on offshore helicopter operations in harmonization with a dynamic ship and its landing deck in the open sea environment, differences raise due to the “moving” landing place:

- Therefore, the moving ship landing deck is detected via image-based algorithms to offer the pilot an outside scenery conformal landing aid superimposed to the ship.
- Next, the appurtenant dynamic “virtual glide path” visualizes an optimal glide slope to allow a precise and safe approach and landing in all weather conditions.
- Finally, the HMD gives important visual cues to counteract visual confusion in such harsh conditions, which may lead to Controlled Flight into Terrain (CFIT) or Controlled Flight into Obstacles (CFIO).

To maximize the benefits of HMDs, the investigations of a potential PAS are sustained to the following aspects:

- Development along established (naval) procedures and standards.
- Consideration of technical requirements to not interfere with cockpit instrumentation and outside scenery.
- HMD representation of synthetic visual cues in a natural manner so that information is processed by the pilots intuitively.
- And finally, the visualization of flight information and visual cues are projected in a consistent information form to be useful in all weather conditions.

1.2.2 Methodology

Different phases of flight in standard naval operation procedures are analyzed and investigated using pilot-in-the-loop tasks. Detailed requirements for helicopter offshore maneuvers result in a systems requirements matrix linked to DVEs and good visual environments (GVEs) conditions. Resulting requirements are discussed with maritime test and fleet pilots ending up in functions for a PAS design. These requirements culminate in the investigation of the PAS and the helicopter ship interface including a maritime environment. Integration, test, verification, and validation is guaranteed within repeated pilot-in-the-loop simulations together with maritime test and fleet pilots.

In detail, needed parameters to be displayed to the pilot flying during approach and landing on a moving ship deck are determined and developed in a real-time augmentation design via a head-tracked HMD for the eyes-of-of-the-cockpit tasks. A ship detection and visual augmentation scheme is designed and integrated to the Trivisio HMD LCD29 within the fixed-base Rotorcraft Simulation Environment (ROSIE) to face challenges of information overload, reduce pilot workload, and increase SA. To evaluate the visual and control augmentation concept, maritime test and fleet pilots from industry (Airbus, Boeing, Kopter, Sikorsky), public authorities (Federal German Police), and armed forces (German Bundeswehr, US Navy) were invited to fulfill missions [105] [140] broken down into different mission task elements (MTEs) [2] of ship deck approach and landing operations in two pilot-in-the-loop simulator flight test campaigns.

1.2.3 Assumptions

The following assumptions were made for the development, validation, and verification of the present HMD/PAS as well as for proceeding the pilot-in-the-loop simulator experiments.

1. The focus of this work is straightforward to a maximum Technology Readiness Level (TRL) 2, as the HMD/PAS is a potential application to be validated. Basic principles are observed and reported (TRL1).
2. A dynamic rotor inflow model coupled to the ship surface is implemented within the test environment, see [11], but not validated [90] [102].
3. No critical system failures are expected during the experiments, which might lead to a hazardous event in flight. Hence, needed simulated sensor information for ship detection [93], as well as available visual and control augmentation modes [52] are always available.

1.2.4 Functional Requirements and Performance Parameters

This section summarizes the functional requirements and performance parameters for a PAS, integrated functions, and the environment of the experiment.

The demand for a PAS during helicopter near-ship operations arises from:

1. Pilot synthetic visual cueing for precise helicopter shipboard approaches and landings within a highly dynamic and harsh environment.
2. Enhancement of flight operation by decreasing helicopter pilot's workload and increasing SA in DVEs and GVEs.
3. Helicopter-ship platform independent usability of the developed helicopter PAS.

Therefore, the functions of the PAS are summarized as follows:

1. Development of a head-worn visual augmentation scheme. The cluttered and dynamic augmentation modes visualized by a see-through HMD offers the pilot the ability to focus on the helicopter ship deck approach and landing with constant, and weather independent synthetic 2D and 3D visual cues, and having main helicopter parameters in sight at same time. Scene linked clutter modes of the visual augmentation concept based on procedural and human centered requirements are considered.
2. Integration of the visual augmentation scheme to a platform independent low-cost HMD. Wisely, landing platform detection, hence its visualization is provided by integrated image-based ship tracking methods, which can be used in accordance with sensors mounted on actual maritime helicopters in real world conditions.
3. Coupling of visual and control augmentation modes in flight. Needed parameters are tailored to advanced flight control modes, Translational Rate Command (TRC) and Acceleration Command Velocity Hold (ACVH).

The functional requirements and performance parameters to the experimental environment are as follows:

1. Appropriation of a dynamic maritime environment. The visualization of the maritime environment within ROSIE includes a highly realistic and dynamic 3D open sea wave model.
2. Integration of a high resolution and realistic ship interface presented via the representation of an original ship model and its movement data. Therefore, the Systematic Characterization of the Naval Environment (SCONE) database [98] is provided for the simulated deck motions using a state-of-the-art, non-linear seakeeping code. The data includes full and consistent sets of six degrees of freedom ship deck motion data for a generic surface combatant ship, DTMB Model 5415 hull, which is a representative of a DDG-90-type destroyer, as typically used for helicopter shipboard operations.
3. Fusion of the dynamic maritime environment with the ship model and visualization of a highly realistic ship sterns and wake's field angle according to the waves and ship model setup, and a high-resolution weather model simulating DVE conditions.
4. Integration of a user-centered front end for adjustments of environmental conditions and ship motions configurations due to needed experiments setups.

2 State-of-the-Art Technologies and Human Visual Perception

Landing on unprepared sites in bad weather conditions is a typical mission in helicopter operations [162]. When outside visual cues fade away, the overall workload on the pilot and the loss of SA increases [38]. Wartmann et al. characterize in the final report of HELI-X [149] outside visual cues disappear caused by situations where the helicopter's main rotor downwash raises surrounding particles like dust (brownout) or snow (whiteout). These situations may lead to incidents like obstacle or ground hits. Padfield et al. [110] identify and transfer similar situations arising during helicopter offshore operations in coordination with ships. Within this chapter available ships and helicopters' landing aids to face these challenges are introduced. A possible coupling of these sensors to an HMD projection are presented along actual developments used within onshore operations. With a focus on a human centered design of the PAS, human information processing is introduced according to design principles, human perception, related workload, and SA. Finally, HMD induced symptoms and effects caused by the maritime environment are discussed.

2.1 Helicopter Ship Deck Operations Landing Aids

Operating maritime helicopters to naval ships at open sea is often a difficult and dangerous task. A restricted landing area which is pitching, rolling, and heaving, the pilot also deals within a harsh maritime environment where bad weather conditions often come across. Modern combat ships, e.g., frigates and destroyers, operate with maritime helicopters. The task of approaching and landing the helicopter in bad weather situations is acknowledged as being both demanding and dangerous. Moreover, the pilot must contend with a restricted landing area [35] [88], as seen in Figure 2-1 (author's courtesy).



Figure 2-1: Helicopter during final approach over ship landing deck

For typical procedures [99], in detail helicopter ship deck approach and landing maneuvers, mission safety is enhanced by offering the pilots aids on helicopter and ship side. The land-based limitations are extended to the shipborne environment due to the factors listed below and due to the combined effects of the following factors [13], also see Figure 2-2:

- Ship airwake/ turbulence,
- Ship motion,
- Confined landing area, and
- Visual cue limitations.

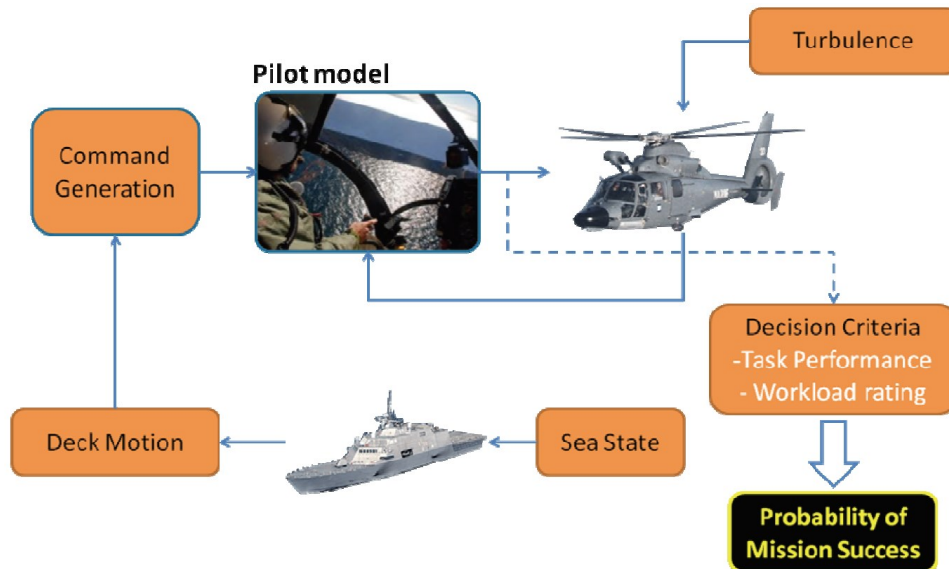


Figure 2-2: Dynamic interface simulation environment [13]

To obtain the maximum operational capability combined with best safety practices, tailored helicopter/ ship sensorics are required. Strategies for a sensor-based approach-to-land [162] supported by ships and helicopter sensors [163] have been investigated and implemented to helicopters in the last decades. However, solutions [48] bringing sensor results visually to the pilot by using head-worn displays are not yet used in the maritime environment. Hence, this chapter investigates in two sections of helicopter landing aids used within a maritime environment:

- Sensor-based landing aids supported by ships and helicopter side sensors, and
- Assistance systems related to state-of-the-art visual augmentation systems.

2.1.1 Ship Sensor Augmentation for Piloted Operations

In the following, three ship installed sensors are introduced. A Ships Helicopter Operational Limit Display System (SHOLDS) [122] established by the Aeronautical & General Instruments Limited (AGI), a glide slope indicator, and a horizontal reference bar offered by cilas ariane group within SAFECOPTER [19] as a ship installed helicopter visual landing aid system.

SHOLDS, mainly used for helicopter ship approaches, provides the ship crew dynamic up-to-date information on wind and ship's motions, superimposed on diagrams as used within actual research, among others like Forrest et al. [35], both see Figure 2-3.

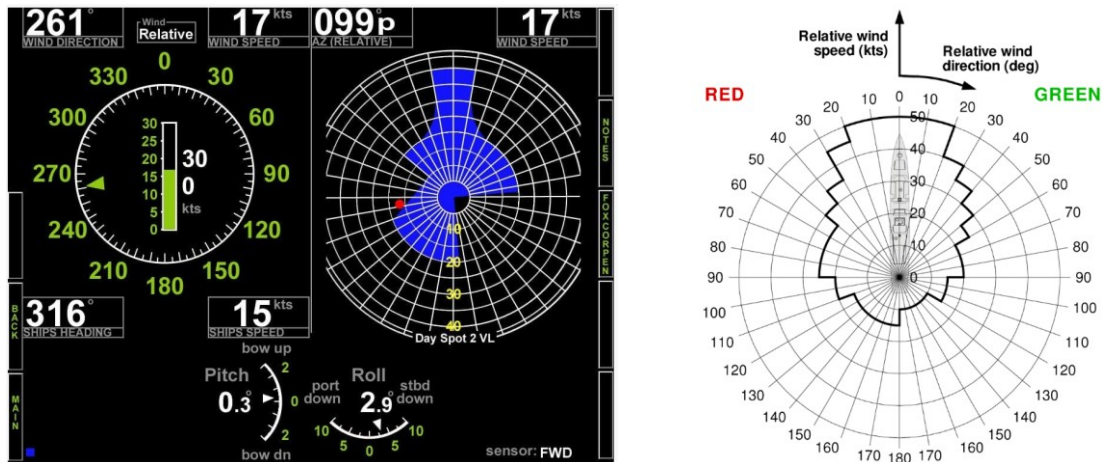


Figure 2-3: SHOLDS GUI [122] (left) and typical SHOL diagram [35] (right)

SHOLDS offers the ship’s crew a visualization of ships relative wind, superimposed on a pre-selected helicopter operating limit procedure. The system indicates a green (go, as seen in Figure 2-3, left image) status if the wind is within limits, and a red (no go) if outside the limits to assist the flight deck officer giving the helicopter a landing clearance via radio communication. To reduce the latency within communication and prevent misleading or broken communication, precisely for these reasons, the visual augmented information of SHOLDS will be integrated to the HMD/PAS developed within this thesis.

Helicopter visual landing aids for take-off and landing, by name a Digital Glide Slope Indicator (DGSi) and a Horizon Reference Bar (HRB), provide the pilot flying an indication of the right approach path during his landing procedure and an actual horizon reference independent from the ship rolling during hover over deck and land. DGSi and HRB, both as seen in Figure 2-4, are installed at the ships rear side vertical board, and thereby in the FoV of the helicopters pilot during the approach and landing maneuvers. [87]

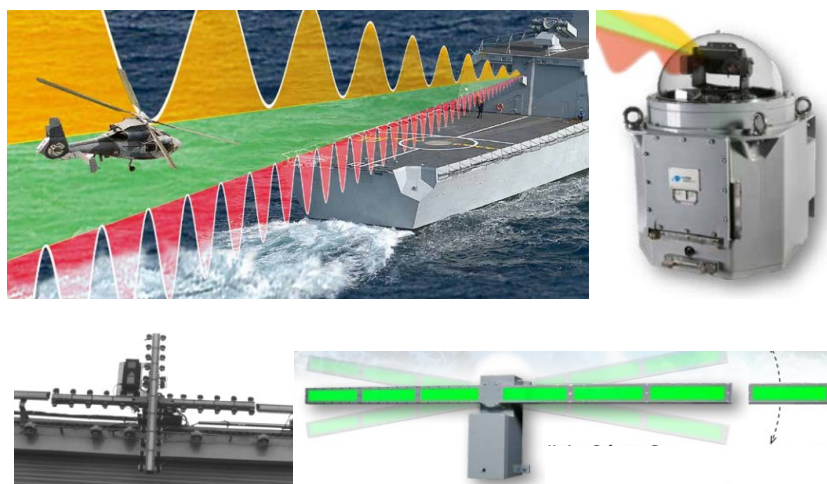


Figure 2-4: DGSi [19] (upper images), HAPS [87] and HRB [19] (lower images)

To be visually independent from any adverse weather conditions and to offer a ship platform independent use of the long lasting and well accepted [87] Hover and Approach Positioning System (HAPS) system, main visual aids of these three systems are integrated to the

HMD/PAS within its HMD visual augmentation concept. HAPS has already been tested with success within an HMD symbology format [87], and is implemented due to state-of-the-art capabilities of color coding for see-through displays [12] and declutter modes [44] within the used HMD of this work. Overall, DGSI, HAPS, and HRB elements are integrated to the HMD visual augmented modes within the HMD/PAS. [104]

2.1.2 Helicopter Visual Augmentation Systems

Visual augmented pilot assistance systems, developed for onshore low-level helicopter operations in DVE [25] [103], as seen in Figure 2-5, aim at giving back the essential visual cues to lower risks.

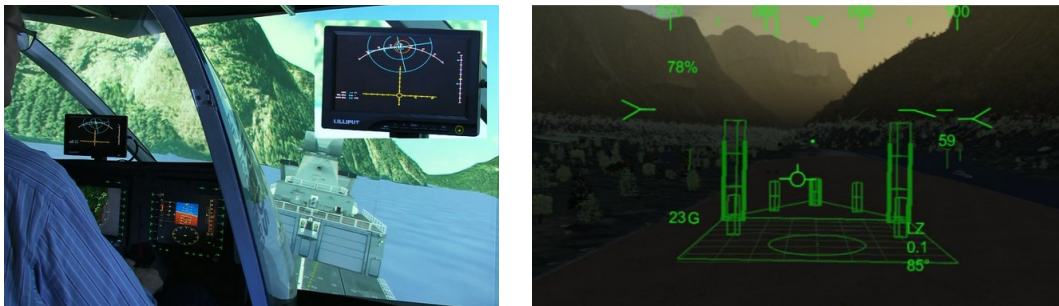


Figure 2-5: 2D and 3D symbology on HDD (left) [25] and on HMD (right) [103]

Therefore, helicopter onshore pilot assistance systems which have the potential to be used for helicopter shipboard operations are introduced:

- Take-off and landing visual augmentation: DeckFinder™ [25],
- A 2D landing symbology for DVE landing maneuvers, named as HMD Brownout Symbology System (BOSS) and the corresponding visual conformal 3D perspective landing display. [27], and
- SferiAssist® of SFERION [103].

First, DeckFinder is a Global Navigation Satellite System (GNSS) independent local positioning system which enables accurate navigation for helicopters during approach to a moving ship. Acting as a pilot assistance for operations in low reference environments, like within flight over open sea, relative position and heading of the own helicopter towards the related ship are visualized on an HDD. Therefore, DeckFinder needs ship and airborne installed segments, like deployable landing deck station units and relating airborne antennas.

Second, proposed HMD 3D perspective display format as investigated from Doehler et al. [27] [28] translated the well-known 2D HMD BOSS into a more intuitive understandable 3D visualization of the helicopters flight situation and its environment: The symbology concept for pilot cueing, as seen in Figure 2-6, is integrated to a state-of-the-art HMD from Elbit Systems (Jedeye) [70] consisting of following visualization parts:

- Helmet aligned elements: Main helicopter parameters of speed, altitude, and engines.
- Aircraft aligned elements: Helicopter attitudes.
- Outside world aligned elements: Horizon line, optional tunnel in the sky, and landing zone symbol.

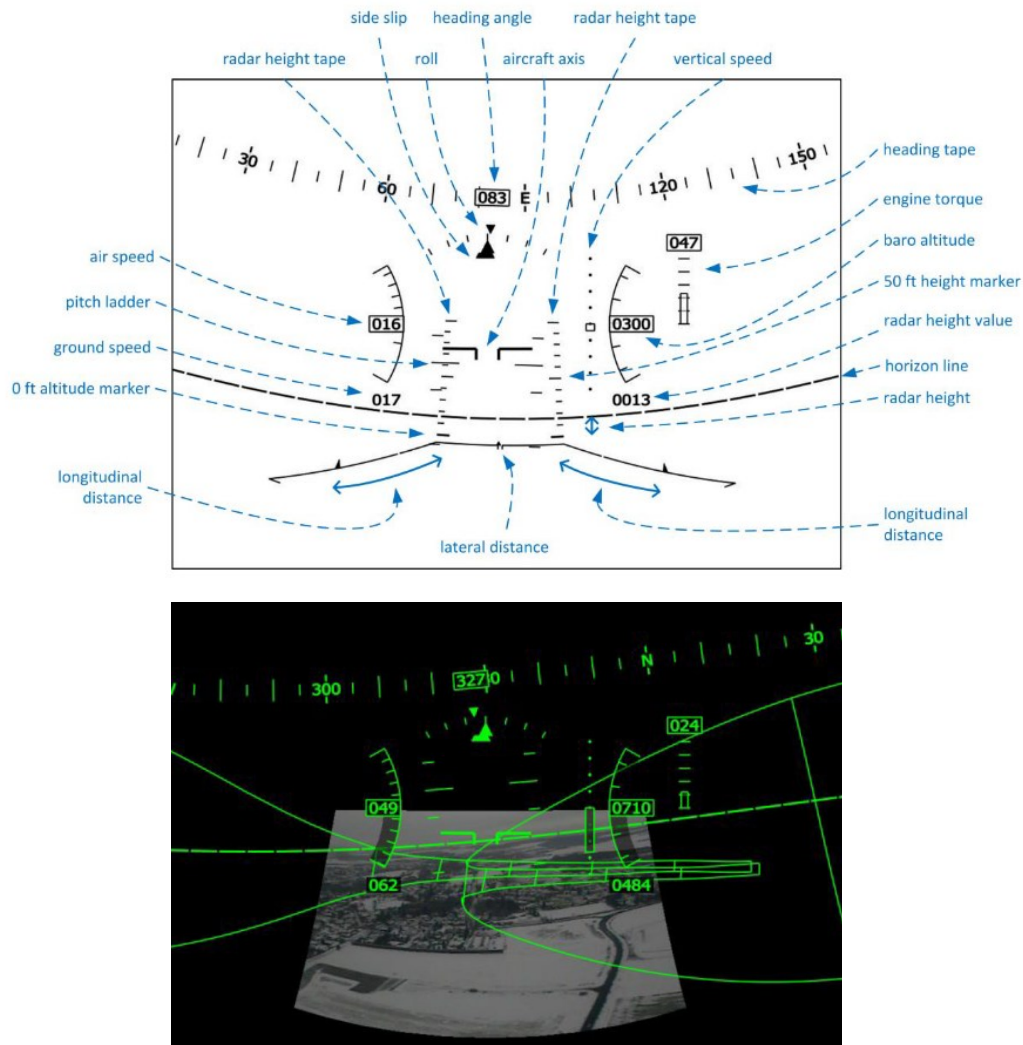


Figure 2-6: 3D symbology (upper image) and seen through HMD (lower image) [27]

The information displayed on the HMD is based on fused data from the 3D LiDAR sensor SferiSense®. The visual augmentation does not intend to present a fully synthetic imagery on the HMD. This would mask the remaining outside view, with all consequences like different visual cues and missing outside scenery of the real image of the landing zone. Walters et al. [146] examined how these cueing settings impacted pilot workload for helicopter shipboard missions. A “tunnel in the sky” and a “follow the leader” 3D visual cueing set, as seen in Figure 2-7, were visualized by a Head Up Display (HUD). Pilots reported lower workload with the use of the 3D conformal cueing. However, pilots were unable to effectively follow the 3D cueing at night and during limited visibility conditions with no external visual references presented. [103]



Figure 2-7: HUD presented tunnel in the sky (left) and cueing set (right)

Third, investigations and developments on pilot assistance systems like SferiAssist® arise among others from flight test results of a sensor enhanced 3D conformal pilot support system [129]. Capabilities of visual augmented sensor systems for helicopter approach and landing, as seen in Figure 2-8, have been demonstrated. The HMD demonstrated a cockpit look-through and an enhancement of see-through capabilities by increasing receiver sensitivity in DVE conditions.

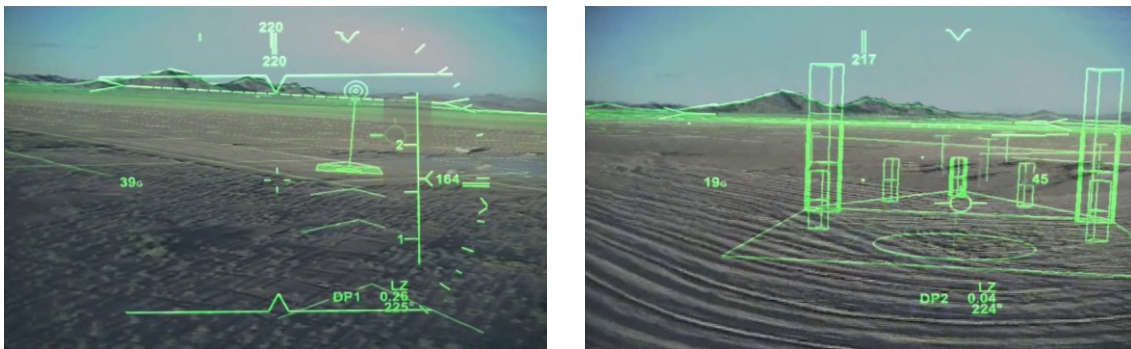


Figure 2-8: HMD symbology during approach (left) and before touchdown (right) [102]

2D DeckFinder augmentation and the 3D visual augmented approach and landing symbology do all have important visual cues, which are extended within this work for offshore operations as follows:

- Integration of an intuitive visualization of the helicopter and environmental related information using 2D and 3D symbols,
- Synthetic external visual references,
- Scene linked clutter modes, and
- Use of a color-coding concept [8] to enhance symbology perception.

Stanton et al. [127] explored the concept of distributed SA within the maritime helicopter domain and concluded a demand for the development of future rotary-wing cockpit technologies to increase the operational capacity of helicopter crafts in DVE conditions. Here, the utility of HMD augmented reality (AR) showed a great capacity to reduce workload and increase SA at same time for simulated maritime operations [90].

2.1.3 Advanced Helmet-Mounted Display Technologies

Developments in electronic display technologies offer benefits for the usage in avionics [135]. Industry and academia alike have presented a variety of external Human Machine Interfaces (HMIs) for airborne vehicles, as investigated below: Efficiency and safety of operations can be enhanced by using synthetic vision and associated technologies, employed on an HMD. Hence, advanced HMDs and corresponding visual augmentation concepts can improve performance and perception [6]. Hereafter, some examples of advanced HMD technologies and visual augmentation concepts used within the helicopter operations are introduced. Major manufacturers arise from BAE Systems, Thales Avionics, and Elbit Systems. The integrated HMDs on helicopters like the NH-90, UH-Tiger, Rooivalk, Cobra, and Mangusta used for flight information and guidance are:

- BAE Systems Striker II Colour [130],
- Thales Avionics TopOwl [138], and
- Elbit Systems Jedeye [70].

BAE Systems Striker II HMD has a visor projected see-through visual augmentation with a $40^\circ \times 32^\circ$ field of view (FoV) and a 1.280 x 1.024 pixels' resolution. The head tracked HMD uses optical trackers (120Hz update rate) installed in the helicopter cockpit to detect and calculate pilots head motions and visualize required parameters plus overlay sensor information with outside scenery cues, as seen in Figure 2-9.



Figure 2-9: Striker Colour helmet (left) and display system (right) [68]

Just like the other two HMDs introduced within this chapter, Striker II enables pilots to fly “heads up and eyes out of the cockpit” by displaying vital information fully colored in a stereoscopic manner directly on to the visor. Striker II HMD visualizes main helicopter parameters and the outside scenery visualization from a Forward Looking Infrared (FLIR) system. The helmet system has an integrated ISIE-11 [55] digital night-vision camera (resolution: 1.600 x 1.200 pixels) situated in the ‘Cyclops’ position, negating the current need for the pilot to wear night-vision goggles (NVG) underneath the visor. However, integrated NVG is visualized monocular on both eyes.

Thales Avionics TopOwl® [82] Helmet Mounted Sight and Display (HMSD) is a full see-through HMSD with a visor projected monochrome augmentation. The TopOwl helmet is

designed with a 40° x 34° FoV and has a 1.280 x 1.024 pixels' resolution. The head tracked HMSD uses electromagnetic trackers (60Hz update rate) mounted inside the helicopter cockpit. TopOwl provides generation and display of 2D and 3D symbology parameters, as seen in Figure 2-10, with binocular intensified image (coming from integrated Image Intensifier Tubes – IITs) with a full overlap of outside scenery.

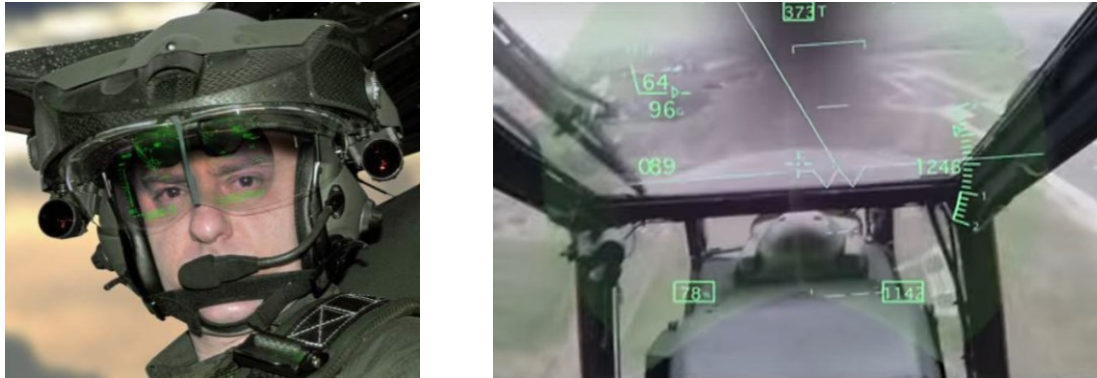


Figure 2-10: TopOwl helmet (left) [82] and display system (right) [139]

The Elbit Jedeye [34] HMD device offers a binocular monochrome green visual augmentation with a wide FoV of 80° x 40° and has a 1.920 x 1.080 pixels' resolution. The head tracked HMD can use optical and electromagnetic trackers. Jedeye provides a picture-in-picture display besides sensor and symbology visualization, as seen in Figure 2-11.



Figure 2-11: Jedeye helmet (left) and display system (right) [34]

At the time of investigation, Jedeye did not offer any helmet integrated NVGs. Table 2-1 gives an overview of introduced HMDs and the HMD, Trivisio LCD29, as used for investigations within this work. More information about the Trivisio LCD29 can be found in [141].

HMDs	Horizontal and vertical resolution per eye (pixel)	Horizontal and vertical FoV per eye (degree)	Color Coding	Display	Stereoscopic projection available
BAE Systems Striker II	1280 x 1024	40 x 32	Fully Color	Visor projection	Yes

Thales Avionics TopOwl	1280 x 1024	40 x 34	Monochrome green	Visor projection	Yes
Elbit Jedeye	1920 x 1080	80 x 40	Monochrome green	2 flat panels display	Yes
Trivisio LCD-29	800 x 600	23 x 17	Fully color	2 flat glasses display	Yes

Table 2-1: Key parameters of HMDs

With access to digital technologies as detailed above, HMDs have become more useful in all stages of flight, even in harsh situations like DVEs. Peinecke et al. [113] describe the development of conformal displays in HMDs during the last half of the century: Conformal symbologies have been developed from helicopter parameter visualization towards a broad variation of nearly all cockpit-related virtual instrumentation.

2.1.4 Simulated Helicopter Ship Operations and Visual Augmentation

Research projects like HELIcopter Situation Awareness für eXtreme Missionsanforderungen (HELI-X) [149] and [80] investigate in displaying an adequate symbol set to the pilot in a harsh maritime environment. In the following, two recent projects examining helicopter shipboard operations and display layouts are presented:

- DLR: Helicopter Flight Safety in Maritime Operations (HELMA) [123] and Helicopter Deck Landing Assistance (HEDELA) [26] using the findings from HELMA to examine offshore flights in DVE conditions with the assistance of AR systems.
- Review of head-worn outside scenery conformal displays. Display of synthetically generated highway in the sky and flight parameters via scene linked, augmented reality. [27]

DLR investigated in HELMA together with German Federal Police in maritime helicopter missions in offshore wind parks. The research focused on enhancing the operational efficiency and safety of maritime helicopter missions. Project HELEDA as the continuation project examines helicopter offshore flights with a focus on helicopter ship interface and AR head-worn systems, as seen in Figure 2-12.



Figure 2-12: DLR helicopter ship interface (right) and see-through HMD view [26]

Within HELMA, a maritime simulation environment within the DLR air vehicle simulator (AVES) was established. AVES is designed as a modular, flexible platform for numeric simulations and experimental flight operations. With the head worn AR system, testing of multiple external head trackers, integration, and certification to DLRs' experimental helicopter Advanced Control Technology/Flying Helicopter Simulator (ACT/FHS), and pilot-in-the-loop symbology concepts are investigated. Simulated and test flights in the projects HELMA as well as HEDELA showed a great benefit of using AR systems in flight to lower pilot workload and enhance SA, even within DVE conditions. [90]

Schmerwitz et al. [120] hold a long-lasting experience in routing information, navigation aids, specialized landing displays. Pilot-in-the-Loop investigations focus on tunnel and landing displays for onshore operations and its evaluation: Here, a too naturalistic representation via HMD synthetic visual augmentation may mislead the pilot to false assumptions, as discussed together with pilots during several flight test campaigns [103]. The use of a scene linked symbology showing obstacle symbols, virtual flight path, and a safety line is stated to be useful. For this reason, HMD displays with conformal symbol sets can support the approach and landing phase of a helicopter [119]. Here, pilots benefit from a virtual representation of the landing pad consisting of a rectangular shape with the near edge missing. During the landing procedure, flight parameter and basic navigation information, and a synthetic horizon are visualized on the HMD, as can be seen in Figure 2-13.

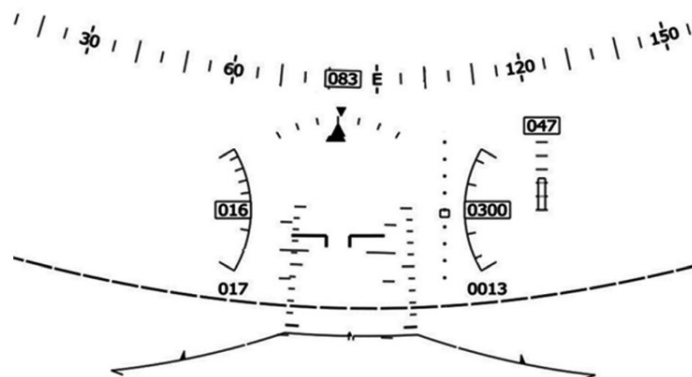


Figure 2-13: Virtual conformal landing display [119]

The HMD symbol set facilitated the precision throughout approach and landing phases. Within these conditions, the superiority of HMDs becomes very evident. [119]

2.2 Human Information Processing

The helicopter ship approach and landing maneuvers are complex tasks addressing a variety of demands on human information processing. These tasks comprise the reception of sensory stimuli, processing of received information by detection, recognition, identification (DRI), evaluation and decision-making processes, and finally the execution of action [156]. Human information processing includes active and passive, conscious, and unconscious, automated, and deliberately controllable processes [116]. Human processing capabilities are limited among others to subjective workload which can be overloaded due to different factors. Therefore, human information processing [41] is considered to identify the potentials and risks related to design principles for HMD visual augmentation, pilot workload and SA, visual perception, and object recognition. Finally, typical symptoms and effects of flying a helicopter with an HMD are illuminated.

2.2.1 Visual Cueing and Design Principles

Pilots use different resources to manage different kind of tasks. Wickens et al. [152] lay out the rationale for the multiple resource theory and the 4-D multiple resource model. The 4-D model puts a focus on multiple human resources and mental workload, see Figure 2-14, which integrates four dimensions of human information processing:

- The stages of processing: Perceptual and cognitive tasks use different resources from those underlying the selection and execution of action.
- The codes of processing: Spatial activity uses different resources than does verbal.
- The perceptual modalities indicate that auditory perception uses different resources than does visual perception.
- The visual channels distinguish between focal and ambient vision.

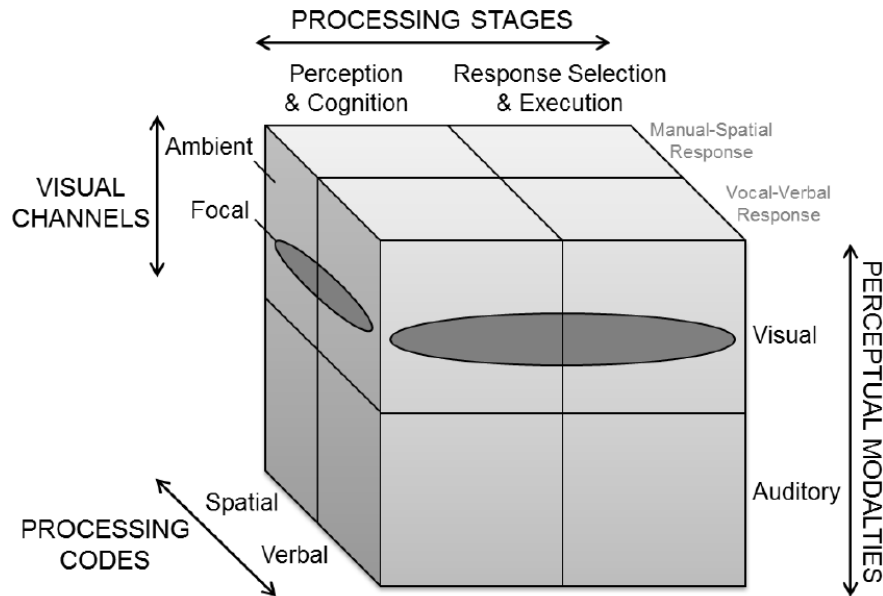


Figure 2-14: The 4-D multiple resource model [152]

In detail, the visual channel focal vision, primarily foveal, supports object identification and recognition, and acuity perception (e.g., reading flight parameters). Ambient vision distributed across the entire visual field and (unlike focal vision) more focuses on peripheral vision and perception of orientation and movement (e.g., approaching towards the ship deck). In accordance with visual cueing principles, the control behavior of pilots depends on the (visual) information available. The three basic control mechanism used within the design of the visual augmentation of this work are as follows:

- Compensatory: The error of parameter to be tracked is displayed, e.g., landing pad.
- Prospective: The whole course or trend of the parameter is displayed, e.g., tunnel in the sky.
- Pursuit: A command value is displayed, e.g., a flight director.

Compensatory and tracking displays have been developed and tested with success within several helicopter approach and landing tasks in DVE conditions [110]. Current 3D-conformal display concepts are mainly based on prospective information, which offers the pilot to anticipate the position of the helicopter in the outside scenery [144]. Predictive approaches, like a projected safety line [96], calculate the minimum flight path altitude for not hitting the obstacles. Moreover, merging control mechanism with the layout for a visual augmentation on an HMD, design principles of Goldstein et al. [46] and Palmer et al. [112] should be considered:

- Principle of closeness: Elements, which are arranged closely together, are perceived as one unit.
- Principle of similarity: Elements which are like each other (e.g., in terms of shape, color, size) appear belonging together.

- Principle of conciseness (or simplicity/ clear design): An arrangement of elements is perceived in such a way that the resulting structure is as simple and memorable as possible.
- Principle of good progression (or continuation/ continuous line): Lines are perceived as if they follow the simplest path. For example, two lines crossing each other are perceived as straight lines, and not as bending off at the point of intersection.
- Principle of common destiny: Elements that move simultaneously in the same direction are perceived as belonging together.
- Principle of familiarity: Elements are more likely to be perceived as belonging together if the resulting arrangement/ grouping appears familiar or meaningful.
- Principle of the common region: Elements that are located in common, separated areas are perceived as belonging together.
- Principle of connectedness: Connected elements are perceived as a unity.
- Principle of temporal synchronicity: Elements that change simultaneously are perceived as belonging together.

The grouping according to the principles detailed above occurs quasi automatically and without conscious attention [116]. The consideration of the design principles in combination to control mechanism is there for highly relevant for the displayed scenery within the HMD. Moreover, the advantage of binocular displays of an HMD, visualizing a stereoscopic conformal picture, is based on mental integration of information in the outside scene and the symbology presented [153]. This includes to provide benefits regarding guidance and navigation as well as reduction of attentional capture, and mental workload [75]. Swan et al. [133] and Morland et al. [100] detail benefits and challenges using depth judgments, visual perception of motion and color coding in optical, see-through AR displays.

In sum, aspects from above lead to a superimposed symbology approach within the FoV of the used HMD: Creating a symbol set that is embedded to the scene (e.g., using 3D visual conformal symbol sets), rather than overlaid on it, greatly improves what is called “scene awareness”. Results of NASA flight tests [106] with different symbol sets indicate that pilots perform significantly better when using world fixed symbology over the standard screen-fixed symbol set. Regarding brightness, contrast, and luminance following colors are identified highest for full-color, see-through HMDs within natural scenes: White (R 255, G 255, B 255), green (0, 255, 0), cyan (0, 255, 255), and magenta (0, 255, 0) [54].

Overall, an intuitive, scene-linked, and highly outside scenery conformal HMD visual augmentation concept is strongly coupled to pilot’s workload and SA. Therefore, these visual cueing and design principles are considered for the HMD/PAS design.

2.2.2 Helicopter Pilot Workload and Situational Awareness

Helicopter flights can be broken down in different phases, each entailing different levels of pilot workload. Recent studies claim that the final phases of flight, e.g., approach and landing are the most demanding. Results of several simulator as well as operational flight tests identified low visibility conditions and rough sea having a detrimental effect on pilots perceived workload [3].

The University of Liverpool has a long-lasting experience investigating in helicopter flying qualities in critical offshore missions [110] using Ship-Helicopter Operating Limits (SHOLs) [121]. Much of its work has involved the HELIFLIGHT-R motion-base flight simulator [115]. The simulation includes among others a representation of a next generation UK frigate Type 26. The difficulty of approaching and landing a helicopter on a moving landing deck with limited size of these type of ships, even in bad weather conditions, is well known. The main challenges, which Perfect et al. [115] identify arise from the small landing deck coupled motions in pitch, roll, and heave axis. Therefore, HELIFLIGHT-R ship's simulation includes a ship motions computation, named as ShipMo3D. The motions of a well-validated type 23 frigate ship model arise from the Defense Research and Development Canada (DRDC). Small, mid, and large ship sizes are used to simulate different ship movement levels in roll and heave axes, as can be seen in Figure 2-15.

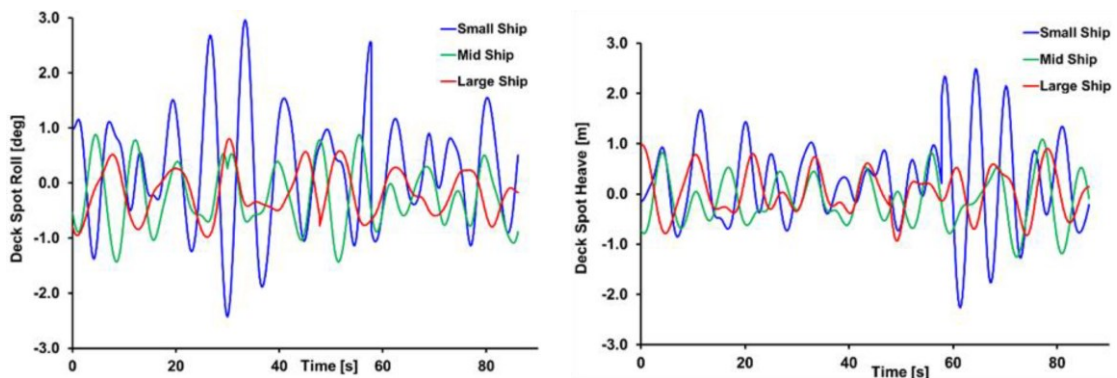


Figure 2-15: Computed displacements of three ships landing spots [121]

Corresponding simulator tests are mainly conducted at HELIFLIGHT-R together with UK Royal Navy helicopter test pilots. The approach and landing tasks are defined along Royal navy port-side approach [140], as among others [105] used within this work. Normally, pilots are asked to provide workload ratings using the Bedford workload rating scale and Deck Interface Pilot Scale (DIPES), see A.1. Previous studies have shown that it can be more difficult to land to a large ship than a smaller one, even it had a bigger landing deck, as can be seen from Figure 2-16. Pilots awarded the greatest workload rating to the hover task over the smallest ship.

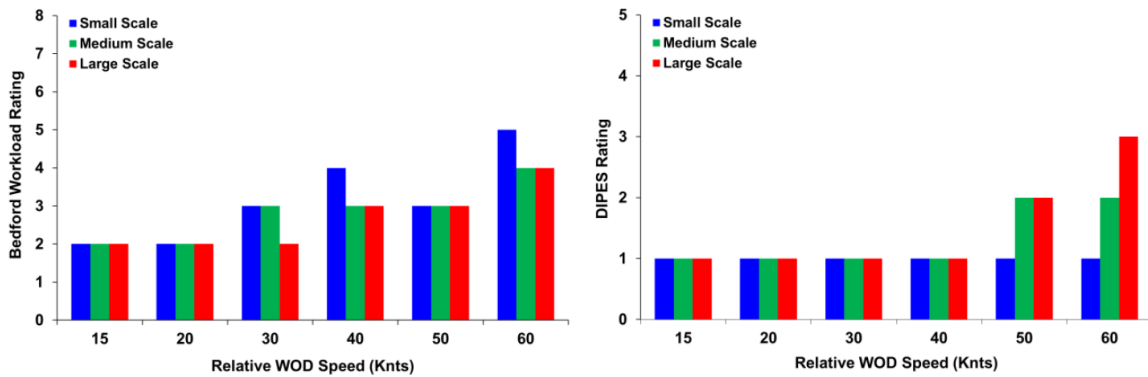


Figure 2-16: Pilot ratings for hover over deck task [121]

Moreover, a long row of simulated helicopter ship approach experiments offers insights into pilot’s control inputs. Largest excursions for lateral and longitudinal cyclic control inputs are observed for the larger ships, while the smaller ships show the smallest excursions. Greatest activity in the collective inputs is for the hover task over the small ship. Same situations for pedal control inputs. An overview is given in Figure 2-17.

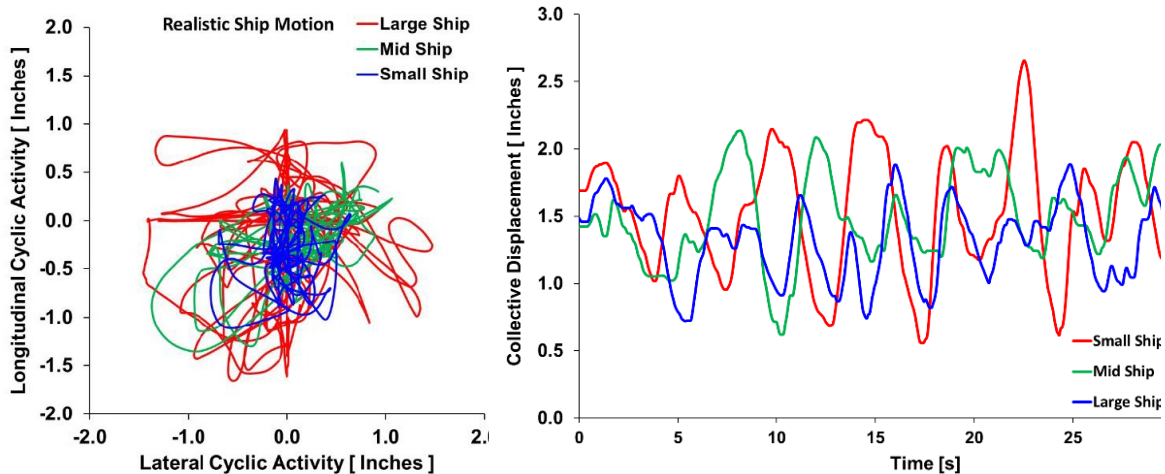


Figure 2-17: Pilots control activities during hover task over landing spot [121]

However, flying a helicopter even towards a moving landing place needs an amount of workload of the pilot. The less effort it takes; the more resources can be spent on enhancing SA.

2.2.3 Visual Perception and Object Recognition

For this purpose, one of the main benefits of the HMD - HMI is to reduce pilots’ workload and increase SA in all phases of flight. Münsterer et al. [102] investigations in HMI workshops together with helicopter pilots have shown that the preferred HMD display information depends on the phase of flight, the current environmental conditions, and the visibility of the moving landing zone. Figure 2-18 gives an impression how different perception of the environment can be in different phases of flight using an HMD in flight: Zimmermann et al. [161] investigated in HMD visual augmentation, landing zone detection and visualization in flight using the ACT/FHS of the Deutsches Zentrum für Luft- und

Raumfahrt e.V. (DLR). The SferiAssist® [59] combined tunnel in the sky symbology with dynamic path visualization based on a LIDAR sensor.

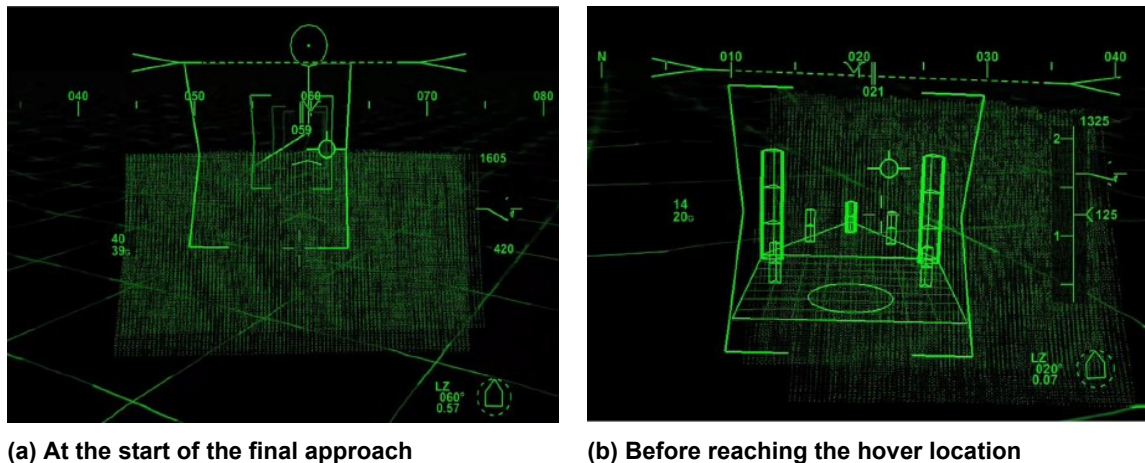


Figure 2-18: SferiAssist at two points along an approach to a fixed landing point [161]

Therefore, main aspects of visual perception and object recognition are investigated along well-known theories in the physiology of behavior [15] and cognitive neuroscience [40]: First, perception of object motion in relation to own motions is introduced. Second, based on the own motion, the optical flow delivers further information for own perception during locomotion. Lastly, the role of the visual association cortex for visual information processing is introduced. These aspects will have a strong impact in the design of the HMD visual augmentation concept.

Important aspects within motion recognition concerns the differentiation between perception of motion of surrounding objects and the own observer locomotion. Gibson et al. [15] described that out of the motion within an optical surface layout, which surrounds a person, both individual objects and surfaces as well as own active locomotion is perceived. Moreover, own locomotion is allocated by the motoric activity. Local motion within the field of regard (FoR): Gibson et al. focused during their analyses mainly on the information “outside” of a person, which means in this case the motion in the surrounding optical arrangement. He described the perception of object motions by focusing on the relationship between the moving object relative to the background. Progressive concealment and release are main characteristics for motion perception. Since the eye is sensitive to motion, and since vectors can be used to represent that motion, the relative velocity of any point in the optical array ought to be represented by a vector in the picture whose length corresponds to that velocity, as can be seen in Figure 2-19.

Optical flow and the motion it evokes in the FoR of the observer: Figure 2-19 shows three of Gibson's earliest images of optical flow during flyby (left image) over the landing field, (middle image) a landing, and (right image) a flyby to the left.

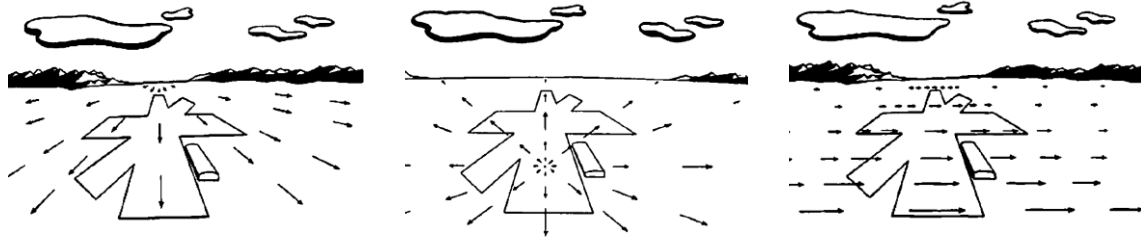


Figure 2-19: Optical flows of pilots' view [23]

Therefore, following scheme scenario has a high validity: While moving forward and looking within 45° of the (flight) path, where the pilot spends 90% of our looking time, advantage is taken out of the relative motion of objects around where the observer is looking. These have following characteristic patterns: Objects converge towards one another, they decelerate apart, or they accelerate apart, and fixation on one member of such pairs makes the relative motions easier to recognize. Pairs in the first two categories yield unambiguous information about heading: It is always to the outside of the nearer member of a pair that is converging or decelerating apart. These are, based on Gibson et al., invariant pairs where there is an invariant relation among the observer, the pair of objects, and heading that is independent of translational velocity. The latter kind of pair are those with objects accelerating apart, yields only for probabilistic information.

Own (observers) and surrounding object motions embedded to the principle of optical flow is part of the processing done by the visual association cortex. Functional-imaging studies among others from Carlson et al. [15] indicate that specific areas of the cortex are involved in perception of form, movement, and color. The visual cortex consists of the striate cortex and two streams of visual association cortex. The ventral stream is involved with perception of objects. The dorsal stream is involved with perception of movement, location, visual attention, control of eye and hand movement. In sum, two dozen different sub regions of the visual cortex are arranged in a hierarchical fashion. Each region analyses a characteristic of visual information and passes the results to other regions in their hierarchy: Striate cortex processes visual information across entire visual field of contralateral eye, dorsal/ ventral analyzes form and processes color constancy, lateral occipital complex is responsible for object recognition, medial temporal/ medial superior processes the perception of motion, and among others caudal intraparietal area establishes perception of depth from stereopsis. The view depends on the own vantage point. Each vantage point reveals new views on the scene, including objects that were obscured from the other vantage point. Moreover, the outside scenery colors may change, depending on environmental conditions, e.g., clouds versus clear sky. Despite this variability, the pilot still can recognize all scenes. However, when pilots operate a helicopter equipped with an HMD visual augmentation system, different effects may arise.

2.2.4 Symptoms and Effects of HMD Augmentation

The use of an HMD during helicopter operations within DVE conditions can pose to different symptoms and effects: Main symptoms are introduced as originating from the HMD itself, named as hyperstereopsis and parallax error, culminating in spatial disorientation induced by high pilot workload.

At first, the initial effects of hyperstereopsis and parallax error on visual perception in helicopter pilots flying with a see-through HMD are well known [30] [117]. Priot et al. [117] investigated the effects of hyperstereopsis on visual perception while using HMD projecting an image for flight guidance with the help of a FLIR or image intensifier tubes in flight, even during DVE conditions. Moreover, Priot et al. summarized out of recent studies hyperstereopsis affects near- and intermediate-distance viewing of static (distance, height, depth, size) and dynamic (speed, time-to-contact) navigation viewing parameters. One of the main reasons of hyperstereopsis is based on the mismatch of the eyes horizontal distance and the horizontal distance of the image intensifier tubes or FLIR cameras [141] [144]: Here the image intensifier tubes are mounted to the sides of the pilot's eyes, and FLIR cameras horizontal positioning to each other is normally not equal to pilots eyes horizontal distance. The presence of multiple, interacting (synthetic) depth cues, and cognitive factors such as a familiar-size scene, means that hyperstereopsis in operational environments generates complex sensory illusions. As it has a near- to intermediate-range effect, it is a particular concern when landing, and in low-altitude phases of flight.

Second, the mismatch of the eye point of the pilot's eyes and the FLIR cameras mounting is extended by a second phenomenon observed during operating a helicopter with the help of a FLIR camera mounted on the front side of the helicopter: the parallax error. Moreover, motion parallax cues also enhance stereoscopic depth. The lack of motion parallax cues during hovering tasks is likely to hamper height perception. Conversely, the role of vertical disparities is likely to be minimal in operational environments because the contribution of vertical disparities to distance perception depends on the size of the FoV of the HMD and is limited to near fixation distances.

Finally, while subjective workload now increases and so SA decreases, spatial disorientation comes on top. Knabl et al. [76] describe spatial disorientation as unawareness of lateral drifts prior to touchdown, illusion of self-motion, and somatotropic illusion. Consequences such as roll-over, CFIT and CFIO may arise.

3 Concept of Design for the Visual Augmentation Scheme

The following chapter describes the main offshore approach procedures for helicopter operations in the near-ship environment based on two main international naval standards [105] [140]. Next, the resulting requirements matrix unifies standard procedures of helicopter ship deck recovery tasks with “Pilot-in-the-Loop” operational needs. Finally, fundamental functions for a visual and control augmentation scheme are given based on the established requirements.

3.1 Process of Integration and Validation

User, costumer, and operational guidelines represent different, complementary, and contradictory demands [92] on the design of aeronautical equipment [124] [16]. Therefore, a systematic requirements analysis [24] is used for elicitation, traceability, and testing of a visual and control augmentation scheme for maritime helicopter operations. The following steps summarize the integration, validation, and verification process of the HMD/PAS into the experimental setup ROSIE:

1. HMD/PAS and maritime environment system requirements specification establishment along international naval procedures and accompanying design workshops [49] together with two maritime test pilots from German Armed Forces.
2. Integration of a visual and control augmentation scheme based on 1. into ROSIE and extension of the experimental environment by integrating a dynamic maritime environment.
3. Separate workshop and naval flights to increase the authors experiences in “flying and approaching to ship decks over open sea” together with six maritime fleet pilots from Wiking Helicopters. [154]
4. Verification and validation of the visual and control augmentation scheme within two simulator flight test campaigns.

3.2 Phases of Flight during a Helicopter Near-Ship Mission

Helicopter pilots challenge different phases of flight towards a moving ship deck. Hence, standardized procedures for the ship approach and landing are highly desirable to operate safely and efficiently. Therefore, Helicopter Operations from Ships other than Aircraft Carriers (HOSTAC) [105] specifies helicopter cross operations to air-capable ships. In parallel the SBAS Offshore Approach Procedure (SOAP) [140] describes the development and assessment of offshore approaches. HOSTAC is produced by North Atlantic Treaty Organization (NATO) and non-NATO international working groups while SOAP is established for the UK Civil Aviation Authority (CAA). Following chapters investigate in both

procedures to fulfill the approach and landing maneuver starting from the Initial Approach Fix (IAF) until station keeping over the deck [140].

3.2.1 Helicopter Ship Approach and Landing Procedure

The HOSTAC program is designed to specify and standardize procedures for helicopter and ship cross operations. The HOSTAC operations offer the pilots of a helicopter to always use the standard SCA (Ship-Controlled Approach) procedure [105] for maneuvering and deck handling procedures of the host ship. Therefore, this section includes a brief description of the SCA procedure of the ship dynamic interface [87].

The standard SCA procedure of a naval helicopter, as shown in Figure 3-1, starts when the helicopter passes at a range of 3 NM oriented from the centerline of approach from 150° to 210° relative to the ship and ends with the station keeping of the helicopter over the landing deck.

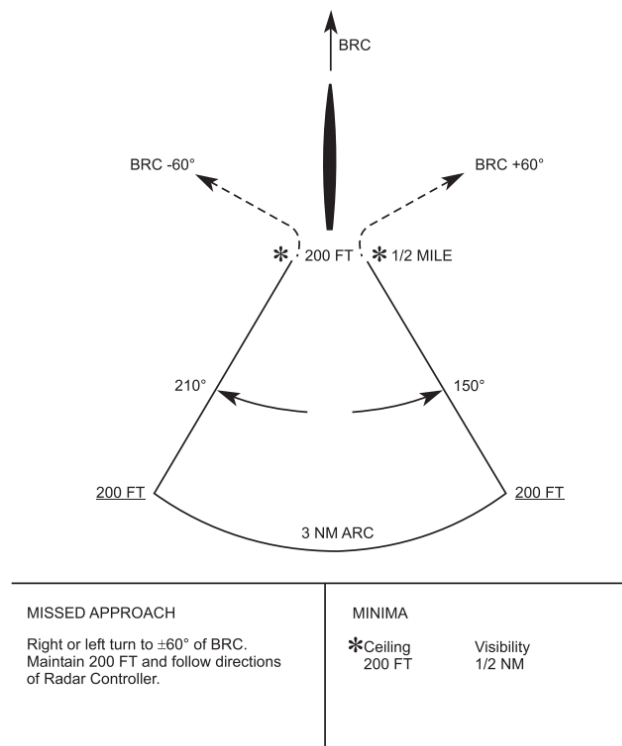


Figure 3-1: Standard SCA approach chart [105]

At the starting point of this final approach procedure, the helicopter must be at an initial height of 200 ft over the flight deck according to the altitude as detailed in chapter 3.2.2. First phase, named as phase **prior to final**, ends at the gate of 2 NM behind the ship deck. Regarding flight parameters during this phase, the helicopter pilot gets information from the helicopter air controller. The Standardization Agreement (STANAG) 1154 [126] provides the standard qualifications for controller enhancing operational safety for approaches and landings. The information from the helicopter air controller includes the relative wind, speed of the ship, flying course of own helicopter, and the request for the approach speed. Next,

the pilot begins to descend the helicopter at the range of 2 NM with a descent rate up to the pilot's discretion, preferably in accordance with receiving ship's equipment specifications [87] [105]. Second phase, named as **descent**, ends 0.5 NM behind the ship deck at the Missed Approach Point (MAP). At that point, the ship deck must be visual to the pilot flying. Otherwise, the pilot must proceed a missed approach according to a standard procedure as given in Figure 3-1. Finally, the helicopter station keeping over deck and landing is specified as phase **landing**. There are five types of approach that a pilot can make to ship flight decks:

- a) Straight-in,
- b) Oblique port to starboard *or* starboard to port,
- c) Lateral: port *or* starboard,
- d) 45° approach: port *or* starboard, and
- e) Athwartships: port to starboard *or* starboard to board.

Since c), as shown in Figure 3-2, is identified by the HOSTAC as the common standard approach, the lateral port approach is used for investigations within this work.

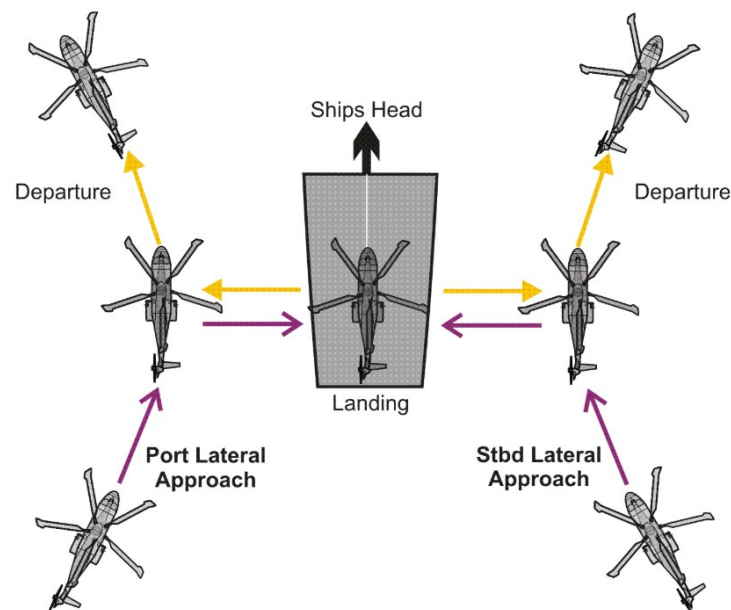


Figure 3-2: HOSTAC shipboard landing - lateral approach [105]

3.2.2 Ship Controlled Final Approach Procedure

Investigations of the potential to provide a practical GPS offshore approach guidance system are in the focus of the SBAS SOAP [140]. SBAS describes the development and assessment of a new type of offshore approach procedure named as SOAP. SOAP is based on the new Approach with Vertical Guidance (APV) defined by the ICAO (International Civil Aviation Organization). This section contains a description of the final approach segment of the SBAS SOAP procedure. Therefore, the approach task is subdivided into the arrival segment, the initial approach segment, the final approach segment, and the final stages of the recovery.

The arrival segment starts at the last en-route navigation fix and ends at the Initial Approach Fix (IAF), see Figure 3-3. Next, the initial approach segment, named as the phase of **navigation**, commences at the IAF, and ends at the FAF. At the FAF, the helicopter enters the descent segment, named as the phase of **descent**, at a constant airspeed and a fixed glide path angle of 4° until it reaches the Minimum Descent Altitude (MDA). Subsequently the phase named as **level** continues from the MDA to the MAP, where the helicopter must align to the MDA over the whole phase. The MAP is defined as the closest point to the destination from which it is safe to decide to land. The distance of the closest point to the landing spot, named as Minimum Decision Range (MDR), is under normal circumstances 0.75 NM from MAP, where the helicopter has a maximum ground speed of 80 kts. The MDA will be 200 ft or helideck height + 50 ft by day and 300 ft by night.

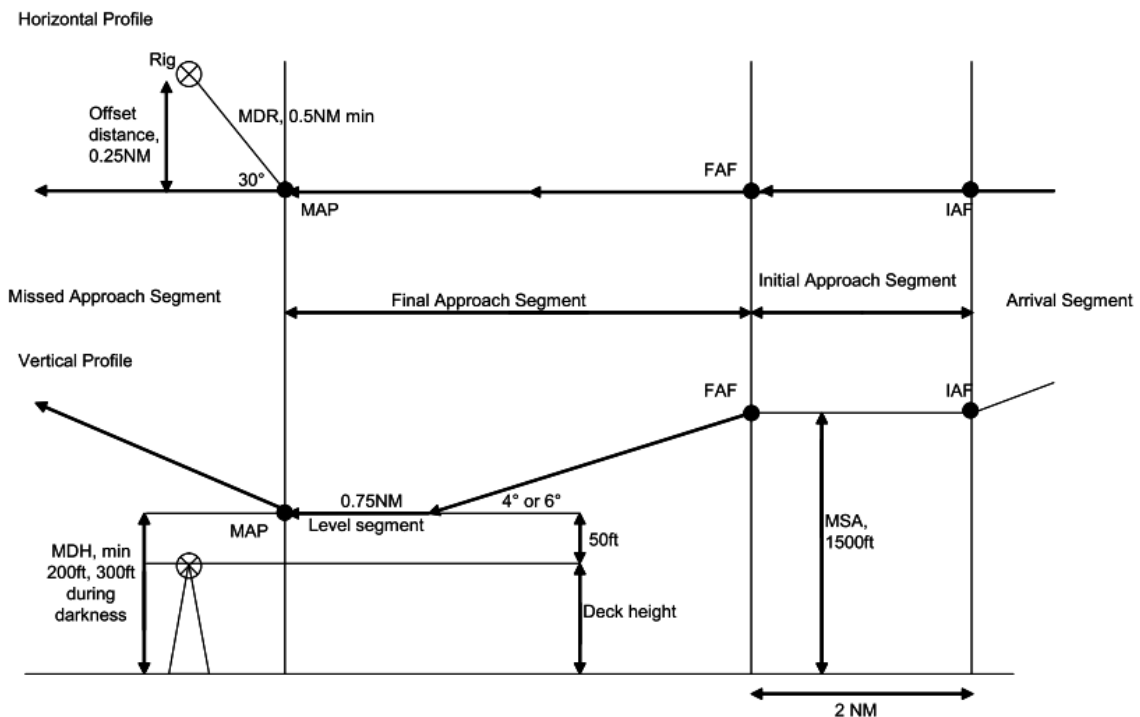


Figure 3-3: Overview of approach parameters [140]

However, the final stages of recovery are not described in detail in the SOAP. Owen et al. [109] describe these stages of the recovery as deceleration to hover alongside, hover alongside, sidestep, station keeping above flight deck, and landing during a quiescent period, as shown in Figure 3-4.

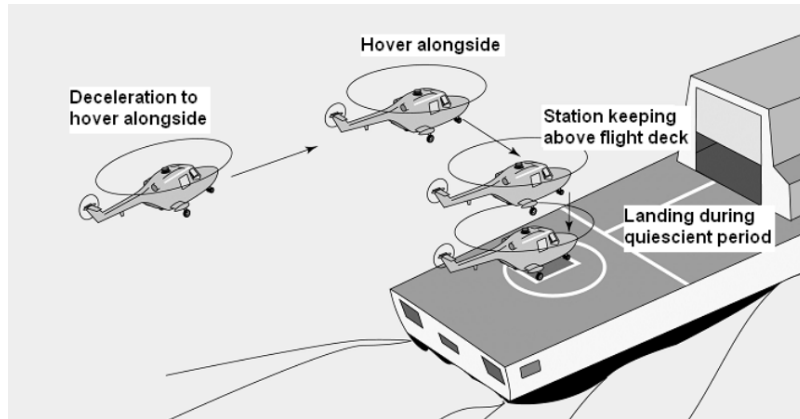


Figure 3-4: Final stages of the recovery of a helicopter to a ship deck [109]

Within this final recovery maneuvers, the pilot positions the helicopter parallel to and alongside the side of the ship deck. The pilot then fulfills the sidestep with the helicopter heading towards the ship deck, with the eye-line at about hangar height until he positioned above the landing spot. During a quiescent period in the ship's motions, the pilot descends to the deck and lands. These final stages of the recovery named as phase **land** starts with the deceleration and ends with landing the landing on the deck.

3.3 Requirements for a Visual Augmented Helicopter Shipboard Approach

As HOSTAC and SOAP mainly describe similar procedures during a helicopter shipboard approach, this section summarizes and illustrates both procedures. However, as the procedures differ in detail, main stages of flight named as navigate, descent, and land are addressed to later perform simulator flight tests. Table 3-1 illustrates the combined phase model of the HOSTAC approach and landing procedure, and the SOAP final approach procedure.

HOSTAC	SOAP							
	Arrival	Navigate	Descent	Level	Deceleration	Hover alongside	Station keeping	Land on keck
Prior to final	NAV							
Prior to final		NAV						
Descent			DESC					
Descent				DESC				
Landing					LAND			
Landing						LAND		
Landing							LAND	LAND

Table 3-1: Combined phase model for helicopter ship deck approach

The main stages of the helicopter ship interface during the recovery task are summarized as follows:

1. Navigation (NAV): Detect and find the ship in all weather conditions to start the approach procedure from IAF.
2. Descent (DESC): Descent from the IAF to the MAP towards the ship along, mainly along the HOSTAC procedures.
3. Landing (LAND): Operating the helicopter from the MAP towards the moving ship deck and proceed the sidestep landing procedure, as given in the SBAS SOAP.

3.3.1 Problem Statement of Helicopter Ship Interface

The combination of the procedures within the experiments is highly desirable to evaluate the pilot assistance system functions with the focus to operate a helicopter safely, efficiently in a maritime environment, closely to a moving ship, and even in harsh environmental conditions. However, two more items are mandatory for any cross operation: Insights on the receiving ship's landing area, support facilities, deck markings, location of obstructions, and other physical details which influence the helicopter landing. Detailed knowledge of the helicopter to be landed on the ship's landing area, including rotor diameter, gross weight, fuselage length, and landing gear specifications. Here, the problem description for the ship deck recovery is given and detailed on respective ship approach and landing MTEs.

The approach task, as shown in Figure 3-5, mainly follows the maneuvers from SBAS SOAP final approach procedure. In detail, the following MTEs [14] are proceeded by the pilot flying:

- MTE (0, all as labeled in Figure 3-5) approach to the deck: The helicopter enters the visual augmented IAF and proceeds the ship approach along the moving glide path up to MAP.
- MTE (1) hover behind and alongside the deck with a constant speed holding the helicopter in parallel to the rear left side of the landing deck.
- MTE (2) sidestep, hover over deck, and land: where the helicopter passes the MAP and enters the final landing phase (3) and (4)) towards the moving ship (all in cyan).
- MTE (3) hover alongside the deck, where the helicopter passes the edge of the landing deck, hover over the deck and land during a quiescent period of ship motion.

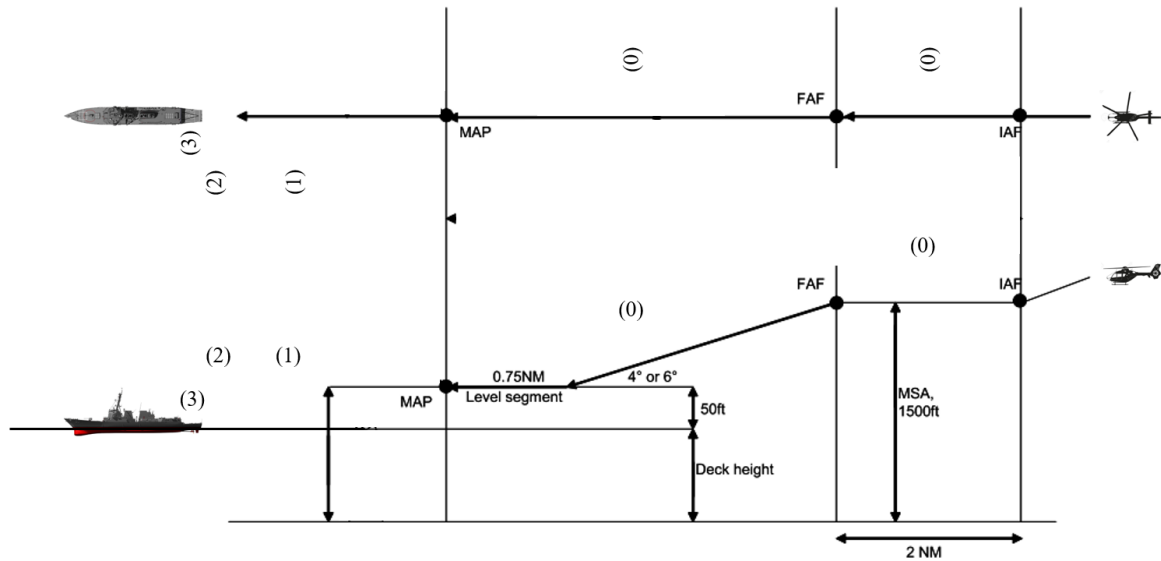


Figure 3-5: Side and top view of the approach trajectory, figure not to scale

Here, the HMD/PAS faces following challenges to decrease pilot’s workload and enhance visual cues [28] within this phase of flight caused by possible upcoming DVE conditions:

- The ability to detect and find the IAF with the assistance of the HMD visual augmentation [77] to engage the approach towards the moving landing point with precision and a reasonable amount of aggressiveness.
- The requirement to keep a constant and precise glide path, in detail sink rate, speed, and heading towards the moving ship.
- The capability to attain the MAP at the end of the glide path while keeping precise relative position, altitude, and heading behind and above the moving ship deck.
- To fulfill the landing during a quiescent period of the moving ship deck with acceptable workload and high precision at same time.

Moreover, the standard ship-controlled landing procedures have been used to isolate the landing sequence for a helicopter, see Figure 3-6. The landing task essentially combines the bob-up and bob-down [14] maneuvers. Here, the pilot fulfills the following MTEs [14]:

1. Hover alongside the deck (MTE1, (1)),
2. Sidestep (MTE2, (2)),
3. Precision hover over deck (MTE3, (3)),
4. And land on the deck (MTE4, (4)) from [140].

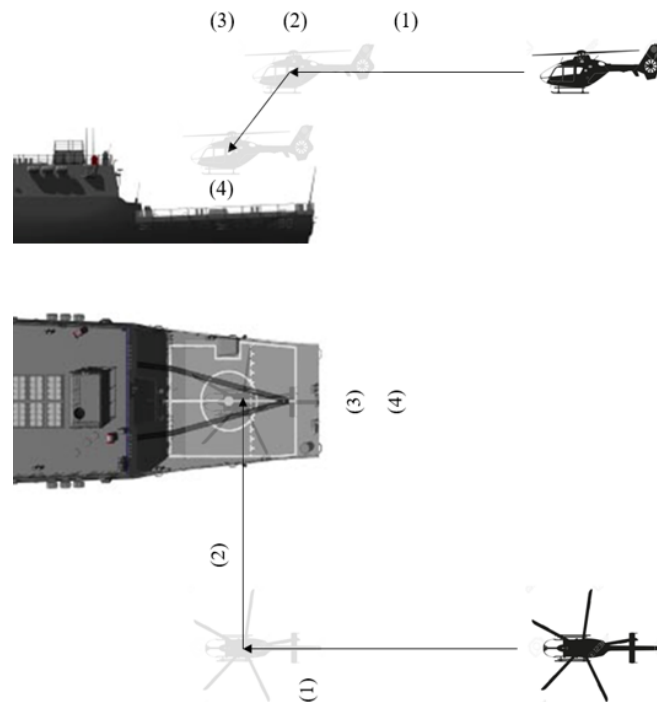


Figure 3-6: Side and top view of the landing trajectory, figure not to scale

During this final phase of flight, the HMD/PAS fulfills following requirements to decrease pilot's workload and increase pilot's SA [67]:

1. The ability to decelerate from translating flight to a stabilized hover alongside the ship deck with precision and a reasonable amount of aggressiveness.
2. The competence to keep a precise relative position, altitude, and heading alongside the moving ship.
3. The capability to sidestep to the center of the ship deck landing pad while keeping precise relative position, altitude, and heading above the moving ship deck.
4. The power to keep precise relative position, altitude, and heading above the moving ship deck landing pad.
5. Landing during a quiescent period of the moving ship deck with a safe distance of the rotor diameter to obstructions and facilities of the ship.

Minotra et al. [97] summarized alike the helicopter ship deck approach within a cognitive task analysis and knowledge audit together with four rotorcraft pilots, as shown in Figure 3-7.

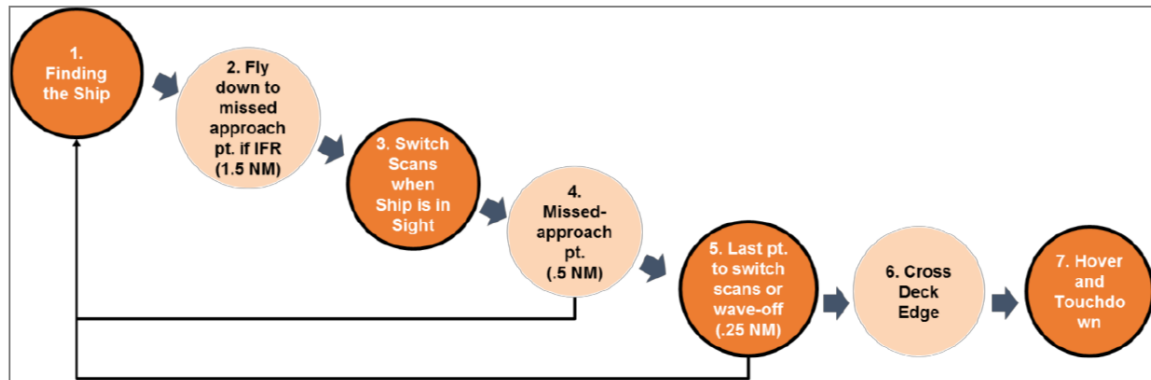


Figure 3-7: Pilot cognition of surface-level interview [97]

Taking procedures and mitigation strategies of the approach and landing tasks both into account, the resulting operational requirements are summarized in the following.

3.3.2 Fundamental Requirements for a Pilot Assistance System

The basic requirements of the PAS are developed along the aeronautical system engineering and project management process, see [83]. A review process of defined operational needs was proceeded during a workshop together with two maritime test pilots of German armed forces culminating in a PAS systems requirements matrix (SysReqM) [64] [120]. Finally, following main operational requirements for the PAS [57] had been identified:

1. The visual augmentation of the PAS must be head-worn. [74]
2. The PAS must display the following main flight parameters of the rotorcraft: Altitude, speed, vertical speed, heading, helicopter attitude, and engine information.
3. As a backup system, main parameters from 2. must be displayed in a visual layout to the head-down instrumentation, in detail the PFD of the rotorcraft.
4. The PAS must visualize the main parameters of the standard procedure glide path towards the ship, the landing deck, main obstructions, and facilities of the ship.
5. The PAS must display the main outside scenery visual cues such as an artificial horizon and guarantee a high outside scenery conformity.
6. The PAS must keep nonconformity as low as possible.
7. The PAS should harmonize visual and control augmentation [50].

Needed operational requirements for a safe ship recovery task with a focus on the PAS using an HMD [42] were further discussed in a workshop together with two experienced maritime test pilots (mean flight hours on rotary systems 3631,86 h, SD 2053,79 h) from German Armed Forces, Wehrtechnische Dienststelle der Luftwaffe 61 (WTD61, Technical Center for Aircraft and Aeronautical Equipment, Manching, Germany). Both pilots hold several helicopter licenses, such as for CH53, H135, MK88, NH90, Sea Lynx, UH-1D, and UH-Tiger with both having a long-lasting experience in flying with HMDs in real flight (mean HMD flight hours on rotary systems 381,00 h, SD 507,00 h) and in simulators (mean flight

hours on simulator rotary systems 94,60 h, SD 113,86 h). The main goals of the workshop were as follows:

1. Analysis of all system requirements as established in the PAS SysReqM from pilots' point of view.
2. Design of a prototype for an HMD ship deck landing symbology concept, based on 1.
3. Extension of the prototype of HMD symbology concept by test pilot's experiences of flying helicopters over open sea or in DVEs [134], especially in inadvertent visual flight rules (VFR) to instrument meteorological conditions (IMC). [102]

Looking at workshop goal 1, the PAS SysReqM had been confirmed and supplemented from pilots' point of view as follows:

1. Both pilots confirmed to benefit during flights in DVEs from head-worn systems [28] and acknowledged the visual augmentation concept of the HMD/PAS for offshore operations [107]. As there is by the time of the design of this work no HMD visual augmentation concept available on the market for helicopter ship deck operations, two promising symbology concepts for the Ship Deck Approach and Landing are considered: the (Enhanced) Ship Deck Approach Symbology ((E)SAS) and the (Enhanced) Ship Deck Landing Symbology ((E)SLS). [72] [161]
2. Different variants of primary and advanced flight control modes in accordance with the SAS/ ESAS and SLS/ ESLS modes had been recommended by both pilots and are therefore taken into account in the experiments, see also [52].

Consequentially, the layout of the HMD visual augmentation is designed along a color-coding concept [43], especially used in rotorcraft systems operating with an HMD equipped, based on [142]. Main color differentiation within the HMD (E)SAS and (E)SLS is implemented as follows based on [21]:

- **Magenta:** All helicopter navigation symbols.
- **Green:** Ship approach path visualization.
- **White:** Ship landing deck augmentation.
- **Red:** Synthetic horizon.

In addition, the HMD visual augmentation must provide relevant three dimensional (3D) visual cues to assist the pilot during shipboard launch and recovery operations. A detailed description of the final HMD symbology concept can be found in chapter 4 and [93].

Regarding workshop goal 2, following concept is proposed from the author together with the maritime test pilots for an HMD/PAS: The HMD 2D primary flight display information is visualized via a helicopter fixed and head-fixed symbology concept and had been transferred from on shore operations in DVE as used in [142]. The ship approach and

landing information is visualized in a 2D, and 3D manner based on [128], all symbology related to the actual ship position.

Finally, looking at workshop goal 3, following extensions to the HMD visual augmentation is purposed to be integrated from pilots' experience. Both test pilot suggested enhancements based on their experiences flying in simulated maritime environments: In detail, they recommended adding a room-stable symbology to the HMD SLS on the flight deck, which displays the line-up line [12] of the landing pad for giving a longitudinal reference. Therefore, a virtual line-up line, see chapter 4, was integrated in a dual use concept according to ADS-33 PRF [1] and HOSTAC [140] standards: The additional 3D lines are visible at all times through the HMD, and operate as a room-stable hover symbology according to the standard course layout of the hover MTE [1], and as successfully used during simulated onshore operations [144]. Besides the SLS and ESLS for the final recovery maneuvers, the visual augmentation types for the approach phase, namely SAS and ESAS, are designed equally, taking actual developments [28] [74] [77] of HMD visual augmentation methods for onshore operations into account. Regarding the needed dynamic of SAS and ESAS, main challenge of the visual augmentation concept is to visualize the standard approach procedure, guaranteeing a highly precise relative positioning to the moving deck. Figure 3-8 illustrates a general overview of the HMD/PAS developed within this work.

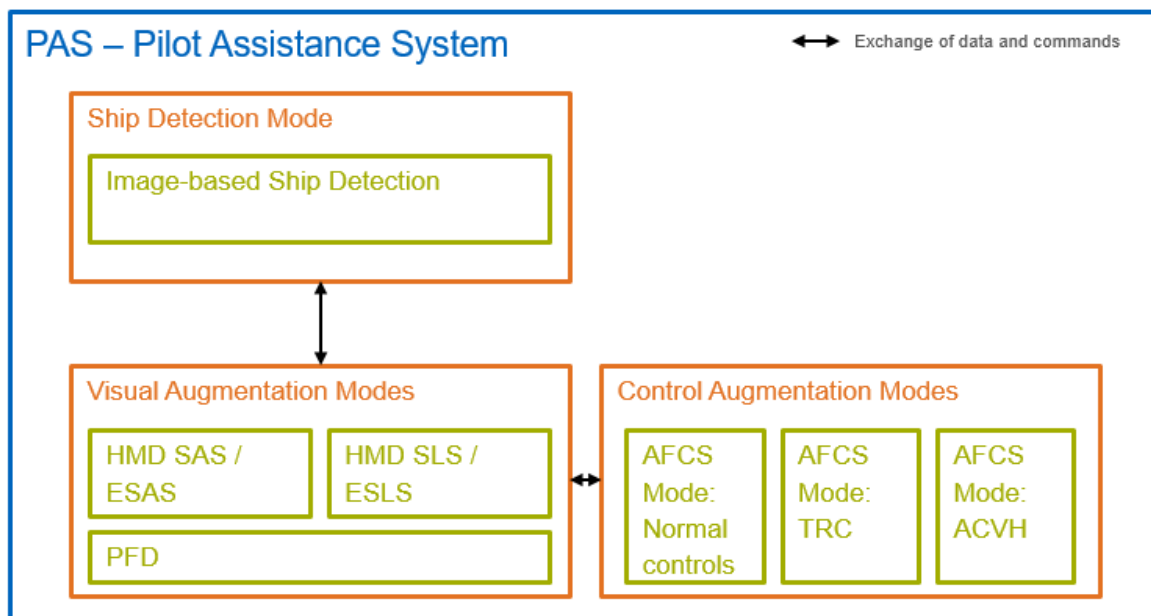


Figure 3-8: PAS including main systems (orange) and subsystems (green)

The PAS comprises of three main systems: Ship detection methods, HMD visual augmentation, and control augmentation modes. Insights of advanced flight control modes are investigated in chapter 4, and further given in [50] and [52]. An overview is given in

Table 3-2, which allows a requirement related system testing, validation, and verification [24] of the PAS.

PAS SysReqM	PAS SysSpec											
	1	2	3	4	5	6	7	8	9	10	11	12
ID												
Ship Detection				X	X	X	X	X			X	
Visual Augmentation	X	X	X	X	X	X	X	X	X	X		X
HMD SAS / ESAS	X	X		X	X	X	X	X	X	X		X
HMD SLS / ESLS	X	X		X	X	X	X	X	X	X		X
HDD PFD		X	X			X	X	X		X		X
Control Augmentation												X
AFCS: Primary FCS												X
AFCS: TRC												X
AFCS: ACVH												X

Table 3-2: PAS SysReqM connected to PAS SysSpec

4 Functions for a Pilot Assistance System during Near-Ship Operations

The newly developed visual and control augmented PAS for helicopter shipboard operations is presented within this chapter. The PAS incorporates an image-based ship detection method to estimate ships actual and predicted position for a visual augmentation. The HMD/PAS uses then a commercial but modified HMD to visualize a scene-linked enhanced ship deck approach and landing symbology, named as the ESAS and ESLS. Finally, the HMD/PAS includes two advanced flight control modes [50] [51].

4.1 Image based Ship Detection

Within this work, the ship decks localization in the simulation environment is detected via estimating the 6D pose of the landing deck: The corresponding computer vision based methods can be categorized into sparse feature-based, template-based, and learning-based methods [11] [78] [136]. Therefore, well known approaches for real-time 6D pose estimation are analyzed within this work: Pose CNN [157], PV Net [114], Dense Fusion [148] and Single Shot 6D Pose [136]. Once the results have been compared in datasets such as Line MOD [65] and methodologies, the method Single Shot 6D Pose with self-generated input images was chosen for detecting the ship within the maritime environment of ROSIE. The method allows an object (3D translation vectors and 3D rotation matrices) to be detected in an RGB image without multiple hypotheses needing to be examined.

At first, to detect the moving ship in the scenery, two basic datasets for a static ship were created. For both datasets, the ship center was set to correspond to the screen center, and the ship's nose and stern were barely truncated. Second, three more datasets using SCONE data were generated: In the first dataset, the ship is moving while the ship center still stays in the center of the analyzed image. In the second dataset, either the ship's nose, stern or side is truncated, while the ship center is not outside of the image. Third, a dataset according to the second dataset was established, in which a linearly scaling fog (DVE condition) is added and the transparency of the fog changes during the data generation process [45] [85]. Figure 4-1 gives an overview of the different coordinate systems and matrices which must be considered for the calculation of the 6D pose of the ship deck: local space, world space, view space, clip space, and, finally, screen space.

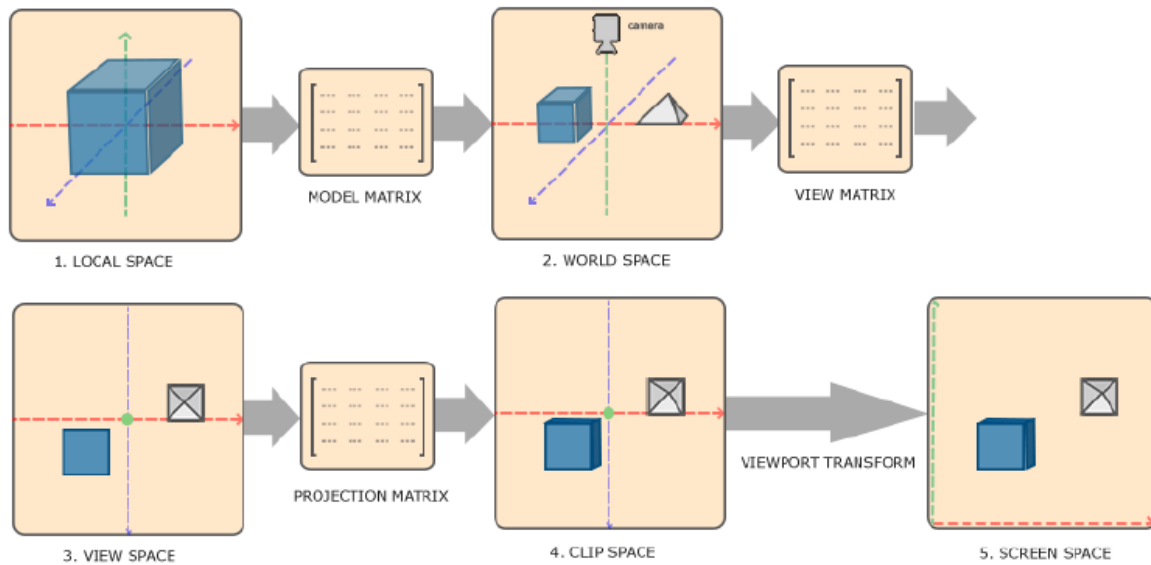


Figure 4-1: Viewing transformations from local space to screen space

A data generation handler creates one label file in common TXT format for every screenshot to store the 21 numbers. In each frame, this class records nine vectors, which store the 3D coordinates of the center point and eight corner points in world space. Each of them is multiplied with the model matrix, the view matrix, and the projection matrix to compute the 2D coordinates and normalize them in the range of -1 to 1 in the clip space. The respective matrices result from the coordinate systems as given above. Results are ranged from 0 to 1 and then stored in the label files, which the SingleShot6DPose network needs for training. To visualize the resulting points via a bounding box in the image, as can be seen in Figure 4-2, in DVE conditions such as limited visibility (left image) and fog (right image), the results need to be multiplied finally with a viewport transform matrix.

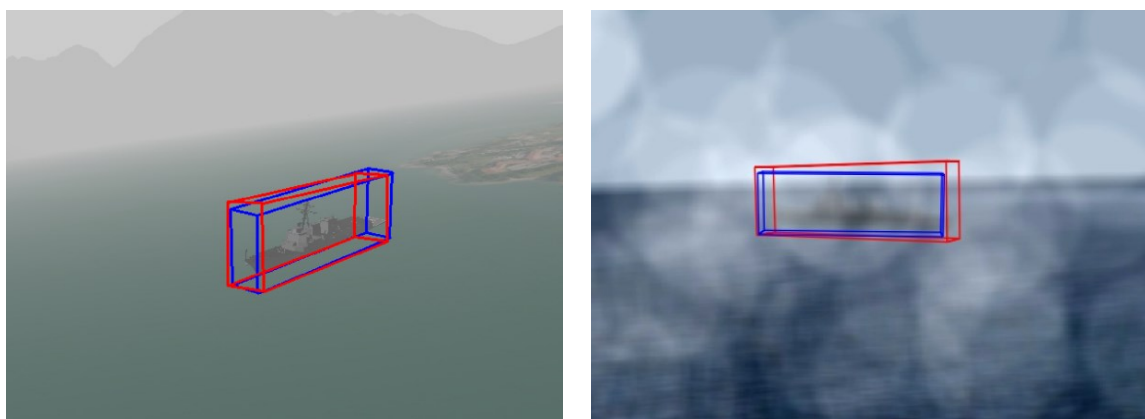


Figure 4-2: Ship detection in DVEs with ground truth (blue) and prediction (red)

Although the SingleShot6DPose does not show clearly yet to detect the ship model with truncation, an attempt was made for comparison's sake. By training the network without clamping the bounding boxes' corner points to the range of 0 to 1, the method was able to predict the bounding box corners outside of the image. Nevertheless, the center points of the bounding box or the center of the segmentation mask must still be inside of the image.

However, a state-of-the-art application of an image-based detection method has been used to detect the simulated moving landing platform and bring this position visual to the pilot's eyes on an HMD.

4.2 HMD Visual Augmentation Modes

Zimmermann et al. investigated in [161] HMD visual augmentation and landing zone concepts in flight operations using the ACT/FHS of the Deutsches Zentrum für Luft- und Raumfahrt e.V. (DLR). The SferiAssist® [59] combines tunnel in the sky symbology with dynamic path visualization. The HMD/PAS extends the benefits from these onshore operations to offshore procedures, even within DVE conditions. A detailed view of the capability of the HMD visual augmentation in low visibility conditions is given in Figure 4-3.



Figure 4-3: HMD view during approach (upper row) and landing (lower row)

The HMD visualization concept is subdivided in deck approach and landing visualization modes along standards of recent international VFR and IFR offshore procedures [1] [105] [140], combined with well-accepted onshore visual clutter concepts [97]. In the following, the HMD visual augmentation modes used for the helicopter ship approach and landing procedures are introduced in detail. The related advanced flight control modes chosen are TRC and ACVH. Detailed information about the advanced flight control modes can be found in chapter 4.3 and [50] [51] [52]. The following scene linked modes and types of HMD visual augmentation are designed along the corresponding phases of flight, see chapter 3.2:

- Mode 1: 3D outside scenery conformal visual augmentation for a safe and precise helicopter ship approach trajectory in DVE conditions.
- Mode 2: 3D visual augmentation for precise maneuvering and landing on the moving ship platform including a visualization of the relevant ship deck installations.
- Both modes are related to the ships position and its motions in all axes, superimposed with a synthetic horizon and 2D flight parameters.

HMD/PAS types:

- Within mode 1:
 - Type: SAS – Ship deck approach symbology displaying the ideal flight path via a glide slope trajectory towards the moving landing deck.
 - Type: ESAS – Enhanced ship deck approach symbology visualizing horizontal and vertical boundaries of an IFR procedure-based approach glide slope trace towards the moving landing deck.
 - Both types include a so called “ship flag” representing the ships landing deck position from a distant point of view.
- Within mode 2:
 - Type: SLS – Ship deck landing symbology visualizing the main deck obstructions superimposed to the rolling and heaving landing deck. Helicopter related height bars connected to the landing rectangle, represent the altitude and position of the approaching helicopter in relative to the landing deck.
 - Type: ESLS – Enhanced ship deck landing symbology offers the pilot besides all elements of the SLS an elevator bar, and a virtual space-stable line-up line symbology.

The visualization of mode 1 begins at the IAF. Next, mode 1 switches automatically to mode 2 at MAP. Mode 2 is projected on the HMD until landing. However, if the pilot needs to do a go-around, mode 1 is visualized automatically again, in case of a decision to a missed approach after the helicopter reached the MAP, to guarantee the pilot to find back to the IAF flying “eyes out of the cockpit”. Independent from modes and types of ship approach and landing symbology, main helicopter flight parameters are visualized constantly to the pilot flying to enable a constant “heads up” flying.

4.2.1 Head Up Flight Parameters

The 2D HMD symbology visualizes the main helicopter flight parameters separated into head-fixed and helicopter fixed symbology. While the head-fixed symbology visualizes the primary helicopter state information, the helicopter fixed symbology projects helicopters orientation. Head-up flight parameters are grouped in a “T-Arrangement”, as used in most head-down helicopter PFDs. The head-up flight parameters visualization has already been

successfully tested during onshore operations [120] [144], and therefore taken for offshore operations as well. Everything shown in black within the figures of this chapter conforms to the transparency on the HMD. The main parameters, as can be seen in Figure 4-4 and Figure 4-5, are as follows.

The head-fixed visualization, given in Figure 4-4, includes airspeed and a speed tape, ground speed, a vertical speed bar, barometric altitude and altitude tape, radar altitude, heading and rotating heading tape, and engine torque with limit indicators. The symbology follows the head of the pilot flying and is arranged to the top of the display to have a clear view during the approach and landing on the ship to reduce the occlusion of the important lower part of the display. Moreover, the heading tape rotates in alignment with the synthetic and the outside scenery horizon.

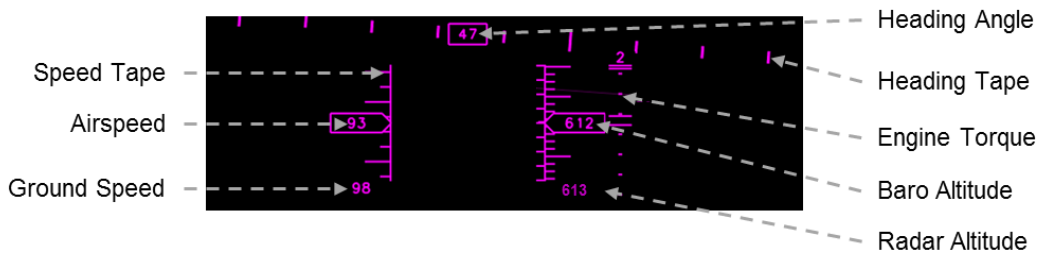


Figure 4-4: HMD Head Fixed Symbology

The helicopter fixed information, given in Figure 4-5, consists of the attitude indicator, symmetric pitch ladders, and an aircraft symbol. The helicopter fixed symbology is aligned to the longitudinal extension of the helicopter to decrease mental rotations and to increase visual conformity.

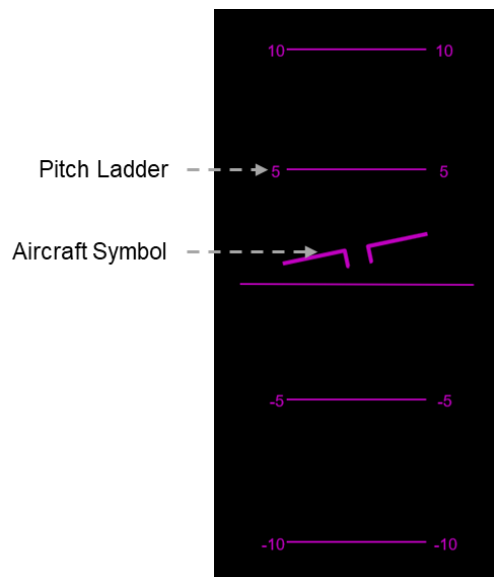


Figure 4-5: HMD Helicopter Fixed Symbology

The 2D primary flight display information is visualized to the pilot on the HMD at all stages of flight to ensure a constant “eyes out of the cockpit” flying during the ship approach until a safe landing on the moving deck.

4.2.2 Ship Approach Visual Guidance

The standard ship-controlled approach procedures [105] [140] have been used to isolate and visualize the ship approach sequence for a helicopter. The two available types of (E)SAS, both see Figure 4-6, can be visualized each during the ship deck approach task from IAF to MAP.

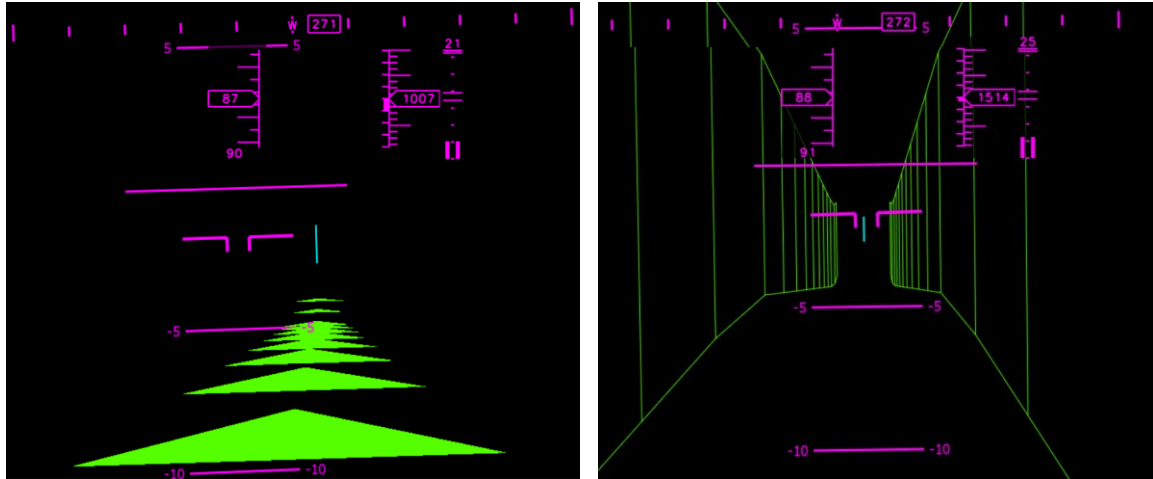


Figure 4-6: HMD SAS (left) and ESAS (right) as seen through HMD during approach

The ship following green colored arrows and the green colored garden fences approach guidance information both visualize the optimal glide path towards the moving ship and ship flag, colored in cyan. Therefore, the HMD visual ship approach guidance (AG) is dependent on the moving central landing point of the landing deck of the ship in lateral and longitudinal position, but independent from ship motions in roll and heave axis. The projection of the AG begins at the IAF and ends at the MAP. Pilots must decide before flight between the “arrows” (SAS) and the “garden fence” (ESAS) visualization type.

The arrows of the AG, see Figure 4-6 left image, have a width expansion of 10m and 600m in length each, visualizing a 1% fault tolerance in lateral axis of the ideal approach. The arrow “line”, representing the longitudinal visualization of the approach, is made up of the sum of arrows positioned with its tip heading towards, and on the optimal and precise approach path in longitudinal axis to the ship. Arrow’s “slide” is specified as the side view of the AG shows arrows positioned vertically on the minimum needed altitude for a safe approach.

The garden fence of the AG, see Figure 4-6 right image, is dimensioned each with 200m in height expansion visualizing the maximum and minimum needed altitude from the IAF down to the ship until MAP. The fences of the AG are positioned horizontally each 150m to the ideal flight path from the middle line. The garden fences upper and lower borders are positioned vertically on the maximum and minimum needed altitude for a safe approach. The symmetric vertical “gate” distance is specified by 600m regarding dividing the 12km (7NM) lasting approach. These dimensions in creating a vertical and horizontal corridor

allows the pilot to achieve a safe approach to the ship based on the IFR setup [105] [140] made visually with the HMD.

Apart from this, SAS and ESAS include a visualization of the general position of the ship, visualized by a moving cyan colored ship flag. In case, the ship flag is positioned visually in extension to the furthestmost tip of the green arrows, respectively in the middle of the two furthestmost vertical garden fence lines, the helicopter is mainly within the optimal flight direction during approach. However, only if the tip of the furthestmost arrow/ garden fence vertical lines, the cyan ship flag, and the magenta 2D helicopter fixed aircraft symbol are positioned in line, as can be seen in Figure 4-6 right image, the helicopter is on optimal flight track.

AG ship related visualization types, SAS as well as ESAS, enable the helicopter pilot a visual augmentation during approach which is independent from outside scenery conditions, such as DVEs. Hence, the pilot is always connected to the actual ship position and movement by a real-time visual augmentation, even during a missed approach, as can be seen in Figure 4-7.



Figure 4-7: In-flight HMD tunnel view after missed approach

In preparation for landing on the ship, the visual approach guidance switches automatically to the landing and obstacle awareness visual augmentation when the helicopter passes the MAP.

4.2.3 Precise Landing and Obstacle Awareness Information

The standard ship-controlled landing procedures [105] [140] and ADS-33 standards [2] have been also used to isolate and visualize the landing sequence for a helicopter as shown in Figure 3-6 from MAP until the final touch down on the moving landing deck. The two available types of (E)SLS, see Figure 4-8, visualize the ideal landing point on the moving

ship. The dynamic 3D visual augmentation types represent the restricted landing area of the moving ship deck, and ESLS offers on top further external synthetic visual cues by a space-stable symbology concept, for ship-independent precise maneuvering (sidestep and hover) of the helicopter, based on the ADS-33 precise hovering task layout [2]. In the final development phase of the HMD symbology concept, a helicopter test pilot of the WTD 61 (German Armed Forces, Technical Center for Aircraft and Aeronautical Equipment) evaluated the display concept and provided valuable feedback regarding improvements on the design of the SLS, and simulator flight test procedures of the experiment. The test pilot (age 41y) has a flight experience of 2,400 hours (h) as Pilot in Command (PIC) for rotorcraft systems and multiple type ratings for NH90, BELL UH-1D, and EC135 (including VFR and IFR). He has practical experience in flying with Night Vision Goggles (NVG, 400h), using HMDs either in real flight (NH90, 300h), or various HMD types in simulation (30h). Besides holding a test pilot license (TP 1), he reported to have encountered DVE conditions below 800 m while flying VFR over open sea.

Regarding SLS augmentation enhancement, he recommended to add a space-stable symbology set on the flight deck that displays the line-up line of the landing pad, see Figure 4-9. Therefore, a line-up line was added to the ESLS type in a dual-use concept according to ADS-33 PRF and HOSTAC standards: The magenta line-up line, as shown in Figure 4-9, is visible through the HMD during the final recovery as a space-stable hover symbology. This space-stable symbology has also been used successfully in onshore precision hover tasks in DVE conditions, see [144].

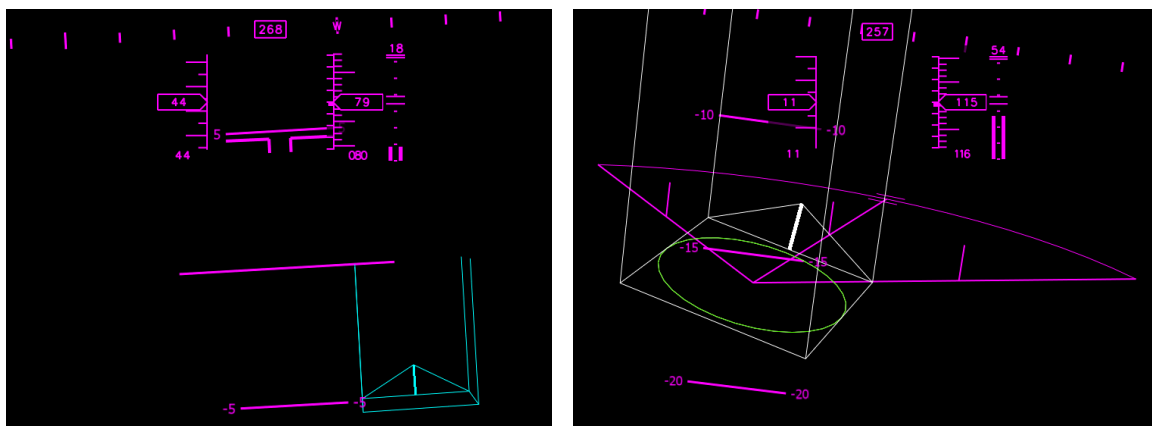


Figure 4-8: HMD SLS (left) and ESLS (right) as seen through HMD during landing

(E)SLS extend previous experimental works on visual cueing enhancements for DVE conditions and adapts the symbol concepts for shipboard launch and recovery missions.

The SLS and ESLS, as shown in Figure 4-9, are composed of four main elements:

1. A green precise landing circle connected via four height bars showing the altitude and position of the approaching helicopter relative to the landing deck.

2. A cyan (SLS) or white (ESLS) rectangle representing the landing deck and a cyan (SLS) or white (ESLS) triangle visualizing the front wall of the deck.
3. Two vertices of the triangle show the lower two corners of the front wall and the third vertex represents the midpoint of the front wall.
4. A cyan (SLS) or white (ESLS) elevator bar displaying the midpoint of the landing deck in lateral axis and the required final altitude of the helicopter relative to the deck.
5. The continuous displayed red prominent synthetic horizon, see Figure 4-7.

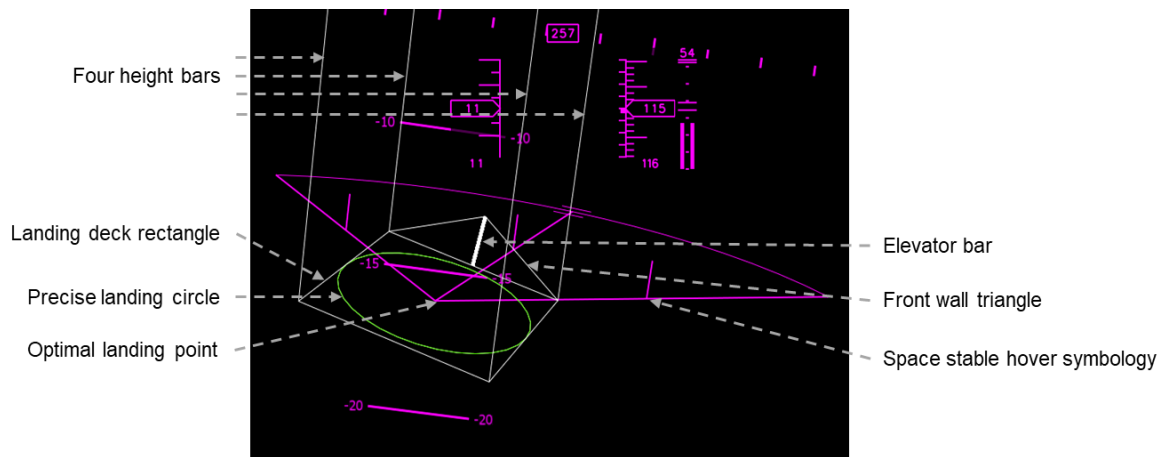


Figure 4-9: HMD entire moving landing symbology

Overall, the HMD visual augmentation is offered to the pilot flying during the helicopter ship approach and landing, or if necessary, after a missed approach. Besides head-up flying, the integration of a color and automatic clutter concept linked to the two respective stages of flight, approach, and final recovery, have been established.

4.2.4 Automatic Visual Clutter

The HMD synthetic visual cues were intended to overlay the actual outside environment. Therefore two clutter modes with a constant coloring setup were chosen to reflect this. Green color was chosen for the 3D approach guidance. Cyan color was taken for the landing deck dimensions. To assist the pilot while the approach and landing task with synthetic visual cues, the HMD includes two modes of 3D visual augmentation, one for ship approach trajectory and one for the final approach, changing automatically during flight when reaching designated points. On top, a 2D constant projection of important helicopter flight parameters and a continuous represented earth-referenced synthetic horizon may offer aspects of a safety line in the special case over open sea. Symbology elements were chosen to create salient and outside scenery related visual cues that help pilots to adapt to automatic control responses. In detail, such time varying, and constant-colored displays respond to skill-based behaviors under the skills-, rules, and knowledge –based behavior design as also

successfully used during onshore operations in DVE conditions. Hence, (E)SAS and (E)SLS were implemented as follows. All numbers here as in Figure 4-10:

- From (1) to (2): (E)SAS is projected. The helicopter enters the visual augmented IAF (first virtual green arrow or first virtual vertical front edges of the garden fence in green color) and proceeds the ship approach along the moving glide path (all in green color) until reaching the MAP, designated as the end of (E)SAS augmentation.
- At (2): Mode switches from (E)SAS to (E)SLS while the primary helicopter flight information (all in magenta color) and the synthetic horizon (horizontal red line) are still displayed.
- From (3) to (4): (E)SLS is projected. The helicopter passes the MAP and enters the final recovery phase towards the moving ship (all in cyan color). Here, the outside scenery conformal (E)SLS visual augmentation is displayed to the pilot on the HMD.

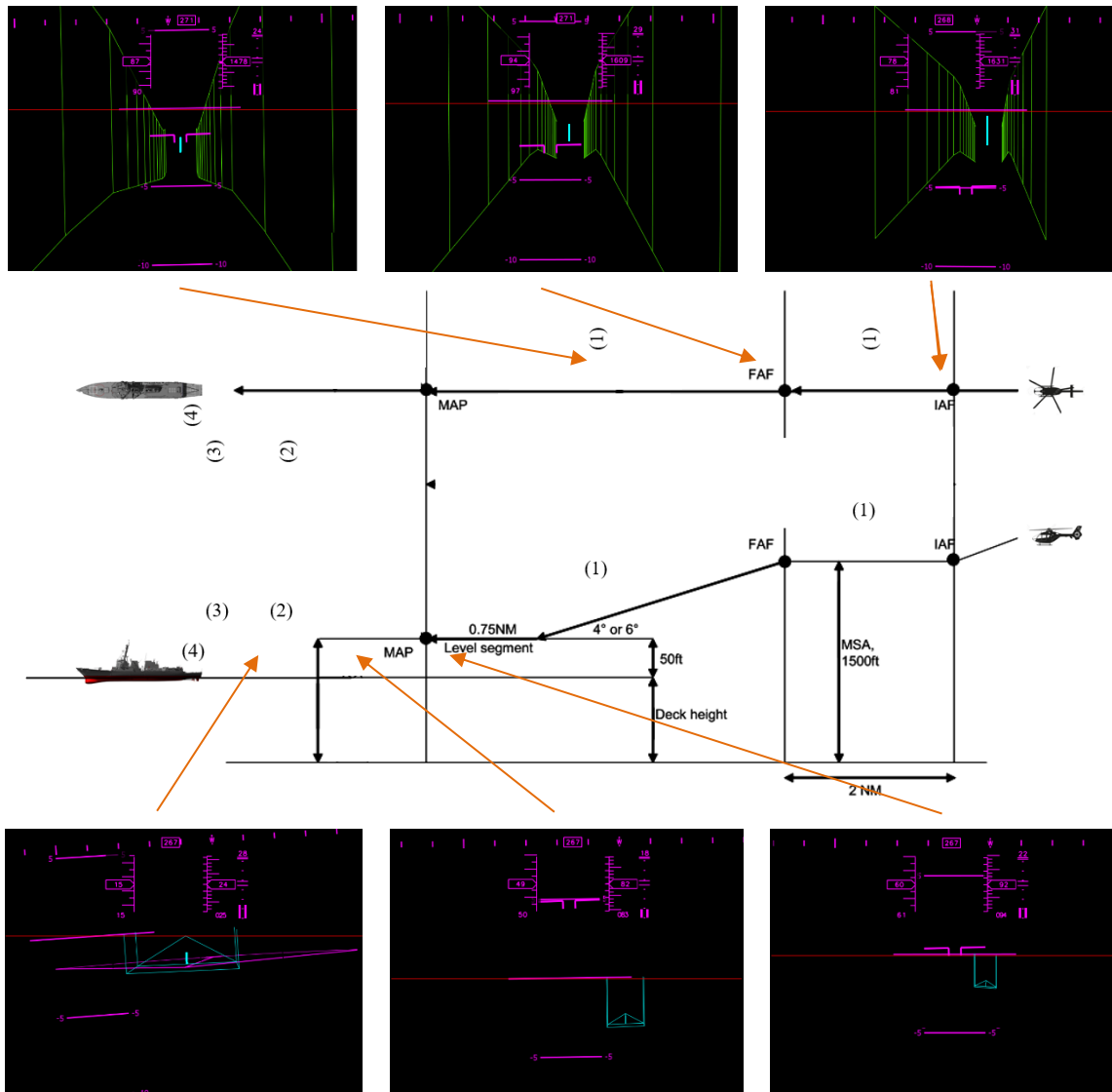


Figure 4-10: PAS ESAS (upper row) and ESLS (lower row) declutter modes

The dynamic and ship related symbology displayed during ship approach and landing includes chevrons indicating the approach towards the moving ship, a synthetic horizon,

and the moving rectangle showing the image-based detected heaving and rolling landing deck area [104]. Besides the visual augmentation, two advanced flight control modes are offered to the pilot during flight.

4.3 Control Augmentation Modes

Two advanced flight control modes are harmonized and evaluated in combination with the visual augmentation modes since these advanced flight control modes are available on modern maritime rotorcraft systems. In the following, two advanced flight control modes are given which are used besides conventional controls while operating the HMD/PAS. The cockpit setup includes the conventional pilot controls: a center stick, a collective lever, and foot pedals. The center stick includes a force trim system and allows the pilot to change the detent position using beep switches. The collective stick and pedals, however, do not include a force trim. Two advanced response-types are offered in flight: TRC and ACVH. For basic investigations, conventional mechanical controls (MECH) are used within simulated flights.

For the TRC response-type, the pilot commands on the cyclic inceptor are mapped onto the commanded translational rates in the local inertial reference frame. Thus, a longitudinal cyclic deflection yields a proportional forward velocity, and a lateral cyclic deflection yields a proportional lateral velocity. Cyclic detent holds the helicopter's current position.

For the ACVH response-type, the pilot commands on the cyclic inceptor are mapped onto the commanded translational accelerations in the local inertial reference frame. Thus, a longitudinal cyclic deflection yields a proportional forward acceleration, and a lateral cyclic yield a proportional lateral acceleration. Cyclic detent holds the helicopter's current velocities. The attitude command, attitude hold (ACAH) response-types for the pitch and roll attitudes are synthesized in the inner-loop for TRC and ACVH execution. Furthermore, the pilot's collective stick deflection yields a proportional inertial vertical speed. Collective detent holds altitude, and so this response is modeled as a rate command, height hold (RCHH) response-type. An overview is given in Figure 4-11.

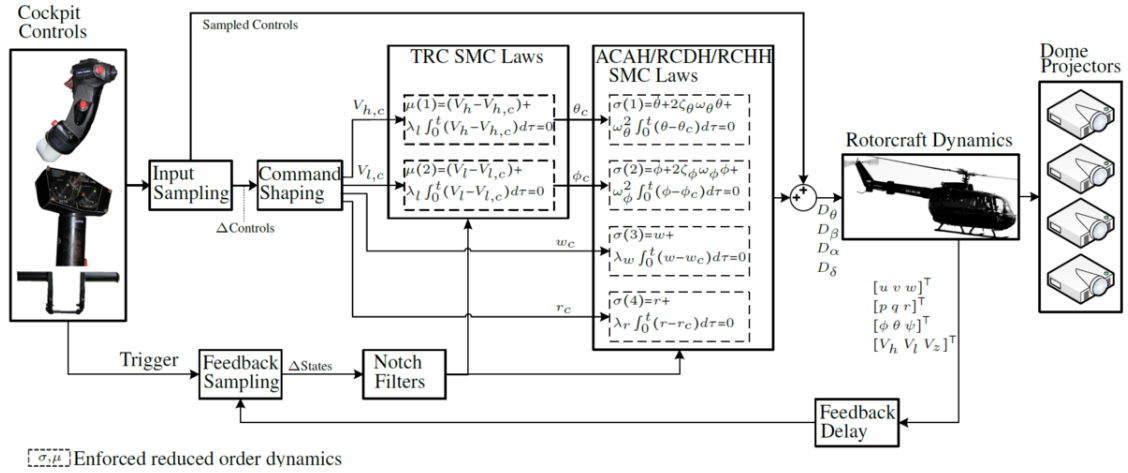


Figure 4-11: Closed-loop flight control and simulation setup

Lastly, the pilot's pedal deflection yields a proportional yaw rate. Pedal detent holds heading, and so this response is modeled as a rate command, direction hold (RCDH) response-type. To satisfy ideal, lower-order responses using ADS-33 criteria [1], ACAH is modeled as a second-order transfer function, and RCDH and RCHH are modeled as first-order transfer functions. Further details on the synthesis of robust control laws to satisfy the TRC and ACVH can be found in [51].

Towards transforming the piloting task into a task of precisely steering the helicopter during the landing phase, the response-types developed for the vertical and yawing motion are the well-known vertical rate command, height hold (RCHH), and yaw ratecraft command, direction hold (RCDH), respectively. The flight envelope of interest was restricted to the hover and low-speed flight regime (up to 25 m/s forward speed). The synthesis of these different response-types is described next.

First, the TRC response-type maps the pilot's cyclic inceptor command as a linear function of the horizontal translational rate command. From the cyclic stick detent position in hover, a longitudinal cyclic command ($D_{\beta,c}$) yields a proportional change in the forward velocity ($V_{h,c}$), whereas a lateral cyclic command ($D_{\alpha,c}$) yields a proportional change in the lateral velocity ($V_{l,c}$).

$$V_{h,c} = k_h \Delta D_{\beta,c} \quad (1)$$

$$V_{l,c} = k_l \Delta D_{\alpha,c} \quad (2)$$

where k_h and k_l are constant gains in the command model, and Δ denotes a change from the detent position. Returning the cyclic stick to the detent position commands zero translational rates ($V_{h,c} = 0, V_{l,c} = 0$), and the helicopter is expected to return to stable hover. Simplified helicopter translational equations of motion then yield the required pitch attitude change ($\Delta\theta = \theta_c - \theta_{trim}$) and the roll attitude change ($\Delta\phi = \phi_c - \phi_{trim}$) for the helicopter ground velocities (V_h, V_l) to track the commanded values.

$$\Delta\theta \approx (V_h - V_{h,c})/g \quad (3)$$

$$\Delta\phi \approx (V_l - V_{l,c})/g \quad (10)$$

Second, the ACVH response-type maps the pilot's cyclic inceptor command as a linear function of the horizontal translational acceleration command. From the cyclic stick detent position, a longitudinal cyclic command ($D_{\beta,c}$) yields a proportional change in the forward acceleration ($\dot{V}_{h,c}$), whereas a lateral cyclic command ($D_{\alpha,c}$) yields a proportional change in the lateral acceleration ($\dot{V}_{l,c}$):

$$\dot{V}_{h,c} = k_h D_{\beta,c} \quad (11)$$

$$\dot{V}_{l,c} = k_l D_{\alpha,c} \quad (12)$$

where the constant gains k_h and k_l are not necessarily identical to the values of the gains in the TRC response-type. As before, returning the cyclic stick to the detent position should command zero acceleration, and the helicopter is expected to hold the ground velocity value at the time of return to detent. The required pitch and roll attitude commands in this case are:

$$\Delta\theta \approx \dot{V}_h/g \quad (13)$$

$$\Delta\phi \approx \dot{V}_l/g \quad (14)$$

Third, the RCHH response-type maps the pilot's collective inceptor command ($D_{\theta,c}$) as a linear function of the inertial vertical speed command ($V_{z,c}$) as follows:

$$V_{z,c} = k_z \Delta D_{\theta,c} \quad (15)$$

where k_z is a constant gain. An inertial to body transformation yields the commanded normal speed (w_c) as:

$$w_c = \frac{u \sin \theta - v \sin \phi \cos \theta + V_{z,c}}{\cos \theta \cos \phi} \quad (16)$$

Finally, the RCDH response-type maps the pilot's pedal command ($D_{\delta,c}$) as a linear function of the body yaw rate (r_c) as follows:

$$r_c = k_r \Delta D_{\delta,c} \quad (17)$$

where k_r is a constant gain. It is noted that the input command shaping constants (k_h, k_l, k_w, k_r) were determined to offer a balance between precision and aggressiveness; smaller gains allow finer, precise maneuvering but require considerable control deflections for aggressive maneuvers. Initial piloted simulation with the experimental test pilot of the German Armed Forces allowed fine-tuning of these gains.

The aforementioned input-command-shaping functions collectively yield a command vector $\mathbf{r} \equiv [\phi_c \ \theta_c \ w_c \ r_c]^T$, which the helicopter output vector $\mathbf{y} \equiv [\phi \ \theta \ w \ r]^T$ is required to track robustly (i.e., in the presence of any modeling uncertainties). For the subsequent attitude and rate control design, the nonlinear helicopter dynamics model described previously is linearized about equally spaced airspeed intervals between hover and 25 m/s forward speed. The linearization process uses a built-in trim subroutine in the nonlinear

model. Numerical perturbations about the trim states then yield the following linear state-space form:

$$\dot{x} = Ax(t) + Bu(t) \tag{18}$$

$$y = Cx(t) \tag{19}$$

where $x \equiv [\phi \ \theta \ u \ v \ w \ p \ q \ r]^T$ and $u \equiv [D_\theta \ D_\alpha \ D_\beta \ D_\delta]^T$ are the state and control vectors, respectively, (u, v, w) represent the fuselage translational components in the body-frame, and (p, q, r) represent the fuselage angular rates in the body-frame. Further, A, B are matrices containing the stability and control derivatives, respectively, and C is the output matrix. Stability analysis of this linear state-space model shows that the phugoid mode is unstable, the Dutch roll mode is stable but has low damping with a variable period, and the high frequency rotor lead-lag mode has very low damping [108]. These flight characteristics make the piloting of the helicopter difficult. They also corroborate the findings of previous studies that highlight low HQ levels for precision maneuvering tasks [108].

The flight controller in this work employs the sliding mode control technique for generating the necessary actuator commands on the main and tail rotor blades for robust output tracking, such that $\lim_{t \rightarrow \infty} \|y - r\| = 0$. The subsequent steps in the sliding mode flight controller synthesis are identical to those described in Ref. [51], and are therefore omitted here for brevity. Reference [51] also discusses the level of agility, axial decoupling, and predicted HQ levels achievable by the sliding mode flight controller. The pilot controller in ROSIE is a conventional center stick for cyclic control, a collective lever, and foot pedals. For the TRC response-type, the pilot commands on the cyclic inceptor are mapped onto the commanded translational rates in the local inertial reference frame. Thus, a longitudinal cyclic deflection yields a proportional forward velocity, and a lateral cyclic deflection yields a proportional lateral velocity. Cyclic detent holds the helicopter's current position. Lastly, the pilot's pedal deflection yields a proportional yaw rate. Pedal detent holds heading, and so this response is modeled as a rate command, direction hold (RCDH) response-type. To satisfy ideal, lower-order responses using ADS-33 criteria, ACAH is modeled as a second-order transfer function, and RCDH and RCHH are modeled as first-order transfer functions. Table 4-1 summarizes the visual and control augmentation modes within the HMD/PAS. All modes can be operated in all combinations.

Visual augmentation modes	Control augmentation modes
Primary HDD	Primary FCS (MECH)
HMD + SAS & SLS	TRC/PH + RCDH + RCHH (TRC)
HMD + ESAS & ESLS	ACVH + RCDH + RCHH (ACVH)

Table 4-1: Available visual and control augmentation modes

5 Helicopter Shipboard Operations Environment

The challenges of the helicopter ship deck landing tasks arise among others from aspects of the helicopter ship interface, and the maritime environment. Recent studies [97] [125] focus on relation between ship air wake data, pilot workload and handling qualities. This work focuses on the pilot-in-the-loop by investigating the interaction between pilot workload, different motion intensity levels of the moving ship deck, and corresponding DVEs. The simulator flights of the helicopter ship deck operations were conducted at ROSIE [144].

Therefore, the HELIOP environment, as detailed in this chapter, takes four main elements into account: ROSIE, the simulated moving ship, the dynamic maritime environment, and the visual augmentation. Moreover, this chapter investigates in the characteristics of the open sea environment in ROSIE, ship implementation, visualization and motions, and a pilot fitted HMD visual augmentation for offshore operations during DVEs.

5.1 ROSIE Helicopter Ship Interface

ROSIE is a fixed-base rotorcraft simulator with a realistic cockpit and a high-fidelity visual system, see Figure 5-1. It utilizes a nonlinear flight model with the blade aerodynamic model based on blade element/momentum theory with an analytical downwash model and rigid blades. The flight model is defined to represent the H135, a twin-turbine, lightweight utility helicopter. Helicopter dynamics of the H135 models can be simulated using the software package GenSim hosted in a Matlab/Simulink framework [50] [52]. GenSim simulates aerodynamic effects of the main rotor, tail rotor, fuselage, vertical fin, and horizontal stabilizer. It uses a rigid blade assumption and simple analytical downwash models to simulate rotor dynamics up to the first harmonics of the flap, lead-lag, and torsion modes. More details about ROSIE and GenSim can be found in [142] [143].



Figure 5-1: Outside view of ROSIE during pilot-in-the-loop flight

First, main identified head-down instrumentations, see Figure 5-2, are modified to naval operations: The glass cockpit instrumentation offers two 15" touch screen displays. A PFD visualizes two-dimensional head-down instrumentation. Lower second digital touch display, see also Figure 5-4, visualizes a digital moving map (Sky-Map).



Figure 5-2: ROSIE HDD instrumentation modes

Both, PFD, and Sky Map are tailored to naval operations, based on ongoing research regarding HMI analysis of innovative landing aids [120] for rotorcraft in DVE, and taking existing instrumentations [20] into account. The PFD offers two modes to the pilot flying for naval operations. A PFD and an enhanced PFD mode. Basic helicopter parameters are displayed in both modes to the pilot in a similar way. Basic flight parameters include:

- Helicopter attitudes,
- Helicopter velocities and altitudes,
- Engines, battery, and fuel parameters,
- Cautions and warnings, and
- Compass rose.

Transferring the cockpit instrumentation from a real helicopter to the simulation environment, ROSIE PFD offers two modes for helicopter shipboard operations: First mode, named as PFD, includes the main helicopter instrumentation and basic flight parameters as described above. The second mode is specified as the enhanced PFD, which is namely the PFD extended by the following enhancements superimposed on the ADI: A drift indicator is added based on aeronautical standards [7] and ongoing research [86] for precise landing maneuvers on a moving platform: As given in Figure 5-3 left image, the helicopter CoG position (magenta) moves with 20kts GS forward. The speed component in the helicopter lateral axis is zero. Range between each circle (white) represents 10kts GS. Next, a helicopter ship longitudinal and lateral deviation indicator was added. The deviation indicator is based on the Course Deviation Indicator (CDI) instrument flight rules (IFR) instrumentation [7]. The deviation indicator (combined layout as seen in Figure 5-2) is separated in Figure 5-3 for description to axes. Figure 5-3 middle image: The ship is 90°

left in relation to the current heading of the helicopter (magenta), so flight direction must be corrected to the left. Range between two horizontal aligned small circles represents 45° deviations in lateral axis. Figure 5-3 right image: The helicopter is aligned to the ship in lateral positioning and the distance of the helicopter to the ship is around 9.8 NM. The range between two horizontal vertical aligned short lines represents 2NM in longitudinal axis.

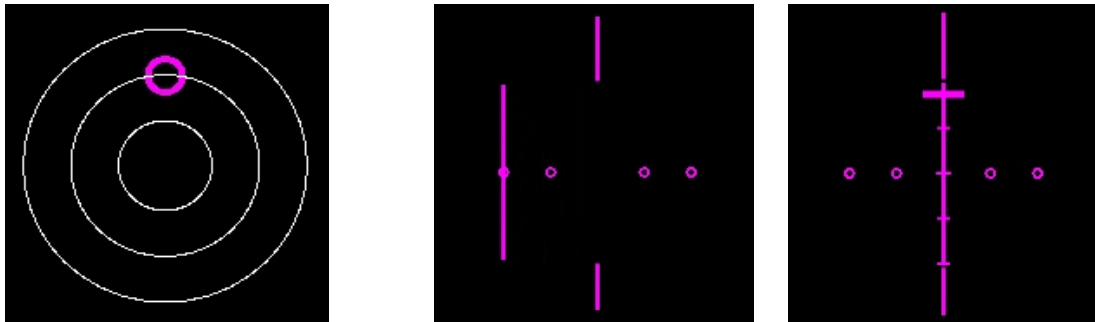


Figure 5-3: Drift indicator (left) and deviation indicator (right)

Finally, a sky map displays the actual flight path of the helicopter from gods' eye perspective. The visualization includes the expected path of the moving ship, given in Figure 5-4 (1), and the helicopter position and flight direction, see Figure 5-4 (2), all displayed on a standard aeronautical map.



Figure 5-4: Sky Map with ship alignment line, figure to scale

The head-down visualization concept is designed in harmonization with the head-up instrumentation. However, differences in layout and design arise besides HMI aspects [86], technical requirements [107] [120] such as pilot's eye point position, parallax error, and dynamic vergence correction to avoid binocular disparity [141]. All displayed parameters are taken from actual HMI primary flight instrumentation design [86], see also Figure 5-5.



Figure 5-5: H135 cockpit flight instrumentation during ship approach

The photo was taken during offshore flights of the author proceeded together with naval fleet pilots within a workshop at Wiking Helicopter at North Sea, Germany. More details about the workshop can be found in chapter 4.

5.2 Visualization of the Maritime Environment

The visualization of the dynamic maritime environment in ROSIE consists of a simulated and rendered ocean [137] scene, an adjustable 3D Gerstner waves model with convenient wave foam including a Fourier synthesis to the ocean [91], and a real-time animation and rendering of ocean whitecaps [31]. Main investigations and integration work of the maritime environment visualization in ROSIE are:

- (1) Animation of dynamic ocean waves and dispersion (frame rate higher than 30 f/sec).
The waves simulation is based on an ocean wave spectrum and improved Gerstner model [159], and includes a visualization of waves white caps. The Gerstner's wave model is defined as a two-dimensional nonlinear-periodic travelling wave at the surface of a flat element of infinite depth [58]. Fournier et al. [37] established the Gerstner wave model for ocean wave graphics as used within this work.
- (2) Building up a random ocean wave height field and rendering of 3D ocean waves white caps within the visual system of ROSIE [17].
- (3) Simulation of waves in 3D, non-periodic in line, and random in total of waves [22]. Adjustable 3D waves are harmonized with configurable waves, ship foam, and ships motions.
- (4) Visualization of a realistic ship sterns and wake's field angle [89] matched to integrated wave and ship model.

Regarding (1), the simulation of an ocean environment and global illumination look are like those of any other radiosity challenges. Although, the volumetric specification of environmental components, like the level of salinity and underwater streams, complicate a general implementation considerably [137]. Optimizations are integrated to improve the geometry of the sea surface, computing rate and Level of Detail (LoD) [17]. The ocean wave representation based on ocean wave algorithms is as follows:

- Gerstner waves approximation solution to the fluid dynamic equations of Fournier and Reeves [137].
- The physical model is detailed by the surface in terms of the motion of individual points on the surface itself. Regarding the approximation, all points with its coordinates $x_0 = (x_0, z_0)$ of the surface of the water pass a circular motion, as a wave passes by. Therefore, the height is defined as $y_0 = 0$. Then, as a single wave with amplitude A passes by, and the point on the surface is displayed at time t to

$$x = x_0 - \left(\frac{k}{k}\right) A \sin(k * x_0 - \omega t) \quad (4)$$

$$y = A \cos(k * x_0 - \omega t) \quad (5)$$

The vector k , named as the wave vector, is defined as a horizontal vector which points in the running direction of the waves. The magnitude k of the wave related to the length of the wave (λ) is calculated by

$$k = 2\pi/\lambda \quad (6) .$$

The frequency ω for a given wave number k is approximated by

$$\bar{\omega}(k) = \left[\frac{\omega(k)}{\omega_0} \right] \omega_0 \quad (7)$$

where $[[a]]$ describes the integer part of the value of a , and $\omega(k)$ is defined as dispersion. The frequencies $\bar{\omega}(k)$ are a quantization of the dispersion surface. Turning from (1) to (2), building a random ocean wave field and rendering it in ROSIE mainly offers following challenges:

- Implementation of Gaussian random numbers of waves with a spatial spectrum of a prescribed foam.
- Realization of waves with a sufficient height may break at the top, generating a new set of physical phenomena in foam, splash, bubbles, and spray [137].

Figure 5-6 gives an example of rendering several waves with low (left), reasonably average (middle), and high (right) number of waves.

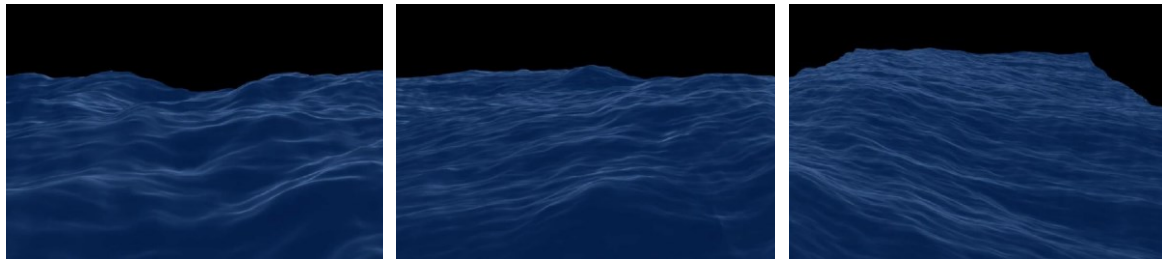


Figure 5-6: Low (left), medium (middle), high (right) numbers of waves [137]

Figure 5-7 visualizes an optimized simulated wave surface without (upper image) and strong (lower image) choppy algorithms, as integrated within the maritime environment.

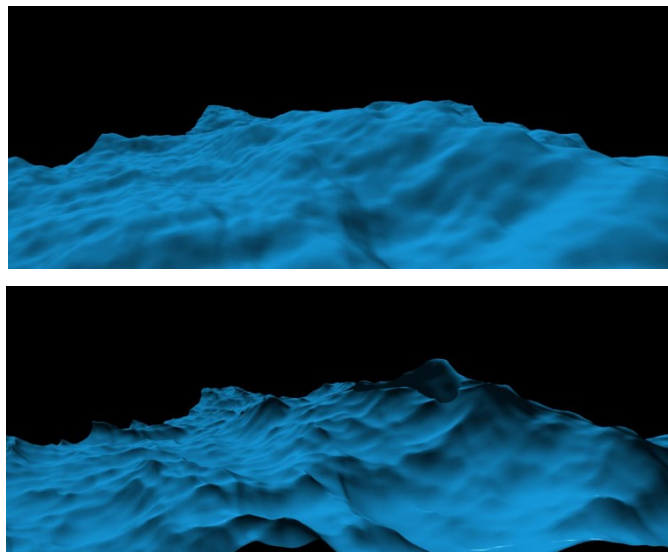


Figure 5-7: Simulated wave surface without (top) and strong (down) chops [137]

Details about the mathematical design of the used Fourier domain, amplitudes of a wave height field, and creating choppy looking waves can be found in [91] and [137].

Focusing on (3), a scalable method to animate and render ocean scenes with whitecaps is integrated to ROSIE as follows: The Tessendorf method [137] is implemented in C++ using OpenGL, which runs on all 6 IGs of ROSIE. At first, evaluations of equations of the wave and white cap model, see [31], as well as the discrete generation and storage of the whitecap model are calculated and stored in 2D textures with mipmaps. Next, the projected grid in a vertex shader is rendered and equations of the surface are run in a fragment shader [69]. The 3D graphics of ROSIE maritime simulator's visual system is based on OpenSceneGraph (OSG). OSG uses a tree-structure to manage the data. Therefore, the sea surface is connected to the scene tree as a geode, and the surface geometries are linked to the geode. According to three ship motion levels as detailed in chapter 5.4, following ocean waves scale is implemented for the helicopter shipboard operation simulations, see Table 5-1 and corresponding Figure 5-8. The sea states in the maritime environment are defined along the World Meteorological Organization (WMO) sea state code, as used as in recent studies [66] [145] [158].

WMO Waves Description	Wave Height and Characteristics	SCONE Levels within ROSIE	SCONE Original Ship Levels
Slight	0.0 to 0.5m, Smooth (wavelets)	1	Low
Moderate	0.5 to 4.0 m, Slight to moderate	2	Moderate
Rough	4.0 to 6.0m Rough to very rough	3	High

Table 5-1: Ocean waves scaling within ROSIE



Figure 5-8: Animated waves in low (left), moderate (middle), high (right) sea states [17]

Looking finally at (4), to harmonize ocean and ship visualization for pilot’s perception and visual cues, a corresponding ship bow, and stern wake [47] are implemented. In Figure 5-9, L represents ship’s length and B ships width.

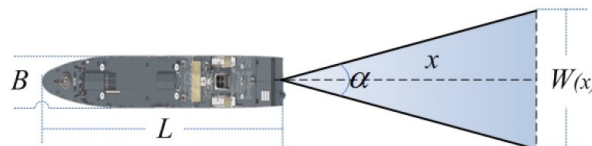


Figure 5-9: Schematic diagram of stern wake’s field angle [89]

The width $W(x)$ is the wake width x meters from the stern. $W(x)$ is calculated by

$$W(x) = \frac{4B}{(4L)^{1/5}} x^{1/5} \tag{8}$$

The design of the ship’s bow and stern wake is as follows: The particle’s initial position is $(0, 0, H)$ where H is the height of stern wave. The particle’ initial velocity v_1 is calculated according to the ship speed from SCONE and wakes’ angle, see (9).

$$\left. \begin{aligned} v_{1x} &= -S * \sin \left(\text{rand} \left(0, \frac{\alpha}{2} \right) \right) \\ v_{1y} &= -S * \cos \left(\text{rand} \left(0, \frac{\alpha}{2} \right) \right) \\ v_{1z} &= -(\text{rand}(0,1) * v_{1x}) \end{aligned} \right\} \tag{9}$$

As in (2), $(\text{rand} \left(0, \frac{\alpha}{2} \right))$ is a random emitting angle from range of 0 to $\frac{\alpha}{2}$. An example of the integrated simulated open sea within the HELIOP environment is given in Figure 5-10 for

low level flight conditions (left image), and of the ship wake (right image) during high altitude flight conditions.

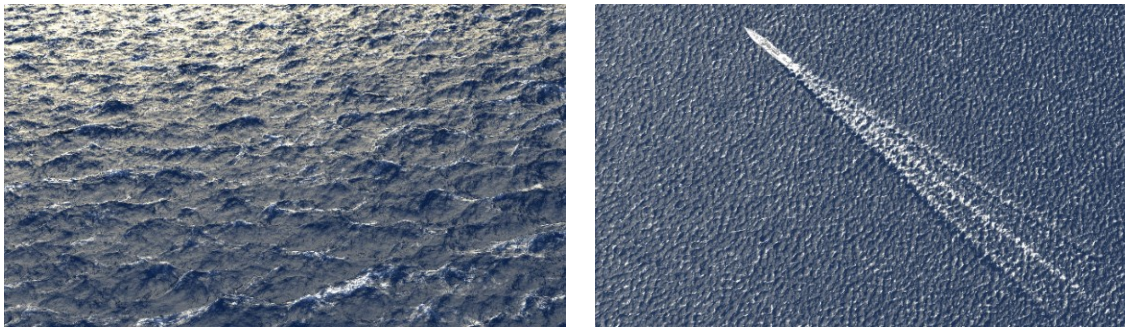


Figure 5-10: Simulated open sea environment (left) and ship wake (right)

In sum, the integrated dynamic 3D ocean surface uses the height map of a discrete point grid. The ocean surface is based on the calculation of a Fast Fourier Transformation (FFT) and an improved Gerstner waves model enhanced by a high LoD, 3D wave chops added to the waves animation to enhance the authenticity, and a highly synchronized projection between all six beamers. An example of a cockpit view of proceeded simulator flight tests is given in Figure 5-11.



Figure 5-11: Cockpit view - Ship operating in low (left) and high (right) sea states

Finally, the method uses as much power as available from the Central Processing Units (CPUs) of the Image Generators (IGs) of ROSIE to optimize the speed and efficiency of the simulation.

5.3 Simulation of a Dynamic Generic Combatant Ship

Sea swell leads to movement of the ship about its degree of freedom in pitch, roll, and heave, causing the landing spot on the rear side of the ship deck to move. To achieve a highly realistic environment for helicopter shipboard operations, a generic ship model including the realistic movement data from SCONE is integrated into ROSIE. The database is provided for the simulated deck motions using a state-of-the-art, non-linear seakeeping prediction code (LAMP). The dataset includes a full, consistent set of six degrees of freedom ship deck motion data for a generic surface combatant ship, DTMB Model 5415 hull, which is a representative of a DDG-90-type destroyer as shown in Figure 5-12. The SCONE

database itself has already been used in the academic research to the topics of the ship approach and landing with deck motion prediction, see [67] and [160].

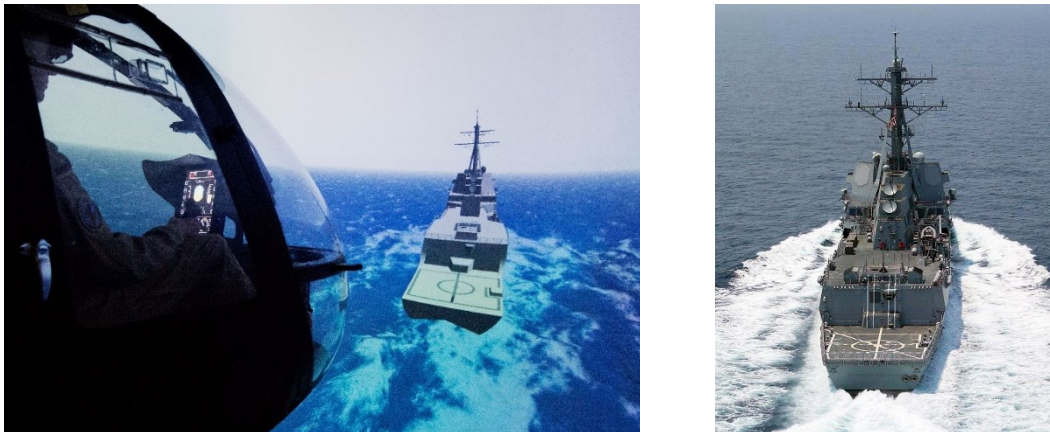


Figure 5-12: DDG-90 ship deck in ROSIE (left) and in real environment (right) [1]

To apply the ship simulation at different locations on the earth else than where the SCONE data was recorded, a calculation of the transformation from local space to world space is needed. Since the movement in the world space is based on the earth model, it must be calculated from coordinates in the local space to latitude, longitude, and height on the earth, followed to the position in the world space as shown in Figure 5-13. The angular velocities in roll (roll rate in °/sec), pitch (pitch rate in °/sec) and yaw motions (yaw rate in °/sec) are used to rotate the ship in the local space.

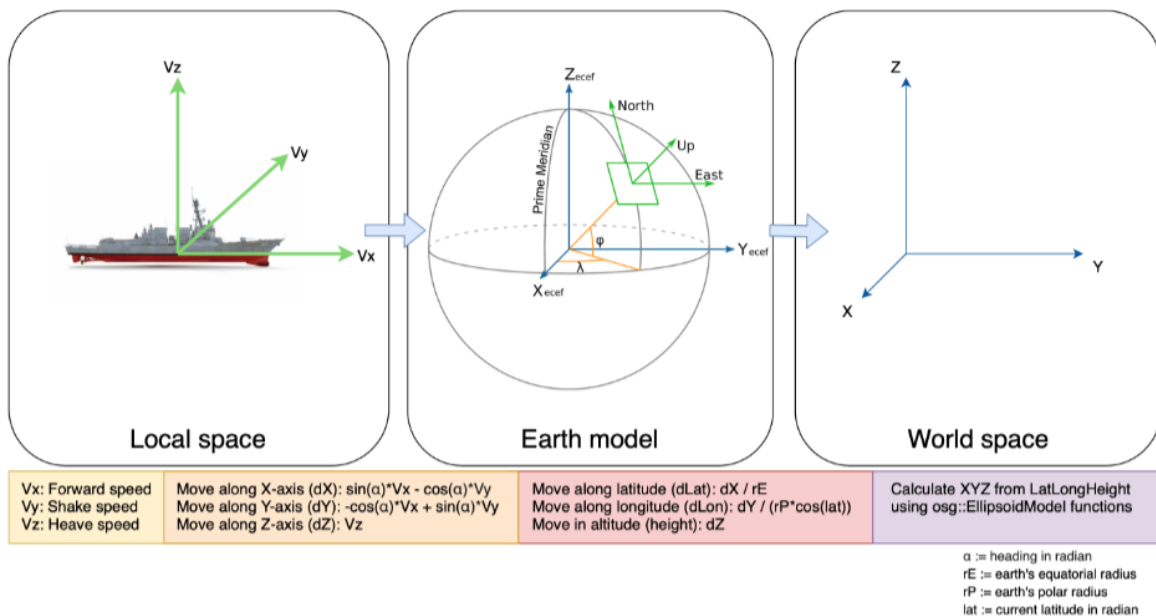


Figure 5-13: Calculation of translations from local to world space coordinates

The velocity along the x-axis, the delta translation in x in a timeunit, represents the speed on the course in the heading direction. The speed along the y-axis, V_y , and along the z-axis, V_z , represent the roll and heave speeds along the y- and z-axes. At first, V_x is rotated towards the given heading direction. Second, V_x and V_y (rad/sec) are computed and added

to the latitude and longitude position of the last time step of the data to get the current latitude and longitude position on the surface of the earth model. Finally, the embedded visualization software of ROSIE, in detail OSG, computes the transformation matrix into the world space coordinates in latitude, longitude and altitude. Thus, the ship is located and animated by the SCONE dataset in the high-fidelity maritime environment for pilot-in-the-loop simulator tests, as can be seen in Figure 5-14.



Figure 5-14: ROSIE cockpit view (right) during ship approach

5.4 Ship Motion based Data for Pilot-in-the-Loop Simulations

The configuration of the visualized ship motions by SCONE-related data [98] from the Office of Naval Research (ONR) allow to operate the ship with no, varying, or a constant ship speed. Additionally, ship motions in the three different SCONE levels of roll and heave intensities can be simulated. SCONE offers a wide range of recorded data from a U.S. Navy destroyer operating in open sea. The individual configuration of the visualized dynamic ship with the SCONE-related motions allows the ship to be operated within a constant or non-varying speed. Velocity and motions in roll and heave can be executed together or separately from each other.

First, regarding the ship speed, the original recorded speed of SCONE data is simulated which is constantly varying around 20 kts (Mean 20,5 kts, SD= 0,56 kts) over all recorded data, and as used in similar research [97]. The propeller of the ship is operated at a constant rotation rate corresponding to a calm water speed, so the basic simulation includes an unsteady variation in speed. However, if needed, other constant and varying speeds can be commanded to the ship.

Second, focusing on the ship motions, all recordings within the SCONE database contain a set of data that describe the different ship deck motions with respect to the roll and heave intensities of the ship. These intensities are described as “low” (level 1), “moderate” (level

2), and “high” (level 3) conditions. For each condition, five simulations were recorded and can be executed with differing, random wave phases. Thus, there are five 30-minute time histories for each deck motion condition. Overall, each file contains five subsets of data with a 20 Hz sampling rate. The LAMP predictions are time-domain simulations that incorporate a nonlinear calculation of the incident wave forcing and hydrostatic restoring, a body-linear 3D potential flow solution of the wave-body hydrodynamic interaction forces (radiation, diffraction, and forward speed), and semi-empirical models for viscous roll damping and drag, appendage (rudder and bilge keel) lift and drag, propeller thrust and hull maneuvering forces. The variation is small for the selected conditions, as detailed below.

Overall, the ship can be operated at the three different levels of roll and or heave intensity levels as seen in an excerpt of the recordings in Figure 5-15. Therefore, Figure 5-15 shows a typical time span for a helicopter shipboard approach. The helicopter landing spot is located 130 m longitudinally aft of the ship’s forward perpendicular (FP), on the ship lateral centerline and 5,0 m above the waterline.

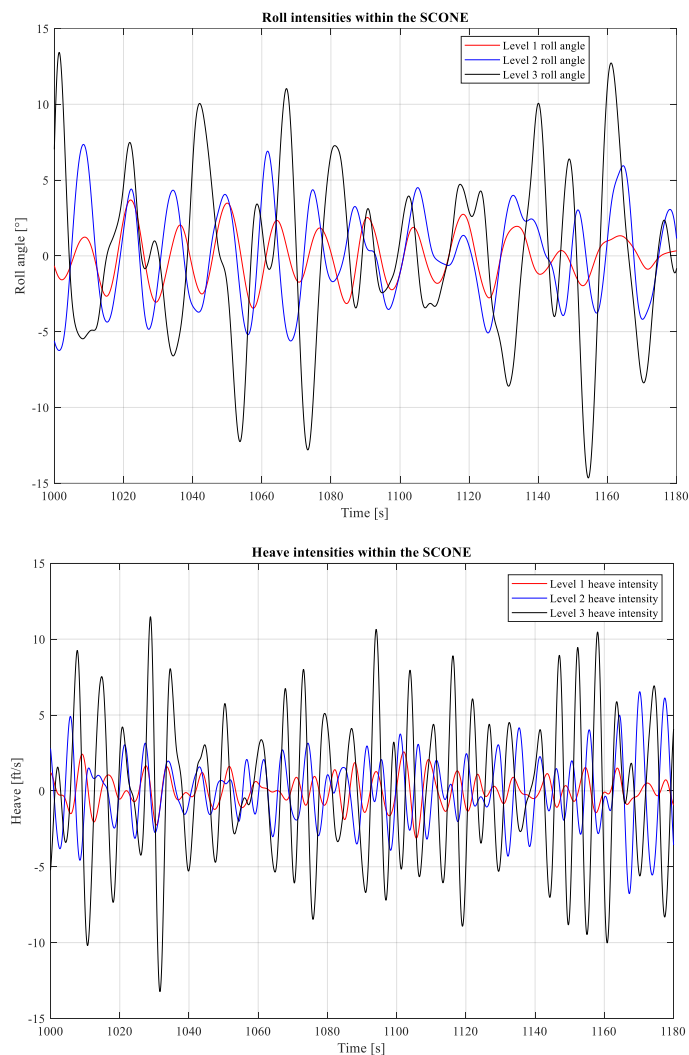


Figure 5-15: Roll (upper) and heave (lower) intensity levels within SCONE

The repeatable motion configurations offer investigations related to specific levels and ship motions. Moreover, the SCONE data sets include two more aspects regarding investigations and the experiment design: Comparison of motion levels related to its heave and roll characteristics, and linearity of all 3 motions levels. Table 5-2 shows the characteristics of the motion levels of the ship in roll and heave axes with increasing values from level 1 (all values in red color), over level 2 (blue), up to level 3 (black). As can be seen in Table 5-2, the roll attitude of the ship is balanced between the rolling motion to the left and right side from the perspective of the flying helicopter behind the deck. The heave levels of the ship between the heave up and heave down are counterbalanced as well.

Ship Motions	SCONE Levels	Mean Values	Maximum Values
Roll left	1	1.95°	7.99°
Roll right	1	- 1.85°	- 7.35°
Roll left	2	4.06°	17.53°
Roll right	2	- 3.90°	- 18.09°
Roll left	3	5.31°	23.74°
Roll right	3	- 5.48°	- 26.92°
Heave up	1	0.98 ft/sec	5.35 ft/sec
Heave down	1	- 0.98 ft/sec	- 5.96 ft/sec
Heave up	2	1.95 ft/sec	11.71 ft/sec
Heave down	2	- 1.91 ft/sec	- 10.83 ft/sec
Heave up	3	3.64 ft/sec	19.18 ft/sec
Heave down	3	- 3.65 ft/sec	- 16.67 ft/sec

Table 5-2: SCONE roll and heave levels

The linearity of the three ship motions mean maxima in total is given in Figure 5-16. The data includes mean roll angles of the different levels which ranges from level 1 with mean overall value 1.9° to level 2 with 3.98°, up to level 3 of 5.39° taking all SCONE recordings into account.

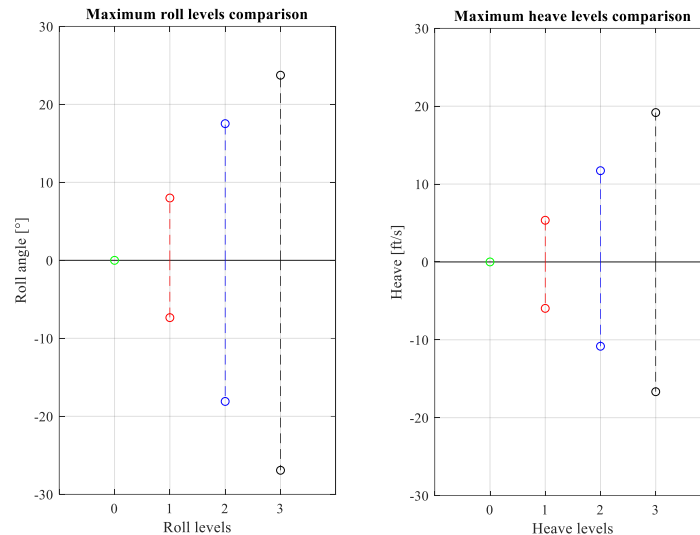


Figure 5-16: SCONE mean maxima roll and heave level values

The mean values in roll angles range from level 1 with 2.92° (SD 1.64°) and -2.78° (SD 1.51°) to level 2 with 5.85° (SD 3.59°) and -5.61° (SD 3.51°), up to level 3 with 7.21° (SD 5.15°) and -7.43° (SD 5.34°). At the same time, mean heave motion levels range from level 1 with 0.56 m/sec (SD 0.27 m/sec) and -0.56 m/sec (SD 0.27 m/sec), to level 2 with 0.84 m/sec (SD 0.56 m/sec) and -0.85 m/sec (SD 0.53 m/sec), and level 3 with 1.63 m/sec (SD 1.02 m/sec) and -1.58 m/sec (SD 0.99 m/sec) taking all recorded SCONE data sets into account.

5.5 HMD Visual Augmentation in DVE

An HMD with see-through capabilities is used for visual augmentation within this work. The visual augmentation is given by a 3D conformal cueing symbology for assisting helicopter pilots during ground-reference [131] operations in DVEs [102] while approaching and landing the helicopter on a moving ship. Hence, this chapter outlines the HMD used within the helicopter shipboard operations in DVEs. Further details about the information displayed on the HMD is given in chapter 4.

A low-cost HMD LCD-29 from Trivisio is taken for visual augmentation, as can be seen in Figure 5-17. The HMD offers a binocular stereoscopic vision with modified combiners (30% reflection and 70% transmission) for a better see-through capability in the simulation environment with limited brightness. A complete description of the basic HMD and its integration is given in [144].



Figure 5-17: Side view of pilot using see-through HMD (left) and close-up (right)

A main benefit of the HMD compared to the head-down instrumentation is the continuous unobstructed view on the outside scenery while having essential helicopter parameters and flight information in sight [28] at the same time. Second main benefit in comparison to other HMDs is that the LCD29 guarantees a stereoscopic fully colored visualization by two separate DVI inputs for two different images. Table 5-3 details the HMDs FoV and resolution.

	Horizontal resolution (pixel)	Vertical resolution (pixel)	Horizontal FoV (degree)	Vertical FoV (degree)	Horizontal resolution (arcmin/pixel)	Vertical resolution (arcmin/pixel)
HMD (Each eye)	800	600	23	17	1.725	1.700

Table 5-3: Resolution and FoV of HMD LCD29

The integrated six degree-of-freedom (DOF) Intersende-IS900 hybrid inertial-ultrasonic head-tracking system does not interfere with any electromagnetic and metallic components of the helicopter simulator. Position measurement culminates in an update rate of 180Hz. Latency is further reduced by inbuilt filters. Accuracy is maintained of 2.0 - 3.0mm translational with a resolution of 0.75mm and an accuracy of 0.25° in pitch and roll as well as 0.5° in yaw with a resolution of 0.05°. However, the drawback of this low-cost system is the limited FoV of 23° x 17° per eye. 2D and 3D-conformal information are displayed on the HMD to visualize a flight guidance information, as well as the main helicopter parameters. For the phases of ship approach and landing in DVE conditions [4], an approach and landing symbology is displayed to the pilot's eyes. Figure 5-18 gives an example of the HMD landing symbology as seen through the HMD during a degraded visibility range of 800m at MAP (left image) and entering final landing procedure behind the ship deck (right image).



Figure 5-18: HMD symbology as seen from MAP (left) and behind the deck (right)

Table 5-4 gives an overview of the IFR categories [4] (CAT) used within the pilot-in-the-loop simulations of this work. [144]

Category (CAT)	Decision Height (DH)	Runway Visual Range (RVR) requirement	Visibility Limits used within ROSIE
CAT I	Not less than 200ft	Not less than 550m or ground visibility not less than 800m	800m
CAT II	Less than 200ft but not less than 100ft	Not less than 350m	400m
CAT III	Less than 100ft or no DH	Not less than 200m or none	200m

Table 5-4: IFR categories and visibility limits within ROSIE

To enable and evaluate the HMD/PAS, the main contributions of this work were as follows:

- Design and integration of visual and control augmentation modes projected on a modified HMD to the pilots' eyes.
- Adaption of enhanced advanced flight control modes for low-speed operations in the vicinity of ship landing platforms.
- Integration of a generic combat ship model and its capability for 6DOF motions close to the reality.
- Embedded to a highly realistic and dynamic new maritime simulation environment.

6 Experimental Setup for Simulated Flights

The simulator flight tests of this work took place at the Rotorcraft Simulation Environment ROSIE. The chapter summarizes the setup of conducted simulator flight test campaigns. Proceedings, subjective ratings, and measurements are introduced along ADS-33 PRF [1] flight test standards. Finally, detailed descriptions of offshore training and operational MTEs and flights [105] [126] are endorsed along simulated environmental conditions.

6.1 Flight Test Campaign Environment

The simulator campaigns focused on the assessment of subjective workload and handling qualities using different modes of the HMD/PAS in training and during operational flights. In the following, main concerned systems are introduced and given valuable feedback from participating pilots.

6.1.1 Test System

Flight training and operating of the helicopter during shipboard maneuvers took place in two environments. Environment 1, named as “Tegernsee” was established for training. Environment 1 includes standard ADS-33 elements such as for the hover task, the sidestep scenario, and short free flights within a realistic and highly detailed outside scenery of the Tegernsee lake and surrounding environment. Environment 2, named as “North Sea” includes a projection of the sea environment and the moving ship with detailed superstructures. Figure 6-1 shows cockpit views during hover tasks in DVE conditions in both environments.



Figure 6-1: Simulation environments Tegernsee (left) and North Sea (right)

Light and weather conditions could be manipulated in both scenarios in the same manner: Visibility ranges were set to different IFR categories, as well as projecting all kinds and types of cloud layers. Sea states and ship motions were put to WMO sea states and/or SCONE datasets.

6.1.2 Test Setup

For this experiment, the in-flight validated dynamics model of a H135 [71] is simulated. Moreover, characteristics of helicopter phenomena, e.g., ground effect over deck, pitch response at higher velocities are used. Coupling of ship air wake and rotor dynamics are not simulated. Previous experiments within this test setup using a DLR turbulence model showed unintuitive effects caused by missing 6DOF motions within the simulator. However, focus of this investigation is a pilot-in-the-loop evaluation of a visual and control augmentation concept, less the dynamic effects of rotor – ship wake coupling [66]. More details about ROSIE and its systems architecture can be found in chapter 5.1, [141] and [143]. For the simulator flight test campaigns, following experiment setup was chosen for all flights:

1. Outside scenery visualization: The six-channel dome projection offers a FoV of 200° (horizontal) and $-50^\circ/+30^\circ$ (vertically). With a focus on visualizing approach, hover, and landing scenarios even within limited visual ranges and high ship motions, FoV downwards is especially important. All six projectors have a resolution of 1920×1200 pixels providing a resolution of three minutes per arc per pixel. Projectors are auto calibrated to ensure a homogenous image. Projectors communicate and synchronize using network communication via Common Image Generator Interface (CIGI).
2. Cockpit configuration: The original Bo105 helicopter frame is positioned within the outside scenery visualization dome. The Bo105 cockpit is used to simulate the category of scout and attack helicopters as specified within the ADS-33 PRF [1] standard during proceeded flight trails and evaluations. This configuration fits very well to operated helicopter categories such as for near-ship procedures [105] [126]. The standard analog instruments have been replaced by a generic glass cockpit configuration. HDD instrumentation is implemented by “2indicate”, a tool developed by the DLR.
3. Pilot seat shaker: It was found [155] that although motion cueing could cause differences in the pilot’s workload ratings, it had no discernible regular trend in the relative GVE. However, in the severely DVEs, the motion cueing effect was more significant. The pilot’s workload ratings and control activities on control sticks and pedal were normally higher without motion cues. To provide valuable feedback about the control augmentation and the load factor by simulating the vibrations caused by the main rotor, a seat shaker is installed on the rear side of the experimental pilots’ seat. Even without having a 6DOF platform, the produced oscillations from 5Hz to 200Hz matched very well to simulate the vibrations induced by the main rotor harmonics with an amplitude depending on the load factor.

4. Pilot controls: The original Bo105 flight controls, namely cyclic with trim function, collective, and pedals were used during flights. Mechanic artificial force feedback and cyclic trim actuators ensured a realistic control feeling. The basic beep-trim functionality with a four-way switch has been extended by a follow-up trim function, in which the actuators are automatically driven to the current cyclic stick position to lower forces on pilot's right hand and to reach a trimmed position during flight. The collective lever offers a friction brake, which also can be positioned to an individual stable position by the pilot lowering forces on pilots' left hand.

Figure 6-2 gives a detailed view of the cockpit configuration during simulated flights with the pilot wearing the HMD, seats shaker installed to the pilot's seat, and pilot control instruments.



Figure 6-2: Test setup cockpit configuration during experiments

5. HDD and HMD visualization: A standard state-of-the-art HDD approach was used during flights subdivided into a PFD, and a digital moving map visualized on a separate MFD below the PFD. While the PFD visualized H135 PFD information, the digital moving map showed helicopters position on a typical aeronautical map (Scale 1:100.000). Figure 6-3 visualizes a detailed view on the HDD display configuration, PFD (left image) and moving map (right image) during simulated flights.



Figure 6-3: Test setup display configuration during experiments

The HMD itself and the HMD/PAS concept, as detailed in chapter 4.2 and chapter 5.5, are aimed to make classical HDD instrumentation obsolete and instead offering pilots unobscured view on the flight path and the landing deck

6. DVE condition settings: For the simulated flights DVE condition “degraded visual range” was chosen [97] [104]. Therefore, standard IFR categories [4] were used to define values for the helicopter shipboard approach and landing scenarios. The three decreasing visibility ranges were 800m, 400m, and 200m to all directions from the helicopters CoG. Table 6-1 states described test setup values.

Category (CAT)	Visibility Limits
CAT I	800m
CAT II	400m
CAT III	200m

Table 6-1: Visibility limits during experiments

7. Ship motions settings: The visualization of the generic combatant ship and its 6DOF motions were used to investigate in aspects of a moving landing platform during approach and landing scenarios. The two ship configuration settings chosen were SCONE Level 1 (low) and Level 3 (high) with related ship constant speeds of 20kts to 23kts and a constant heading of 270°. Table 6-2 details the test setup values of the ship.

Ship Motions	Ship Motion Limits (SCONE Level)	Mean Values	Maximum Values
Roll left	1	1.95°	7.99°
Roll right	1	- 1.85°	- 7.35°
Heave up	1	0.98 ft/sec	5.35 ft/sec
Heave down	1	- 0.98 ft/sec	- 5.96 ft/sec
Roll left	3	5.31°	23.74°
Roll right	3	- 5.48°	- 26.92°
Heave up	3	3.64 ft/sec	19.18 ft/sec
Heave down	3	- 3.65 ft/sec	- 16.67 ft/sec

Table 6-2: Ship motions during experiments

6.1.3 Simulation Fidelity

In addition to the experiments, the simulation environment was evaluated by participating pilots. The goal is to evaluate how realistic the simulation environment is represented to all participating test pilots with regards to the human-in-the-loop experiments and investigations. The data are collected because the fidelity of helicopter flight simulators and training devices [5] plays an important role towards the realistic presentation of the outside scenery including the ship and the inside of the cockpit. The rating was based on a four-point Likert scale (1: Agree, 2: Rather agree, 3: Rather disagree, 4: Disagree). The questionnaires began with questions on the maritime environment, followed by the evaluation of the projected ship model, and the cockpit environment. All tables within this chapter show the subjective rating results with mean values and standard deviations. Corresponding similar results with median, minimal, and maximal values are given in [53] and [95].

Table 6-3 shows pilots' evaluations on the LoD of the visual presentation of the outside scenery and the ship itself, when finally flying very close to the sea surface and the shipboard. All pilots agreed that the maritime environment is visualized in a realistic manner. Even the synchronization of the dynamic waves projected to the six beamers was accepted well by all pilots. When it comes to flying close to the ship, ship motions were experienced as highly realistic. However, ship motion in heave axes when flying remarkably close to it, was observed by some pilots not perfectly as a fluent motion. Finally, the visualization and the LoD of the open sea was accepted well by all pilots. Here, waves were rendered in the HELIOP environment with a grid size of 7 x 7m, coming very close to real waves cluster.

Questionnaire item	
6.7	The level of detail of the waves model has almost no negative influences on fulfilling all MTEs. (Mean 1.0, SD 0.0)
6.6	The visual presentation of the waves model has almost no negative influences on fulfilling all MTEs. (Mean 1.0, SD 0.0)
6.5	The visual presentation of the maritime environment including waves and weather model enables an adequate realistic presentation of a navy environment. (Mean 1.13, SD 0.36)
6.4	The behavior of the ship model in forward speed enables an adequate realistic presentation of a navy ship behavior when coming very close to it (<100m). (Mean 1.25, SD 0.47)
6.3	The behavior of the ship model in heave enables an adequate realistic presentation of a navy ship behavior when coming very close to it (<100m). (Mean 1.38, SD 0.75)
6.2	The behavior of the ship model in roll axis enables an adequate realistic presentation of the ship behavior when coming very close to it (<100m). (Mean 1.25, SD 0.47)
6.1	The visual presentation of the ship model enables an adequate realistic presentation of a navy environment when coming very close to it (<100m). (Mean 1.13, SD 0.36)

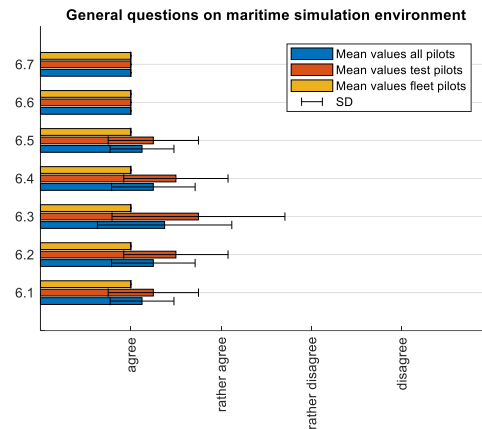


Table 6-3: Subjective pilot evaluations of the maritime simulation visualization (N=10)

Table 6-4, gives an overview of visual perception and perceived behavior of the ship model from pilots' perspective. The ship visualization in general was rated as being realistic in matter of visualizing the superstructures and the landing deck of the ship, as well as the motion behavior of the ship within the sea. One of the most experienced maritime pilots (PID3) stated the motions of the ship being almost even as realistic to a real ship setup by the sentence "every seventh wake is a good wake". It means, that pilots observe the ship motions while hovering behind or alongside the ship to detect a kind of repetition of waves and corresponding ship motion in roll and heave. Therefore, they try to detect a quiescent period to land the helicopter on the deck. This procedure is well known in the maritime helicopter world and was stated from several pilots during the experiment.

Questionnaire item	
7.5	The behavior of the ship model in forward speed enables an adequate realistic presentation of a navy ship behavior. (Mean 1.13, SD 0.36)
7.4	The behavior of the ship model in heave enables an adequate realistic presentation of a navy ship behavior. (Mean 1.25, SD 0.70)
7.3	The behavior of the ship model in roll axis enables an adequate realistic presentation of the ship behavior. (Mean 1.13, SD 0.36)
7.2	The level of detail of the landing deck enables an adequate realistic presentation of a navy deck scenario. (Mean 1.25, SD 0.47)
7.1	The visual presentation of the ship model enables an adequate realistic presentation of a navy environment. (Mean 1.13, SD 0.36)

Table 6-4: Subjective pilot evaluations of the ship simulation visualization (N=10)

Finally, Table 6-5 shows pilots evaluations of the three basic subsystems of ROSIE: the visual cueing system, the flight dynamics, and the cockpit. Pilots stated the outside visual cues as acceptable to proceed the flights without any visual or computing disturbance. Here, the evaluation of the visual cues took among others brightness and contrast, update rate, and homogeneity of the dome projection into account.

Questionnaire item	
8.4	The cockpit concept with the reduced head-down instrumentation complemented the HMD concept. (Mean 1.13, SD 0.35)
8.3	The flight controls were adequate (e.g. control forces). (Mean 1.25, SD 0.5)
8.2	The flight dynamics simulation was adequate. (Mean 1.25, SD 0.5)
8.1	The outside visual cues were adequate. (Mean 1.25, SD 0,46)

Table 6-5: Subjective pilot evaluations of ROSIE (N=10)

The flight controls and dynamics were accepted in general. However, some pilots mentioned to be used to fly with a Force-Trim Release (FTR). Within ROSIE and the original Bo-105 controls, only a Force-Trim was available. Overall, no pilot had problems with

adapting to the flight controls for the given tasks. ROSIE slim cockpit configuration in interaction with the used HMD was accepted well by all pilots. However, pilots were instructed to use as much as possible the HMD during flight.

6.2 Experimental Simulation Methodology

The experimental methodology introduced in this chapter considers an introduction of participating test subjects and its clustering. Measurements and ratings are chosen along standard flight test procedures in the rotorcraft world [1], naval helicopters operations [105] [126], and ergonomic guidelines [46]. Finally, an overview of the test schedules and connected ratings and questionnaires within training and operational flight blocks is given. A benefit of the test design may be the comparability, repeatability, and transferability to experiments [53] [94] which had been conducted in parallel or are planned to be proceeded in the near future.

6.2.1 Participating Helicopter Pilots

The simulator flight test campaign involved a total of ten maritime test and fleet pilots, all with naval experience. Participating pilots, each ascribed by a specific PID number, have extensive years' experience on AS350, AW139, AW189, Bell UH 1D, Bell-205, Bell 407, Bell 412, Bo-105, CH-47, CH-53, EC-155, H-135, H-145, NH-90, Sea King, Sea Lion, Sea Lynx, Super Puma, UH-Tiger, UH-60, and multiple experimental helicopters such as ACT/FHS and MAT. The PIDs were structured as follows:

1. Maritime test pilots (TPs) ($N=6$) from German and U.S. armed forces, Airbus, Kopter Group, Boeing, and Sikorsky.
2. Maritime fleet pilots (FPs) ($N=4$) from German armed forces, and federal German Police.

All pilots (mean age 43.7y, $SD= 11.2y$), see also Table 6-6, were asked about their flight experience (stated in flight hours) in real life (mean = 3537.5fh, $SD = 2054.9fh$), using Night Vision Googles (NVG) (mean = 253.0fh, $SD = 161.2fh$), and an HMD (mean = 381.0fh, $SD = 507.1fh$), simulator flying (mean = 670.0fh, $SD = 835.7fh$), all as Pilot in Command (PIC) in terms of being able to achieve the tasks at least at an adequate level.

Number of PIDs	Category (TP, FP, Sum)	Pilot ID	Experience in H/C flying Mean (SD)
6	TP	1, 3, 4, 5, 8, 9	4133,3 fh (1875,8 fh)
4	FP	2, 6, 7, 10	2643, 8 fh (2242,3 fh)
10	Sum	1 - 10	35.375,0 fh

Table 6-6: Evaluation pilots for pilot-in-the-loop experiments

Nine out of ten participating pilots stated to have experience in flying in a maritime environment. PID7, which was from the Federal German Police, stated to be planned for offshore operations, but at the time of experiments he entered the training phase which contains flying in simulators offering a maritime environment. All pilots acknowledged to have entered different DVE conditions in their career, and even a minimum of one situation of degraded visibility down to 100m. Insights during discussions about using HMDs in flight showed that all test pilots had extended experience in flying actual available and future technology HMD systems. In total, eight out of ten pilots had access to HMDs at the time of experiments. The remaining two pilots (PID6, PID7) were open minded to HMD technologies as well as the other participating pilots. It should be mentioned that two maritime test pilots from German Armed Forces (PID1, PID3) participated also in the design process of the maritime environment and the HMD/PAS. In detail, based on their flight and test experience, outside scenery conditions were tried to be setup as realistic as possible (visualization of bad weather conditions to corresponding ship motions), and symbology concepts were setup and improved (SLS and ESLS) closely together in two workshops, see chapter 3.2.2. The cluster of participating test and fleet pilots from different countries (France, Germany, U.S.) and heterogenic disciplines (armed forces, public authorities, and civil industry) may offer a wide perspective of feedbacks and ratings, as well as possible differences in flying and evaluations.

6.2.2 Measurements and Ratings

When it came to prepare, proceed, and evaluate the simulator campaigns, tools for a quantitative analysis, subjective ratings, and observations of flight and human parameters were established to record valuable feedback before, during, and after experiments, and for data post processing.

Quantitative evaluations of training and shipboard operations were guaranteed by recording all flight parameters with a frame rate of 100Hz of the helicopter and the ship, the HMD/PAS, and outside scenery conditions. In addition, all flights were observed by a camera mounted

inside the cockpit. As in real experimental helicopter flight tests, the pilot in controls was sitting on the right front side of the cockpit. In the backyard of the helicopter, the observer (normally the place of the test flight engineer) was sitting being offered to be part of the operations and always have the pilots' HMD view in sight: The actual visual augmentation of the HMD image was rendered simultaneously to a screen next to the observer's seat. The observer could also take down notes from the pilots given feedback during flight on a kneeboard.

Subjective evaluations were done after each proceeded short flight and additional remarks were written down. To give structured and valuable subjective ratings, well established rating scales were offered to the pilots. Two subjective workload rating scales for airborne operations [134], named as Bedford Workload Scale [36] and DIPES [35] were used. An introduction to the flight test standard rating scales and standards [1] [105] [122] was part of the briefing before the flights started. By starting the first flight, pilots were asked for a rating for subjective workload for each defined MTE after each flight, and a rating for the overall task in common, directly after finishing the short flight. Moreover, using a scale from 0 to 100 in gradient steps of 5, workload had to be tailored to six categories using the pilot workload weighting scale [1]: mental demand (MD), physical demand (PD), temporal demand (TD), performance (P), effort (E) and frustration (F). To evaluate the HMD visual augmentation in categories of human behavior, a visual cue rating (VCR) [1] [39] was asked to the pilot after each flight of training and operations. The VCR ranges from 1 to 5 in gradient steps of 1. Linked ratings [9] towards the evaluation of the advanced flight control modes of the HMD/PAS as well as basic flight controls were proceeded by using the Cooper Harper Handling Qualities Ratings (HQRs) [1] after fulfilling each MTE. Consequently, workload, HQRs, and VCRs were assessed after each training and operative simulator test flight.

Finally, following questionnaires were given to the pilots after finishing the whole experiment: Directly after the last flight, a simulator sickness questionnaire (SSQ) [73] was filled out by each pilot measuring pilots' level of sickness symptoms regarding the fixed-base simulator and its environment. Moreover, a separate questionnaire focused on the HMD visual augmentation concept, the maritime environment, and ROSIE. The questionnaire used a 4-point Likert scale in gradient steps from "agree", "rather agree", "rather disagree" to "disagree". Finally, before an open discussion debriefing started, pilots filled out a biographic questionnaire collecting details on pilots' experience and education, actual licenses, and experiences in flying under different conditions.

6.2.3 Simulator Flight Test Procedures

The simulator flight test plan was made up of two simulator campaigns. Both campaigns lasted in sum one day (8,5 hours) for each pilot. First simulator campaign focused on

helicopter shipboard approaches and landings in DVEs. Second campaign concentrated on helicopter shipboard final approaches and landings during DVEs and different ship motion states. Both campaigns involved different visual and control augmentations, as well as both scenarios: One for training, named as “Tegernsee”, and one for operational blocks, named as “North Sea”. The schedule of the simulator campaigns is given in Table 6-7.

Simulator flight test program		Timeline
Briefing	Motivation, training, and operational environments, display concepts, tasks and missions' explanation	08:00 – 08:45
Training MTEs	<ul style="list-style-type: none"> • Familiarization with ratings (Bedford, HQR, DIPES, VCR, NASA-TLX) • Simulator and HMD/PAS handling • Proceeding of free flight, hover and sidestep MTEs according to ADS-33 PRF standards (Bedford, HQR, VCR) 	09:00 – 10:30
Short break		
Operational block 1	<ul style="list-style-type: none"> • Helicopter shipboard approaches in different ship motions and DVE categories • Different visual cues (PFD, no HMD, HMD) • Different advanced flight control modes (normal controls, TRC, ACVH) (Bedford, HQR, DIPES, VCR)	10:30 – 13:00
Lunch break		
Operational block 2	<ul style="list-style-type: none"> • Helicopter shipboard final recoveries in different ship motions and DVE categories • Different visual cues (PFD, no HMD, HMD) • Different advanced flight control modes (normal controls, TRC, ACVH) (Bedford, HQR, DIPES, VCR, NASA-TLX) <ul style="list-style-type: none"> • Simulator Sickness Questionnaire (SSQ) 	14:00 – 16:30
Short break		
Debriefing	<ul style="list-style-type: none"> • Questionnaire on study • Questionnaire on display concepts • Biographical questionnaire and discussion 	16:30 – 17:30

Table 6-7: Simulator flight test program

Each test day started with a briefing in the morning which included an introduction to the simulator, its main systems and controls, and the HMD/PAS. The visual augmentation concepts, as well as advanced flight control modes were given to the pilot with a presentation and inside cockpit sitting explanation for familiarization. Besides that, the flight test procedures and ratings standards were presented in detail. To guarantee that the pilot could fully focus on the given tasks, procedures and ratings were recapitulated before each block again. Moreover, none of the pilots wore glasses which could cause effects with the HMD during flight. Almost all pilots were asked to wear their flight suits, gloves, and shoes to further generate a close to reality situation.

First flight block included a structured training with a short free flight and ADS-33 MTEs hover and sidestep. Because these maneuvers are later integrated to the MTEs in the operational blocks, respective MTEs were proceeded in all combinations of advanced flight control modes. MTEs were rated to give valuable basic feedback on simulator flight control devices, advanced flight control modes, visual cues, and the cockpit environment.

After a short break, the scenery was switched to the North Sea environment. Pilots then had to proceed six short flights to approach and land safely on a moving ship within the maritime environment in GVE and DVE conditions. After every flight, each was given ratings along subjective workload, HQR, benefits or disadvantages of the HMD/PAS modes, and further comments. Operational block 2 was further proceeded after lunch break in the same matter as operational block 1, but with increasing DVE conditions. Since the most demanding task was expected to be with the lowest visibility range and highest ship motion states, it was put at the end of the experiment. Directly after the last flight, each pilot filled out the SSQ. After a further short break, debriefing was proceeded along prepared questionnaires focusing on the simulator, the maritime environment and ship visualization, detailed questions on HMD symbology concepts, and finally an open discussion. Here, the pilots could use a pencil and a board to visualize their ideas on further improving the visualization concepts and procedures. Checklists were used by the author to monitor the varying conditions and to guarantee equal settings and conditions for each pilot. A detailed description of the training and operational phases and tasks is given in the next chapter.

6.3 Helicopter Shipboard Operations

The following chapter details proceeded simulator experiments. First, the training phase was conducted to familiarize the pilots with the simulation environment, MTEs, operational procedures, and corresponding ratings. Moreover, during MTEs training phase, main maneuvers for ship approach and landings were conducted, and visual and control augmentations were trained. Second, operational blocks were executed in different DVE conditions, mainly with staggered visibilities and ship motion levels using variants of visual

and control augmentations. DVE conditions were defined along aeronautical standards [4], and ship motions were specified to SCONE levels as detailed in chapter 5.4.

6.3.1 Mission Task Elements Training Phase

The simulation campaign began with a training phase subdivided into three parts: Basic training, proceeding of MTEs, and training of operational flights. A detailed schedule is given in Table 6-8. MTEs of the training phase was proceeded to familiarize the pilots with the simulation environment and basic flight dynamics. Training started with short free flights using available flight controllers, followed by proceeding of MTEs hover and sidestep [1], and ended in operational flights in the maritime environment to get familiar with the visual and control augmentation. Structured execution of different MTEs allowed the pilots to practice the later available visual and control augmentation combinations. Moreover, the training phase was used to give the augmentations separately and in combinations a basic rating, and simultaneously to improve flying skills of the pilot in the simulator. Hence, all pilots had to adapt their control behavior to the flight dynamics of the simulator. To mitigate the influencing effects for the results, the training phase was conducted with a focus on the visual and control augmentation setups in combination to available outside visual cues. The training phase was completed with the first flights in DVE conditions of 800m visibility, before heading to the first operational ship approach and landing tasks. Table 6-8 gives a detailed overview of the training blocks for each pilot in the morning, starting with the basic training (FRE_1_1 – FRE_1_3), proceeding of MTEs (HOV_1_1 – SID_0_3), and training of operational flights (SID_2_1 – SID_2_3) before break. The level of difficulty had been increased step by step over the three blocks. Order of proceeding for MTEs, training of operational blocks, and fulfillment of both operational blocks in the afternoon had been randomized to encounter training and fatigue effects. However, basic training was executed in the same manner because advanced flight control modes build up on the unaugmented flight control.

ID	Test point	Environment	Flight control mode	HMD mode	Duration (min.)
FRE_1_1	Free flight	Tegernsee	unaugmented	No HMD	5
FRE_1_2	Free flight	Tegernsee	TRC	No HMD	5
FRE_1_3	Free flight	Tegernsee	ACVH	No HMD	5
Short break					
HOV_1_1	MTE Hover	Tegernsee	unaugmented	No HMD	5
Questionnaire Ratings					
HOV_1_2	MTE Hover	Tegernsee	TRC	No HMD	5
Questionnaire Ratings					
HOV_1_3	MTE Hover	Tegernsee	ACVH	No HMD	5
Questionnaire Ratings					
Short break					
SID_0_1	MTE Sidestep	Tegernsee	unaugmented	No HMD	5
Questionnaire Ratings					
SID_0_2	MTE Sidestep	Tegernsee	TRC	No HMD	5
Questionnaire Ratings					
SID_0_3	MTE Sidestep	Tegernsee	ACVH	No HMD	5
Questionnaire Ratings					
Short break					
SID_2_1	Ship recovery	North Sea	unaugmented I	HMD	5
Questionnaire Ratings					
SID_2_2	Ship recovery	North Sea	TRC	HMD	5
Questionnaire Ratings					
SID_2_3	Ship recovery	North Sea	ACVH	HMD	5
Questionnaire Ratings					
Short break					

Table 6-8: Simulator flight test points – training phase

Part one basic training, as well as part two proceeding of MTEs were executed in the “Tegernsee” environment. Part three, training of operational flights was conducted in the operational environment “North Sea”. Part two reflects the main maneuvers of the operational blocks. Hence, maneuvers of part two were embedded to operational conditions in part three. Both parts, one and two prepared pilots for the operational blocks in the afternoon. In the following, part two and three are described in detail.

Part two, proceeding of MTEs was subdivided into the main maneuvers needed for a safe helicopter ship approach and landing [105], namely “sidestep” and “hover” taken from ADS-

33 PRF [1]. Besides practicing maneuvers for later operational flights, MTEs hover as well as sidestep are established and used to rate augmentations among pilot workload and handling qualities. Objective of MTE hover, as seen in Figure 6-4, was to inspect for undesirable handling qualities in a moderately aggressive hovering turn, check ability to recover from a moderate rate hovering turn with reasonable practice, and finally test for undesirable interaxis coupling.

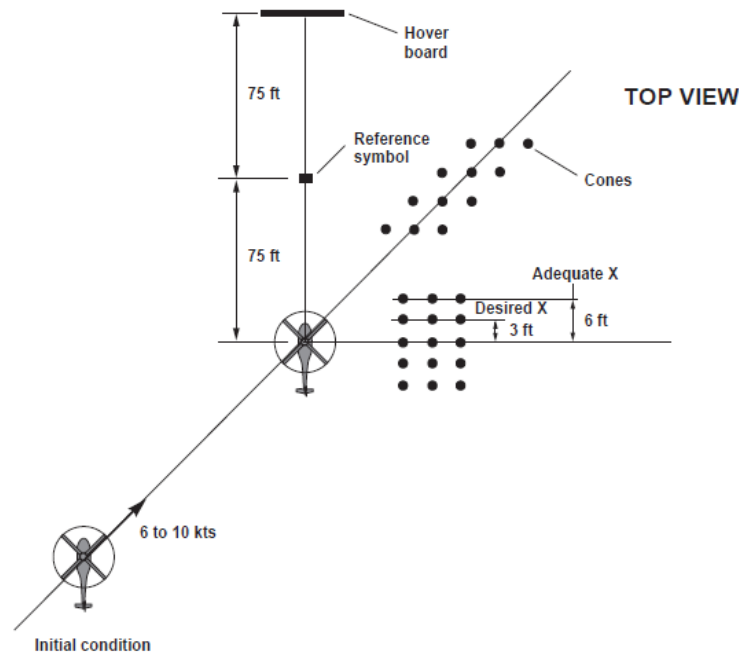


Figure 6-4: Top view of suggested course for hover mission task element [1]

Two example runs of the MTE sidestep of two pilots, one navy fleet pilot (PID6) and one navy test pilot (PID9), are given in Figure 6-5. Left hand figure shows two unaugmented runs, while the right-hand figure displays augmented runs using ACVH. The final hover points are situated in the lower right corner of the figures.

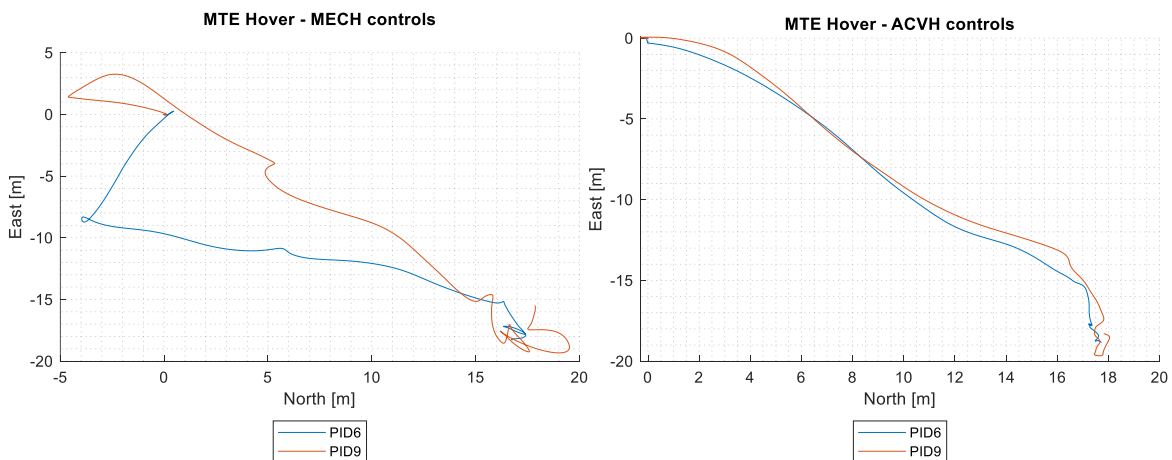


Figure 6-5: Two example runs of the hover MTE

Objective of MTE sidestep, as given in Figure 6-6, was to overhaul lateral-directional handling qualities for maneuvering near the augmentation limits of performance, survey for

interaxis coupling as well, and finally to check ability to coordinate bank angle and collective to hold constant altitude.

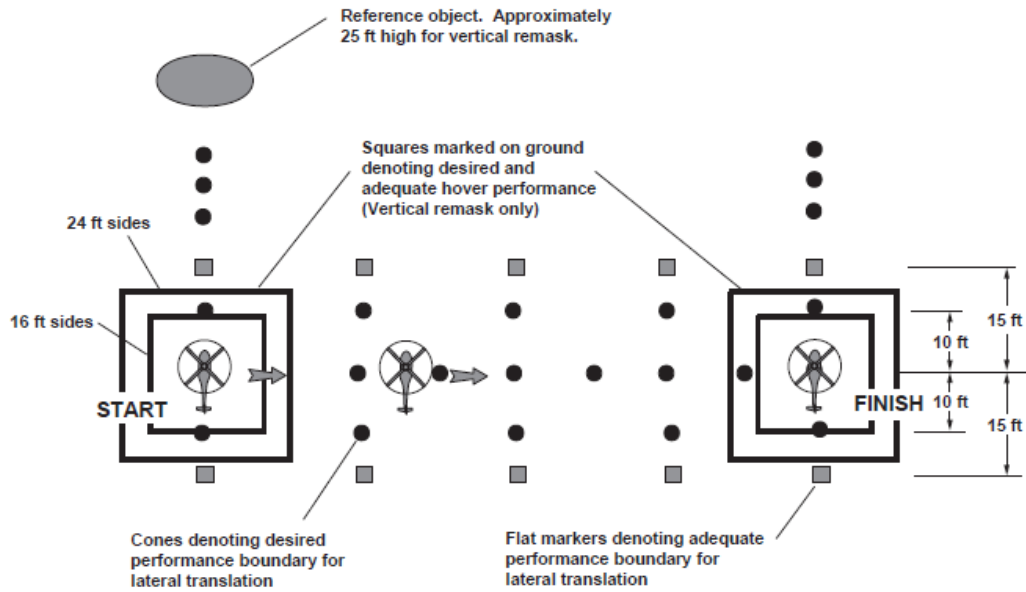


Figure 6-6: Top view of suggested course for sidestep MTE [1]

Two example runs of the MTE sidestep of two pilots, again one navy fleet pilot (PID6) and one navy test pilot (PID9), are given in Figure 6-7. Left hand figure shows two unaugmented runs, while the right-hand figure visualizes augmented runs using ACVH response type. Moreover, Figure 6-7 includes desired performance boundaries [1] visualized as horizontal dashed lines, which were used during experiments to rate HQs along defined values within the Cooper-Harper HQRs.

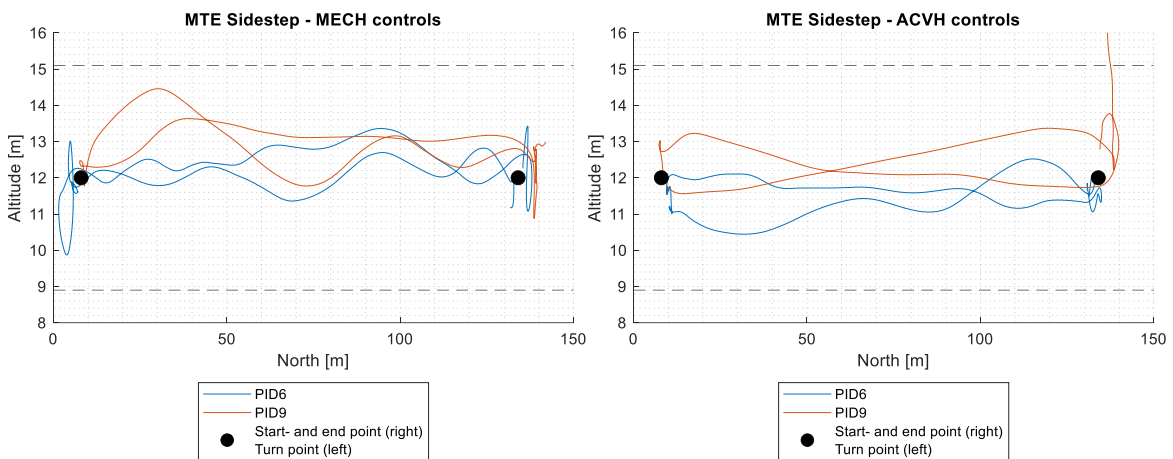


Figure 6-7: Two example runs of the sidestep MTE

Part two was used to train and rate the control augmentation modes which were used within the experiments. The maneuvers included the degree of needed aggressiveness and divided attentions during operation, as well as the “applicability of rotor start and stop capabilities for shipboard operations” [1]. However, with limited duration of the training phase, MTE acceleration-deceleration was embedded to the free flights. A separate flight campaign was established focusing on the three MTEs hover, sidestep, and acceleration-

deceleration to reflect control augmentations on isolated sequences of helicopter shipboard operations. More details about the flight campaign can be found in [53].

With increasing maneuver complexity, and to practice and combine visual and control augmentations, pilots flew the operational test points afterwards. Now, it was not any more the main priority that pilots were able to achieve the desired or adequate values within the maneuvers. The focus of part three was to familiarize the pilots with the operational environment, proceeding of the missions in the afternoon, and to rate basic workload and HQs during basic setups of environment and ship motions. Before proceeding part three, pilots were introduced to the HMD fitting to ensure proper wearing, readability of visual augmentation and check head tracking alignment. Therefore, a verification process [144] of correct HMD fitting through the pilot was done each before part three and both operational blocks in the afternoon. After fitting the HMD, the pilots familiarized with the visual augmentation concept and practiced operational tasks. For the ship approach and landing tasks, two clutter modes were applied, as seen in Figure 6-8. The training of operational flights included basic visual and control augmentation combinations. It should be mentioned, that without the visual augmentation set-up, it would not have been possible to fly the ship approach task even at visual ranges of 800m, and for the ship landing task at visual ranges below 400m.

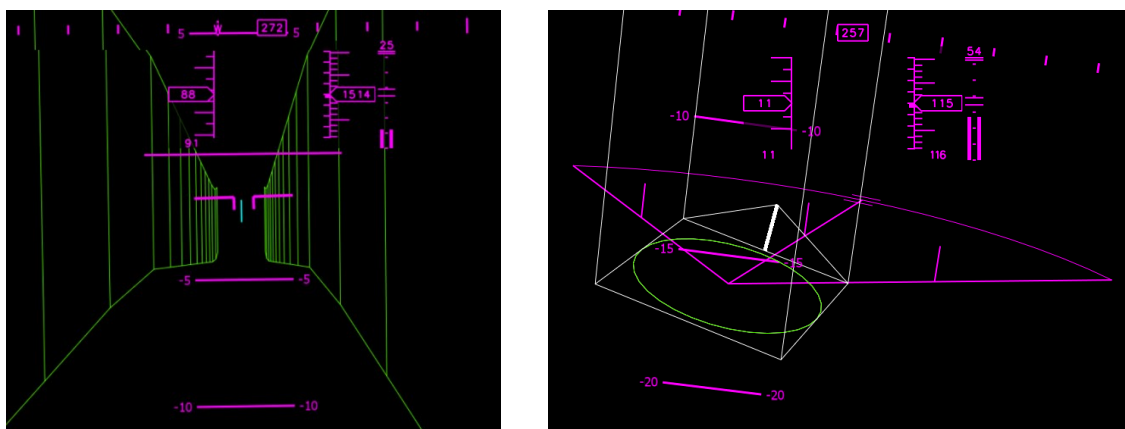


Figure 6-8: Basic display modes for ship approach (left) and landing (right)

As in part one and two, pilots were trained in part three the basic and advanced visual and control augmentations. Bedford workload ratings, HQRs, and VCR ratings were conducted for training purposes and to rate visual and control augmentation modes separately. The MTE training phase concluded in the basic DVE setup for the operational flights with a decreased visibility of 800m and ship motion level 1.

6.3.2 Helicopter Shipboard Approach Sequence

Block one of the helicopter operations simulator flight tests focused on the visual approach and landing segment towards a moving ship in DVE conditions. The scenario was used to demonstrate the usability of visual and control augmentation modes and its combinations

within different levels of degraded visibility. Hence, following research questions raised: How could a PAS maintain the pilot during approaching the helicopter towards the ship in a DVE? Does a PAS increase flight stability during near-ship helicopter operations in a DVE? Currently, maritime helicopters are only allowed to launch and recover in open sea environment when visual conditions are above 800m visibility. Below 800m, ships must provide guidance for helicopters final approaching via IFR flight rules. Though conflict scenarios raise from available GPS assisted approaches, where the GPS signal over sea is denied. Moreover, weather conditions often quickly change over sea. Therefore, the HMD/PAS might offer a ship independent possibility to find, approach, and land on the ship even in harsh conditions such as within minimum visibility ranges. To answer those research questions, a helicopter ship approach scenario with standardized approach MTEs has been developed. The scenario covers international ship approach procedures [105] [140] and is broken down simultaneously into ADS-33 PRF [1] flight test standard sequences. The final approach and landing phase were further detailed and investigated during operational block two, see chapter 6.3.3. Table 6-9 gives a detailed description of research questions and corresponding hypotheses for the simulator flight tests.

RQ 1	How could the PAS assist the pilot during approaching the helicopter towards the ship in DVE condition?
H1	Pilot workload is at a lower level using visual and control augmented PAS than visual augmented PAS during decreasing visibility ranges within the approach segment.
H2	Pilot workload is at a lower level using the enhanced visual augmentation mode (ESAS) than the visual augmentation mode (SAS) during decreasing visibility ranges within the approach segment.
RQ 2	Does the PAS increase glide path stability during approaching the helicopter towards the ship in DVE condition?
H3	Helicopter flight envelopes are closer to optimal glide path using visual and control augmented PAS than while flying visual augmented PAS during decreasing visibility ranges within the approach segment.
H4	Pilot command input rates using visual, and control augmented PAS are lower than visual augmented PAS during increasing ship states within the final approach phase.

Table 6-9: Research questions and hypotheses

Piloted simulation using advanced response types such as ACVH and TRC during helicopter shipboard operations indicated best performance while workload decreased in several studies [90] [94]. Almost Level 1 handling qualities and low pilot workload were

achieved as supported by time domain metrics [118] [125]. However, flight tests identified DVEs on pilot workload as first limits for safe operation [81]: DVEs and turbulence increased workload, reduced piloting performance, and had an impact on control input activity. On top, fulfilling specific rotorcraft tasks, such as hover behind, alongside and over the ship deck, and land, the motion cueing effect turned out to be more significant during DVEs than ship air wakes [81]. In Ref. [147], a motion cueing simulation study of lateral sidestep maneuver indicated the importance of motion cueing. The study reported that without motion cues the pilot could not achieve the desired accuracy [2] without heavily over-controlling. Proceeded test points showed motion cueing could cause differences in the pilot's workload ratings, and it had no discernible regular trend in the relative GVE. However, in the severely DVEs, the motion cueing effect was more significant. The pilot's workload ratings and control activities on control sticks and pedal were normally higher without motion cues. Consistent with previous studies [18] [147], the findings suggest that external visual cueing is vital for a successful landing, during the last phases of approach and landing. Therefore, improvements of external visual cues that have the potential to reduce pilots' workload and improve the overall safety of landing operations are provided. During operational flight tests, pilot's workload ratings and control activities were normally higher without any motion cues [147]. Therefore, one of the main benefits of a visual augmentation [97] is to reduce pilots' workload and increase SA in all phases of flight. Münsterer et al. [103] analyzed together with helicopter pilots that the preferred HMD display information depends on the phase of flight, the current environmental conditions and the visibility of the moving landing zone, the ship deck. Hence, the simulated flight scenarios, as detailed below, focus on shipboard approach and landing during DVE conditions - reduced visibility and variable ship motions. Inside the scenarios, visual augmentation is offered to the pilots activated for approach and landing scenario, and deactivated (outside visual cues stay apparent) for basic investigation. Advanced flight control modes are activated and deactivated alike to examine visual and control augmentation coupling.

6.3.2.1 Scenario Design during Degraded Visibility

The focus of operational block one was to investigate in helicopter ship approaches fulfilling standard maritime IMC approach procedures [105] flying visual with the HMD/PAS in bad weather conditions. The procedure comprised a 'straight-in' approach providing a minimum lateral separation from the approach track to the nearest part of the ship deck landing platform. It did not include any course reversal, racetrack or arc procedure, or any turn or change of course.

Meaning in detail, the approach segment commenced at the IAF, where visual augmentation of the SAS/ ESAS also had its visual entry point represented on the HMD. The helicopter started in a stable in-flight hover position one mile straight behind the IAF in

1500ft AGL. The IAF segment had to be flown at a constant altitude of 1500 ft with a constant speed between 80 to 100 kts IAS. The purpose of the initial approach segment was to align and prepare the helicopter for the final approach by the pilot with acceptable workload and maintaining procedure flight parameters. During the IAF segment (IAF to FAF), the helicopter had to finalize its heading in line with the ship and decelerate to the final approach airspeed, around 80 kts IAS. The final approach segment further continued fluent at the FAF and ended at the MAP. At the FAF, the helicopter entered the descent segment and began to descend at a constant airspeed and a fixed glide path angle of 4° with around 60 to 80 kts GS until the helicopter reached the MDA. Reaching MDA, the helicopter continued in stable forward flight (still 60 to 80 kts GS) until MAP was reached. At MAP SAS/ ESAS switched automatically to SLS/ ESLS visual augmentation. From MAP on, the pilots had to proceed a well-known “HOSTAC SHOL—Port Lateral & 45-Degree” [105] final approach and landing. Final approach maneuvers consisted of hover behind and alongside the deck, sidestep (from left to right), and land during a quiescent period, meaning when ship deck was approximately aligned with the outside scenery horizon.

The intend during flights from IAF down to the final landing was to proceed all maneuvers with acceptable workload and control inputs. On top, due to degrading visibility, pilots were instructed to be aware to not hit the sea while approaching (CFIT). Table 6-10 summarizes the approach procedure of each short flight.

ID	Helicopter ship approach	Duration (min.)
MTE 0	Approach towards the ship	4
MTE 1	Hover behind and alongside (left side) the deck	3
MTE 2	Sidestep (from left to right)	1
MTE 3	Hover over the deck and land	2

Table 6-10: MTEs – operational block 1

Each flight had an endurance of 8 to 10 minutes depending on the speed and the final decision of the pilot to land the helicopter on the deck. In sum, 12 flights were executed. Visibility was reduced in a sequence of three flights (800m, 400m, 200m) while offering four times different combinations of visual and control augmentation modes to the pilot. After each flight, pilot workload, HMD visual cues, and HQs were rated by the pilot respectively for each MTE. A compendium of used rating scales is given in A.1. Table 6-11 shows the detailed schedule of proceeded flights using combinations of visual and control augmentations.

ID	Test point	North Sea Environment (all SCONE level 1)	Flight control mode	HMD mode	Duration (min.)
1_1_1_800m	Approach	800m visibility	unaugmented	SAS+SLS	10
Questionnaire Ratings					
1_1_1_400	Approach	400m visibility	unaugmented	SAS+SLS	10
Questionnaire Ratings					
1_1_1_200	Approach	200m visibility	unaugmented	SAS+SLS	10
Questionnaire Ratings					
1_2_1_800	Approach	800m visibility	unaugmented	ESAS+ESLS	10
Questionnaire Ratings					
1_2_1_400	Approach	400m visibility	unaugmented	ESAS+ESLS	10
Questionnaire Ratings					
1_2_1_200	Approach	200m visibility	unaugmented	ESAS+ESLS	10
Questionnaire Ratings					
Short break					
1_1_3_800	Approach	800m visibility	ACVH	SAS+SLS	10
Questionnaire Ratings					
1_1_3_400	Approach	400m visibility	ACVH	SAS+SLS	10
Questionnaire Ratings					
1_1_3_200	Approach	200m visibility	ACVH	SAS+SLS	10
Questionnaire Ratings					
1_2_3_800	Approach	800m visibility	ACVH	ESAS+ESLS	10
Questionnaire Ratings					
1_2_3_400	Approach	400m visibility	ACVH	ESAS+ESLS	10
Questionnaire Ratings					
1_2_3_200	Approach	200m visibility	ACVH	ESAS+ESLS	10
Questionnaire Ratings					
Lunch break					

Table 6-11: Simulator flight test points – operational block 1

Hence, first six flights included visual augmentation and no control augmentation, while second six flights contained combinations of both. Flights without visual augmentation were not proceeded, because even with 800m visibility, pilots were not able to reach the ship visually. However, IFR procedures could have been proceeded orally but were not in focus of operational block one. Therefore, operational block two, as detailed in chapter 6.3.3, included flights with visual and control augmentations each activated separately. The intend

of the schedule of operational block one was to enhance pilot assistance in two steps, while DVE condition constantly decreased during all flights from 800m, to 400m, and finally to minimum visibility range of 200m. Figure 6-9 illustrates example runs of a test (PID4) and a fleet pilot (PID10) of first six and second six flights.

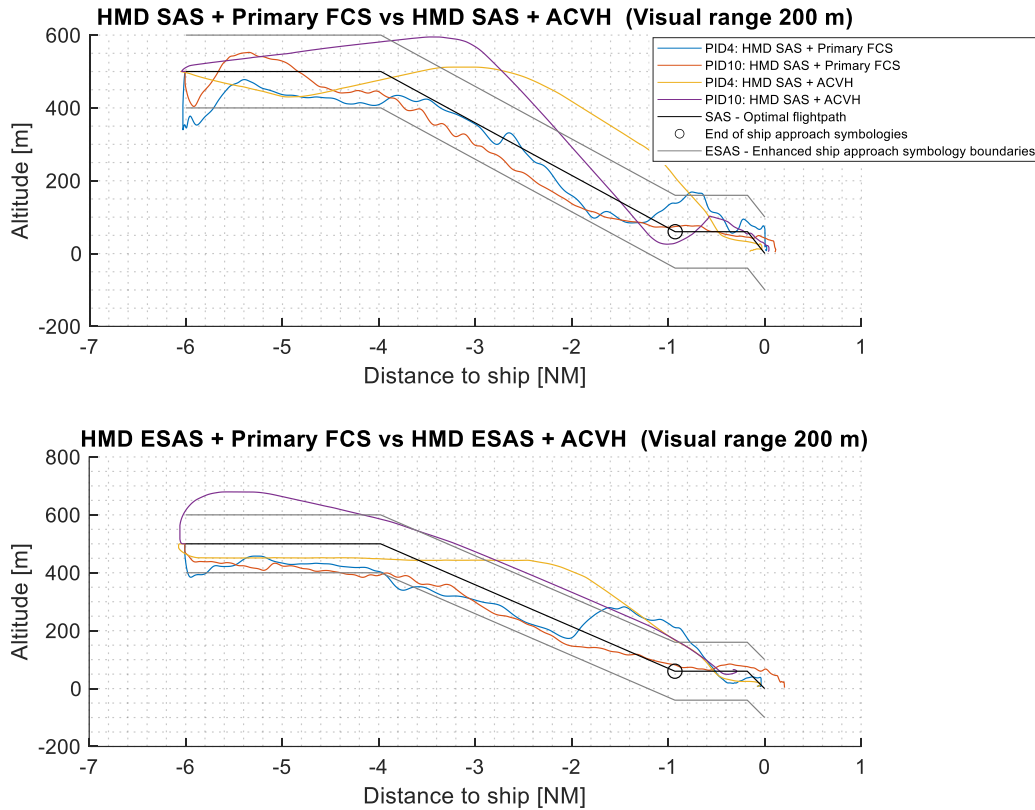


Figure 6-9: Side view of eight example runs of the approach scenario

The consolidated three independent variables (treatments) for operational block one were DVE condition visibility (800m, 400m, 200m), advanced flight control mode deactivated (unaugmented) and activated (ACVH), and HMD visual augmentation modes SAS and ESAS. Ship motion level was set to level 1 for all flights. Granular investigations in the final landing phase, as detailed in chapter 6.3.3, will include outstanding independent variables such as different ship motion levels, both advanced flight control modes (TRC, ACVH), and HMD visual augmentation activated and deactivated (both flying eyes out of the cockpit). In the following, dependent variables (measurements) corresponding to operational block one are introduced.

6.3.2.2 Dependent Variables for the Visual and Control Augmentation

The dependent variables of operational block one are listed in Table 6-12. As similar established for both scenarios, dependent variables are of subjective assessments for proceeded MTEs during each flight and recorded helicopter flight data. The main considered flight parameters are deviation from optimal flight path and cyclic control inputs. VCRs were given to evaluate the HMD visual augmentation, and HQRs were performed to

rate the control augmentation. While the control augmentation was measured by control inputs aggressiveness, the HMD visual augmentation could not be measured objectively so far. Therefore, complementary to the VCRs, pilots head motions were recorded during experiments to discuss the line of sight (LOS) during flights.

	Group of dependent variables	Parameter classification
Subjective ratings	Pilot workload and handling qualities	Bedford rating, DIPES scaling, HQR (Rating: 1 – 10, 1 – 5)
	Visual Cue Rating (VCR)	Attitude, Horizontal Translational Rate, Vertical Translational Rate (Rating: 1 – 5)
	Questionnaires	Dynamic 3D ship approach guidance, 3D-conformal landing deck visualization, flight guidance parameters and general aspects (all Likert scaling)
Objective observations	Flight data	Deviation from optimal flight path, deviation from optimal glide path altitude (all RMSE)
	HMD	Head motions
	Control augmentation modes	Deviation from controls input center positions (RMSE), controls input aggressiveness (Scale 1 – 10)

Table 6-12: Group of dependent variables of the operational block 1

6.3.3 Helicopter Shipboard Final Approach Sequence

Block two of the helicopter operations simulator flight tests investigated in the final approach and landing phase onto the moving landing deck within different ship motion states in a DVE condition. Meaning ship motions were increased from SCONE Level 1 (low) to Level 3 (high) while the DVE condition was fixed to 800m visibility range. The main difference to operational block one is the opportunity to investigate in flying the helicopter without and with the assistance of HMD visual augmentation, and the evaluation of both advanced flight control modes TRC and ACVH. However, with respect to the time schedule and pilot fatigue, SCONE Level 2 was taken out. Therefore, the idea was to use minimum and maximum ship motions to proceed from average to hardest conditions at the end of operational block two, which was the end of the experiment at same time.

Currently, helicopter pilots benefit from ship installations and deck markings to proceed a safe landing. However, influencing factors such as spray on the windshield arising from helicopter rotor downwash lead to reduced outside scenery visibility coming on top to DVE

conditions and high ship motions [150]. Therefore, the visual augmentation is intended to support the pilot to be aware of upcoming obstacles such as the landing deck and the rear wall of the ship [97], named as the capability “Obstacle Awareness”. Moreover, the control augmentation is offered to the pilot to hold a stable position during all phases of the final approach with minimum needed control inputs for workload reduction. In sum, the goal of the visual and control augmentation during the final approach and landing the helicopter is increasing SA. Hence, following research questions were defined: How could a PAS maintain the pilot during landing the helicopter on the ship in DVE condition? How could a PAS assist the pilot during landing the helicopter towards the ship within different ship motion states? Does a PAS increase flight stability during helicopter ship deck landings in DVE? And finally, does a PAS enlarge helicopter time over deck needed for a safe landing with the landing deck set to different motion levels?

To answer those research questions, a helicopter ship final approach and landing scenario with MTEs harmonized to those used in operational block one has been proceeded. Again, the scenario covers international ship approach procedures [105] [140] and is broken down into ADS-33 PRF [1] maneuvers.

6.3.3.1 Scenario Design during different Ship Motions

The focus of operational block two was to examine in helicopter ship final approaches and landings in standard and challenging maritime IMC approach conditions [105] using the visual and control augmentation. Both augmentations were offered to the pilot during low and high ship motions coming on top to the DVE condition decreased visibility range (now fixed to 800m). The procedure comprised a “HOSTAC SHOL—Port Lateral” [105] final approach and landing, as typically used during most international helicopter shipboard operations [97]. It did not include any go-arounds, turns, or change of course. Red and green winds [105] were no factor due to not being activated for both operational blocks. Winds were not activated, because pretests with a maritime test pilot from German Armed Forces showed winds in combination to the fixed-based simulator using the seat shaker for motion cueing were from adequate level. This fact may lead the pilots to more concentrate on flight parameters instrumentations than in real flight conditions. Nevertheless, the motion cueing of the simulator with the dome projection was rated well from all pilots.

Looking at the final approach maneuver in detail, the port lateral final approach and landing essentially combines the bob-up, bob-down maneuver and the sidestep maneuver from ADS-33E-PRF [2]. Each flight began with the helicopter starting in a stable in-flight hover position. The helicopter was staggered to the left rear side of the moving ship in a stable hover at 60m AGL, defined as starting point for the final approach. [105]

Thus, the mission sequence for testing purposes was defined using four contiguous MTEs from the MAP until touchdown on the landing deck. The mission sequence includes hover

alongside the left side of the deck (MTE1), sidestep (MTE2) from the left to the right, until precision hover over the deck (MTE3), and finally land on the deck (MTE4), see Table 6-13. The sequence of MTEs required the pilot to execute the following tasks: Accelerate to 30kts GS and then decelerate from translating flight to a stabilized hover alongside the moving ship deck (20 – 23 kts GS) with precision and a reasonable amount of aggressiveness. Keep altitude of 60ft AGL and harmonize the helicopter with ship speed, which is continuously around 20 to 23kts. Thereafter, hold relative position, altitude, and heading alongside the ship deck. Next, proceed a sidestep to the center of the ship landing deck and attain a stabilized hover. Hold the relative position, altitude, and heading above the landing deck. Finally, descend the helicopter until touchdown during a quiescent period of the ship’s roll and heave motions.

The intend of operational block two was to proceed all maneuvers with acceptable workload and control inputs. Because of different ship motions setup (SCONE Level 1 and 3), pilots were instructed to be aware of the heaving landing deck during different ship motions settings (CFIO). Table 6-13 summarizes the final recovery procedure of each short flight.

ID	Helicopter ship final approach	Duration (min.)
MTE 1	Hover behind and alongside (left side) the deck	5
MTE 2	Sidestep (from left to right)	2
MTE 3	Hover over deck	2
MTE 4	Land on the deck	1
Questionnaire Ratings		

Table 6-13: MTEs – operational block 2

All flights had an endurance of 8 to 10 minutes’ dependent on the decision of the pilot to perform the sidestep and to land the helicopter on the deck during a quiescent period. Again, as in operational block one, 12 flights were conducted. During first six flights, SCONE level 1 was adjusted, and SCONE level 3 during second six flights. After each flight, pilot workload, NASA-Task Load Index (TLX) weighting, and HQRs were conducted for each MTE. Table 6-14 lists the detailed schedule of operational block two for basic investigations on visual augmentation being deactivated and activated, and different ship motions while using combinations of visual and control augmentations.

ID	Test point	North Sea Environment (all in 800m visibility)	Flight control mode	HMD mode	Duration (min.)
SHIP1_1_1	Ship recovery	SCONE L1	normal	No HMD	10
Questionnaire Ratings					
SHIP1_1_2	Ship recovery	SCONE L1	TRC	No HMD	10
Questionnaire Ratings					
SHIP1_1_3	Ship recovery	SCONE L1	ACVH	No HMD	10
Questionnaire Ratings					
SHIP1_2_1	Ship recovery	SCONE L1	normal	ESLS	10
Questionnaire Ratings					
SHIP1_2_2	Ship recovery	SCONE L1	TRC	ESLS	10
Questionnaire Ratings					
SHIP1_2_3	Ship recovery	SCONE L1	ACVH	ESLS	10
Questionnaire Ratings					
Short break					
SHIP3_1_1	Ship recovery	SCONE L3	normal	No HMD	10
Questionnaire Ratings					
SHIP3_1_2	Ship recovery	SCONE L3	TRC	No HMD	10
Questionnaire Ratings					
SHIP3_1_3	Ship recovery	SCONE L3	ACVH	No HMD	10
Questionnaire Ratings					
SHIP3_2_1	Ship recovery	SCONE L3	normal	ESLS	10
Questionnaire Ratings					
SHIP3_2_2	Ship recovery	SCONE L3	TRC	ESLS	10
Questionnaire Ratings					
SHIP3_2_3	Ship recovery	SCONE L3	ACVH	ESLS	10
Questionnaire Ratings					
Debriefing					

Table 6-14: Simulator flight test points – operational block 2

Consequently, first three flights were executed without HMD visual augmentation, while second three flights were conducted with visual augmentation. Within first three flights control augmentation was set from no augmentation (MECH), to TRC, ending up in ACVH advanced flight control mode. After first six flights, ship motions intensity was increased to a higher level to further proceed same six flights as before. Figure 6-10 represents a final

approach until landing on the deck of a test pilot with deactivated and activated HMD visual and control augmentation.

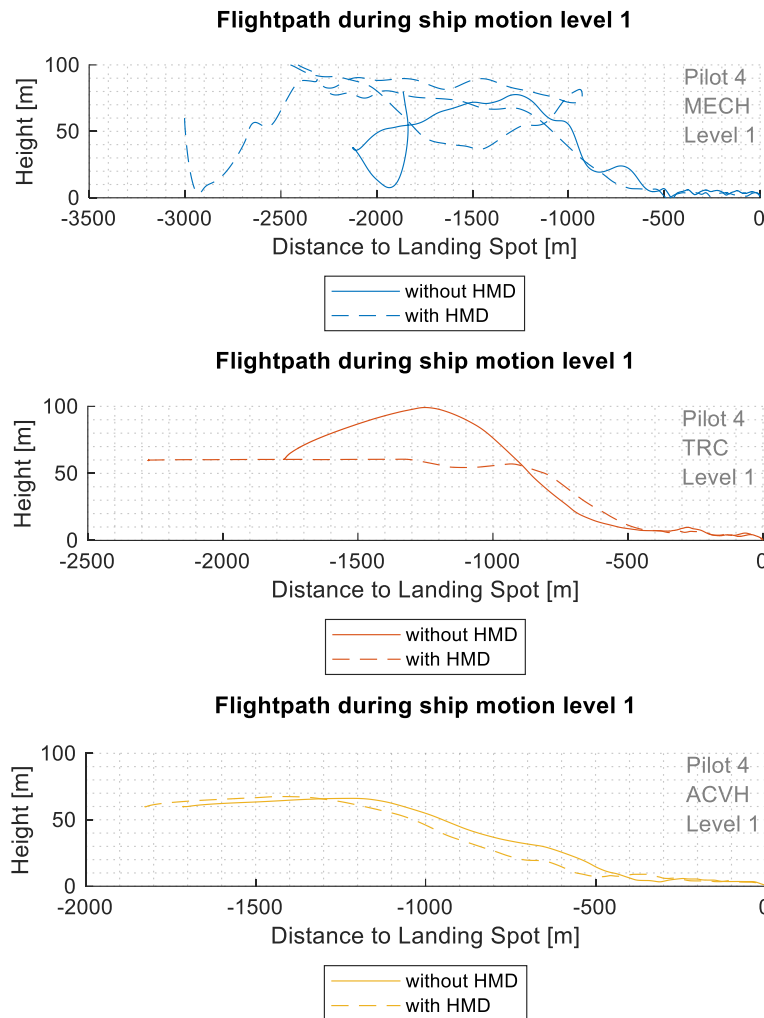


Figure 6-10: Side view of four example runs of the final approach scenario

Taking operational block one into account, three independent variables remain for operational block two: HMD visual augmentation deactivated and activated (no HMD or ESLs), ship motion level (SCONE level 1 and 3) and remaining advanced flight control mode ACVH compared to TRC and unaugment control (MECH). DVE condition was set to 800m visibility for all flights. In the following, dependent variables for operational block two are defined.

6.3.3.2 Dependent Variables for the Visual and Control Augmentation

Table 6-15 presents dependent variables of operational block two. The focus of observed flight parameters was the positioning of the helicopter for the last 40 sec of flight and giving insights into precision hover over the deck and landing maneuver.

	Group of dependent variables	Parameter classification
Subjective ratings	Pilot workload and handling qualities	Bedford rating, DIPES scaling, HQR (Rating: 1 – 10, 1 – 5)
	Pilot workload weighting (NASA-TLX)	Mental demand, physical demand, temporal demand, performance, effort, frustration (Rating: 0 – 100%)
	Questionnaires	3D-conformal landing deck visualization, flight guidance parameters and general aspects (all Likert scaling)
Objective observations	Flight data	Cyclic, collective, and pedals input (all RMSE)
	Displays	Head motions
	Obstacle avoidance	Avoidance maneuver distance to obstructions during landing (last 40 sec of flight)

Table 6-15: Group of dependent variables of the operational block 2

Pilot control inputs, mainly of cyclic and collective control for positioning the helicopter over the deck, were considered. Pilots head motion is from interest during HMD visual augmentation as being activated. The focus with HMD visual augmentation off was also to not wear the HMD for any negative effects on fulfilling the tasks. Hence, head motions could only be observed during HMD worn flights. Complementary to pilot workload ratings, the NASA-TLX task-load-index workload weighting was proceeded for each MTE to further detail the workload into the six categories of mental demand (MD), physical demand (PD), temporal demand (TD), performance (P), effort (E), and frustration (F) level. A detailed description of all ratings is given in A.1.

7 Results and Discussion of the Simulator Flight Tests

In the following, the results of the simulator flight tests are given for the training phase and each operational block. For the training phase as well as for all operational missions, performance evaluations are investigated, and a concluding discussion is given for each phase of the simulated flights. Pilot workload ratings, HQRs, VCRs, NASA-TLX weightings, and questionnaires complement the objective pilot behavior measurements. Moreover, a mathematical handling qualities model is established for helicopter near-ship operations based on the simulator flight test data. Finally, results of the simulated image-based ship tracking data onto the HMD visualization are given.

The present work has demonstrated the utility of in-cockpit, eyes-out display concepts for helicopter shipboard recovery operations. It has also confirmed the effectiveness of advanced response-types for near-ship maneuvers. A judicious combination of control and visual augmentation has the potential to offer operational benefits to naval helicopter pilots in the GVE and DVE environments. However, further research is necessary to understand the impact of advanced eyes-out concepts and advanced response-types for shipboard recovery in the DVE and during emergency procedures.

7.1 Handling Qualities during Training Phase

During the training phase, specific ADS-33 PRF [2] maneuvers using unaugmented (MECH) and augmented controls (TRC, ACVH) were performed and evaluated. Although, both control augmentations TRC and ACVH were practiced, this section focuses on the effects between unaugmented and augmented controls. Further results are given in [53].

The focus of the training phase was to familiarize the pilots with the simulator, its control devices, and control augmentations. Moreover, this segment was used to evaluate the advanced flight control modes separately within the ADS-33 PRF setup. Proceeded tasks of hover and sidestep have a strong connection to the main tasks during the helicopter ship deck final approach phase [105] [140]. To enable ratings of precision and aggressiveness within desired and adequate performance, ADS-33 PRF standards for each task are listed separately for the used rotorcraft category cargo/ utility in GVE conditions. All data are presented in mean values (M), SD and RMSE facing the total amount of pilots. Finally, data is presented to a test and fleet pilot's breakdown for further discussions.

7.1.1 ADS-33 MTE Hover

The main goals for all participating pilots to fulfill the hover MTE with unaugmented and augmented controls were as follows: familiarize with unaugmented (MECH) and augmented (ACVH) controls. Check the ability to transition from translating flight to a stabilized hover with precision and a reasonable amount of aggressiveness and tolerable workload. And

finally, maintain a precise position over the designated hover point, heading, and altitude with the given outside visual cues from the environment. Figure 7-1 shows the pilot performing the transition (left image) and hover (right image) maneuver.



Figure 7-1: Views during MTE hover in the Tegernsee environment

The pilots started the maneuver in a stable position on ground to the rear left side of the precision hover point, as specified within the ADS-33 PRF [2] for the hover MTE: Pilots began the maneuver after lifting the helicopter at a GS of between 6 and 10 kts, at an altitude less than 20 ft AGL. The target hover point was oriented approximately 45° relative to the heading of the rotorcraft, which is a repeatable, ground-referenced point from which rotorcraft deviations were measured. The ground track should be such that the rotorcraft will arrive over the target hover point in a 45° moving of the helicopter. Pilots were offered to use for operation the cockpit visual cues of the PFD information for attitude, speed, altitude, heading and outside visual cues of the MTE hover itself. As seen in Figure 7-1 (right image), pilots could benefit from a visual reference and feedback to keep the hover position: When the green balls on the upper end of the poles stay within the grey segment of the boards, a HQR rating of “desired” is recommended. “Adequate” performance rating is advised when staying within the surrounding red borders could be achieved. Finally, “outside adequate” values should be given when the green balls are observed by the pilot outside the red borders. It should be noted that corresponding pilot workload ratings mostly go along with the HQRs. [36]

Results of Bedford [110] pilot workload ratings and HQRs for the MTE hover and sidestep are given in Figure 7-2. First, Bedford workload ratings for MTE hover indicated that pilots rated unaugmented controls within level 2, while the advanced flight control mode ACVH was continuously placed within level 1. Bedford ratings between numeric values of 3 (enough spare capacity for further tasks) and 4 (insufficient spare capacity for further tasks) play an important role due to corresponding desired (rating value 3) and adequate (rating value 4) HQRs.

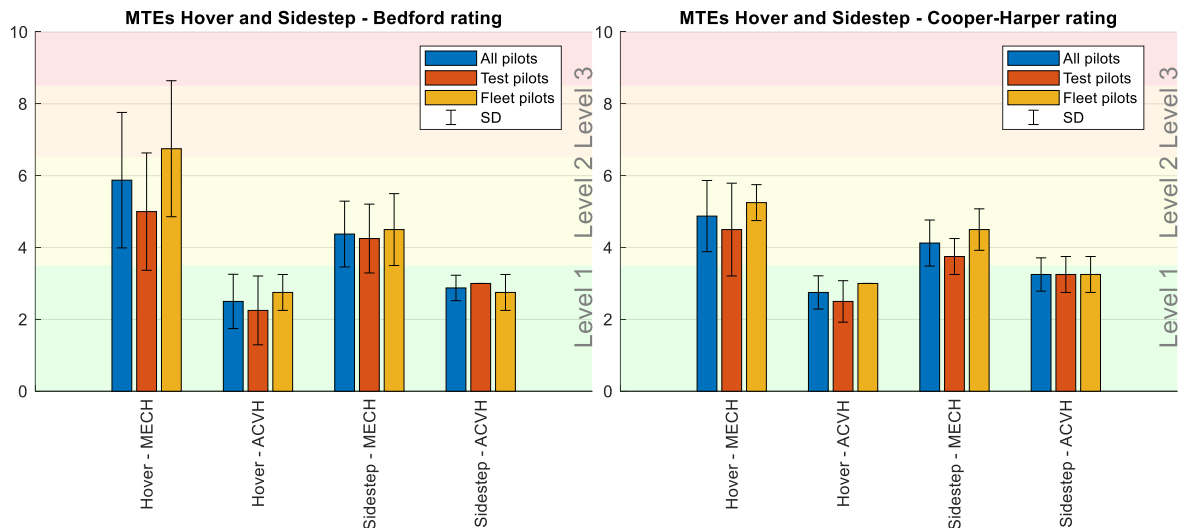


Figure 7-2: MTEs Hover and Sidestep – pilot ratings, $N=10$

Participating pilots stated that the most challenging demand during the MTE hover was to perform the deceleration and a continuous (almost 30 sec.) stable hover, especially when flying unaugmented. Moreover, when reaching the final hover position, pilots' efforts were to keep all outside visual markers in sight at same time, mainly due to aspects of the cockpit layout: The cockpit frame, especially the right A-frame of the front cockpit window covered the unobstructed view on the right-hand hover board. When flying augmented, most of the pilots reported the acceleration and deceleration behavior of the advanced control mode were intuitive and with less workload to fulfill, even because controls were decoupled. Hence, pilots characterized to be able now to focus more on the outside visual cues to perform not only a stable hover but try to reach the precise final position for desired values. However, with acceptable workload. Pilots' workload ratings showed acceptable and even low workload when operating the helicopter with control augmentation. The nascent spare capacity was used by all pilots to focus on the cockpit instrumentation and outside visual cues, and so keep within a precise and stable hover position.

Equivalent HQRs for MTE hover, as seen in Figure 7-2 right image, go along with Bedford ratings from above. Unaugmented controls were rated all inside level 2 which might confirm the realistic behavior of the H135 flight model and the opportunity to perform all tasks with given modes MECH and ACVH. Augmented controls were rated within the higher level 1. Pilots commented the aggressiveness of the advanced flight control mode were being well balanced when they had to bring the helicopter to a stop, accelerating, or decelerating. This might be an outcome of including a maritime test pilot from German Armed Forces having extensive experience in optimizing the advanced response types during the control augmentation finalization phase, where gains and latencies were tuned together with this test pilot. Results on these experiments are given in [93].

Observation of corresponding flight performance see Figure 7-3, may substantiate the subjective ratings. Figure 7-3 illustrates the top view of the helicopter flight paths with

unaugmented (left image) and augmented (right image) controls. The final hover point is illustrated in the lower right corner of Figure 7-3.

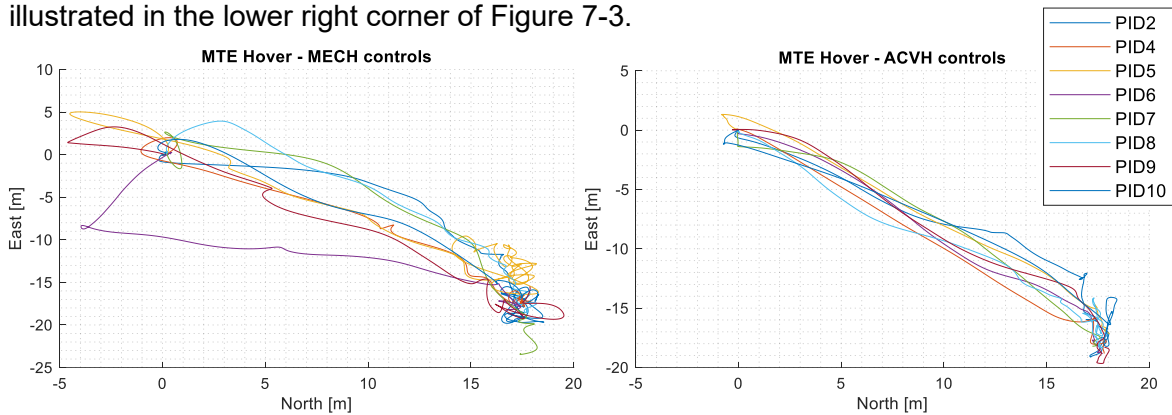


Figure 7-3: MTE Hover – top views flight paths

Observations confirmed the given feedback from most of the pilots: Flying unaugmented might result in an “overshoot” when coming to a stop on a predefined position is needed. This aspect even plays an important role, when obstructions like a rear deck wall of a ship are close to this position. On the other hand, when flying the task with control augmentation, all pilots were able to follow the visual guidance line on the ground which indicates the optimal flight path during transition to hover. Finally, when the final hover position was reached, pilots had to pay more attention to keep the helicopter within a stable position while flying unaugmented. In contrast to that, flying augmented allowed the pilots even to hover “attentive hands on” the control devices while focusing more on the outside visual cues than during unaugmented flight. However, a comparison in deviation of the ideal flight paths (RMSE) as given in Figure 7-4 indicates good performance for unaugmented, as well as for augmented flights. Finally, the evidence of a higher error correction to maintain within ADS-33 PRF desired flight parameters while operating the helicopter without control augmentation, given as SD in Figure 7-4, should be outlined.

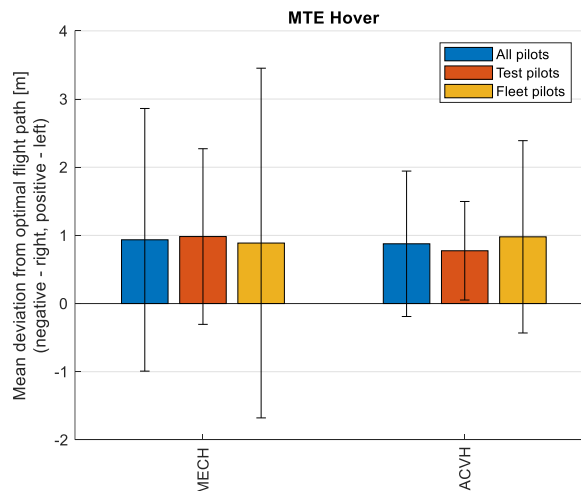


Figure 7-4: MTE Hover – deviations from ideal flight paths

Taking subjective ratings and observations both into account, the following main results might be given for the MTE hover:

1. All participating pilots were able to fulfill the given task MTE hover within acceptable pilot workload and needed pilot input performance.
2. Augmented flights (level 1) in comparison to unaugmented flights (level 2) culminated in HQRs for “adequate” and “desired” performance, in accordance with given Bedford pilot workload ratings of level 1 (augmented controls) and level 2 (unaugmented controls).
3. Free mental capacity during augmented flights was used to pay more attention on the outside visual cues to fulfill the given task within a higher precision.
4. Test pilots as well as fleet pilots’ ratings showed similar ratings.

Next, after a short break the MTE sidestep was performed within the same control configurations as for the MTE hover.

7.1.2 ADS-33 MTE Sidestep

Alike the hover maneuvers, second MTE sidestep was proceeded as given in ADS-33 PRF [2]. The main goals of fulfilling and evaluating the task with unaugmented and augmented controls were as follows: further familiarization with the simulation environment and helicopter control inputs in aggressive and precise maneuvering. MTE sidestep focused on practicing and checking lateral - directional handling qualities for aggressive maneuvering near the helicopter limits of performance. Regarding the control augmentation modes, the focus was to check for objectionable interaxis coupling (unaugmented) and decoupling (augmented). Finally, participating pilots were invited to fulfill and evaluate the ability to coordinate bank angle and collective control to keep a constant altitude, as being necessary during helicopter ship interface maneuvers [105] [140]. Figure 7-5 illustrates the pilot performing a lateral sidestep (left image) and hover (right image) maneuver using outside visual cues as specified in [2].



Figure 7-5: Views during MTE sidestep in the Tegernsee environment

The MTE sidestep started with the helicopter being on ground with the longitudinal axis of the helicopter oriented 90° to the reference line marked on the ground at the right end side of the MTE sidestep course. Second, pilots fulfilled a takeoff coming visually with the horizontal green bars inside the grey segment of the boards. Again, as during MTE hover,

red and green markings of the boards gave visual feedback on “adequate” and “desired” performance. Next, pilots were instructed to proceed a rapid and aggressive lateral acceleration (less of 40 kts GS), holding altitude at a constant level with power. Pilots had to keep target velocity for at least 5 sec., followed by initiating an aggressive deceleration to hover at a constant altitude at the left end side of the MTE. The peak bank angle during deceleration should occur just before the helicopter comes to a stop. Finally, pilots had to establish and maintain a stabilized hover for 5 sec., followed immediately by repeating the maneuver in the opposite direction with coming to a stabilized hover again at the right end side of the MTE course.

Figure 7-6 shows the recorded flight paths top views of all pilots fulfilling the maneuver sidestep with unaugmented (left image) and augmented controls (right image). Dotted lines in Figure 7-6 represent the ground reference lines to achieve desired longitudinal performance.

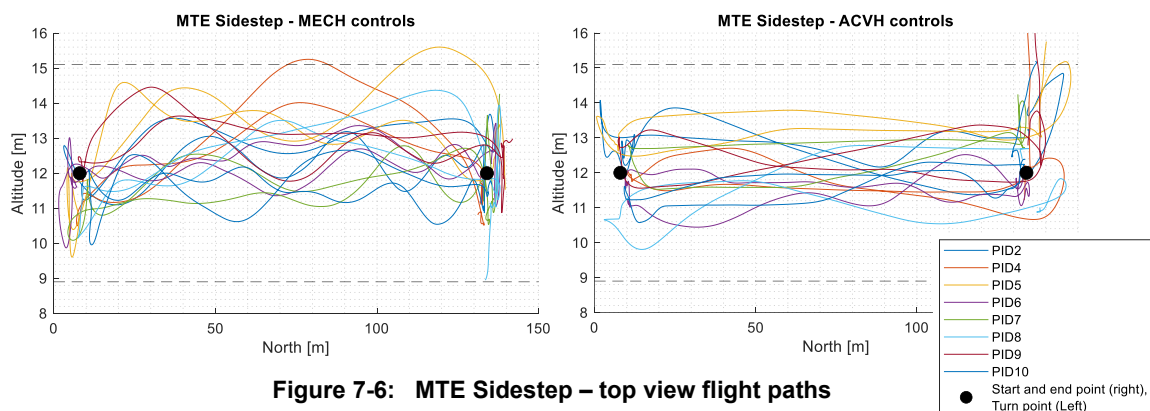


Figure 7-6: MTE Sidestep – top view flight paths

Pilots noticed to focus mainly on the lateral cyclic inputs operating in augmented mode ACVH. This effect was constituted by most of the pilots as follows: When the altitude of the helicopter was set to ideal position, pilots could focus on cyclic control work. However, collective control was kept “attentive hands on”. Moreover, most of the pilots reported that during the aggressive sidestep maneuver, cyclic inputs had to be given mostly to lateral axis. Although, augmented controls were not equipped with an automatic heading hold mode, pilots reported to set their foot not on but close to the pedals, being attentive on to react in case of any event. From pilots’ point of view, the usage of augmented controls allowed to fulfill the MTEs hover and sidestep more aggressive and precise at same time, compared to unaugmented controls.

Taking the results from subjective ratings from above into account, all pilots fulfilled the maneuver within given values from ADS-33 PRF standard reaching HQRs level 2 flying unaugmented. Moreover, operating the helicopter with augmented controls, pilots were even able to stay inside desired values, culminating in HQRs of level 1. Again, as for MTE hover, Bedford workload ratings, see Figure 7-2, showed an equivalent trend starting from level 2 flying unaugmented, leading to level 1 ratings when operating the helicopter with

augmented controls. However, a direct comparison of the deviation from the ideal flight path (RMSE), as given in Figure 7-7 for longitudinal axis (left image) and in helicopter altitude (right image) shows different results: With the increasing aggressiveness flying augmented controls, precision for unaugmented controls in longitudinal axes as well as for helicopter altitude were higher than during augmented flights. However, it should be noted, that pilots stayed within desired values flying unaugmented as well as augmented controls.

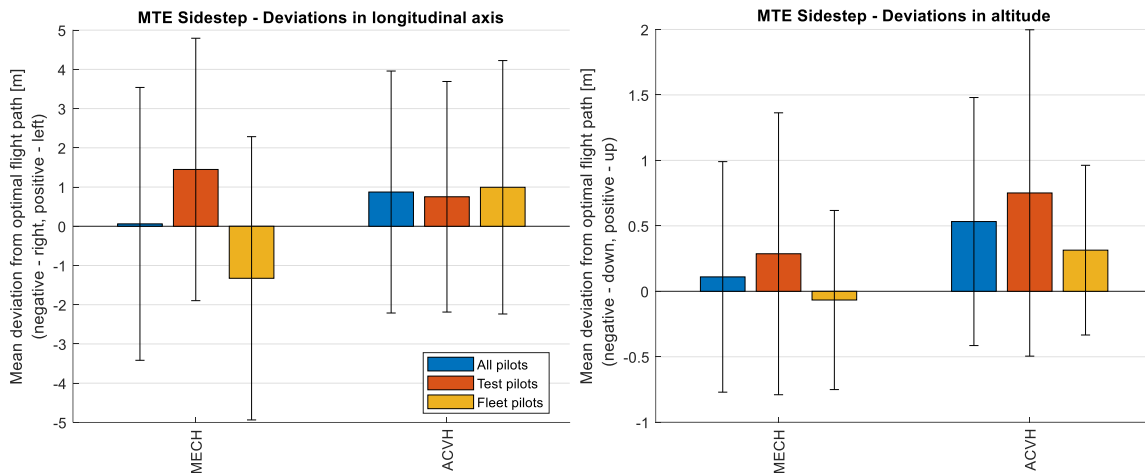


Figure 7-7: MTE Sidestep – deviations from ideal flight paths

Again, observations from above acknowledge pilots' comments to operate the helicopter more aggressive within acceptable workload during augmented controlled flights. Having a view on test pilots versus fleet pilots' results, another effect was observed: While test pilots tried to get as close as possible to the front boarder of the course layout, fleet pilots tried to stay within a safe distance leading to a position rather to the longitudinal back border line, see also Figure 7-6 and Figure 7-7. The consolidated results for MTE sidestep may offer the following main conclusions:

1. The behavior of the basic H135 flight model was accepted well by all participating pilots for low-speed maneuvers such as hover and sidestep.
2. Proceeded unaugmented and augmented flights confirmed a steady improvement in the average assigned HQRs mainly within level 1, and a significant reduction in pilot workload from level 2 (unaugmented controls) to level 1 (augmented controls).
3. The contribution of the ACVH response-type to HQRs enhancement was less significant than its contribution to workload alleviation. The ACVH configuration received mostly level 1 HQRs with a correspondingly very low workload rating (level 1) for both MTEs under consideration. For this configuration, although the HQRs in the sidestep MTE were borderline level 1-2. A ground position control capability in a position hold mode might be likely to improve HQRs during low-speed operations.

Beside the proceeded simulator flights, [93] describes the full development and piloted evaluation of further advanced helicopter response-types using the sliding mode control (SMC) technique within the training phase setup for the full spectrum of unaugmented and

controls for MTEs hover, sidestep, and acceleration – deceleration [2]. The required closed-loop response characteristics were acknowledged as ideal, lower-order, axial transfer functions that conform to predicted level 1 handling qualities. Two-loop, full-authority, output-tracking SMC laws were then synthesized to enforce the closed-loop performance, and to track pilot commands robustly and accurately. Analytical proofs for SMC gain tuning were given for the closed-loop performance to remain robust to unknown, but bounded uncertainties in the input channels, as well as to the effects of rotor modes on closed-loop stability. Finally, [93] includes detailed reports on a further simulator campaign conducted with four experimental test pilots out of the test group of the experiments described in here. Again, the simulation results indicated improved mission task performance, HQRs up to level 1, and a significant decrease in pilot workload to level 1 as compared to unaugmented controls (level 2).

Next, after a short break, the test system environment was changed from “Tegernsee” to “North Sea”. Then, all pilots could practice the helicopter shipboard approach maneuvers using visual and control augmentation modes within three free flights, see Table 6-8. Focus of these flights was to explain and familiarize the pilots with the visual augmentation modes in flight. When no more questions raised, operational block one and two were proceeded after another short break.

7.2 Pilot Workload during Helicopter Ship Approaches using a PAS

Both operational blocks focused on the research questions as given in chapter 6.3.2 and chapter 6.3.3 for helicopter ship approach and landing maneuvers during varying DVE conditions, and varying ship motion states. Proceeded missions proved the expectations about pilot behavior when flying with visual and control augmentation in a harsh maritime environment. Block one mainly investigated on approaching and landing on the ship during decreasing staggered visibility ranges using different modes of visual and control augmentation. In addition, block two concentrated on proceeding near ship maneuvers during low and high ship motions while benefitting from activated modes of visual and control augmentation and flying both augmentations deactivated as basic setup.

As during the training phase, pilot workload ratings, HQRs, VCRs, NASA-TLX weightings were proceeded along ADS-33 PRF standards [2] for given missions subdivided into MTEs. All subjective ratings were assessed along mean values and SD. Flight data observations are introduced to mean and SD values, and by investigating in RMSEs. The statistical analysis was performed by using MATLAB. The three DVE visibility conditions of 800m, 400m, and 200m, two visual augmentation and two control modes resulted in a three (visibility) x two (display) repeated measures matrix. The alpha level of .05 was set for significance. Sign rank tests and Friedmann tests were conducted focusing on the

combinations of the two visual, two control augmentation modes, and DVE conditions. Again, as during the training phase, data is illuminated along a test and fleet pilots' breakdown.

7.2.1 Visual Guidance during Ship Approach in Degraded Visibility

The evaluation of the helicopter ship approach scenarios focused on the research questions and hypotheses as given in chapter 6.3.2. For example, which benefits can the control augmented (ACVH), and enhanced visual augmentation concept (ESAS/ ESLS) offer to the pilot to fly at smoother glide path stability with same workload compared to the basic visual augmentation concept (SAS/ SLS). Table 7-1 specifies the nomenclature of given figures and tables for complemented twelve offshore flights of each pilot.

No.	Label	DVE visibility range (m)	Visual augmentation mode	Control augmentation mode
1	1-1-1-	800	SAS+SLS	MECH
2	1-1-1-	400	SAS+SLS	MECH
3	1-1-1-	200	SAS+SLS	MECH
4	1-2-1-	800	ESAS+ESLS	MECH
5	1-2-1-	400	ESAS+ESLS	MECH
6	1-2-1-	200	ESAS+ESLS	MECH
7	1-1-3-	800	SAS+SLS	ACVH
8	1-1-3-	400	SAS+SLS	ACVH
9	1-1-3-	200	SAS+SLS	ACVH
10	1-2-3-	800	ESAS+ESLS	ACVH
11	1-2-3-	400	ESAS+ESLS	ACVH
12	1-2-3-	200	ESAS+ESLS	ACVH

Table 7-1: HELIOP test procedures and modes

Pilot workload ratings: While DVE conditions constantly increased over the flights, the workload and HQRs, see Figure 7-8, of all pilots almost always remained within level 1 when pilots operated the helicopter with visual and control augmentation. It was found that the decreasing visibility ranges had no significant ($F = 7.0, 1.4, 1.0, 2.33$; $p = 0.008, 0.279, 0.393, 0.134$) influence except the degraded visibility of 800m. The similarity of ratings of test and fleet pilots may be associated with the fact that HMD and control visual augmentation design was established together with further maritime test and fleet pilots, who pointed out the need for low latency in control design, and the high outside scenery conformity of superimposed 3D symbology, which was rated as accepted well by most of the participating pilots.

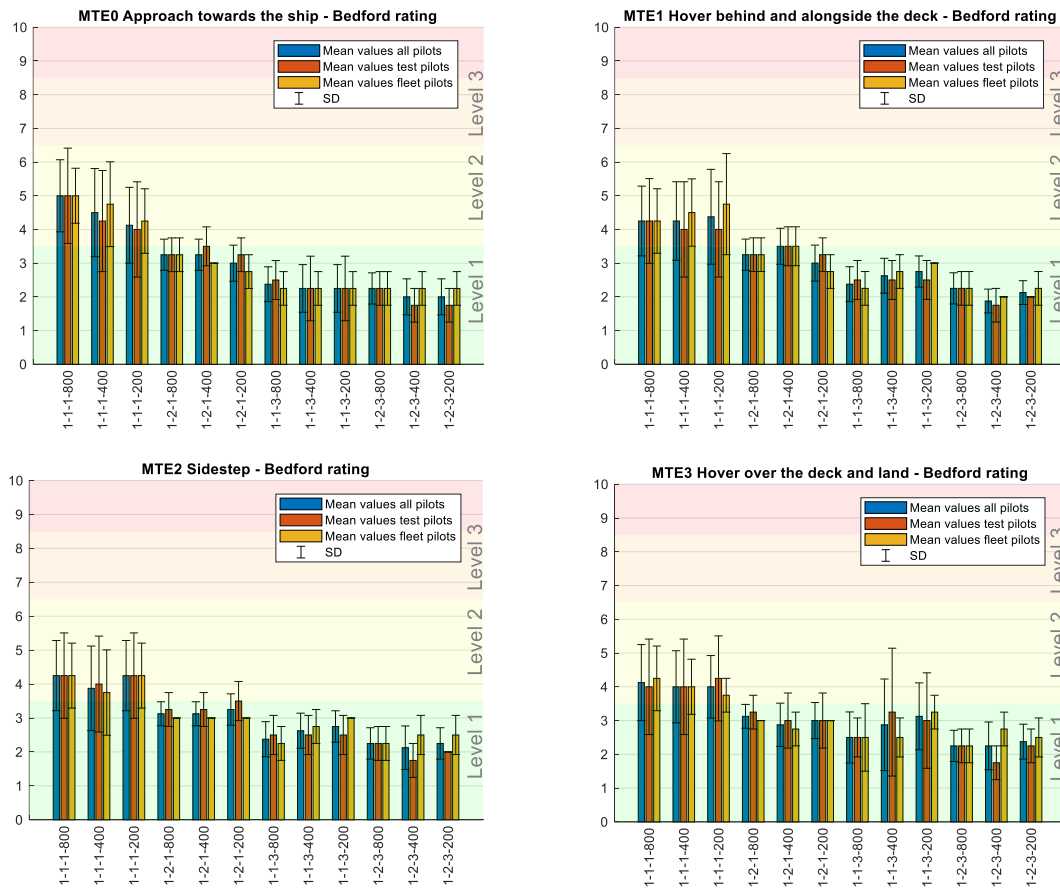


Figure 7-8: Bedford ratings of helicopter ship approach and landing, N=8

Regarding flying in basic mode MECH and then control augmentation mode ACVH, here most of the pilots noted being able to even more focus on the visual augmentation modes. During all DVE visibility ranges, the ESAS design offered the pilots an intuitive and ideal way to position the helicopter in lateral axis and optimal glide path altitude (MTE0). In contrast, the pilots benefitted flying with the SAS design in higher visual feedback to precise the flight path in lateral axis, but also less in altitude. Some pilots commented that it might be an option to combine both SAS and ESAS. When it came to the final approach phase (MTE 1, 2, and 3), all pilots benefitted from the SLS and ESLs visual augmentation to bring the helicopter to a stabilized hover position near to the left back side of the ship with acceptable workload. This was even possible during a minimum visual range of 200m, where the ship was not visually yet in site at the MAP. Moreover, pilots stated to be able to fly with lower effort in flights with ACVH control augmentation mode during all DVE visibility ranges. Finally, when pilots proceeded the hover over deck and landing maneuvers, they stated to benefit more from control than from visual augmentation: It turned out, that visual augmentation reached its limits when it came to the restricted FoV of the HMD operating the helicopter over deck with much head movement needed for lateral repositioning the helicopter to an ideal landing position. This challenge was compensated by most of the pilots with now (MTE3) focusing on the outside scenery ship deck wall and the

superimposed visual augmentation, in detail the elevator bar, at same time while keeping the helicopter with minimum control inputs over the ship deck. Finally, taking hypotheses H1 into account, following main findings are given:

1. Visual augmentation activated, and control augmentation deactivated: The HMD visual augmentation had a significant effect ($V = 7$; $p = 0.016$; $ZD = 1$) on lowering pilot workload ratings during the DVE visibility range of 800m while control augmentation was deactivated. Moreover, strong effects on decreasing pilot workload ratings were found when control augmentation was deactivated during the DVE visibility range of 400m ($V = 6$; $p = 0.125$; $ZD = 3$), and 200m ($V = 7$; $p = 0.070$; $ZD = 2$).
2. However, pilots benefitted from both visual augmentation approach types of SAS/ESAS during 800m, 400m, and 200m visibility range ($V = 4, 5, 5$; $p = 1.000, 0.727, 0.727$; $ZD = 7, 6, 6$) while control augmentation was activated.
3. All pilots evaluated the subjective workload significantly lower ($V = 8$; $p = 0.008$; $ZD = 0$) when operating the helicopter with control augmentation being in mode ACVH in DVE conditions of 800m and 400m with the assistance of both approach visual augmentation types (SAS and ESAS).
4. Finally, the DVE condition visibility had a significant impact on pilot workload ratings during the ship approach when SAS visual augmentation was activated only ($F = 7.0$; $p = 0.008$, $ZD = 0$). However, remaining three variants, MECH+ESAS, ACVH+SAS, ACVH+ESAS ($F = 1.4, 1.0, 2.3$; $p = 0.279, 0.393, 0.134$) indicated that pilots relied on the HMD visual augmentation during flight.

In sum, the H1 “Pilot workload is at lower level using visual and control augmented PAS than visual augmented PAS during decreasing visibility ranges within the approach segment” can be taken as accepted for RQ1. Pilot workload ratings were at a median of 3 (level 1) while flying visual augmented. Moreover, when control augmentation was activated on top, pilot workload further decreased to a median of 2 (constant level 1). However, the DVE condition visibility range turned out to be not statistically significant during the helicopter ship approach. Therefore, training effects of repeated flights should be considered as well.

Pilot HQRs: Besides subjective workload ratings, pilots gave valuable feedback on corresponding HQRs for the control augmentation after each flight. Workload ratings and HQRs, see Figure 7-9, indicated similar trends.

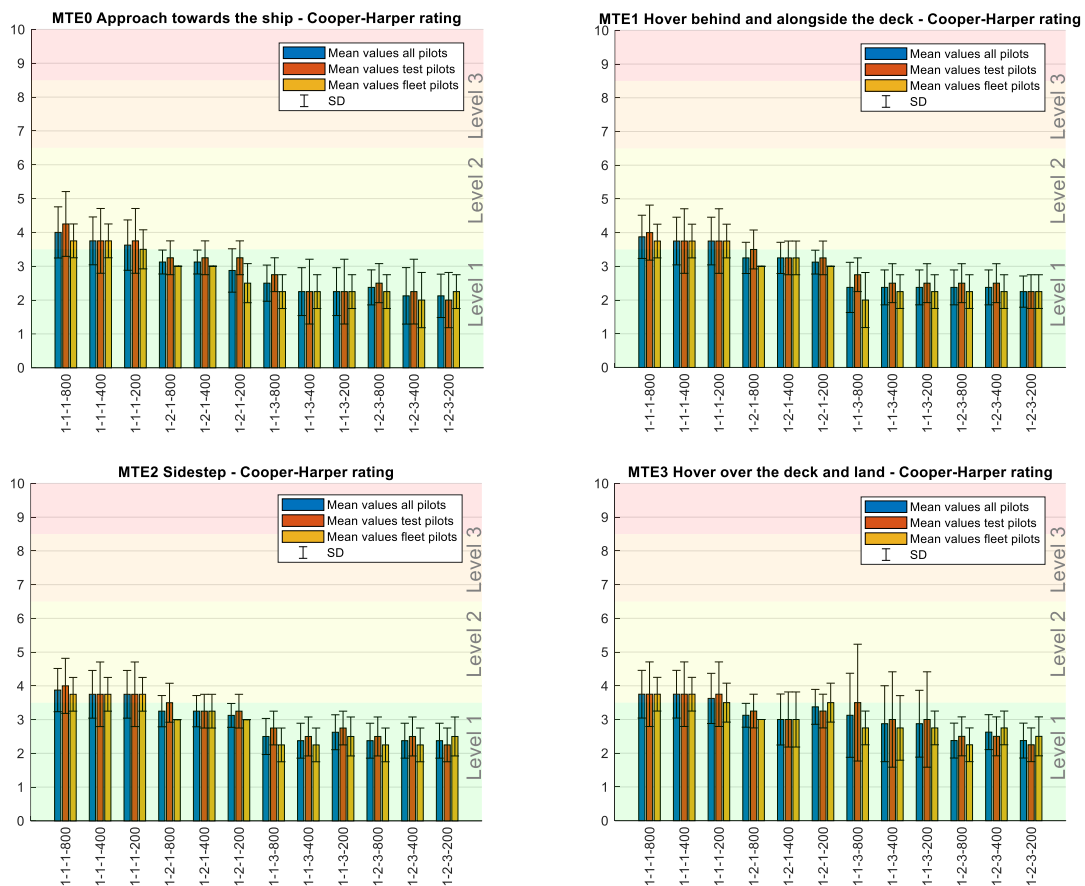


Figure 7-9: Cooper-Harper ratings of helicopter ship approach and landing, N=8

Pilots HQRs almost reached borderline between level 2 and level 1 while flying unaugmented (MECH) during all MTEs. When pilots were offered to operate the helicopter with the advanced flight control mode ACVH, HQRs turned out to be all at almost inside level 1 during all MTEs. Regarding the ship approach (MTE0), pilots noted the main difference between flying control unaugmented and augmented as follows: While flying with the activated advanced flight control mode, generally fewer inputs were needed when a constant glide path was set once by the pilot. During MTE0 pilots mainly focused on giving collective inputs, while during the final approach and landing (MTE 1 – 3) pilots gave more cyclic control inputs. Pilots recommended that fewer needed inputs were needed in general while flying with control augmentation, culminating in a flying “attentive hands on”, and level 1 HQRs. During the sidestep maneuver, pilots were able to fulfill the task without entering heavy Pilot Induced Oscillations (PIOs) as suspected from experiences during real helicopter ship maneuvers. Pilots recommended to enter small PIOs when rolling and heaving outside visual cues as the ship where in the central FoV during MTE1 – 3. However, motion cueing of the simulator was stated to be realistic from all pilots, even since the simulator is a fixed-base simulator. The wide dome projection, the dynamic and highly detailed maritime environment, the realistic feedback from the controls, and the H135 GenSim flight model were referenced by most of the pilots for giving this positive feedback.

Pilot effort ratings: In addition to the Bedford workload ratings and HQRs, the five-point DIPES scale offered pilots to rate the difficulty of the deck approaches and landings. Again, as for all subjective ratings, DIPES ratings were given by all pilots after each flight for each MTE, see Figure 7-10. It was found that the decreasing visibility had no influence on the ratings, meaning almost all DIPES ratings were within acceptable level between ratings of 1 – 3. An important fact for the DIPES scale is that ratings are given on perceived ability of an average fleet pilot, so although a highly capable test pilot may be able to safely land for a given DVE condition, a rating is awarded which excludes that point from the rating if it is deemed too difficult for a fleet pilot to perform.

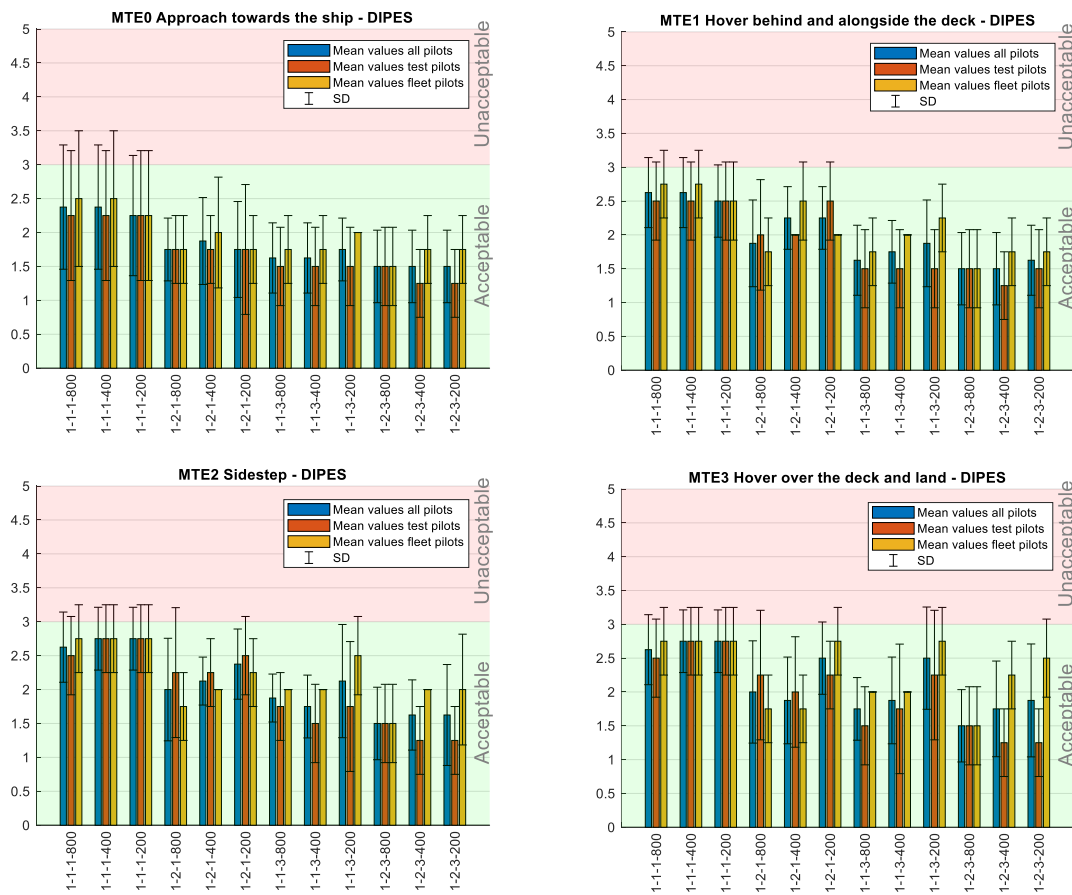


Figure 7-10: DIPES ratings of helicopter ship approach and landing, N=8

All pilots were able to perform all flights with a successful landing. Pilots recommended that decreasing visibility had no influence on their effort until they reached the rear side of the ship deck at the end of MTE0. This effect was justified by all pilots that the HMD visual augmentation gave a highly intuitive synthetic projection for the approach when no outside scenery was visible at all. The 3D conformal ship approach visual guidance in combination with the head up flight parameters offered all pilots to proceed the IMC approach with flying “eyes out of the cockpit” constantly. Even this opportunity was emphasized by most of the pilots to be able to localize in parallel the sea surface and the moving ship visually at MTE1. However, pilots commented challenges were rising when the visibility range was decreased

during sidestep and landing maneuvers (MTE2 and 3). Here, pilots reported to rely on the HMD visual augmentation as a visual benefit to be aware from the deck wall, but preferred as expected, HMD visual augmentation overlapping with the outside scenery ship in sight: During visibility ranges of 800m and 400m this was feasible, but at minimum visibility range of 200m pilots were not till then able to localize the deck visually when they were almost above the landing deck.

Visual cue ratings: Regarding the rating of the HMD visual augmentation usability in flight itself, given VCRs of the pilots were transferred into the Usable Cue Environments (UCEs). The corresponding UCE levels, see Figure 7-11 (No. 1 – 12 for given pilot assistance see Table 7-1), show an enhanced usability of the HMD visual augmentation, all almost inside UCE level 1, while DVE visibility was constantly decreasing. Moreover, ESAS/ ESLS (No. 7 – 12) were rated higher than SLS/ SAS (No. 1 – 6) in general for all MTEs.

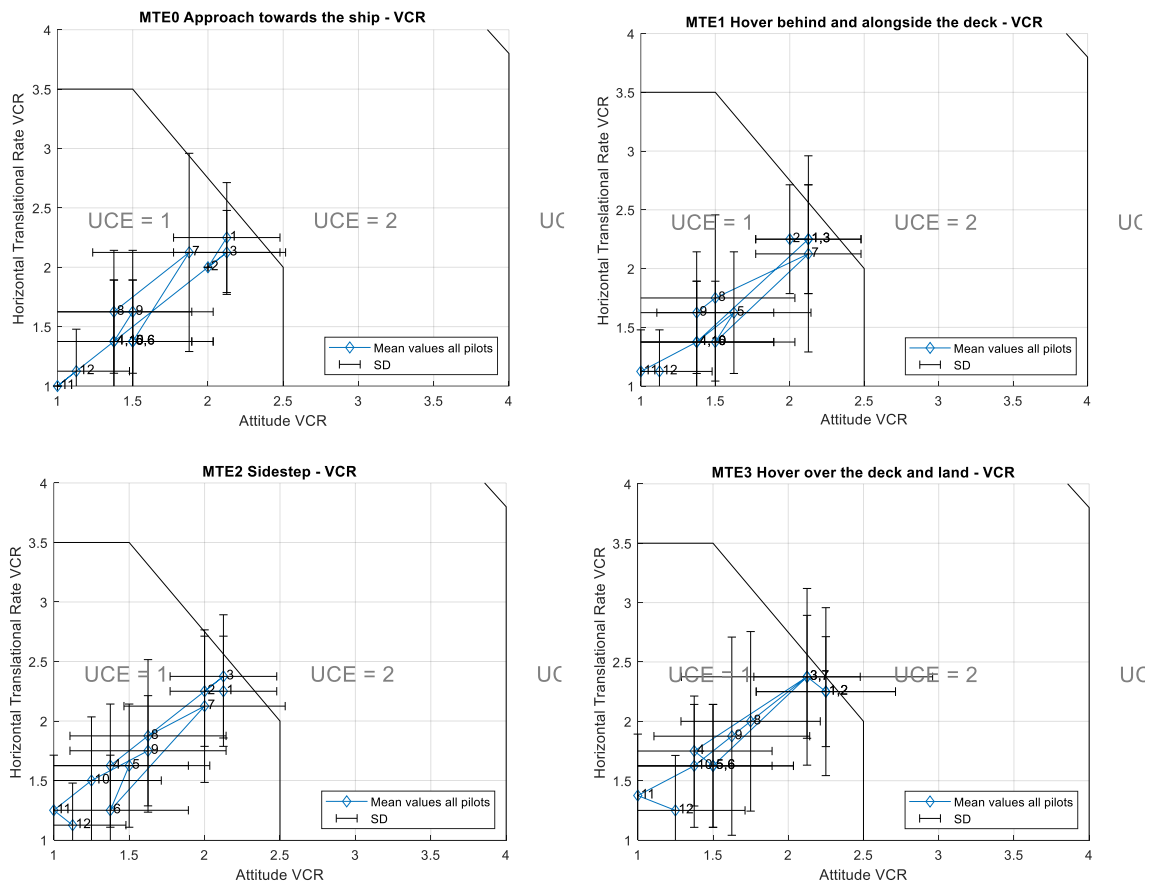


Figure 7-11: VCR ratings of helicopter ship approach and landing, N=8

Pilot stated the main issues in rating the SAS/ SLS and ESAS/ ESLS as follows:

1. For all the MTEs, the VCRs for the HMD visual augmentation modes are similar with respect to the rating being located inside UCE = 1. This result might be an indication that the information displayed in the HMD for all phases of flight are well balanced.
2. The VCRs got its highest ratings during all MTEs within the worst DVE visibility conditions. Pilots' comments emphasized this finding: The visual augmentation of

3D synthetic visual cues during approach and landing allowed the pilots to fulfill the given tasks even in the harshest DVE condition.

Taking the general combinations of visual and control augmentation within the VCRs, see Figure 7-12, into account, the findings can be extended as follows.

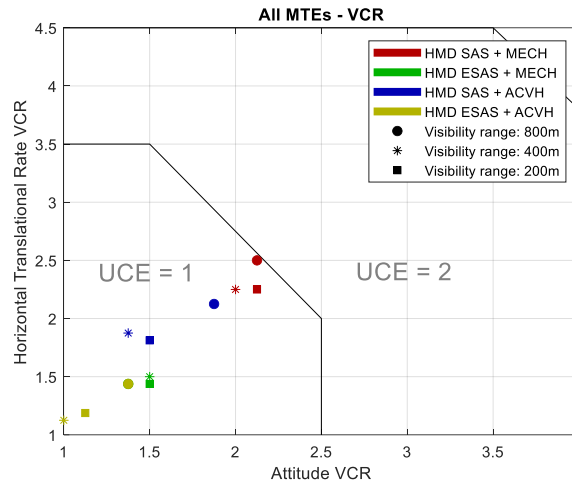


Figure 7-12: Medians of all VCR ratings, N=8

The HMD visual augmentation types are both inside UCE level 1, independent from the control augmentation mode. While control augmentation was activated on top, both modes postponed to highest VCR ratings of UCE level 1 resulting again in ESAS/ ESLS being higher rated as SAS/ SLS. This finding might be an indication that a combination of visual and control augmentation will give pilots the opportunity to use spare capacity given from less attention needed for controls to use for paying more attention on the visual augmentation. Taking hypotheses H2 into account, the following main findings are given:

3. When flying only visual augmented, ESAS showed a higher but not significant effect in comparison to SAS increasing pilots' VCRs during all DVE weather conditions of 800m ($V = 6$; $p = 0.125$; $ZD = 3$), 400m ($V = 6$; $p = 0.289$; $ZD = 4$), and 200m ($V = 6$; $p = 0.125$; $ZD = 3$) visibility range. Moreover, while flying visual and control augmented, given VCRs for ESAS were even higher but still not significant in comparison to SAS VCRs. However, all VCRs of SAS as well as ESAS were within UCE level 1 meaning to be highly usable for flying within the tested DVE conditions.
4. While control augmentation mode ACVH was activated on top, VCRs delivered a significance for DVE condition decreased visibility ranges using SAS+ACVH ($F = 4.79$; $p = 0.026$). However, ESAS+ACVH showed a tendency towards a significance ($F = 2.882$; $p = 0.089$) tending again as described in the results of H1, that visual and control augmentation activated both together delivered best ratings in pilot workload and VCRs.

In sum, the H2 "Pilot workload is at lower level using enhanced visual augmentation mode (ESAS) than visual augmentation mode (SAS) during decreasing visibility ranges within the approach segment" is not supported. However, the visual augmentation concepts SAS as

well as ESAS were accepted for the given tasks by all pilots with a UCE level 1 rating when visual augmentation was activated only. Moreover, VCRs increased to a constant UCE level 1 while flying with visual and control augmentation being activated both. Here, the improvement towards the ideal UCE rating of 1-1 might be an indication, that pilots are even more able to use and benefit from visual augmentation while control augmentation is activated.

In addition to pilot workload and effort ratings, HQRs, and VCRs, questionnaires using a Likert scale were used to further evaluate the elements of the visual augmentation and the corresponding color concept. The questionnaires were proceeded with all participating pilots at the end of proceeded simulated flights. All pilots confirmed that the concepts of the virtual approach and landing symbology were intuitive to be used in flight, even within a short time of familiarization, see Figure 7-13. Moreover, none of the pilots perceived the visualization of the approach symbology as misleading, and did not occlude any outside scenery information, such as the moving ship ahead of the helicopter.

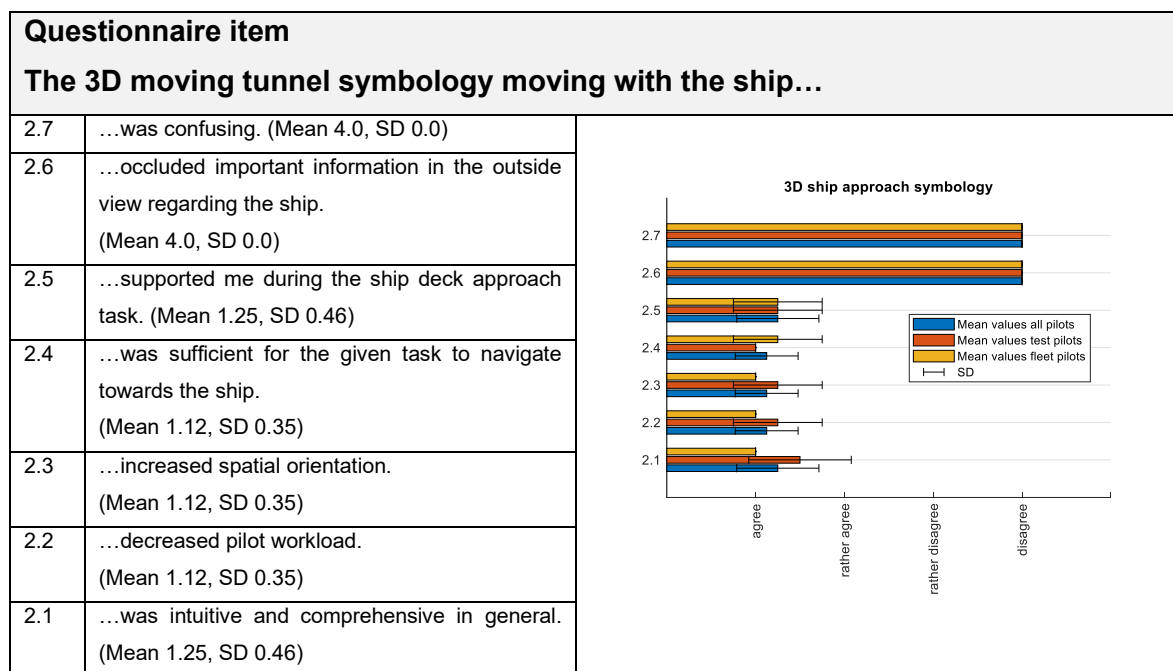


Figure 7-13: Pilot evaluations of the 3D-conformal approach symbology, N=8

Second, the results of the complementary questionnaire for the 3D conformal landing symbology, see Figure 7-14, takes similar aspects into account. As for the approach symbology, pilots also confirmed the landing symbology being highly intuitive in use during flight. However, with respect to the limited FoV of the HMD, pilots recommended that only few elements of the landing symbology, such as the elevator bar within the triangle, were mainly used superimposed with the outside scenery ship deck rear wall during the maneuvers hover over deck and landing.

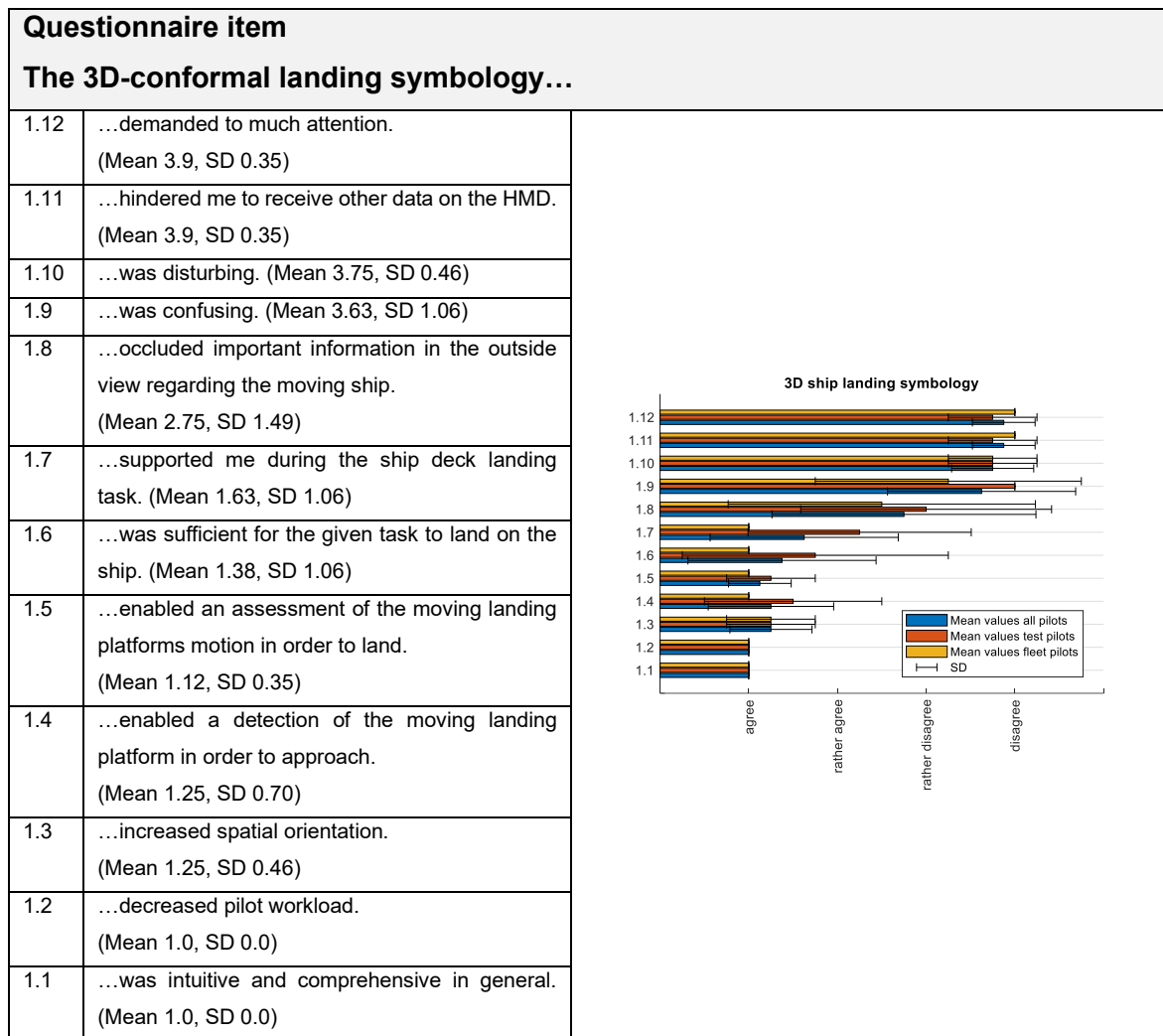


Figure 7-14: Pilot evaluations of the 3D-conformal landing symbology, N=8

Again, none of the pilots stated that decluttered 3D landing and 2D flight parameters information affected each other in a negative way during the two main tasks during the final approach, maneuvering the helicopter over the deck in DVE conditions, and keeping important flight parameters in sight while landing heads-up.

Third, the HMD visual augmentation concept was assessed by all pilots also investigating the visualization of the 2D head-up flight parameters, see Figure 7-15. The ability to identify and distinguish between helicopter and ship information by the arrangement and coloring of the flight guidance information allowed pilots to fly visual augmented at low workload in the end.

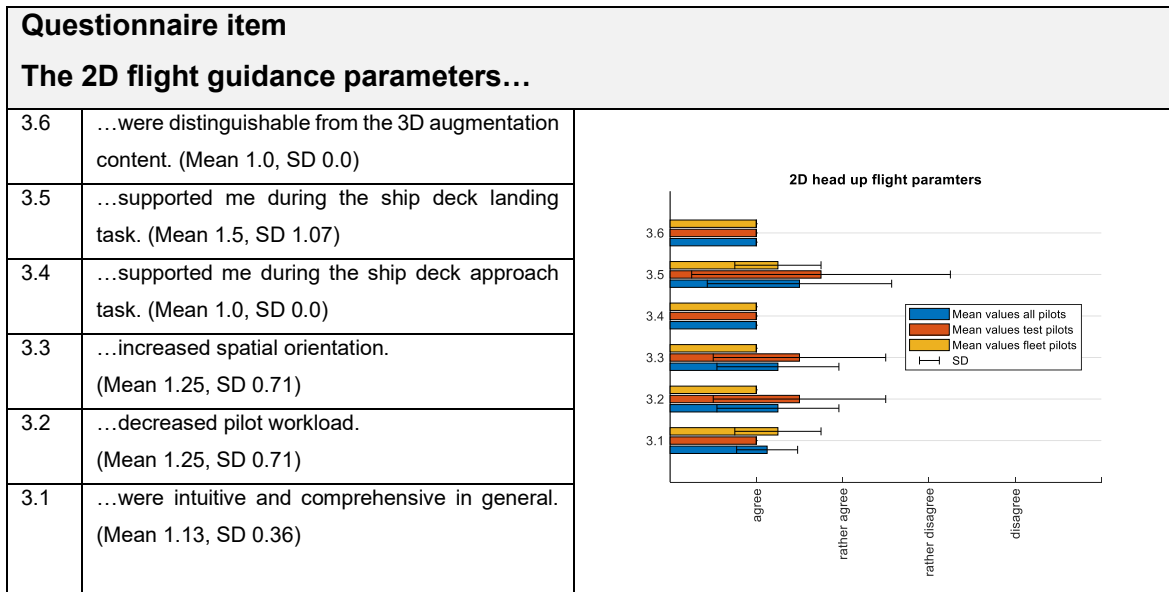


Figure 7-15: Pilot evaluations of the 2D-flight parameters, N=8

All pilots emphasized that the flight guidance information being head fixed was a great benefit to always have the main flight parameters in sight. However, some of the pilots advised to arrange the speed and altitude tape more to the left and right vertical borders to have an even more unobstructed central FoV. Moreover, the 2D flight guidance visualization was almost used exclusively while ignoring the HDD PFD, which more lead to spatial disorientation.

Finally, having a detailed look on the rating of the HMD symbology color concept, see Figure 7-16, pilots stated that the consequent use of colors independent from the visual guidance modes and types during approach and landing offered a continuous allocation of helicopter and ship information.

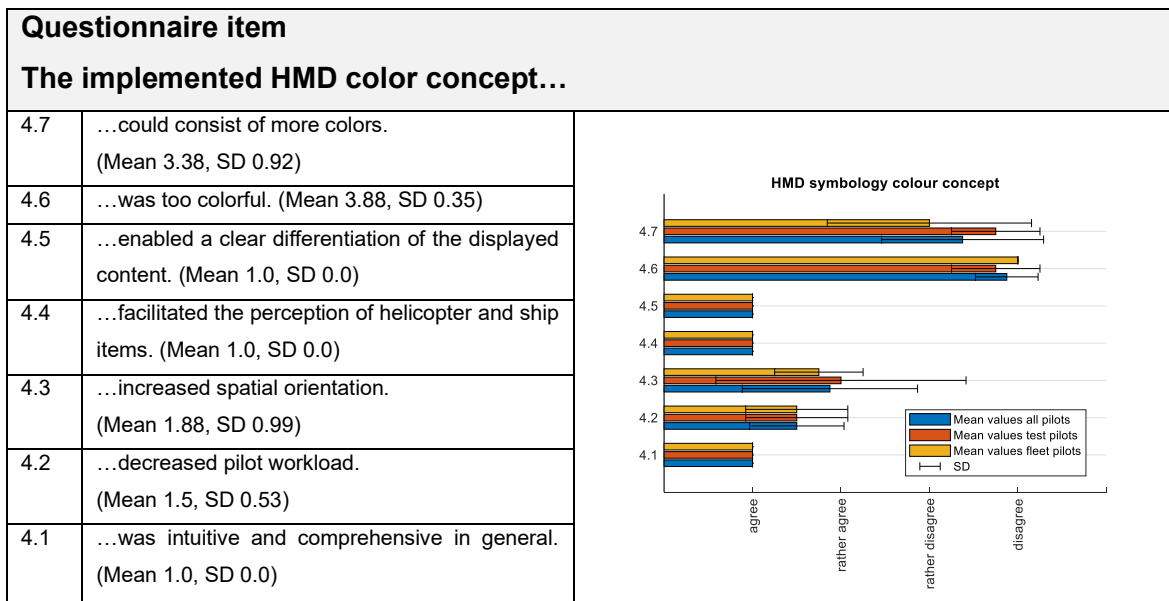


Figure 7-16: Pilot evaluations of the HMD color concept, N=8

Mainly, magenta colors assigned to helicopters parameters and cyan coloring to ship related information harmonized well in terms of brightness and contrast. All pilots advocated

a colored HMD display. It should be noted that HMDs used in real helicopters at the actual stage of this work are of monochrome green coloring. However, the number of colors to be used was set by most of the pilots by not more than three.

Although similar trends can be seen for both the approach and the landing segment, further investigations were proceeded for the final approach segment. The use of different advanced flight control modes, as well as landing on the ship during demanding ship states are from main interest in the following.

7.2.2 Obstacle Awareness during Final Recovery while demanding Ship Motions

The results presented in this section were obtained from operational block two of piloted simulations. Again, the helicopter final approach scenario investigated on the research questions and hypotheses as given in chapter 6.3.2. As per description, does the use of flying with HMD visual augmentation activated or conventional VFR (no HMD) differ in pilot workload in harsh conditions such as during low and high ship states? Which benefits can be taken from different advanced flight control modes (TRC, ACVH) regarding handling qualities and a further workload reduction on top? For the SCONE ship motions to affect the pilot workload and flying qualities, low (Level 1) and high (Level 3) ship motions were simulated during the final approaches. In contrast to operational block one, the DVE condition visual range was fixed to 800m, and focus was set on different ship motions and visual and control augmentations being deactivated or activated while operating the helicopter in the immediate vicinity of the ship.

Pilot workload ratings and HQRs during low and high ship states: Based on the given Bedford workload ratings from the simulated landing tasks, and considering corresponding HQRs, all given in Figure 7-17, a wide spectrum of comparable conventional, visual and control augmented flights have been proceeded. It is interesting to note that repeated flights were conducted using the same SCONE recordings of low and high ship states for all pilots. To appreciate a better difference between the two advanced flight control modes and visual augmentation being deactivated or activated during the final approach, both workload ratings and HQRs are examined next to each other.

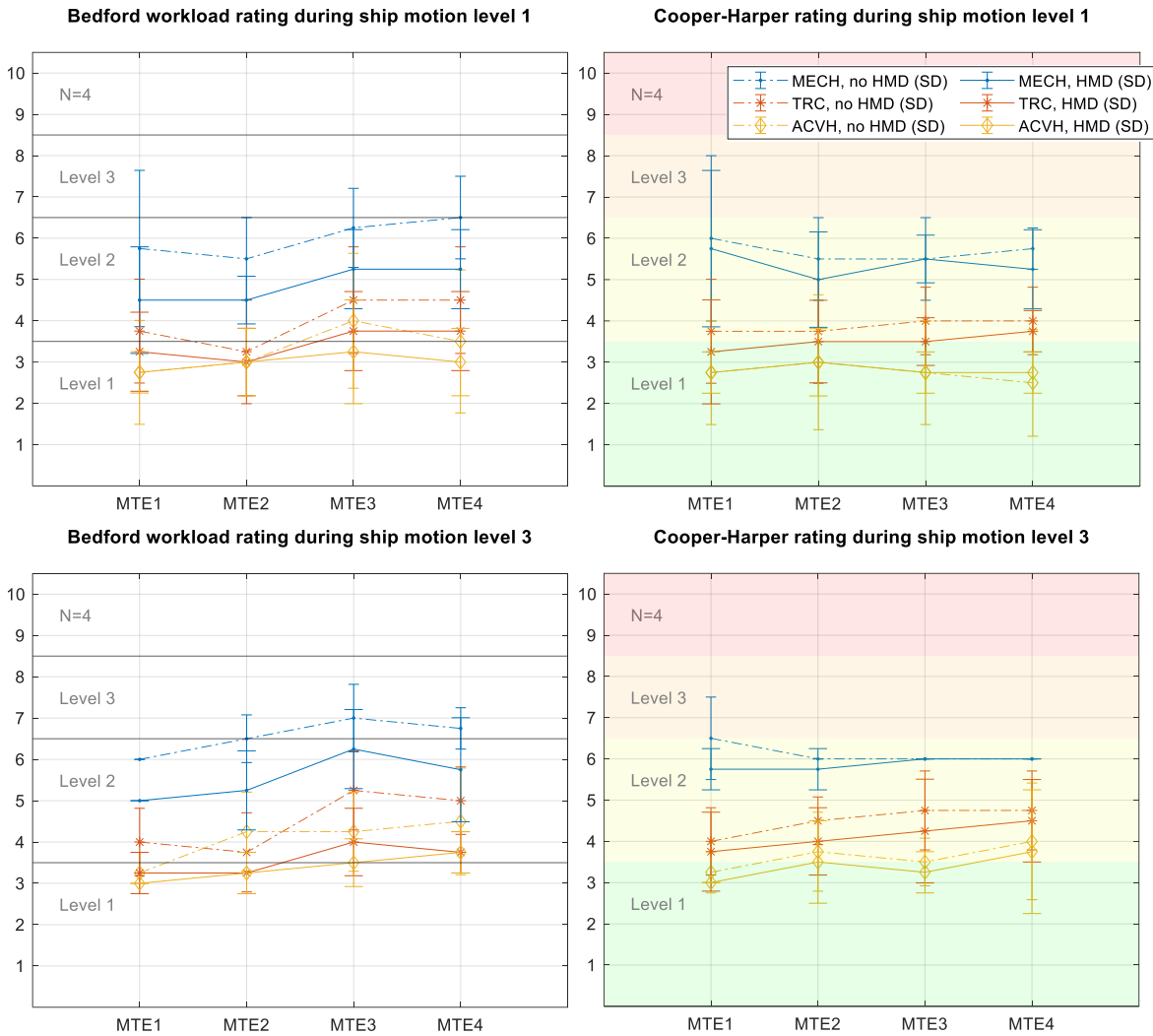


Figure 7-17: Bedford and Cooper-Harper ratings of helicopter ship final recovery

Focusing on Figure 7-17 left row, pilot workload increased with increasing ship motion level. Beyond that, while activated control augmentation reduced pilot workload even to almost level 1 independent from the ship motions level, activated visual augmentation further reduced pilot workload to a constant level 1 pilot workload rating during almost all MTEs. Nevertheless, even while flying conventional VFR (no HMD) with no advanced flight mode being activated, pilot workload was barely acceptable. Although similar trends can be seen for both ship motions levels, a difference is observed for MTE3 hover over deck: Here, the pilot workload increased in general. The task to proceed the sidestep and stopping the helicopter at the optimal point in the middle over the deck was rated as being high demanding from all pilots as the deck is heaving and rolling in parallel. Taking Figure 7-17 right row into account, the advanced flight control modes seemed to compensate this effect, as observed on the HQRs. This result was argued by most of the pilots as the following: While flying with advanced flight control modes being activated, control inputs were focused on the lateral cyclic inputs only when a stable forward flight in an acceptable safe altitude was set once directly before proceeding the sidestep. Consequently, pilots used this spare

capacity to focus on visual augmentation and the outside scenery to reach the ideal position over deck and wait for a quiescent period to land. Again, when the final position over deck was reached, a stable setting of controls and visual cues allowed pilots to wait for the quiescent period even up to one minute for the push down. In sum, taking pilot workload ratings and HQRs into account, the following main results are given:

1. All pilots completed all flights with a successful landing on the moving ship, even in harshest conditions, and while visual and control augmentation were deactivated or activated. While approaching VFR (no HMD) with no advanced flight control mode being activated resulted in just barely level 2 ratings, in contrast operating the helicopter with visual and control augmentation being activated showed up to and inside level 1 ratings.
2. Final approach and landing with control augmentation (TRC or ACVH) being activated generated spare capacity, which pilots stated to use on focusing on the HMD visual augmentation to maneuver the helicopter to an ideal position over deck.
3. Pilot ratings and comments on both advanced flight control modes to use for the sequence of the final ship approach were positive, preferences for TRC or ACVH more depended on pilots' experience and training using the corresponding mode in real flight, rather than in the simulated flights.
4. Low, and high ship motions had not a great impact on pilot workload ratings during the final ship approach when visual and control augmentation were activated simultaneously. The final approach MTEs hover over deck and land turned out to be the highest demanding tasks for most of the pilots.

In the following, the benefits of the HMD and advanced flight control modes for pilots during nearby ship maneuvers, such as reduced workload and improved SA, are further broken down into dedicated items such as mental demand and effort to reveal specific effects of respectively the visual and control augmentation.

NASA-TLX weightings during low ship states: Giving pilots the chance to detail their workload ratings of proceeded MTEs allowed an exploration of the main facets of mental- (MD), physical- (PD), and temporal demand (TD), performance (P) for needed control inputs, effort (E), and finally frustration (F). These six categories range within a linear scaling of “not a factor” (0%) towards “is demanding” (50%) and culminating in “needs almost full attention” (100%). Here, pilots had the opportunity to break down their overall task load (100%), and at same time allocate their comments on a linear distributed scale referring to the specific MTEs of the final recovery mission, as given in Figure 7-18. Figure 7-18 and Figure 7-19 show mean values.

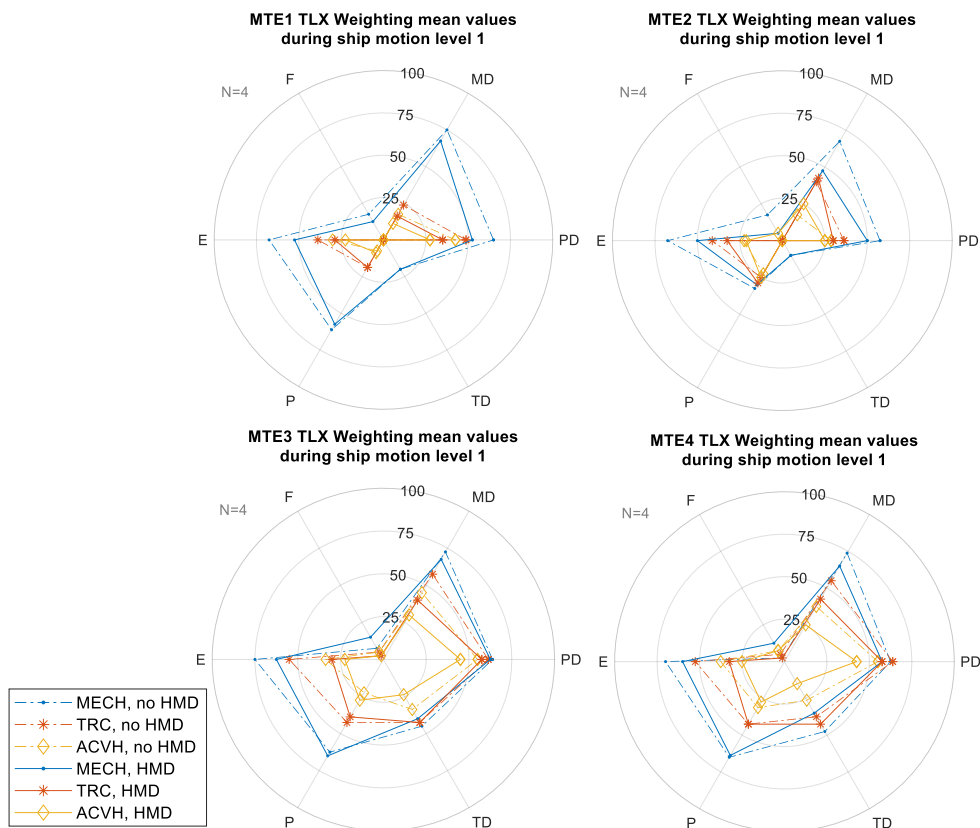


Figure 7-18: NASA-TLX weightings of helicopter ship final recovery – Level 1

When pilots arrived at the ship deck and had to find a basic setup for aligning in speed and direction beside the ship (MTE1), needed control input performance in all axes went along with converging own speed and direction to ships speed and path (MD). Second, proceeding the sidestep (MTE2) was felt by most of the pilots not as highly demanding (MD, PD, TD), however the maneuver cost a lot of coordination effort (E) to keep the helicopters nose aligned with ships heading. Now, when the helicopter reached the edge of the deck, all categories, except frustration highly increased due to factors such as being close to the rear deck wall, the deck itself, and trying to keep a stable hover within a highly dynamic scenery. The task load stayed up high until the landing (MTE4), being the end of the mission. Turning from needed task load dimensions towards differences within its characteristics while using different visual and control augmentations, the following main results are given:

1. Operating the helicopter with visual and control augmentation near the ship, all six categories of the NASA-TLX are at an acceptable level. However, regarding the MTEs hover over deck (MTE 3) and landing (MTE 4), pilots' task load increased when the helicopter crossed the edge of the deck compared to hover alongside and sidestep maneuvers (MTE 1 and 2).
2. Both control augmentation modes TRC and ACVH decreased pilots task loads, originated by less needed pilots control inputs. Nevertheless, a constant high

temporal demand was observed while hovering over the deck (MTE3), turning out to be most demanding task.

3. Visual augmentation further reduced pilots task loads in all phases of the final approach, even during hover over deck and landing maneuvers. Here, pilots strongly benefitted from visual and control augmentation being activated both in parallel.
4. Frustration was not a factor during all MTEs at all. Pilots justified that by the two aspects: A successful proceeding of all missions was possible in general supported by the realistic control behavior of the helicopter and the surrounding highly detailed maritime environment.

In the following, these findings are compared to the last flights of operational block two, where pilots were put into the same situation, but now with the ship operating in high motions.

NASA-TLX weightings during high ship states: The increase of ship motions level from “low” (SCONE level 1) to “high” (SCONE level 3) during the final approach MTEs allowed investigations about influences of different ship states as being often observed during DVEs [97], see Figure 7-19.

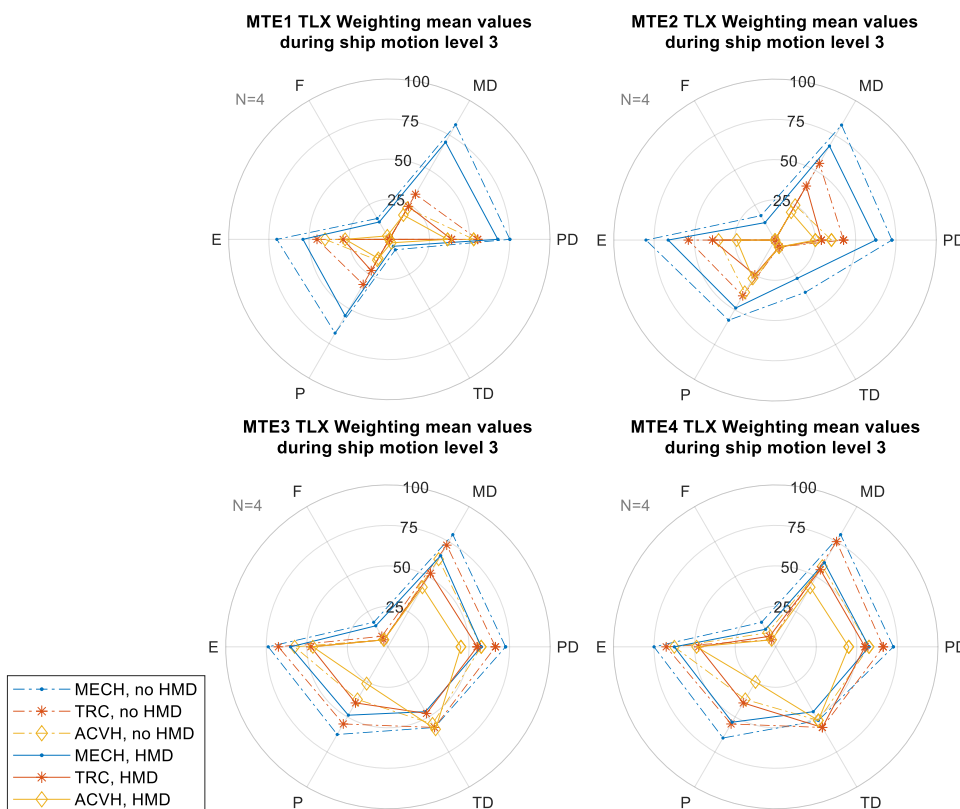


Figure 7-19: NASA-TLX weightings of helicopter ship final recovery – Level 3

Moreover, the repeated flights within the high ship motion level offered a deeper analysis how visual and control augmentation may change pilots task loads in comparison to low ship states, see all Figure 7-18.

When the helicopter arrived again behind the deck (MTE1), pilots stated that task load did not change at all. Pilots strongly focused on the ships behavior to primarily estimate increased heaving and rolling ship motions while keeping the helicopter stable at same time (MD, PD). Proceeding the sidestep maneuver (MTE2) in the following, pilots task load heavily increased in comparison to MTE1, and even unlike to MTE2 during low ship motions. Here, most of the pilots benefitted from activated advanced flight control modes to not run into PIOs when outside scenery visual cues, in detail the rear ship deck wall, were strongly rolling and heaving. The risk of adjusting the helicopters behavior to ships motions turned out to be suppressed by the room-stable HMD hover symbology. Furthermore, flying deactivated in contrast to operating the helicopter with activated advanced flight control modes strongly decreased pilot task loads (PD, P; E), now spent for control inputs. Having crossed the edge of the deck, and finally coming to a stable hover over deck (MTE3), and prepare for landing (MTE4), pilot task loads were at highest level of all MTEs and in comparison, to low ship motions setup. Here, pilots stated that control augmentation created the greatest benefit while visual augmentation was used only with some elements of the symbology: The elevator bar increased pilots SA in combination with the outside scenery substantiated by the capability to not hit the landing deck with the helicopters landing gear while keeping heads up flying.

Taking main findings of proceeding the final recovery within the high ship motions level into account, and at same time comparing all MTEs to low ship motions pilots task load ratings, the following results are given:

1. The most demanding tasks while operating the helicopter in the phase of final approach during high ship motions were the maneuvers hover over deck and land. Here, pilots TLX ratings corresponded with given feedbacks that synthetic visual cues visualized on the HMD highly enhanced SA while operating the helicopter in nearby ship scenarios. Overall, pilots task loads flying with control and visual augmentation activated were at an acceptable level.
2. Control augmentation created the greatest benefits during high ship motions when the helicopter fulfilled the sidestep and hover over deck maneuver. When the helicopter reached the edge of the deck, pilots temporal demand raised even with control and visual augmentation being activated. The increased time pressure was commented by most of the pilots that hover over deck time should be minimized in order to not hit the landing deck or rear ship deck wall, if unexpected ship movements might come up during high ship motions.
3. Taking pilots TLX ratings during low and high ship motions both into account, visual augmentation constantly decreased pilots task loads in all phases of the final recovery. Again, as during the helicopter ship approach, see chapter 7.2.1, greatest

benefits in lowering pilots task loads had been reached when visual and control augmentation were activated both at same time.

4. Again, arranging TLX ratings for low and high ship motions both side by side, nearby ship maneuvers such as when the helicopter crossed the edge of the deck (MTE2 and MTE3) turned out to be the highest demanding during the final approach phase.

For investigating on the benefits and challenges of the HMD visual augmentation during the final approach phase in detail, pilots were asked about all specific elements of the landing and obstacle awareness visual guidance, see Figure 7-20, after having fulfilled all flights. Here, the pilots were asked about the usability of the elements of the 3D landing symbology to keep own position stable besides, along, and while passing the edge of the deck (MTE1 and 2). And, if the obstacle awareness visual guidance supported the pilots to keep relative position over deck and estimating a safe landing position (MTE3 and 4) before landing:

- Usability of the trampoline symbology (MTE1 – 4, x.1, x.2, all as labeled in Figure 7-20),
- usability of the deck marking symbology (MTE1 – 4, x.3, x.4), and
- usability of the synthetic horizon in flight (MTE1 and MTE2, x.5, x.6, x.7) or the elevator bar (MTE3 and MTE4, x.5, x.6).

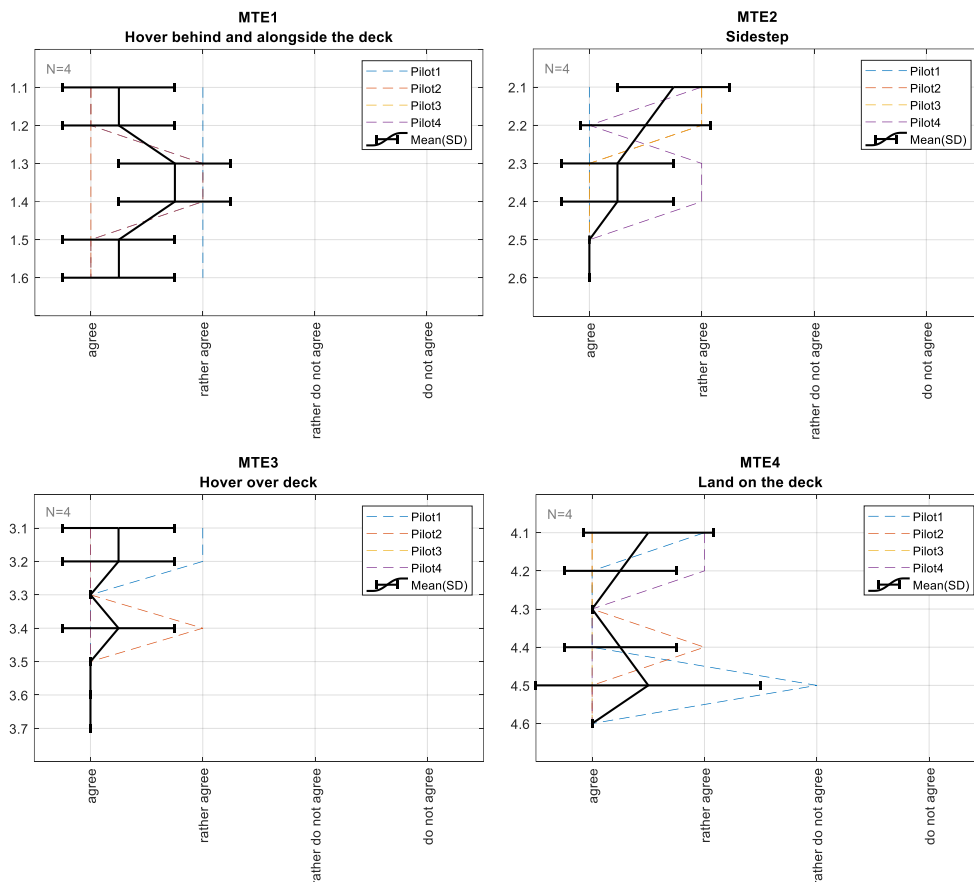


Figure 7-20: Pilot evaluations of the basic 3D-conformal landing symbology

While the precise landing and obstacle awareness symbology, see chapter 4.2.3, enabled the pilots during MTE1 to estimate the altitude of the helicopter relative to the landing area, the deck marking symbology more enhanced pilots' capability to always have the landing and rear ship deck wall in sight during MTE2. These ratings fitted to pilots' comments: While proceeding the sidestep, pilots benefited from the see-through capability of the HMD visual augmentation being able to always have the landing deck in sight, even when the helicopter itself occurred the touch down zone during the sidestep maneuver. Here, regarding the design of the 3D symbology layout, pilots stated this "handshaking" of both visualizations, trampoline circles and deck marking visual augmentation, further strengthened the acceptance of the 3D landing symbology, increased SA, and obstacle awareness. However, when the helicopter hovered over the deck being ready to land, pilots more focused on the outside scenery with the superimposed visual augmented elevator bar to estimate the lateral positioning and altitude of the helicopter above the deck. Due to the fact, that the landing deck had a limited size, pilots tried to stay with minimum but safe longitudinal distance of the rotor disc towards the ship rear wall. Finally, the synthetic horizon gave pilots feedback for own attitude flying behind the rolling and heaving ship, filling almost the whole pilots FoV. Therefore, pilots commented to use the synthetic horizon in combination with the ADI of the HMD visual augmentation as a general reference flying "heads-up" without looking at the HDD PFD.

Results from the current simulator study echo previous work demonstrated that flights in a harsh maritime environment are a great challenge, increase pilot workload and the necessity for pilot performance, and reduce situational awareness. The current study, however, also indicated that these challenges could be greatly reduced and enhanced if pilots have access to advanced response types and an HMD visual augmentation:

1. While ship motions had been increased from "low" to "high", pilot's workload increased, and handling qualities rating decreased simultaneously, however workload kept within an acceptable level.
2. With access to advanced response types, pilot's level of workload decreased from level 2 (primary FCS), up to level 1 using TRC or ACVH. Accordingly, handling qualities of all pilots decreased from level 3 (primary FCS), up to almost level 1 while using both advanced response types. Comparing subjective workload assessments confirmed these results and indicated a pilot's preference for higher degrees of aircraft stabilization in the shipboard environment.

The HMD visual augmentation further reduced a pilot's workload, and decreased TLX weightings based on the main aspects as follows: The intuitive HMD ESLS visual augmentation concept was accepted well by most of the test pilots. However, all test pilots recommended that HMD visual augmentation might even further increase pilots SA when

the helicopter would be operated in a DVE condition such as with a degraded visibility below 800m.

7.3 Flight Envelopes during Helicopter Shipboard Operations

In the following, the results of given pilots' ratings and comments are extended by a detailed investigation of helicopter flight parameters such as for the precise approach and landing maneuvers. Therefore, observations are again subdivided into helicopter ship approach and final recovery scenarios.

First, the approach path of the helicopter is analyzed within the context of degraded visibility ranges while operating the rotorcraft using different modes of visual and control augmentation. Here, another important aspect of the handling qualities analysis is the so-called "pilot gain", which aims to quantify pilot inputs on control inceptors for the purpose of pilot workload quantification. The present work relies on two such methods for analyzing pilot control activity: duty cycle, a time-domain measure; and power spectral density, a frequency-domain measure. Second, landing the helicopter even without in comparison to visual and/ or control augmentation being activated is examined. Moreover, when the helicopter arrived behind the deck, additional observations such as pilots head motions give insights into benefits of the HMD for pilots SA.

7.3.1 Helicopter Maneuver Quality of Execution within decreasing Visibility

In the following, the investigations on flight performance, deviations from optimal approach path, control inputs activity, control aggressiveness, control input power analysis, and head motions are given with mean and SD values for all pilots and extended to test and fleet pilots' results for further discussions.

Precise ship approach: As given in Figure 7-21, heads-up visual augmentation enabled to always approach the helicopter close to the ideal glide path. Here, SAS visualized the optimal glide path, while ESAS projected the tunnel boundaries to pilots' eyes. Both, SAS, and ESAS provided a dynamic ship following 3D visual augmentation to approach safe and successful to the ship. It should be mentioned, that even during lowest degraded visibility range of 800m, the deck and the ocean was not visually in sight until the helicopter reached the end of the tunnel symbology.

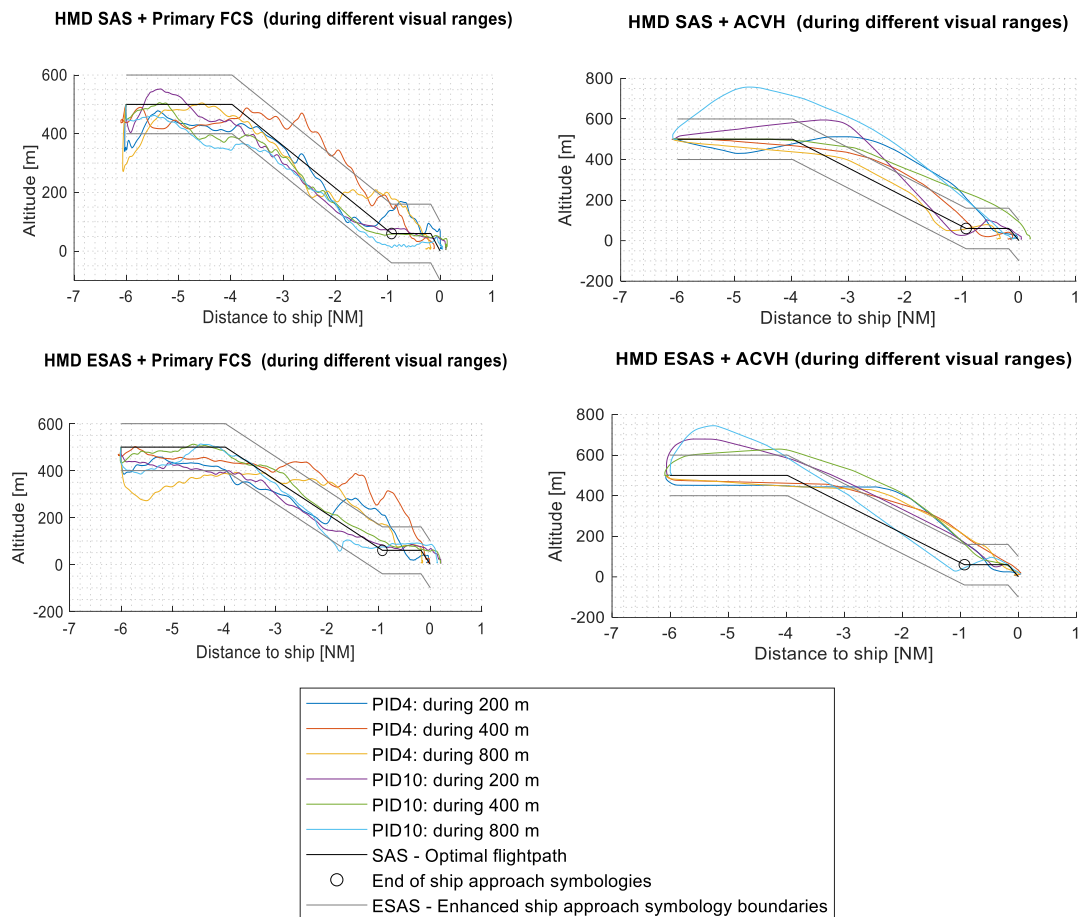


Figure 7-21: Side view of helicopter ship approaches in degrading visibility conditions

For a deeper analysis, representative PID4 (German Armed Forces and industry maritime test pilot, 4000 fh, 1500 fh flying with HMD experience) flight paths performance is plotted besides PID10 (U.S. Navy maritime fleet pilot, 2000 fh, 10 fh flying with HMD experience) recordings. In accordance with pilot workload analysis during ship approaches, see chapter 7.2.1, the control augmentation being activated created a smoother flight profile in all conditions. A successful ship approach would not have been possible without any guidance. The visual augmentation always allowed pilots to fly heads-up, while constantly having the flight path and helicopter parameters in sight. Most of the pilots reported that flying with visual augmentation created a great benefit to not run into spatial disorientation while flying “in the clouds” until reaching the MAP, and not coming too close to the sea surface. Most of the pilots reported, that CFIT was not a factor at all, because SAS and ESAS showed an intuitive “virtual 3D glide slide to run down to the ship deck within a defined safe altitude at the end of the 3D tunnel”. However, no prominent differences were observed while pilots flew SAS or ESAS visual augmentation. Regarding the highly different experience level of the pilots in flying with HMD (and as given in Figure 7-21), it might be concluded that pilots were able to successfully accomplish the missions even with a minimum time of training and familiarization. For proceeding the standard helicopter ship approach [105] [140] with visual and control augmentation, the following main results are given:

1. Visual augmentation: A successful proceeding of the helicopter ship approach was accomplishable by all pilots independent from all given bad weather conditions. Moreover, SAS as well as ESAS visual augmentation allowed a successful fulfillment of the mission and approaching close to the ideal glide path and be aware of CFIT at same time.
2. Control augmentation: The advanced flight control modes created a great benefit to operate the helicopter more stable in comparison to flying unaugmented. Operating the helicopter while control augmentation was activated, pilots recommended being able to focus even more on the HMD visual augmentation because they tended to fly most of the time “attentive hands on” when all parameters for an ideal glide slope along the visual guidance were set.
3. Visual and control augmentation being both activated was highly desired from all pilots. The greatest benefit during the ship approach in degraded visibility was created by the visual augmentation, because not even one approach could have been proceeded successfully even in highest visibility condition of 800m visibility range.

In the following, given in Figure 7-22, mean values of all test and fleet pilots for the helicopter ship approaches are illustrated to enable investigations on flight performance while using the four cases of visual and control augmentation modes. Here the most demanding DVE condition with a minimum visibility range of 200m was chosen, where the ship came visually in sight when the helicopter was flying already behind the deck. Approaches within the DVE visibility ranges of 800m and 400m, see A.3, offer similar results: All pilots were able to fulfill highly precise approaches to the ship deck, even staying within the projected flight path during almost all approaches from the beginning of the mission down to the landing phase. In general, and as often observed during individual flights, test pilots tended to operate the helicopter near the minimum desired altitude, visualized as the lower border of the tunnel symbology. In contrast, fleet pilots showed a trend to fly the helicopter more to the upper border line.

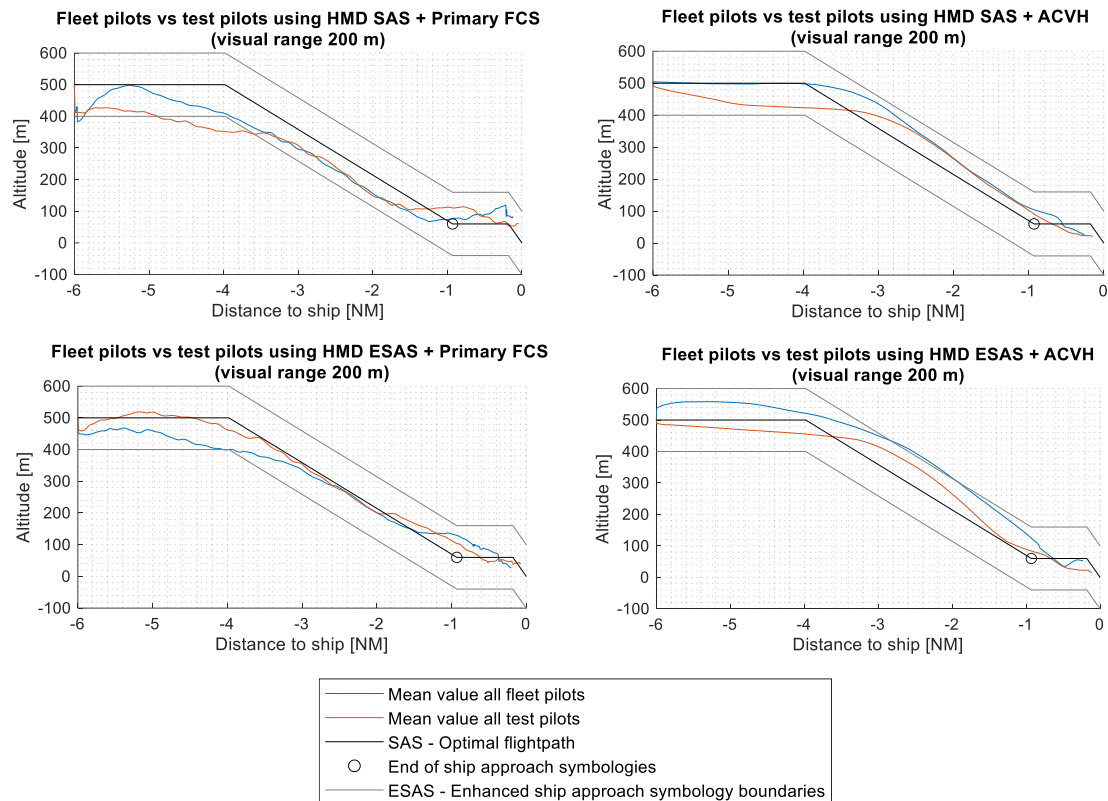


Figure 7-22: Side view of helicopter ship approaches in harsh DVE condition, N=8

Regarding the four cases of visual and control augmentation types tested as for the helicopter ship deck approach maneuver, the outcomes are as follows:

1. Visual augmentation SAS versus ESAS: Almost all helicopter ship approaches were successfully proceeded within given visualized boundaries leading to a successful landing on the deck at the end of the mission. Moreover, flying with ESAS visual augmentation being activated, pilots tended to fly closer to the optimal glide path, which was not projected while flying ESAS, but only while operating the helicopter with SAS visual augmentation.
2. Primary FCS (MECH) versus advanced flight control mode ACVH: In general, pilots approached the ship in a smoother way in mode ACVH. Two maritime test pilots recommended that approaching the helicopter with visual and control augmentation being both activated was “as a piece of cake”. However, it should be noted that these two test pilots (PID3, 5300 fh, 1000 fh flying with HMD experience, 300 ship deck landings, and PID4 with 400 ship deck landings) have extensive experience in flying helicopters equipped with an HMD visual augmentation and proceeding near shipboard maneuvers.
3. Test pilots versus fleet pilots in DVE conditions: All pilots were able to successfully fulfill all helicopter ship approaches, even when control augmentation was deactivated. Fleet pilots as well as test pilots stated to fully rely on the HMD visual augmentation after the first flights. Since flights were proceeded within a safe

simulation environment, safety aspects regarding failures of the HMD visual augmentation of course were discussed, but not in the focus of the flights.

Next, the deviations from optimal flight path, see Figure 7-23, during ship approaches where the helicopter entered the visual guidance for ship approach down to the end of the visual augmentation, are analyzed. Here, deviations from the optimal glide path in vertical and horizontal axes appear to stay within a maintainable level with respect to the glide path horizontal and vertical dimensions of 200m and 300m diameter.

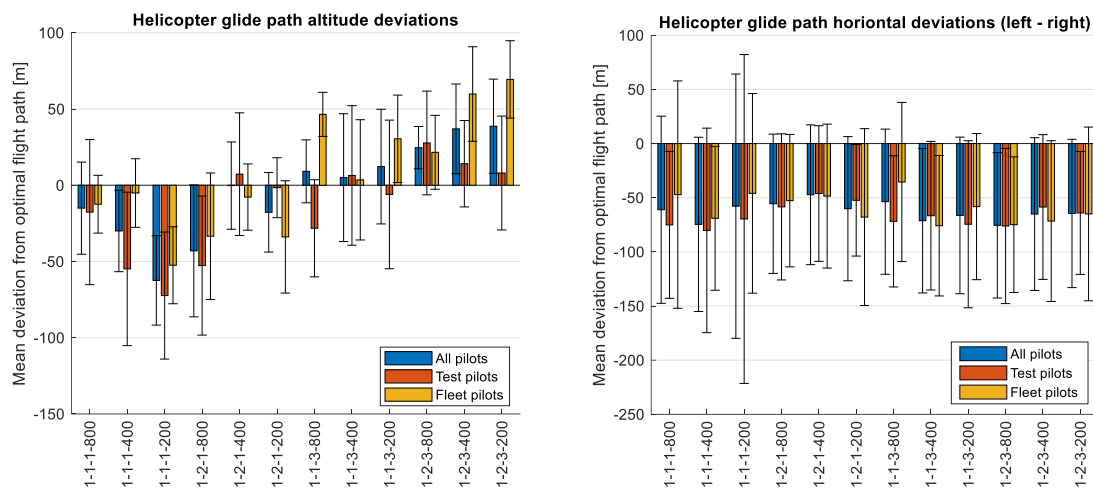


Figure 7-23: Mean deviations from the ideal flight path, N=8

What is remarkable within the vertical deviation, as can be seen in Figure 7-23 left figure, pilots tended to fly below the optimal glide path altitude when operating the helicopter with primary FCS. In contrast, when the advanced flight control mode was activated, most of the pilots stayed above the optimal approach path altitude. This fits to some of the pilots' statements, that while flying with control augmentation being activated, they had more spare capacity to concentrate on the visual augmentation. As a result, approaches were proceeded "more precise at a similar workload level" staying above or close to the optimal glide path altitude. When looking at the lateral deviation from the optimal glide path during the approaches, as given in Figure 7-23 right image, pilots always stayed on the left side of the optimal glide path. This seems to be apparent because pilots were instructed to complete the approach at the MAP behind the left side of the deck, as done during normal helicopter shipboard operations. Hence, all pilots chose an alike approach slightly to the left side of the optimal glide path with the ambition to already align at the end of the tunnel to the left side of the deck. Taking all approaches in different DVE conditions, mean values and deviations from the optimal glide path into account, following additional results might be stated, accompanied by pilots' comments:

1. During the first part of the approach (MTE0) from IAF to the level segment, pilots stated that the moving glide path was an intuitive and easy to understand way visualizing the approach path. When pilots operated the helicopter with control

augmentation activated on top, they attempted to use the additional spare capacity from reduced needed control inputs to even approach on a higher precision level with comparable workload.

2. From the level segment until to the MAP (second part of MTE0), pilots tended to slip the helicopter slightly to the left side at the end of the visual guided approach to get an unobstructed view on the appearing moving ship deck. Here, pilots benefitted from the visual augmentation displaying the ship deck markings which could not be spotted visually during DVE conditions of 400m and 200m degraded visibility.
3. Regarding the subsequent MTEs from hover behind and alongside the deck (MTE1), sidestep (MTE2), hover over deck and finally land (MTE3), pilots were able to fulfill all landings based on the capability to reach the deck, predominant within similar distances and altitudes, provided by the dynamic glide path moving in accordance with the ship.

Control inputs: Besides the flight path analysis, pilots' controls inputs, as given in Figure 7-24 and Figure 7-25, offered valuable clues about pilots control behavior during the approach segment. Given lateral inputs while flying unaugmented showed a tendency to the right from neutral position, as expected for needed compensation of the helicopter tendency rolling to the left in forward flight. While flying with control augmentation, all pilots tended to push the cyclic to the left. Here, given results in combination with recorded pedal inputs indicated that pilots slipped the helicopter constantly to the left from neutral longitudinal axis to have an unobstructed outside view on the approach path. Pilots recommended that effect as being trained to approach towards the ship like this when flying visually, even when visual augmentation always guaranteed a constant view on the virtual glide path. It might be stated that the "see-through" capability of the HMD tended pilots to behave like during a visual approach.

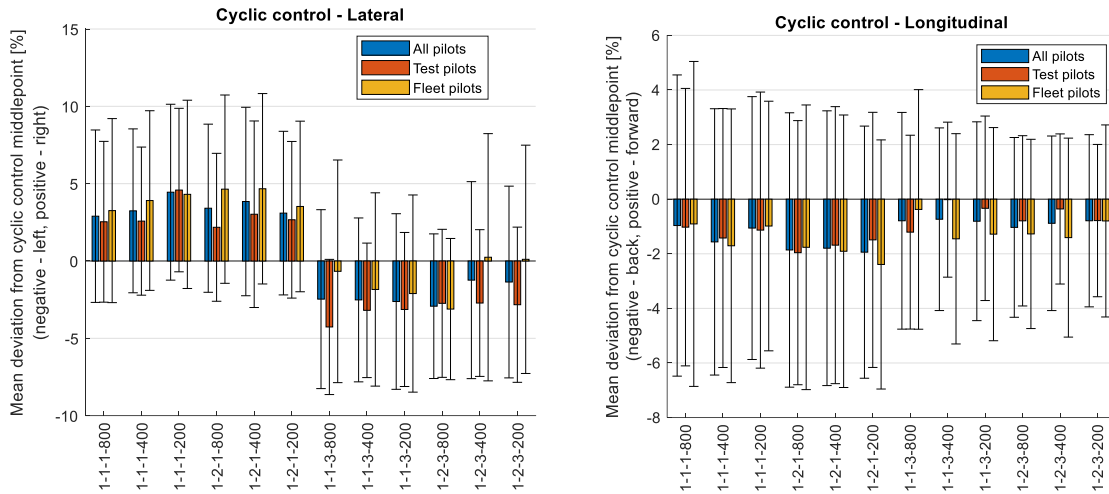


Figure 7-24: Pilots cyclic inputs during flights, N=8

Regarding longitudinal cyclic inputs, see Figure 7-24 right image, pilots gave cyclic inputs with a constant tendency to the back. Here, a reason for that might be that pilots flew the helicopter with an IAS of around 90 kts during all flights, see A.3, and so frequently decelerated the helicopter to stay within the target approach speed of around 80 kts IAS. Taking mean collective inputs of all pilots into account, as given in Figure 7-25, pilots appeared to set the collective control considerably to a lower state while flying with control augmentation being activated.

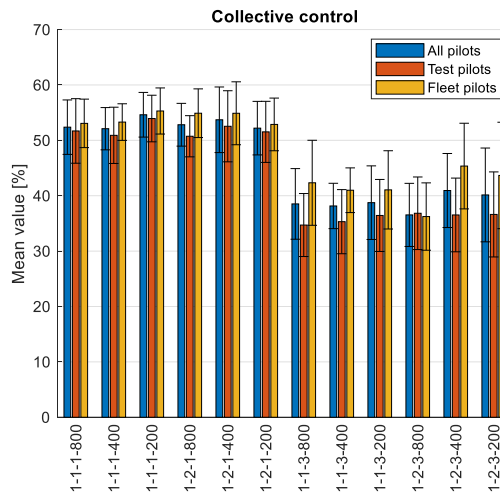


Figure 7-25: Pilots collective inputs during flights, N=8

Test as well as fleet pilots recommended, that when they set once the collective to a certain level during flights with the advanced flight control mode being activated, they did not further change the power setting of the collective during the approach at all. In general, a “normal” pilot control behavior had been observed during most of the flight conditions. Finally, pilots noted again, that liberated spare capacity was used to set an increased focus on the visual augmentation to appoint the helicopter to an optimal glide path setting.

Control inputs aggressiveness: The free spare capacity resulting from decreased pilot workload had been assessed by investigating pilots control inputs dynamics [79]. The

control inputs aggressiveness is an evidence of the magnitude of the control input amplitude during the approach phase starting from the initial trim position. The pilot control inputs aggressiveness is calculated as the time-averaged summation of the difference between the actual control input values of the pilot $\delta(t)$ and the initial trim position $\delta_{trim}(t)$, normalized over the respective total deflection range from the beginning of the approach t_0 until final touch down t_f given as J_A distance to the ship, and time stamps used for flight recordings $\Delta t = 0.01 \text{ sec}$.

$$J_A = \frac{100\%}{t_f - t_0} \sum_{t=t_0}^{t_f} \left(\frac{|\delta(t) - \delta_{trim}(t)|}{\delta_{max} - \delta_{min}} \right) \Delta t \quad (20)$$

The average number of peaks and duty cycles in the longitudinal and lateral cyclic controls, as well as in the collective controls were at a constant low level as can be seen in Figure 7-26. However, the effect in the recorded flight data matches pilots' comments: While flying with control augmentation, pilots stated to be able to fly the virtual approach path more precisely at a comparable aggressive level. At same time, fewer collective inputs were needed while flying with control augmentation being activated, because altitude control was felt to be easier to estimate than while flying with control augmentation being deactivated.

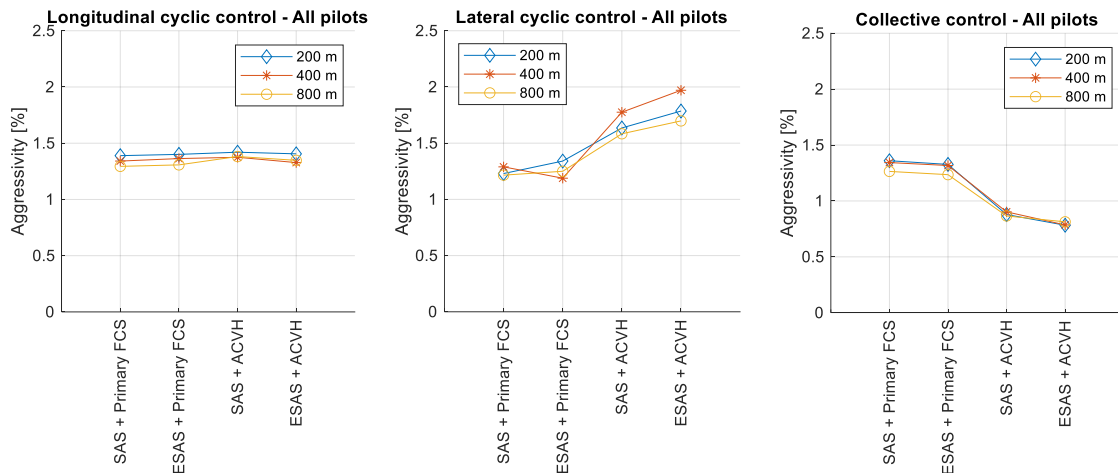


Figure 7-26: Control inputs analysis of average peaks and average duty cycle, $N=8$

The improvements are seen both in the cyclic and collective controls, measured across all DVE conditions:

1. Pilot control inputs stayed within a low level $< 2\%$ during all DVE conditions. A direct association to an acceptable low pilot workload flying with visual and control augmentation can be stated by taking corresponding pilot workload ratings and HQRs within borderline level 1, see chapter 7.2, into account.
2. The increase of cyclic lateral and decreased collective inputs while flying with control augmentation being activated resulted from pilot's effort to fly at a higher precision level regarding the displayed virtual flight path.

3. The height and direction hold capability of the control augmentation allowed pilots to remain attentive hands-on on these inceptors in all DVE conditions, which resulted in low peaks and duty cycles on cyclic as well as collective controls.

Control inputs power frequency spectrum analysis: The power frequency [53], derived from cutoff frequency via wavelet analysis, is introduced as a parameter that relates the frequency of pilot input with the intensity of that input. The analysis is used to transfer subjective pilot workload ratings to an opportunity of objective pilot workload measurement. Scalogram-based time-varying counterparts to both the cutoff frequency and power frequency show how this relationship evolves through a given task. Both the cutoff and the power frequency are calculated for simulator test data on the helicopter ship approach task. The pilot ratings recorded for each evaluation are then compared to both the cutoff frequency and power frequency to determine if a correlation exists [53] [79]. Whereas duty cycle throws light on the amount of pilot activity over time, it fails to capture the frequency spectrum of pilot inputs. For this purpose, the power frequency spectrum is a useful measure. The values are obtained by first applying the discrete Fourier transform to each pilot and each run, and then averaging the power per frequency across all pilots. Figure 7-27 shows the estimated power per frequency averaged for all pilots during evaluated DVE conditions. As can be seen in Figure 7-27, highest cyclic control inputs in pitch (upper row of Figure 7-27) and roll (lower row of Figure 7-27) axis were observed during unaugmented flights. Highest cyclic control inputs at a frequency up to 2 rad/s were given by the pilots during the most demanding degraded visual conditions flying unaugmented. These observations fit to given highest pilots subjective workload ratings as well as HQRs while pilots operated the helicopter unaugmented in most demanding DVE conditions.

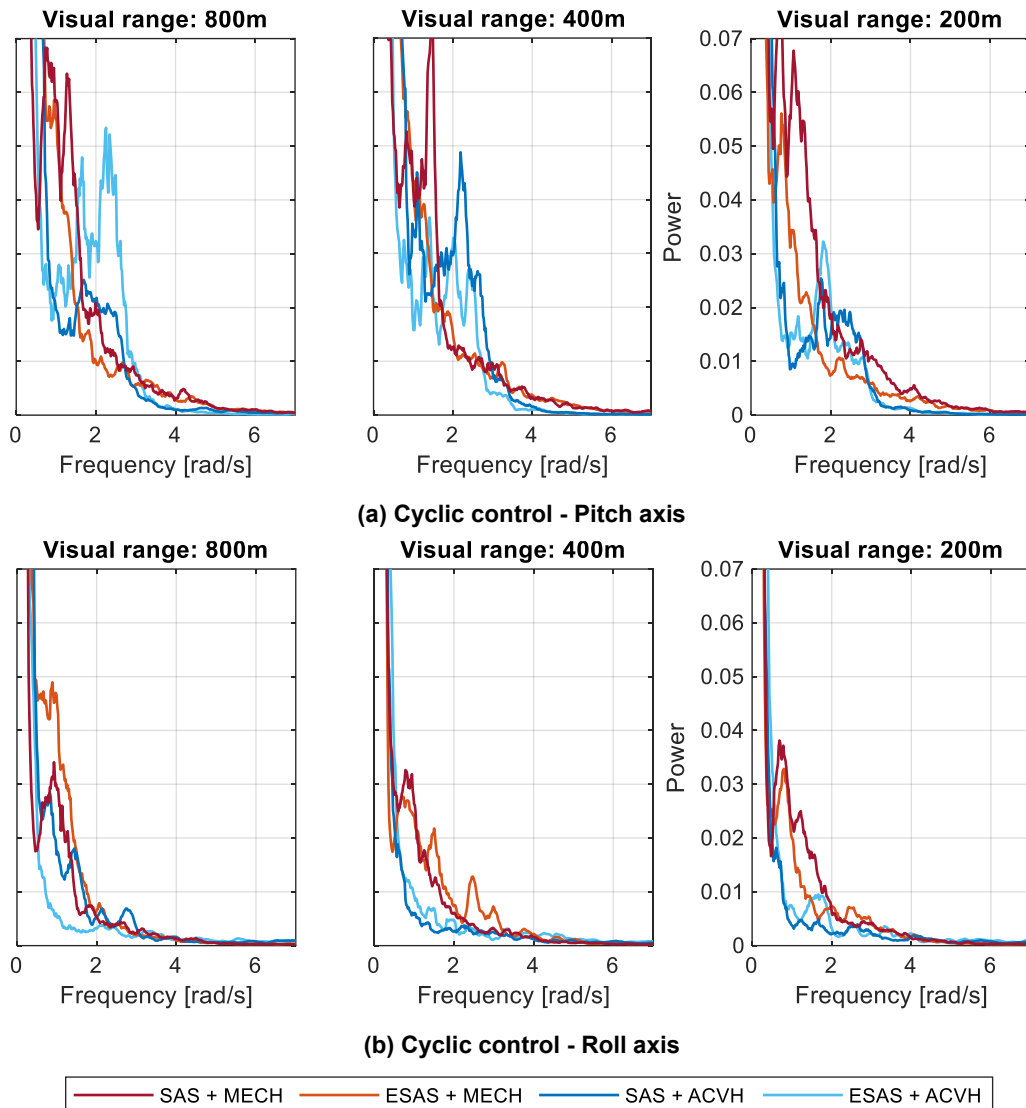


Figure 7-27: Average power per input frequency of pilots' cyclic inputs, $N=8$

The lateral and longitudinal inputs with the ACVH response-types were at lower frequency and average power compared to the unaugmented configuration. Highest frequencies had been observed for pilots' cyclic control pitch inputs: Pilots commented that the most demanding task during the approach phase was to set the optimal glide path angle towards the moving ship. The lowest frequency inputs in all channels were observed with visual and control augmentation being both activated (SAS+ACVH and ESAS+ACVH). It should be noticed, that again fitting to pilot's subjective workload ratings, the DVE condition visibility range had almost no effect on control power input frequencies. However, the difference between the gain and phase margins might indicate PIOs for the precision tasks as hover over deck or aggressive pilot technique. Nevertheless, PIOs had not been observed during simulated flight trials, and the disturbance rejection characteristics of the advanced flight control mode ACVH also lied within level 1 boundary, see [52].

Control inputs times-series analysis: Scalogram-based time-varying counterparts to both the cutoff frequency and power frequency show how this relationship evolves through

a given task. Both the cutoff and the power frequency are calculated for simulator test data on the approach and final recovery task. The pilot ratings recorded for each evaluation are then compared to both the cutoff frequency and power frequency to determine if a correlation exists.

First, 2D pilot cyclic inputs scalograms are investigated for the four combinations of visual and control augmentation types. The scalograms, see Figure 7-28 and Figure 7-29 and, are put side by side for a representative experienced test pilot (PID5, 1900 fh on helicopters, 200 fh with HMD, 200 fh on simulators) and an unexperienced maritime fleet pilot (PID6, 360 fh on helicopters, 0 fh with HMD, 700h fh on simulators). Finally, 2D scalograms are extended to 3D scalograms, see Figure 7-30 and Figure 7-31, taking beside time and frequency also the magnitude into account. These methodologies have been successfully used to estimate and discuss pilot workload along observations within multiple works [79]. The complementary figures for pitch axis can be found in A.3.

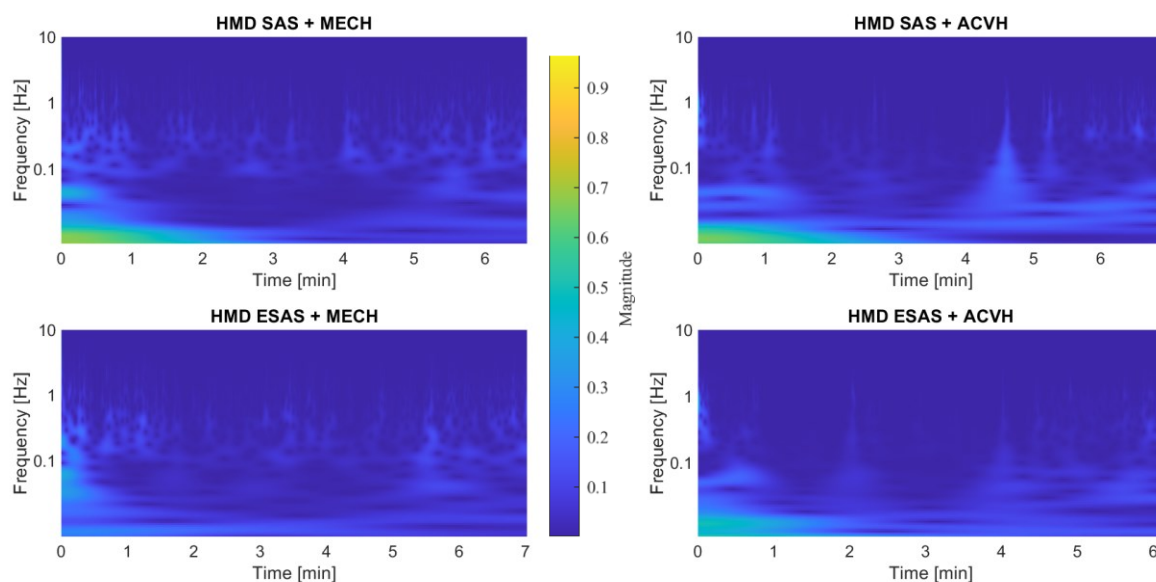


Figure 7-28: PID5 Test pilot cyclic control roll axis scalograms during DVE flights

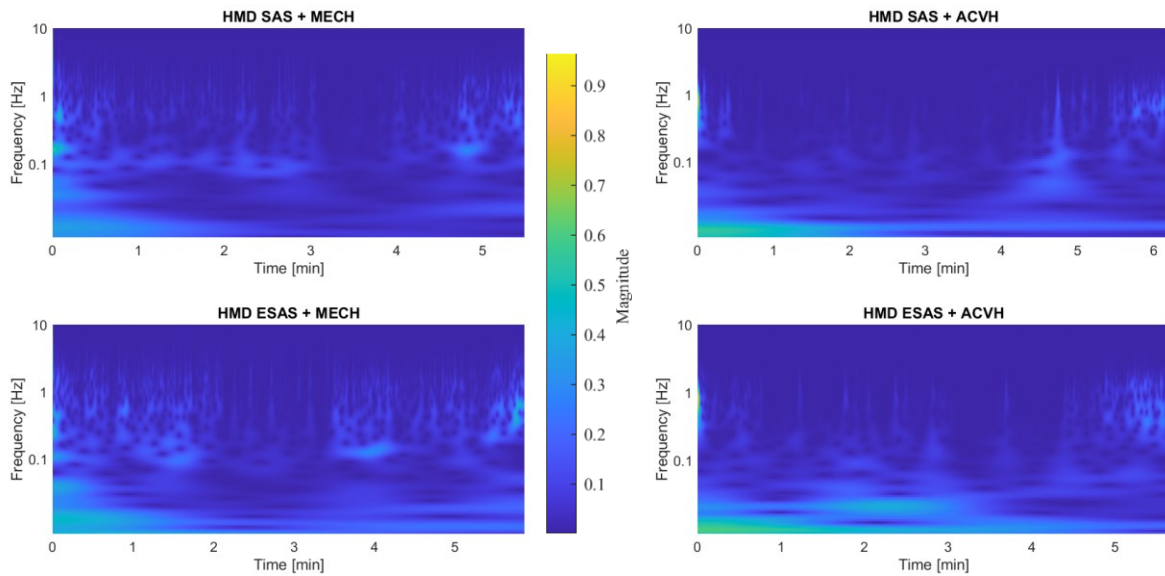


Figure 7-29: PID6 Fleet pilot cyclic control roll axis scalograms during DVE flights

Highest frequency of pilot cyclic inputs had been observed at the beginning of the mission and during the last minutes of flight, where the initial setup for the approach glide path and the final recovery phase took place. This effect fits to most of the pilot's comments: At the beginning of the flight pilots tried to approximate the helicopter to an ideal approach glide path. During the last phase of the flight, pilots had to challenge the final recovery of the helicopter besides and over the landing deck. Here, test pilots as well as fleet pilots showed a comparable input behavior. Flying the helicopter with the activated advanced flight control mode ACVH, frequencies of pilot cyclic inputs were mainly at a low level of < 0.1 Hz, and at lower quantity when a setup for the glide path had been reached and compared to flying in MECH mode. Within this middle stage of the flight, very few inputs had been recorded when pilots approached the helicopter with visual and control augmentation being activated. However, none of the visual augmentation types, SAS or ESAS, showed an improvement over the other in lowering the cyclic input frequencies. By extending the 2D scalograms with the magnitude to 3D scalograms for pilot cyclic inputs, see Figure 7-30 and Figure 7-31, the following results are further given.

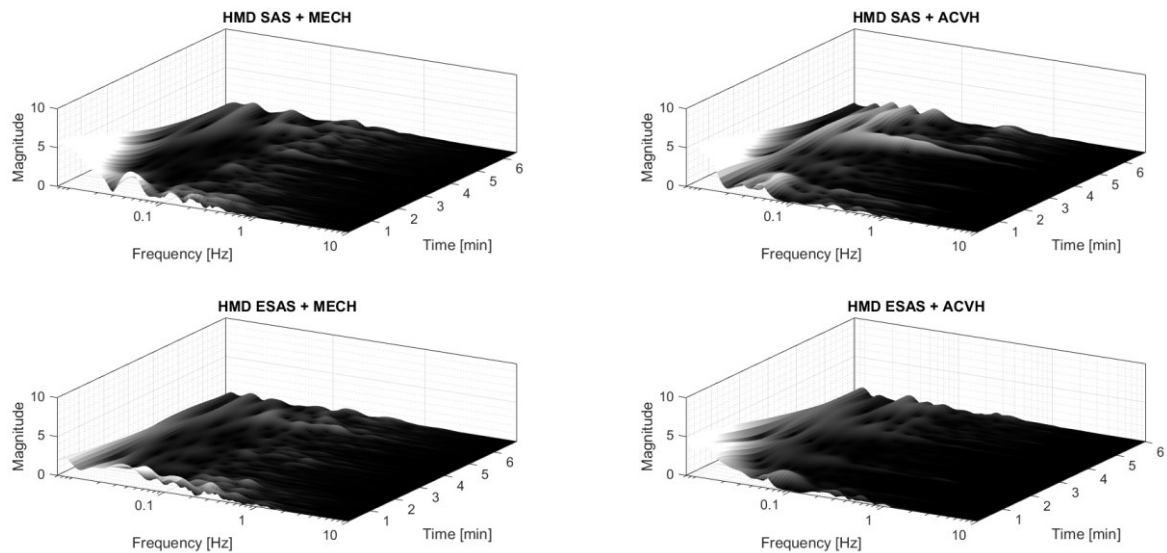


Figure 7-30: PID5 Test pilot cyclic control roll axis scalograms during DVE flights

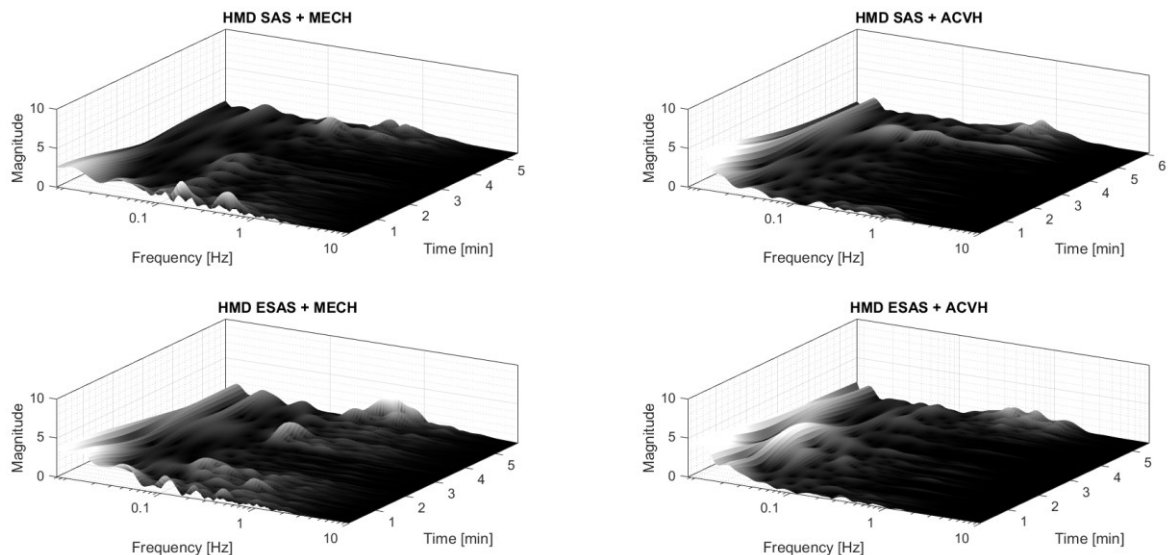


Figure 7-31: PID6 Fleet pilot cyclic control roll axis scalograms during DVE flights

The magnitude of pilot cyclic control inputs was at lower level when the advanced flight control mode had been activated in flight. However, here pilots tended to give more inputs at a constant low frequency. This effect again fits to pilots' comments as they tried to perfectly align to the ideal glide path when flying the helicopter visual and control augmented. The following main results are given for the control inputs times-series analysis taking the subjective workload analysis, see chapter 7.2.1, into account:

1. Pilots were able to operate the helicopter with a low frequency for cyclic inputs when visual and control augmentation had been both activated. The frequency level mostly being $< 0.1\text{Hz}$ fits to acceptable pilot workload ratings of level 2 and 1.
2. Pilots tended to acceptable magnitudes < 5 and frequencies of $< 1\text{ Hz}$ for cyclic control inputs, even when they operated the helicopter in MECH mode and visual control augmentation being only activated.

3. Highest magnitudes were observed during the first and last minutes of the flights. Here, pilots made the initial setup for an ideal approach glide path and conducted the final approach phase besides and over the landing deck. Magnitudes and frequencies fit to highest pilot workload ratings at the beginning and end of the missions of boundary level 2 to 1.

Besides the investigations in different facets of pilot controls inputs, a power spectrum frequency analysis of pilots' head motions indicated that a degradation of the visual range has only little effects, when the pilot was equipped with the visual and control augmented PAS during flight.

Pilots head motions: To obtain effects of control and visual augmentation on pilots' behavior, the physical motions of the pilots were recorded, as given in Figure 7-32. The magnitude of head motions while flying with the HMD equipped, showed that the main view of the pilots was in the lower horizontal central section, probably aiming on the virtual glide path in front.

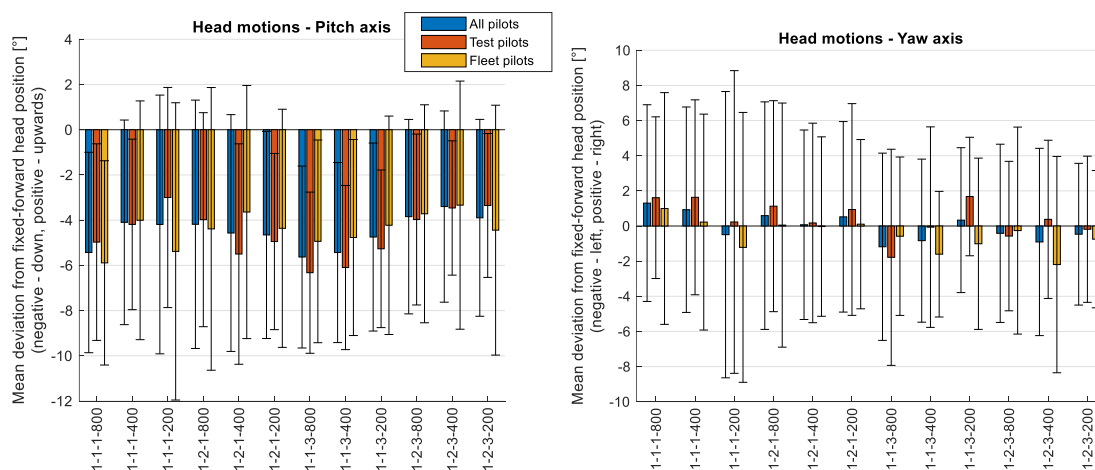


Figure 7-32: Pilots head motions during flights, $N=8$

However, no prominent differences were observed between control augmentation being deactivated or activated. Test pilots stated the following: Flying in DVE conditions without an HMD would implicate increased head motions or a focus to the lower left side. Then pilots would have a need for any outside visual cues or focusing on the HDD PFD in the middle of the simulator's cockpit. As no prominent differences were observed between test and fleet pilots, the visual augmentation displayed on an HMD could be stated as accepted well by most of the pilots. Some pilots advised that an extended FoV of the HMD might further strengthen the benefits of the HMD, such as the see-through capability and the unobstructed view on the scenery independent from any evaluated DVE condition.

Head motions power frequency spectrum analysis: As done for pilots control inputs, the power frequency spectrum analysis was taken to align pilot VCR ratings with head motions observations during proceeded flights. Pilot's pitch and yaw head motions during flights within increasing DVE conditions, see Figure 7-32 for pitch (upper row) and roll (lower row)

axis, match to the VCRs UCE results: Highest head motions were overserved in yaw axes during most demanding DVE conditions culminating in VCRs UCE boundary level 1. Moreover, this effect fits to pilots' comments, that pilots used the visual augmentation for synthetic visual cueing during all phases of flight: the approach and final recovery. Lowest head motions had been observed while the helicopter was operated with control augmentation being activated on top to HMD visual augmentation, whereas VCRs UCE were at constant level 1. Here, pilots stated to be able to shift the focus more to the visual augmentation caused by minimum needed inputs during flight.

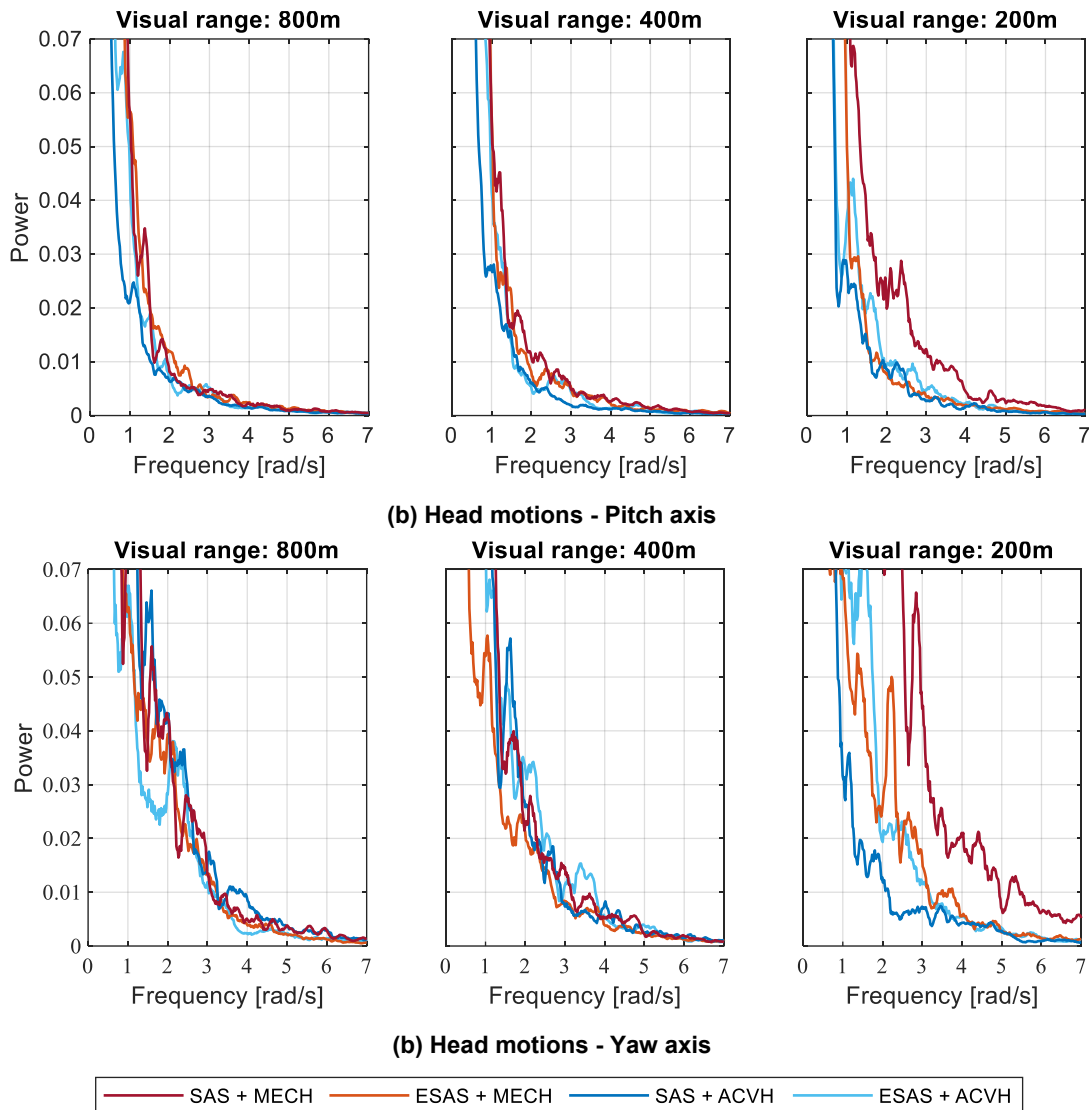


Figure 7-33: Average power per input frequency of pilots' head motions, N=8

Again, as evaluated for the pilots control inputs power frequency spectrum analysis, the increasing DVE condition limited visibility had almost no effect on pilots' head motions, with exception to the visual range of 200m. During the most challenging DVE condition, pilots stated that the missing peripheral outside scenery vision in the close range of the ship deck had a negative effect on their behavior to find any outside scenery visual cues. On the one hand, this effect fits to VCRs within UCE level 1 for both HMD visual augmentation types of

SAS and ESAS. On the other hand, flights without the visual augmentation could not be proceeded during this stage of flight because even at maximum DVE visibility range of 800m, the pilot could not see the ship visually till he passed the MAP. Finally, pilots showed higher power and frequent head motions in yaw axis compared to pitch axis. This effect is consistent with pilots' comments that pilot's greatest effort was to stay within the approach path in lateral axis, and not to drift horizontally while approaching to the deck.

The use of HMD visual augmentation and advanced flight control modes for control augmentation showed a great benefit for operating a helicopter in a demanding DVE condition. To evaluate the full spectrum of the HMD/PAS, detailed investigations on proceeding the final approach phase while flying activated and deactivated of all visual and control augmentation modes are given in the following. Here, different ship motions were taken on top for simulated flights in DVE condition of limited visibility.

7.3.2 Helicopter Ship Recovery while increasing Ship Motions

The flight paths of the helicopter during low and high intensity ship motions and a constant DVE condition (800m degraded visibility) as well as the last 40 seconds of flight, defined as hover over deck and land, are examined in the following. Here, the helicopter operated almost close to the ship deck, starting from the MAP and continuing via a sidestep approach to finally land on the deck. In contrast to the flight performance analysis as given above, here the helicopter had at least the ship foam already visually in sight: Hence, the flight paths analysis, pilots control inputs, and head-motions could be directly compared while flying visual and/ or control augmentation being each deactivated or activated. In addition, the exploration is given for representative test and fleet pilots.

Final approach flight path analysis: Figure 7-34 plots the side views of the flight paths with available modes of visual (no HMD, HMD ESLS) and control augmentation (MECH, TRC, AVCH) being deactivated and activated. During the final approach task, pilots operated the helicopter without as well as with HMD, and TRC and ACVH advanced response types in comparison to the primary FCS (MECH). Next the helicopter traces are plotted on a y-z plane for low and high ship motions, as given in Figure 7-35.

First, modes of visual and control augmentation offered flight performance benefits during the final approach maneuver. Figure 7-34 indicates a more stable behavior of the helicopter at the beginning of the maneuver. However, since the mission started in a trimmed forward flight for all conditions, a more stable start of the maneuver was expected while flying with advanced flight control modes being activated.

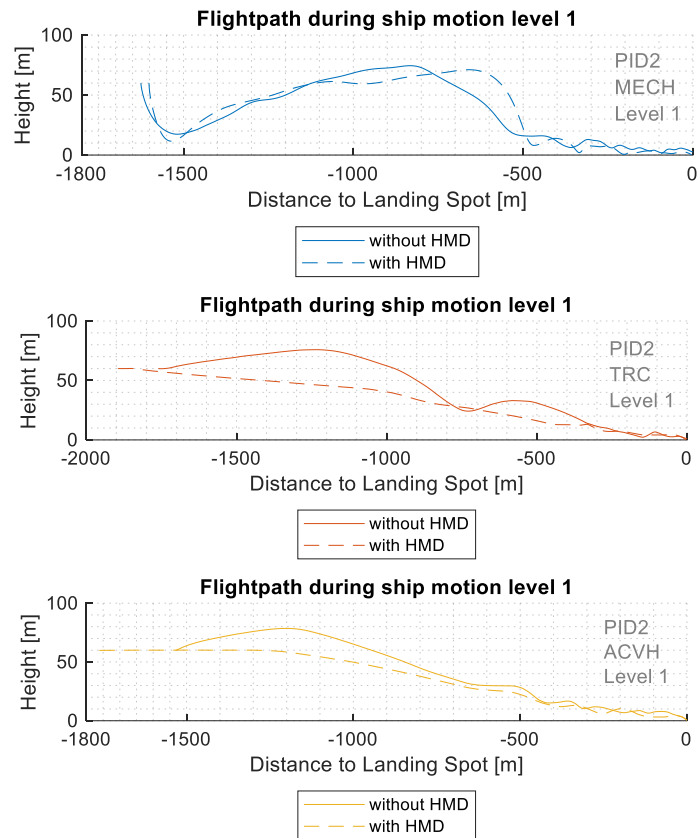


Figure 7-34: PID2 helicopter flight paths during the final approach

In Figure 7-34, a typical final recovery mission is illustrated, which was observed during several approaches. According to the SBAS SOAP procedure, pilots approached towards the ship on a constant glide path. Moreover, a phenomenon is given here, which was monitored during several approaches, flying with visual augmentation: Pilots tended to fly at a lower altitude. The observation is underlined by given pilots feedbacks: Benefits of HMD synthetic outside visual cues raised from a constant available setup independent from any outside scenery condition, finally used always flying the helicopter eyes-out-of-the-cockpit. The HMD visual augmentation enabled pilots to have the main helicopter parameters as well as the virtual landing deck always in sight. In contrast, pilots had to switch between HDD PFD and the outside view when no HMD was available, resulting in “loosing outside visual cues” during the highly dynamic final recovery mission, and a higher chosen altitude of the helicopter in the end. When advanced flight control modes were activated in parallel to the HMD visual augmentation, best approach profiles were reached by all pilots.

Second, Figure 7-35 shows another phenomenon that was observed in many of the approaches. During the hover alongside maneuvers, as the helicopter approached the port-side deck edge, it declined several meters in altitude. This effect was owed to the standard SBAS SOAP approach as the pilot tries to stabilize the helicopter visually at the height of the upper limit of the front wall of the moving deck. Moreover, the pilot operated the helicopter besides the deck for a couple of time to harmonize with the ship's velocity.

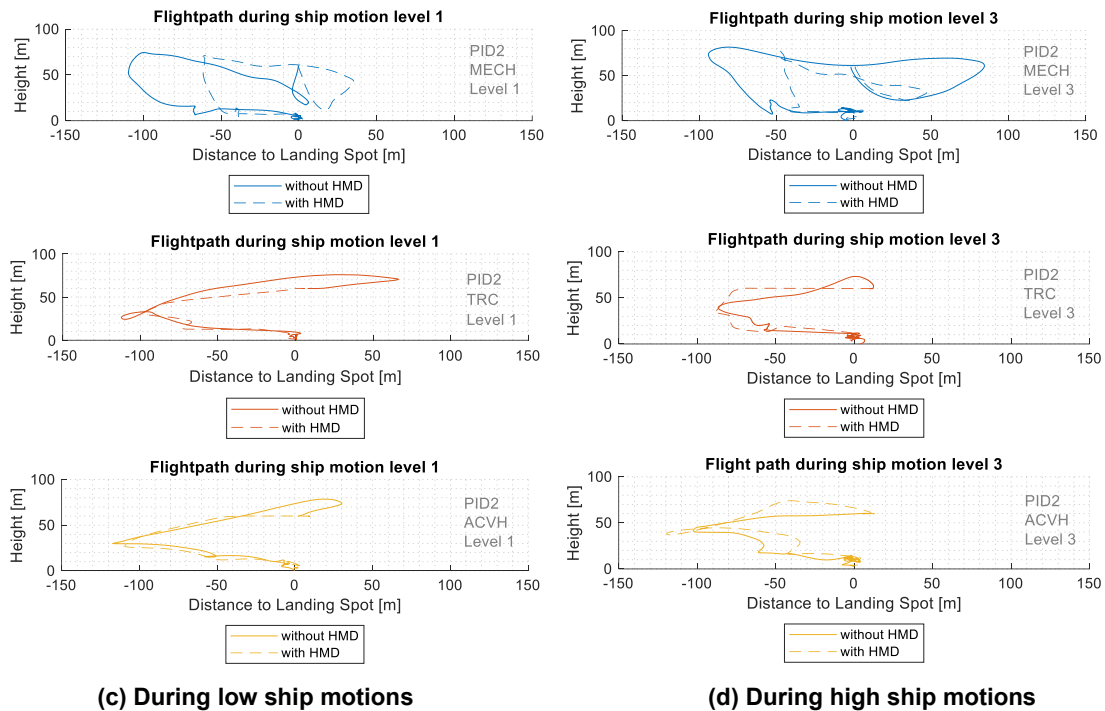


Figure 7-35: PID2 helicopter CG positions from behind during the final approach

Crossing the edge of the deck, a third effect was observed. The helicopter entered into slight PIOs, which raised with increasing ship motion levels from low to high. These PIOs were given via pilots' subjective feedback and observed pilot collective control behavior. Details about the analysis of these PIOs is given in [53]. Pilot comments confirmed that this is a realistic pilot control input behavior as the pilot focuses visually on the rolling and heaving flight deck. In contrast, flying with visual and control augmentation being activated, the pilots reported to be able keeping the helicopter more stable and performing the sidestep maneuver on a constant sidestep glide path without losing altitude due to more focus on the synthetic horizon of the HMD ESLS. The phenomenon is commonly experienced in an approach to frigates using the ACVH mode, where minimal inputs are needed from the pilot to synchronize with the ship's velocity and front wall upper limit height. The main findings while fulfilling the final recovery flying visual and control augmentation modes deactivated and activated are as follows:

1. The use of HMD visual augmentation during the final recovery mission created a great benefit on enhancing pilots SA by having the outside scenery, the ship overlaid by the virtual landing and obstacle awareness augmentation, as well as main helicopter parameters always in sight. The high visual conformity of the virtual landing symbology ESLS and the moving ship deck increased pilots' acceptance of the HMD visual augmentation rated to be good.
2. Both TRC and ACVH advanced flight control modes allowed an enhanced and more precise final approach towards the ship deck until landing. One test pilot from the industry even commented that landing the helicopter on the deck with ACVH and

HMD ESLS as an easy task. It is important to note that this pilot has more than 5,000 fh onshore and even more than 3,000 fh offshore on helicopters. All pilots commented that both TRC and ACVH response-types were sufficiently aggressive for the final recovery mission. Even the latency from input of the pilot until feedback of the helicopter was rated to be good.

3. With access to advanced response types, pilots indicated to operate the helicopter at a higher precision without entering PIOs at any times of the final recovery mission, and independent from low and high ship motions. All pilots desired a preference for higher degrees of aircraft stabilization in the highly dynamic near-shipboard environment.

Last 40 seconds of flight: Next, observations during low and high intensity ship motions while the helicopter hovered directly over the ship deck strengthen the findings from above for the critical tasks over the deck, seen in Figure 7-36 visualizing the last 40 sec. of each flight. When higher control and visual augmentation modes were used in flight, the time duration for station keeping over deck before landing extended at same time. Longest time for the MTE hover over the deck was observed at highest ship motions with advanced flight control modes activated. However, this was expected, because pilots waited for an acceptable quiescent period of the ship deck to finally push down the helicopter while minimum control inputs were needed to keep station over deck.

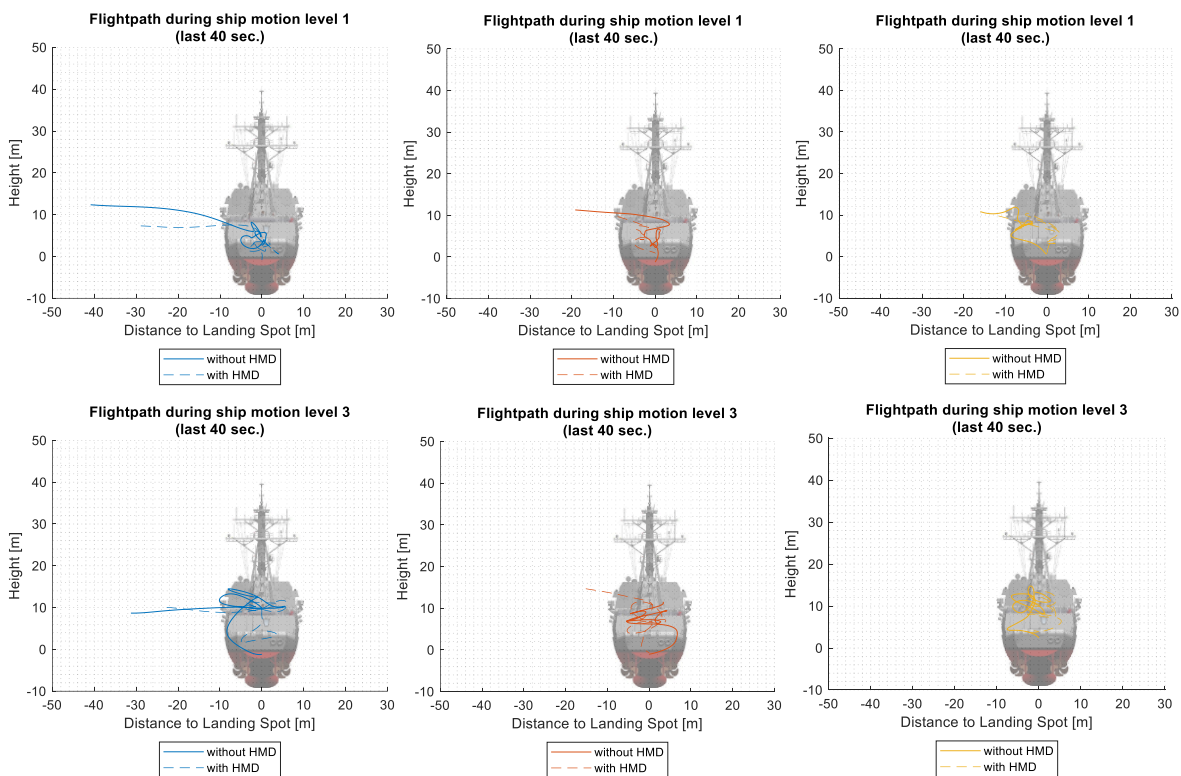


Figure 7-36: PID2 helicopter flight paths last 40 sec in different ship motions

Regarding the visual and control augmentation, two main findings are given. First, most of the pilots fulfilled the sidestep maneuver more stable while flying with HMD visual

augmentation. Comments from pilots substantiated the observation that the synthetic horizon and heads-up main helicopter parameters allowed an outside scenery focused sidestep to the right without losing visual cues by the upcoming rolling ship into the pilots FoR from the right to the left side. Second, station keeping time over deck extended while flying with advanced flight control modes being activated. One the one hand, the hover over deck maneuver was longer at higher ship motions. Pilots tended to wait longer for a quiescent period to land the helicopter safe. The aim of all pilots was to fulfill a precise and soft landing. One the other hand, station keeping over deck also extended during high ship motions. Here, the advanced flight control modes created a great benefit fitting to pilots' comments. With control augmentation modes being activated, the MTE hover deck was not an issue at all, because when all control parameters were set once, only small input had to be given by the pilots to further reach a highly perfect prior to landing position. Finally, when pilots had to position the helicopter in a highly precise "ready to land" position in the middle over the landing deck, pilots stated to use the HMD visual augmentation during this task. However, when the helicopter reached and stayed stable over this position, most of the pilots commented to switch the visual focus onto the ship in the outside scenery to wait for the quiescent period. Then, only main helicopter flight parameters visualized on the HMD were still used by the pilots to fly fully heads-up until pushing down the helicopter on the deck. In sum, the participating pilots of the experiments in this work fulfilled more than 200 ship approaches, all with a successful landing at the end of the mission. No approach was aborted, even during harshest DVE conditions and high ship motions.

Control inputs: Observations of appropriate pilot control inputs for the final approach phase flying with deactivated and activated visual and control augmentation modes illustrates further findings. Figure 7-37 indicates representative lower pilot inputs in the cyclic channels with the activation of control augmentation, even during harsh conditions of high ship motions. These plots corroborate pilot statements that control augmentation simplified piloting, and that the HMD visual augmentation improved SA.

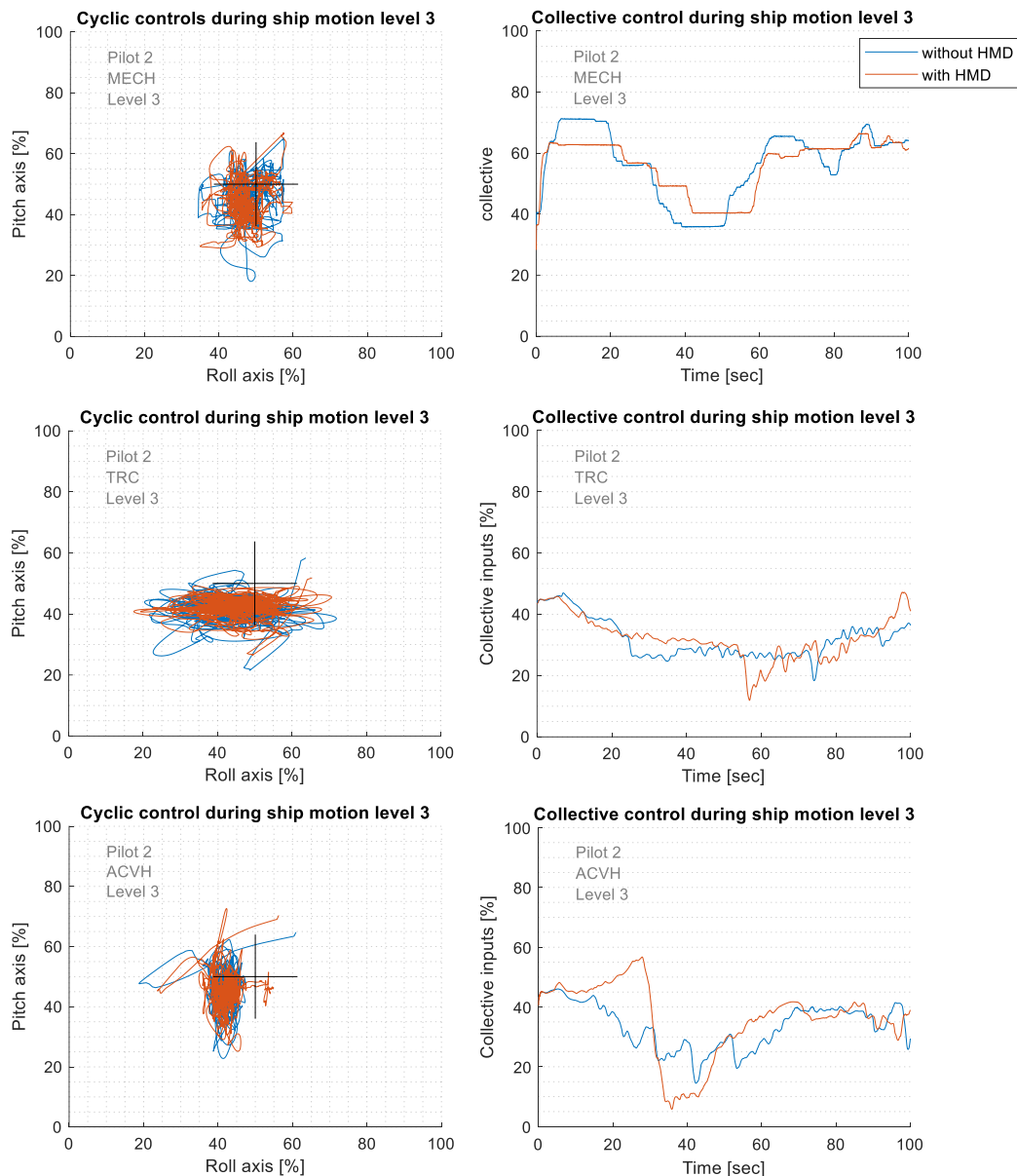


Figure 7-37: Cyclic and collective control activity during a final approach

In the final stages of the approach during sidestep (MTE2) and hover over deck (MTE3), it was apparent that all pilots tended to "drag the spot", to cross over the deck edge aft of the intended landing spot and to progress forward over the ship deck to the spot. Multiple pilots reported a self-observed tendency to drag the spot, and they suggested that this was a result of their efforts to maintain visual contact with the spot in the final stage of the maneuver. Most of the pilots stated to keep a safe distance in longitudinal position to the front wall of the deck by holding the cyclic control inputs in a backward position. The left tendency of the cyclic control inputs may arise from the goal to not overshoot the deck in lateral positioning during final recovery and initial trim configuration. PIOs also turned out to be a factor during MTE3 hover over the deck and land (MTE4). This might be a result from the fact that the moving front wall is now positioned directly in front of the helicopter, and therefore covers most of the pilot's FoR. All pilots reported that they benefitted from the

activated visual and control augmentation at this stage of final recovery: The advanced response types (TRC and ACVH) kept the helicopter in a stable position over the deck with minimal inputs needed from the pilot. Besides that, the pilots benefitted from the visually augmented ESLs; in detail, the elevator bar allowed to keep the helicopter visually in the middle of the deck in the longitudinal axis and at a safe altitude referenced to the rolling and heaving landing spot at the same time. This pilot control behavior may arise from the elevator bar acting as a virtual deck officer [105] to enhance the pilot's control activity with unlimited visual reference in contrast to the deck officer, who is normally hidden by the cockpit instrumentation at some point.

Pilots head motions: Finally, pilots head motions were recorded and investigated to obtain insights into pilot physical behavior in the cockpit. The magnitude of head motion was found to decrease with increased levels of control augmentation, as given in Figure 7-38, for most of the pilots. The main FoR of all pilots was observed in the lower middle central area. However, this was expected during a helicopter ship approach and from participating pilots' comments where pilots tried to always have the virtual landing pad, the ship, and finally the landing site in sight.

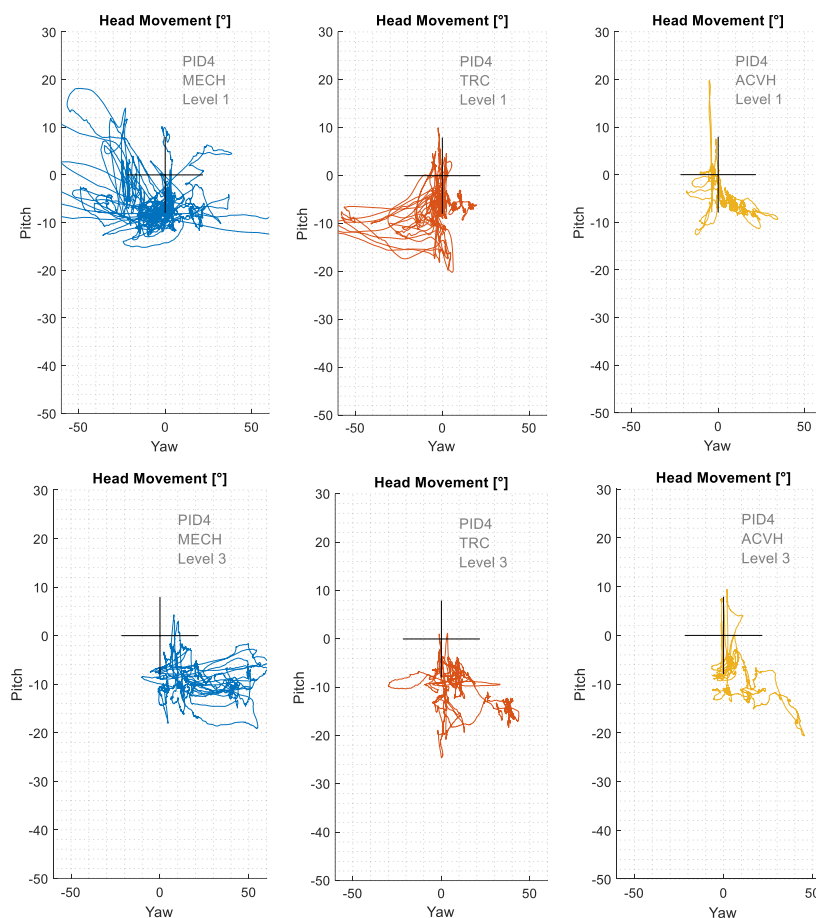


Figure 7-38: Pilot's head motions during low & high (upper & lower row) ship motions

In addition, the visual focus with HMD visual augmentation in the lower middle central area indicates, that pilots mainly used the HMD to monitor helicopter parameters in flight, and

not the HDD PFD which was situated in the upper left FoR. These observations fitted to pilots' comments:

1. During the helicopter ship final recovery, the main FoR of all pilots tended to be in the lower middle section. Pilots used the HMD visual augmentation to benefit from the unobstructed view on the virtual landing deck and the virtual visual cues.
2. The head motions of all pilots decreased with activated advanced response types. All pilots commented that a combination of the HMD visual and control augmentation created the greatest benefits to fulfill the final recovery mission in the given DVE condition, as well as during low and high ship motions.
3. Head motions increased with increasing ship motions. The main FoR in the lower middle section stayed the same as during low ship motions. It might be interesting to note, that pilots recommended that HMD visual augmentation content should be kept to a minimum, meaning all pilots used the elevator bar as well as the helicopter flight parameter information of the HMD visual augmentation for the landing task and to not hit the landing deck and rear deck wall. However, pilots did not benefit from the virtual landing pad when the helicopter reached the final hover over deck position. Here, pilots stated to concentrate on the rear deck wall of the ship with the superimposed elevator bar of the HMD visual augmentation.
4. Due to the diversity of all participating maritime test and fleet pilots with minimal up to extensive experience in flying a helicopter with the assistance of an HMD, it could be stated that even with a minimum amount of training, all pilots were able to fly the maritime missions highly accurately.

A visual and control augmentation scheme gives helicopter pilots the opportunity to operate the helicopter at high precision with acceptable workload, even during demanding ship motions. On top, a demanding DVE condition such as degraded visibility reveals the demand for heads-up flying in the near-ship environment.

7.4 Predictive Handling Qualities Model

Based on the gathered data from the flight test campaigns, a predictive handling qualities model (HQM) was developed and evaluated. Traditionally, handling qualities assessments are performed in real flight tests or pilot-in-the-loop simulations. As these are time consuming and cost intensive procedures, a computer simulation-based evaluation is a cost-effective preflight option like first order estimations of rotorcraft performance to give a first indication for newly developed control augmentation modes. The goal for the development of such a HQM is the opportunity to compare mathematical and pilot rated HQs to give a higher validity of proceeded MTEs.

The HQM model of this work offers modelling, simulation [61], and prediction of flight behavior for standard MTEs of ADS-33 PRF [2]. The HQM model can be adapted to different rotorcraft configurations and control designs. The multi-loop pursuit-control pilot model features a neuromuscular element in order to predict pilot behavior. The closed loop Hess pilot model [62] had been taken as the base line for the HQM model. The Hess model had been successfully used in several MTE-like scenarios to predict pilot behavior for both fixed wing and rotary wing aircrafts, see [60] and [63].

In addition to the neuromuscular element, a pilot aggressiveness parameter, and a visual cue model had been integrated on top, allowing the evaluation of control designs in different UCEs. Since the HQM model, as given in Figure 7-39, was designed in Matlab with the focus of modularity, its field of application is limited to so-called pursuit tracking tasks, meaning the pilot not only receives error information, but is shown both the current state of the aircraft and the target state, he is tasked to perform given from the ADS-33 PRF.

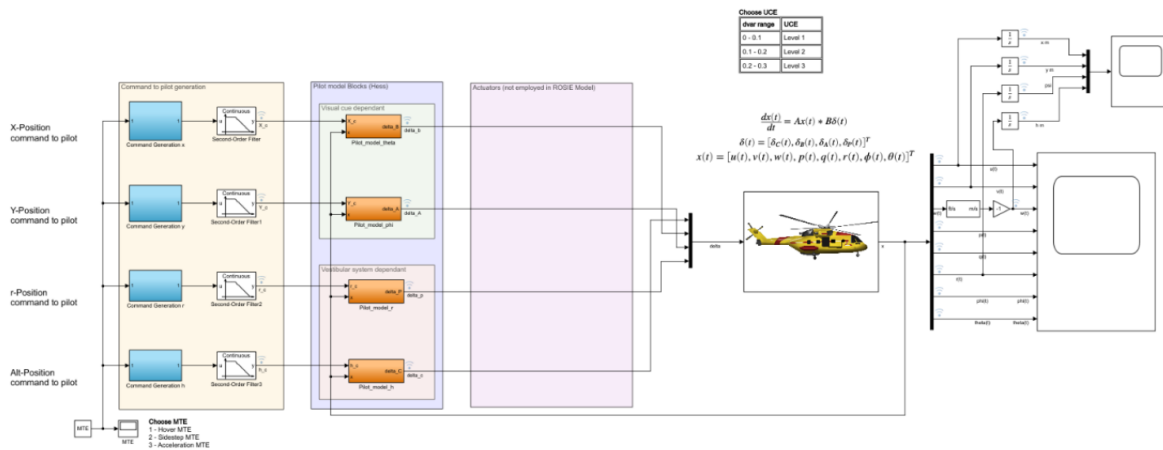


Figure 7-39: Schematic illustration of the HQM model

In order to validate the HQM model and the predictions derived, model results were compared to those of proceeded pilot-in-the-loop ADS-33 MTEs hover and sidestep with the basic control augmentation mode MECH, see chapter 7.1. For the ratings assigned by the pilot, it was found that the model prediction resembled the data acquired from the pilot-in-the-loop experiments. Both, pilots and the HQM model reached a HQ classification of level 2, rating the configurations performance as adequate. The main axis for the HQs measurement in the HQM model was the pitch axis of the helicopter. Similar results were also found with the evaluations conducted by Hess [62]. For the flightpath analysis in this work, two model runs were conducted: One with the standard aggressiveness setting of 1.00, and a second one with an increased pilot aggressiveness of 1.25.

Flight path performance: The HQM model aligns well with the flight tracks, for both the hover and the sidestep MTE, see Figure 7-40 and Figure 7-41. However, subjective pilot ratings of the given MTEs remain as one of the main references for flown HQs. The light

grey boxes represent the area for a desired performance while the darker grey boxes visualize the boundaries for adequate performance according to ADS-33 PRF.

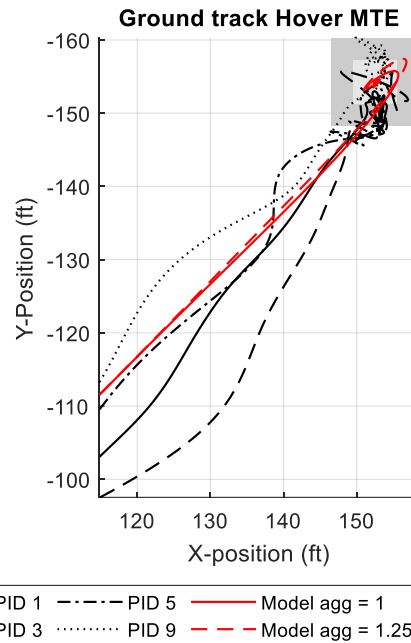


Figure 7-40: MTE Hover - flight path performance of human pilots and pilot model

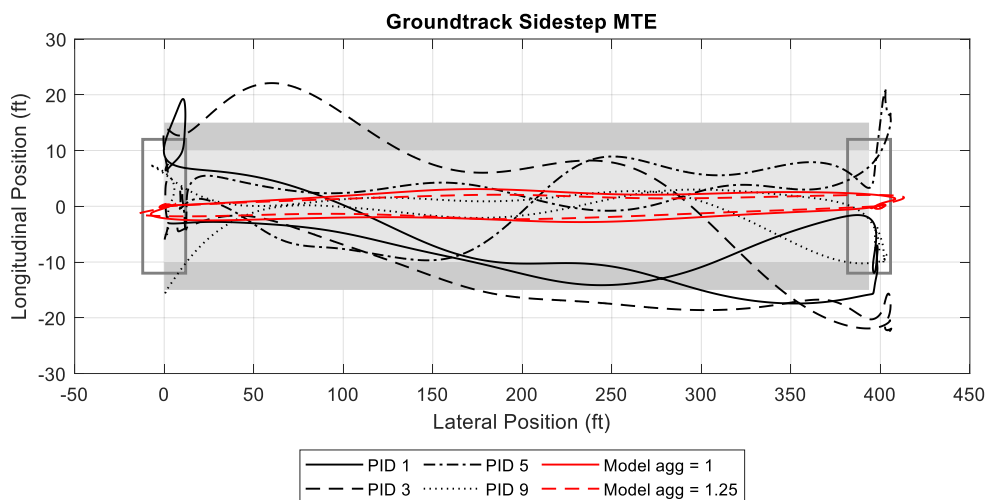


Figure 7-41: MTE Sidestep - flight path performance of human pilots and pilot model

The results indicate that, according to the simulation flights, the HQM would be rated adequate, as two pilots were able to maintain the stable hover inside the adequate limitations. Here, the HQM model predicted better performance: According to the results as given here, the HQM model configuration would be rated as adequate for the higher aggressiveness case and possibly even desired for the lower aggressiveness case.

Altitude and yaw angle performance: The HQM model predicted a better behavior and therefore a better HQ rating for both aggressiveness levels than the pilot in the loop simulations, see Figure 7-42 and Figure 7-43. Two main reasons are derived: First, the HQM model generates less movement in the x-axis. From the pilot simulations data gathered, it seems likely that non commanded axes, i.e. axes with stable target values over

the duration of the MTE, do not provide the instability the pilot in the loop simulations suggest. Second, pilots tend to induce a longitudinal movement in exchange for lateral movement in order to stay within the hover MTE position box limits. This trade-off, whether it is conscious or unconscious, is a human decision the model is not able to simulate. However, even individual pilots performed different in both MTEs.

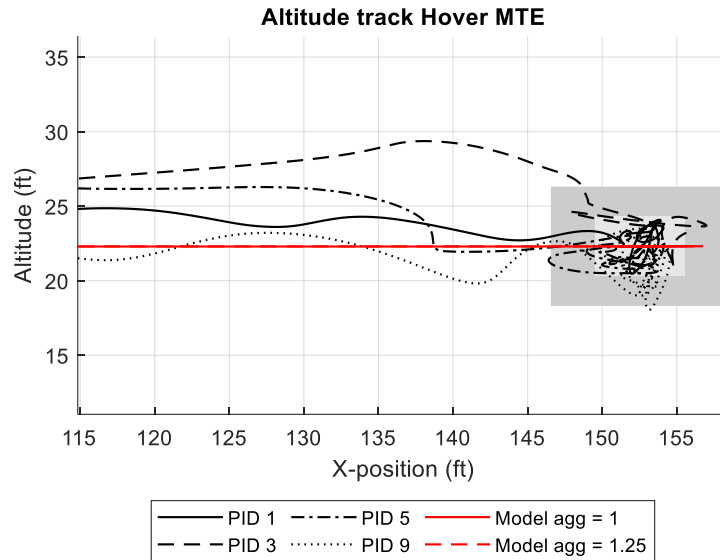


Figure 7-42: MTE Hover - altitude performance of human pilots and pilot model

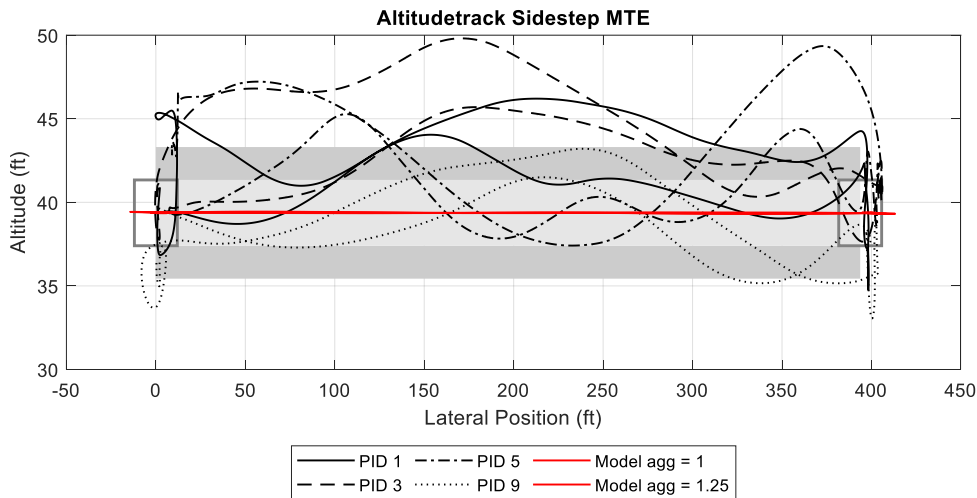


Figure 7-43: MTE Sidestep - altitude performance of human pilots and pilot model

For the yaw angle performance, see Figure 7-44, a similar behavior to the hover MTE can be observed: The yaw angle movement for the HQM model is fairly stable around the -90° target value, while the piloted simulations feature more peak values and general noise. Again, while the model would have predicted desired handling qualities, the simulated flights indicate an adequate behavior for the yaw axis, supporting the expectation that the HQM model provides less fidelity for axis with a stable value command input.

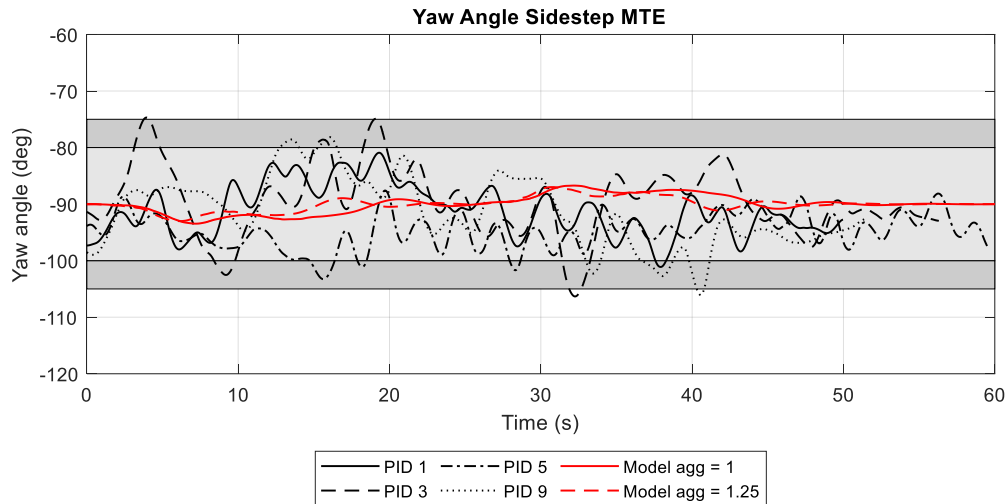


Figure 7-44: MTE Sidestep - yaw angle performance of human pilots and pilot model

The data obtained from commanded axes, i.e. axes with target values changing over the duration of the MTE, indicate that the HQM model predictions for these axis are close to the behavior observed in the simulated flights, both for MTE hover and sidestep. Especially for the higher pilot aggressiveness factor, the effects like over- and undershoot around the target positions were found to be in the same order of magnitude as for the piloted simulations. A second effect had been observed for non-commanded axes, i.e. axes with a stable target value over the duration of the MTE. Axes showed a stable behavior compared to human pilots' inputs. This phenomenon could be due to two reasons: The linearized HQM model may feature too little cross-axis coupling, and the HQM model performs well in compensating the movements introduced by cross axis coupling.

As the HQM model had been developed and tested for the MECH control augmentation mode in the ADS-33 MTEs hover and sidestep, the integration and evaluation of advanced flight control modes, like TRC or ACVH, seems likely. All generated data by the HQM were inside desired performance and therefore showed similar results as generated by human pilots. However, differences in pilot and HQM model behavior had been observed. With respect to helicopter near-shop operations, the HQM model environment could be extended to specific offshore parameters like to simulate sea states and a moving hover MTE box.

7.5 Ship Tracking Model Observations

Image-based object tracking methods can be added to modern sensor images of infrared camera for flight guidance assistance. These tracking methods for moving objects give the opportunity to detect, track, and visualize the landing platform of the ship, even in adverse weather conditions. Moreover, the image-based tracking is independent from any sensors of the ship or any communication between the helicopter and the ship. The goal of the integration of such algorithms to the PAS offers the opportunity to simulate near real world conditions for these helicopter shipboard operations in DVE conditions.

Regarding the trained models of such image-based ship detection methods as the needed information for the HMD visual augmentation, Table 7-2 lists the purposes of four datasets. No occlusion is specified as the target ship is captured on a uniform background, and occlusion connotes the target ship is occluded by the terrain. Under the option "with truncation", the checkmarks indicate that the dataset contains only few images, in which a small part of the bounding box of the ship is truncated. These images with truncation can be ignored, depending on the training purpose.

Datasets	Modal position	With occlusion	Using SCONe	Through fog	With truncation
A	Centered	No	No	No	No
B	Centered	Yes	No	No	No
C	With Offset	Yes	Yes	No	Yes
D	With Offset	Yes	Yes	Yes	Yes

Table 7-2: Purposes of datasets for ship detection

Table 7-3 summarizes the settings of the training processes in the corresponding dataset of Table 7-2. The batch size indicates the GPU in which the training took place.

Dataset	Batch size	Images	Images used	Trained epochs
A	8	4,600	4,600	500
B	3	9,7200	6,800	700
C	3	364,400	9,600	700
D	8	16,200	4,500	250

Table 7-3: Training settings on four datasets for ship detection

All datasets, except dataset A, used the previous trained models as a pre-training. Hence, the last models did not need many epochs to achieve the accuracy shown in Table 7-3: Training settings on four datasets for ship detection "#Images" is the number of all generated images in the dataset, "#Images used" is the number of images used for training. Regarding the ship detection, the SingleShot6DPose project used three standard metrics to evaluate 6D pose accuracy, namely the 2D reprojection error, the intersection over union (IoU) score, and the average 3D distance of model vertices (ADD metric). The accuracy had been calculated as the percentage of correct pose estimations among all predictions:

1. 2D reprojection error. When the mean distance between the 2D projections of the object's 3D mesh vertices using the estimate and the ground truth pose is less than 5 pixels, a pose estimate is correct. It measures the closeness of the true image projection of the object to that obtained using the estimated pose.

2. IoU score. The validation program measures the overlap between the projections of the 3D model given the ground truth and predicted pose. A pose is accepted as correct if the overlap is larger than 0.5. Hence, all poses can be stated as accepted.
3. ADD metric. To compare 6D poses, a pose estimation is seen as correct if the mean distance between the true coordinates of the 3D mesh vertices and those estimated, given by the pose, is less than 10% of the object's diameter.

Table 7-4 shows the evaluation results computed using the three metrics mentioned above.

Dataset	2D reprojection error [%]	IoU source [%]	ADD metrics [%]
A Validation Set	73.32	42.77	77.39
B Validation Set	85.04	48.32	78.86
C Validation Set	67.71	55.64	92.00
D Validation Set	68.62	45.09	81.25

Table 7-4: Evaluation of trained models validating all datasets using three metrics

Regarding the detection of the ship within ROSIE, the accuracy is high enough that the models can be used for 6D pose predictions. Figure 7-45 shows the testing accuracy of the pre-trained model.

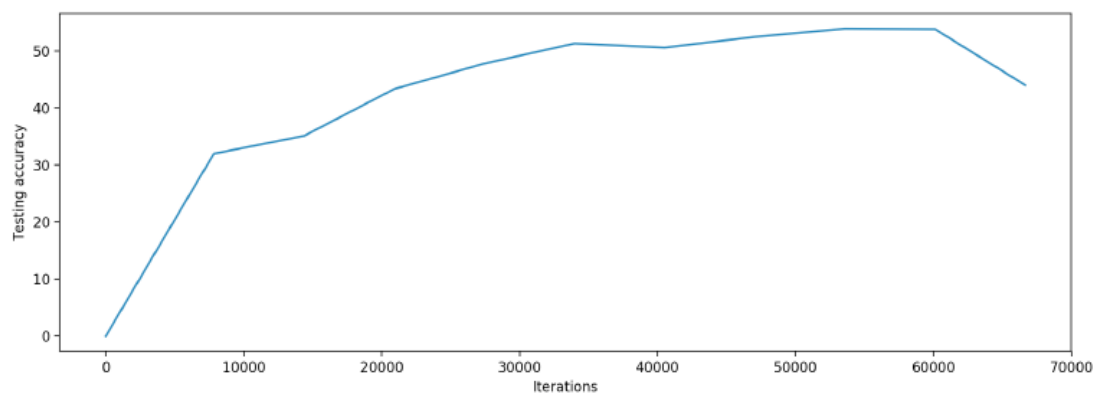


Figure 7-45: Testing accuracy during pre-training

Figure 7-46 compares the testing accuracy of dataset D, trained twice with the optimization algorithms Adaptive Moment Estimation (Adam) and Stochastic Gradient Descent (SGD) with momentum, which are used to find a local or the global minimum of the function, e.g. the neural network.

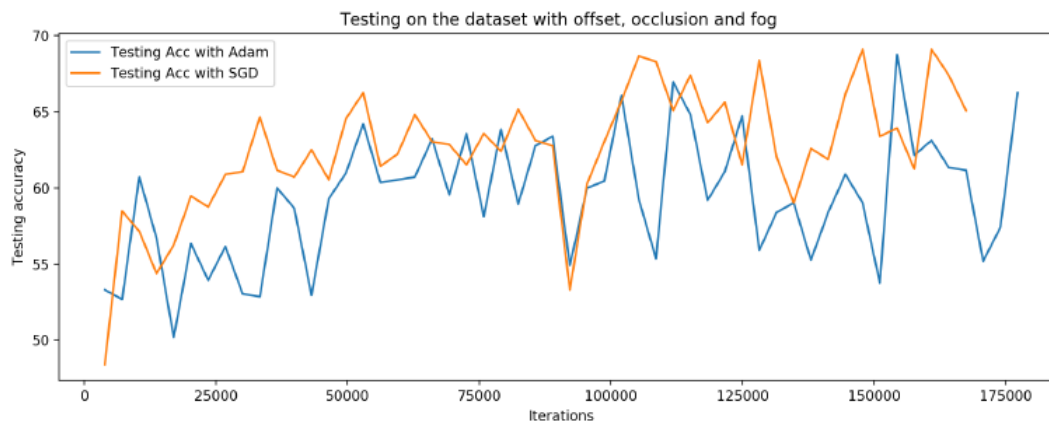


Figure 7-46: Comparison of testing accuracy using SGD and Adam

The smaller fluctuations of the orange curve, which represents testing accuracy with SGD, indicates that the training using the SGD optimizer generally performed in a more stable manner than the one using Adam.

However, in addition to attempting to fine-tune the networks of the currently chosen method further, training with other approaches, such as PoseCNN and DenseFusion might be considered to increase accuracy and reduce computing time of 6D pose estimation. Moreover, another crucial issue is how to detect models with truncation, meaning models partially outside of the screen. Within this work, the detection was computed when the helicopter hovered near the ship, and especially above the ship deck. As SingleShot6DPose uses the PnP algorithm to calculate objects' 6D poses with 2D points, this method rather works, when less than four of the nine points are detected in the image. This is the case when information of feature orientations is not available. The project PVNet might solve the truncation challenge. PVNet is a pixel-wise voting network that regresses pixel-wise unit vectors pointing to the key points and uses these vectors to vote for key point locations using the random sample consensus (RANSAC) algorithm. This approach is also sufficiently efficient for the real-time 6D pose estimation as used within this work. However, further challenges might arise, when these algorithms are taken for an object detection in real world conditions. Nevertheless, actual projects of the industry show promising results on the detection of ship decks for rotary wing – ship constellations.

8 Conclusions and Recommendations

The focus of this work was to prove the capability of a visual and control augmentation pilot assistance system to decrease pilot workload and increase situational awareness benefitting from an affordable Helmet-Mounted Display (HMD) system when performing helicopter shipboard operations. Therefore, the central research question was depicted as: How can a Pilot Assistance System contribute to assist pilots during challenging near-ship missions? These pilot assistance systems mainly used for helicopter onshore operations in degraded visual environment (DVE) conditions have not been investigated in the offshore environment yet. Hence, the examinations and simulator flight test campaigns within this work focus on the potential of such Augmented Reality (AR) systems applied in typical helicopter near-ship operations in representative maritime conditions. The helicopter ship approach and recovery scenarios within harsh maritime conditions such as degraded visibility and high ship motions were selected for the investigation. HMD visual augmentation modes, one for the approach and one for the final recovery tasks, were integrated to the HMD of the fixed-based rotorcraft simulation environment (ROSIE) and subsequently enhanced together with maritime test pilots from German Armed Forces. Additional advanced flight control modes completed the visual and control augmentation system. Pilots benefited from visual and control augmentation modes culminating in acceptable pilot workload and handling qualities at mainly level 1, even in harsh DVE conditions.

During two simulator flight test campaigns, potential benefits of the system were examined together with in sum ten maritime test and fleet pilots from German and US armed forces, industry, and public authorities completing a total over 200 flights. In the first study, an offshore approach scenario was flown by the pilots in degraded visibility conditions down to 200m using the HMD projecting a virtual glide path following the moving ship. As a result of pilots' feedback from the first study, additional three-dimensional synthetic visual cues were added to the cluttered second symbology for the landing phase. This mission phase was assessed in the second campaign with the focus of a final recovery mission in low and high ship motions, and a DVE condition as well. Both scenarios were proceeded along standard offshore procedures [105] [140] including aeronautical design standards [2] for rotorcraft flight tests.

The pilot assistance system consists of an automatically decluttered and scene-linked visual augmentation concept displaying the optimal glide path and an outside scenery conformal virtual landing deck symbology as well as main helicopter parameters to support the pilot's direct perception of critical helicopter operations within the limitations of safety and

performance constraints. The simulated detection of the moving ship deck is investigated by an imaged based deep learning technology. Visual elements of the displayed symbology are color-coded, fit to human information processing, and design principles such as visual perception, object recognition and optical flow. Additional control augmentation modes following pilots' comments and recommendations, focus on rendering pilots' control inputs more precise, while simultaneously decreasing subjective workload. A SMC-based flight controller offering two advanced response-types (TRC/PH, ACVH/PH, RCDH, RCHH) were used for a comprehensive H135 flight dynamics model. Visual and control augmentation were hosted for the purpose of pilot workload and handling qualities evaluation within ADS-33E-PRF mission task elements as well as for operational ship approach and landing missions. To achieve this highly realistic maritime environment for helicopter shipboard operations, an open-sea environment with a modular weather and three-dimensional waves model was implemented to the ROSIE dome projection. Moreover, a dynamic ship model with realistic movement data from the Systematic Characterization of the Naval Environment (SCONE) database [65] from the U.S. Navy had been used for investigations. Sea states and visually coupled ship motions in the maritime environment were defined according to the World Meteorological Organization (WMO) sea state code, as used in recent studies [66] [158].

From the analysis of the two simulator flight test campaigns, see also [93] and [94], corresponding workshops [93], and an additional piloted evaluation of advanced response types, given in [52] and [53], the following conclusions can be drawn.

Handling qualities evaluation:

- Both MTEs, hover and sidestep, unaugmented flights (level 2) in comparison to control augmented flights (level 1) culminated in “desired” and “adequate” Cooper-Harper HQRs, and a significant reduction in pilot workload up to level 1 Bedford workload rating. However, a ground position hold control augmentation was strongly recommended by most of the pilots for low-speed operations.
- The most challenging demands in both MTEs turned out to be flying the helicopter without control augmentation. For the hover maneuver as a part of the MTE sidestep, pilots strongly recommended for an advanced flight control mode. Largest pilots control inputs were observed during unaugmented flights. This effect went along with highest pilot workload and HQ ratings operating the helicopter with the primary FCS.

Reduction of pilot workload and improvement of situational awareness:

Helicopter shipboard approach in decreasing visibility ranges:

- Visual augmentation allowed a helicopter shipboard approach at low workload, mainly at a constant level 1 Bedford workload rating. This was observed even when visibility was decreasing significantly. Successful ship approaches were possible independent from increasing DVE conditions down to 200m visibility while operating the helicopter with visual and control augmentation being activated.
- Head motions power frequency spectrum analysis were at an acceptable frequency and power level in all DVE conditions. Lowest head motions frequencies had been observed while the visual and control augmentation were both activated. However, an increase of head-motions had been observed during the final landing phase over the deck. The head motions analysis fitted to pilot's workload ratings: The degrading visibility had almost no effect, while the greatest benefit had been measured resulting in low power and frequencies of head motions when the control augmentation was activated.
- Control augmentation combined with HMD visual augmentation further reduced pilot workload. Both modes, TRC as well as ACVH, were highly accepted by all participating pilots for low-speed helicopter shipboard maneuvers, culminating in Cooper Harper handling qualities ratings of constant level 1. This enabled pilots to perform precise ship approaches at a constant, low workload level even in harsh environmental conditions.
- Situational awareness increased for ten out of ten pilots up to a constant level 1 UCE while approaching the helicopter with the HMD enhanced ship deck approach (ESAS) symbology. However, even approaching the deck with the ship deck approach symbology (SAS), displaying the ideal glide path towards the moving ship, was rated within borderline UCE level 1 and 2. Degrading visibility ranges (800m, 400m, 200m) did not result in a higher amount of head-motion during the approach segment.

Final ship deck recovery during varying ship motions:

- Pilot workload stayed at borderline level 1 while operating the helicopter with HMD assistance, even during challenging ship motions. When these ship motions were set from "low" to high", also pilot's workload handling qualities rating increased, but both kept mainly within an acceptable level 2.
- Deck interface pilot effort (DIPES) ratings acknowledged and complemented pilot workload analysis. These findings from the DIPES ratings light on the perceived

ability of fleet pilots to benefit from visual and control augmentation. In a high intensity ship motion setup, helicopter maneuvers from the moment of crossing the edge of the deck were perceived by the participating pilots to be too demanding and unsafe for unexperienced fleet pilots, regardless of the use of the proposed control and visual augmentation. Only the ACVH response-type together with the HMD visual augmentation was considered acceptable borderline rating. In contrast, within low ship motions conditions, all MTEs were consistently rated with acceptable effort with the use of the proposed visual and control augmentation modes.

- The limitation of synthetic visual cues became evident when the helicopter crossed the edge of the deck. Here, and as the ship motions intensity increased, the pilots NASA-TLX rating increased, especially during the MTE hover over deck. This observation can be attributed to an increased time pressure and focus on the outside visual cues where in pilots tried to avoid a hard landing on the deck in the presence of higher ship heave motions.
- During the final landing phase with the helicopter over the deck, pilots benefited from HMD projected synthetic deck wall markings for stabilization and for non-interference with the rear deck wall of the ship. Longest time over deck was achieved while operating with both, visual and control augmentation, being activated. Maritime test and fleet pilots were able to proceed sidestep and landing maneuvers with both activated and deactivated HMD. Flying visually (no HMD) versus with HMD turned out to be at a significantly higher workload, effort, and workload weightings, as stated in pilot Bedford, DIPES and NASA-TLX ratings.

Enhancement of helicopter maneuver quality:

- With access to advanced response types, pilot's level of workload decreased from level 3 (no advanced response types, no HMD visual augmentation), down to level 2 (TRC or ACVH, no HMD visual augmentation), and finally achieved level 1 ratings with the HMD ship deck landing symbology (TRC or ACVH and HMD visual augmentation). Accordingly, handling qualities of all pilots decreased from level 3 up to almost level 1 while using each advanced response type and HMD visual augmentation. Observations and pilots' recommendations indicated a preference for higher degrees of aircraft stabilization in the near-shipboard environment.
- An analysis of the control inputs points to low aggressiveness overall when pilots operated the helicopter with HMD visual and control augmentation both being activated. This corresponds to feedbacks from the pilots, using combinations of visual and control augmentation lead to minimum required inputs and allowed flying

heads up, even in degraded environments with limited visibility down to 200m. Higher lateral aggressiveness during the approach was related to the fact that pilots responded to the reliance on the visual and control augmentation, and thus tried to fly more precisely by giving short aggressive cyclic inputs.

- Control inputs frequency domain analysis showed that the SMC laws are capable to offer high bandwidth for the ACVH response type. The difference between the gain and phase margins suggests that the controllers in its present form, both TRC and ACVH, may be prone to pilot induced oscillation for super-precision tasks or aggressive pilot technique, although PIO was not observed during piloted evaluations. The disturbance rejection characteristics of the proposed controller also lay within the level 1 boundary.
- Control inputs power spectrum frequency and times-series analysis carried out segments of high-frequency inputs mainly observed whereas the helicopter was operating over the deck. Pilots control inputs frequency spectrum analysis showed acceptable pilots' cyclic inputs in both axes for all DVE conditions. Lowest bandwidths were observed while the control augmentation was activated. Almost no PIOs were observed during the flights, even while the demanding station keeping over deck maneuver during high ship motions. These analyses and observations conclude that the SMC technique holds promise for robust, high bandwidth flight control for rotary wing platforms. Pilots recommended it would be beneficial to have a selectable heading hold mode available on top to the control augmentation modes TRC and ACVH, especially for low-speed near-ship operations.
- Pilots strongly benefited from the two control augmentations TRC and ACVH during the MTEs hover alongside and sidestep towards the deck. Pilots commented that fewer control inputs were needed to keep the helicopter stable during both maneuvers. Again, as during the approach phase, best results of constant level 1 workload and desired handling qualities were achieved when visual and control augmentation were both activated. The ACVH response-type was rated with slightly better HQRs than the TRC response-type as feeling more "intuitive". Both advanced flight control modes were rated as being aggressive and precise enough for near-ship deck operations resulting in borderline Level 1 Cooper-Harper ratings during low as well during high SCONE ship motion levels.
- Taking visual and control augmentation both into account, all participating test and fleet pilots confirmed ratings to be desirable for higher degrees of aircraft stabilization. Visual and control augmentation being activated at same time manifested in low pilot workload, high situational awareness, and desired handling qualities ratings on the advanced flight control modes. Thus, ideal approach paths

could be achieved by all pilots while corresponding control inputs were at acceptable low aggressiveness level.

As a final conclusion it can be stated the deployment of a pilot assistance system using visual and control augmentation allows the proceeding of enhanced helicopter shipboard operations under DVE conditions and varying ship motions with acceptable workload and precise maneuvering. The utilization of an affordable HMD visual augmentation concept shows the potential to increase situational awareness and decrease pilot workload at same time when performing offshore maneuvers in challenging DVE conditions.

Simulator flight test campaigns environment:

The validity of the test results requires sufficient pilot acceptance of the simulation environment and a sufficient level of fidelity.

- The behavior of the basic H135 flight model with its primary cockpit controls was accepted well from all participating pilots. Both advanced flight control modes used for investigations, namely TRC and ACVH, were rated as being good by most of the pilots for maritime helicopter operations.
- Desired acceptance was stated from all participating maritime test and fleet pilots on the simulation fidelity as well as the maritime simulation environment. Locally even higher texture resolutions were recommended for helicopter low-speed and hover tasks.
- Results on simulator sickness (SSQ) showed acceptable and only slight effects in fatigue and headache at the end of the flight trials of all participating pilots. Most of the pilots were only very slightly affected by the symptoms of vertigo, headache, dizziness, nausea, and general discomfort or had no symptoms at all.

Recommendations for future work:

The intuitive scene-linked HMD enhanced visual augmentation concept was accepted well by all participating pilots operating the helicopter in DVE conditions. The results of this work may demonstrate that access to a pilot assistance system, including pilot-fitted advanced response types and a synthetic HMD visual augmentation concept could allow weather independent operations of the helicopter in the offshore as well in the onshore environment.

- For this purpose, allocating the advanced response types to high speed, low speed, and hover helicopter near-ship maneuvers automatically could even create a benefit regarding an automated helicopter shipboard landing in the long term.

- An expansion of the HMDs limited FoV may allow a more beneficial use of the HMD during hover and station keeping maneuvers, where pilots tended to higher head motions to set and keep up outside and synthetic visual cues.

Detailed test and fleet pilots' feedback on applied maritime conditions led to recommendations for future experimental designs.

- The integration of simulated dynamic elements within in the helicopter-ship-sea environment such as raising water particles caused by the rotor downwash and coupling of rotor inflow to the ship surface to the simulator outside scenery projection are recommended for further investigations in helicopter landing scenarios.
- With the objective of expanding the simulated DVEs of this work, the application of further harsh maritime conditions such as a night environment could be investigated regarding a visual-vestibular motion cueing assessment for maritime helicopter shipboard operations.

Rotorcraft pilots face unique challenges during helicopter shipboard operations, particularly in DVE conditions near the highly dynamic moving landing deck. To expand the envelope of safety, a promising HMD visual and control augmentation concept was developed and tested with success in several simulator flight test campaigns together with a wide spectrum of maritime helicopter pilots. The results of this work reveal elements for such a pilot assistance system that augment decision-making capabilities as well as reduce pilot workload and increase situational awareness. However, this work also identifies areas of interest, which may be useful in future safety evaluations. The predicting handling qualities pilot model might be applied to investigations on SHOL limitations taking human factors into account. Additional cueing technologies such as tactile and 3D audio systems could have the ability to further enhance situational and obstacle awareness by addressing several sensory organs of the pilot. Finally, new sensor imaging technologies produce realistic visuals that may allow offshore helicopter operations with a synthetic panoramic view beyond enhanced visual augmentation as already being started to be implemented for onshore rotorcraft operations, especially as to be used in DVE conditions.

References

- [1] “Aerial stern on view of the US Navy (USN) Arleigh Burke Class: (Flight IIA) Guided Missile Destroyer (Aegis), USS FORREST SHERMAN (DDG 98) underway in the Gulf of Mexico on the builder's sea trials,” <https://catalog.archives.gov/id/6669129>, [retrieved 18 September 2020.781Z].
- [2] Aeronautical Design Standard, Handling Qualities Requirements for Military Rotorcraft, ADS-33D, U.S. Army Aviation and Troop Command, St. Louis, MO, July 1994. [[Link](#)]
- [3] Ahram, T., Taiar, R., Gremeaux-Bader, V., Aminian, K. (Eds.) (2020). Advances in Intelligent Systems and Computing. HUMAN INTERACTION, EMERGING TECHNOLOGIES AND FUTURE APPLICATIONS II. [Place of publication not identified]: SPRINGER NATURE. <https://doi.org/10.1007/978-3-030-44267-5>
- [4] Airbus. Getting to Grips with CAT2 CAT3. Retrieved from <https://www.skybrary.aero/bookshelf/books/1480.pdf>
- [5] Anon., “Certification Specification for Helicopter Flight Simulation Training Devices CS-FSTD(H) Initial Issue,” European Aviation Safety Agency (EASA), 2012.
- [6] Arthur, J. J., Prinzel, L. J., Shelton, K. J., Kramer, L. J., Williams, S. P., Bailey, R. E., Norman, R. M. (2009). Synthetic Vision Enhanced Surface Operations With Head-Worn Display for Commercial Aircraft. *The International Journal of Aviation Psychology*, 19(2), 158–181. <https://doi.org/10.1080/10508410902766507>
- [7] Aviation Handbooks & Manuals (2020, April 3). Retrieved from https://www.faa.gov/regulations_policies/handbooks_manuals/aviation/
- [8] Bazilinsky, P., Dodou, D., Winter, J. de (2019). Survey on eHMI concepts: The effect of text, color, and perspective. *Transportation Research Part F: Traffic Psychology and Behaviour*, 67, 175–194. <https://doi.org/10.1016/j.trf.2019.10.013>
- [9] Berger, T., Blanken, C. L., Tischler, M. B., Horn, J. F. (2019). Flight control design and simulation handling qualities assessment of high-speed rotorcraft. Paper presented at Vertical Flight Society's 75th Annual Forum and Technology Display, Philadelphia, United States. [[Link](#)]
- [10] Bludau, J., Rauleder, J., Friedmann, L., Hajek, M. (2017). Real-Time Simulation of Dynamic Inflow Using Rotorcraft Flight Dynamics Coupled With a Lattice-Boltzmann Based Fluid Simulation. In *AIAA SciTech Forum: 55th AIAA Aerospace Sciences Meeting* (p. 3021). <https://doi.org/10.2514/6.2017-0050>
- [11] Brachmann, E., Krull, A., Michel, F., Gumhold, S., Shotton, J., Rother, C. (2014). Learning 6D Object Pose Estimation Using 3D Object Coordinates. In D. Fleet, T. Pajdla, B. Schiele, & T. Tuytelaars (Eds.), *Lecture Notes in Computer Science. Computer vision - eccv 2014: 13th european conference, zurich, switzerland* (Vol. 157

- 8690, pp. 536–551). [Place of publication not identified]: Springer.
https://doi.org/10.1007/978-3-319-10605-2_35
- [12] Browne, M. P., Moffitt, K. (2018). Feeling a little blue: problems with the symbol color blue for see-through displays and an alternative color solution. In J. Sanders-Reed & J. J. Arthur (Eds.), Proceedings of SPIE: Volume 10642, Degraded Environments: Sensing, Processing, and Display 2018: 17-18 April 2018, Orlando, Florida, United States (p. 24). Bellingham, Washington: SPIE. <https://doi.org/10.1117/12.2309653>
- [13] Carico, G. D., Fang, R., Finch, R. S., Geyer Jr., W. P. (2003). Helicopter/ship qualification testing: Les essais de qualification hélicoptère/navire ([Elektronische Ressource]). AC/323(SCI)TP: Vol. 53. Neuilly-sur-Seine: NATO. Retrieved from <http://www.rta.nato.int/Pubs/RDP.asp?RDP=RTO-AG-300-V22>
- [14] Carignan, S. J. R. P., Gubbels, A. W., Ellis, K., “Assessment of Handling Qualities for the Shipborne Recovery Task-ADS 33 (Maritime),” American Helicopter Society 56th Annual Forum Proceedings, Virginia Beach, VA, May 2–4, 2000. [[Link](#)]
- [15] Carlson, N. R., Birkett, M. A. (2017). Physiology of behavior (Twelfth edition, global edition). Boston: Pearson Education. [ISBN: 9780134080918](#)
- [16] Carter, H., Williams, P., Fitzpatrick, T. (2019?). Foliations of Coverage: Introducing Functional Coverage to DO-254 Verification Projects. In 2019 IEEE Aerospace Conference (pp. 1–7). [Piscataway, New Jersey]: IEEE. <https://doi.org/10.1109/AERO.2019.8741814>
- [17] Chen, L., Jin, Y., Yin, Y. (2017). Ocean Wave Rendering with Whitecap in the Visual System of a Maritime Simulator. Journal of Computing and Information Technology, 25(1), 63–76. <https://doi.org/10.20532/cit.2017.1003327>
- [18] Cheung, B., McKinley, R. A., Steels, B., Sceviour, R., Cosman, V., Holst, P., “Simulator Study of Helmet-Mounted Symbology System Concepts in Degraded Visual Environments,” Aerospace medicine and human performance; Vol. 86, No. 7, 2015, pp. 588–598. [doi: 10.3357/AMHP.4232.2015](https://doi.org/10.3357/AMHP.4232.2015).
- [19] cilas ariane group. SAFECOPTER Helicopter Visual Landing Aid System. Retrieved from <https://cilas.ariane.group/wp-content/uploads/sites/5/2018/07/cilas-safecopter.pdf>, 24.04.2020
- [20] Closing the loop with Helionix Step 3. Airbus. Retrieved from <https://www.airbus.com/newsroom/stories/closing-the-loop-helionix-step-3.html>
- [21] Comstock, J. R., Jones, L. C., Pope, A. T. (2003). The Effectiveness of Various Attitude Indicator Display Sizes and Extended Horizon Lines on Attitude Maintenance in a Part-Task Simulation. Proceedings of the Human Factors and Ergonomics Society Annual Meeting, 47(1), 144–148. <https://doi.org/10.1177/154193120304700130>

- [22] Constantin, A. (2012). An exact solution for equatorially trapped waves. *Journal of Geophysical Research: Oceans*, 117(C5), n/a-n/a. <https://doi.org/10.1029/2012JC007879>
- [23] Cutting, J. E. (2000). Images, imagination, and movement: Pictorial representations and their development in the work of James Gibson. *Perception*, 29(6), 635–648. <https://doi.org/10.1068/p2976>
- [24] Das V-Modell XT (2008). Berlin, Heidelberg: Springer Berlin Heidelberg. <https://doi.org/10.1007/978-3-540-30250-6>
- [25] DeckFinder (2020, May 8.000Z). Retrieved from <https://www.airbus.com/defence/uav/DeckFinder.html/>
- [26] DLR (2020, May 22.000Z). Landing on the deck of a ship – DLR continues its research into maritime helicopter missions. Retrieved from https://www.dlr.de/content/en/articles/news/2019/01/20190320_hedela-landing-on-the-deck-of-ship.html
- [27] Doehler, H.-U., Schmerwitz, S., Lueken, T. (2014). Visual-conformal display format for helicopter guidance. In J. J. Güell & J. Sanders-Reed (Eds.), *SPIE Proceedings, Degraded Visual Environments: Enhanced, Synthetic, and External Vision Solutions 2014* (90870J). SPIE. <https://doi.org/10.1117/12.2052677>
- [28] Doehler, H.-U. (2013). Improving visual-conformal displays for helicopter guidance. *SPIE Newsrooms*. Advance online publication. <https://doi.org/10.1117/2.1201310.005162>
- [29] Doehler, H.-U., Ernst, J. M., Lueken, T., “Virtual aircraft-fixed cockpit instruments,” *Proc. of SPIE Vol. 9471*, *Degraded Visual Environments: Enhanced, Synthetic, and External Vision Solutions*, Baltimore, USA, 2015. <https://doi.org/10.1117/12.2177796>
- [30] Dörner, R., Broll, W., Grimm, P. F., Jung, B. (2013). *Virtual und Augmented Reality (VR/AR): Grundlagen und Methoden der Virtuellen und Augmentierten Realität*. eXamen.press. Berlin, Heidelberg: Springer Vieweg. <https://doi.org/10.1007/978-3-642-28903-3>
- [31] Dupuy, J., Bruneton, E. (2012). Real-time animation and rendering of ocean whitecaps. In Z. Zhang & Z. Li (Eds.), *ACM Digital Library, SIGGRAPH Asia 2012 Technical Briefs* (pp. 1–3). New York, NY: ACM. <https://doi.org/10.1145/2407746.2407761>
- [32] EASA - RPS (2012): CS-FSTD(H) Initial Issue. Online verfügbar unter <https://www.easa.europa.eu/sites/default/files/dfu/Final%20Report%20EASA.2011.02.pdf>.

- [33] Elbit Systems (2020, June 1.000Z). Helmet Mounted Systems Archives - Elbit Systems. Retrieved from <https://elbitsystems.com/pdf-category/company-brochures/helmet-mounted-systems/>
- [34] Ernst, J. M., Doehler, H.-U., Schmerwitz, S. (2016). A concept for a virtual flight deck shown on an HMD. In J. Sanders-Reed & J. J. Arthur (Eds.), SPIE Proceedings, Degraded Visual Environments: Enhanced, Synthetic, and External Vision Solutions 2016 (p. 983909). SPIE. <https://doi.org/10.1117/12.2224933>
- [35] Forrest, J. S., Owen, I., Padfield, G. D., Hodge, S. J. (2012). Ship-Helicopter Operating Limits Prediction Using Piloted Flight Simulation and Time-Accurate Airwakes. *Journal of Aircraft*, 49(4), 1020–1031. <https://doi.org/10.2514/1.C031525>
- [36] Forrest, J., Hodge, S., Matayoshi, N., Owen, I., Padfield, G., et al. (2009): Relationship between Pilot Workload and Turbulence Intensity for Helicopter Operations in Harsh Environments. In: AHS International Forum 65: AHS International. [\[Link\]](#)
- [37] Fournier, A., Reeves, W. T. (1985). A simple model of ocean waves. In D. C. Evans (Ed.), ACM SIGGRAPH: v. 20, no. 4, SIGGRAPH '86 conference proceedings: August 18-22, 1986, Dallas, Texas (pp. 75–84). New York, N.Y: Association for Computing Machinery. <https://doi.org/10.1145/15922.15894>
- [38] Funabiki, K., Tsuda, H., Iijima, T., Nojima, T., Tawada, K., Yoshida, T. (2009). Flight experiment of pilot display for search-and-rescue helicopter. In P. L. Marasco, P. R. Havig, S. A. Jennings, & T. H. Harding (Eds.), SPIE Proceedings, Head- and Helmet-Mounted Displays XIV: Design and Applications (p. 732607). SPIE. <https://doi.org/10.1117/12.819096>
- [39] Funabiki, K., Tsuda, H., Shimizu, A., Sugihara, Y., Tawada, K., and Hasebe, K., “Objective Flight Evaluation of Visual Cue for DVE Helicopter Operation,” AIAA Scitech 2020 Forum, American Institute of Aeronautics and Astronautics, Reston, Virginia, 01062020. <https://doi.org/10.2514/6.2020-0055>
- [40] Gazzaniga, M. S., Ivry, R. B., Mangun, G. R., Steven, M. S. (2009). *Cognitive neuroscience: The biology of the mind* (3. ed., internat. student ed.). New York, NY: Norton. [ISBN 13: 9780393922288](#)
- [41] Gegenfurtner, K. R. (Ed.) (2015). *Lehrbuch. Wahrnehmungspsychologie: Der Grundkurs* (K. Neuser-von Oettingen & G. Plata, Trans.). Berlin, Heidelberg: Springer. [ISBN: 978-3-642-55073-7](#)
- [42] Geiselman, E. E., Havig, P. R. (2011). Rise of the HMD: the need to review our human factors guidelines. In P. L. Marasco & P. R. Havig (Eds.), SPIE Proceedings, Head- and Helmet-Mounted Displays XVI: Design and Applications (p. 804102). SPIE. <https://doi.org/10.1117/12.883859>

- [43] Geiselman, E. E., Post, D. L., Brickman, B. J., Rogers-Adams, B., Hettinger, L. J., Haas, M. W. (1998). Helmet-mounted display targeting symbology color coding: context vs. population bias. In R. J. Lewandowski, L. A. Haworth, & H. J. Girolamo (Eds.), SPIE Proceedings, Helmet- and Head-Mounted Displays III (p. 15). SPIE. <https://doi.org/10.1117/12.317432>
- [44] Geiselman, E. E., Havig, P. R. (2011). Rise of the HMD: the need to review our human factors guidelines. In P. L. Marasco & P. R. Havig (Eds.), SPIE Proceedings, Head- and Helmet-Mounted Displays XVI: Design and Applications (p. 804102). SPIE. <https://doi.org/10.1117/12.883859>
- [45] GitHub (2020, March 30). microsoft/singleshotpose. Retrieved from <https://github.com/microsoft/singleshotpose>
- [46] Goldstein, E. B., Ritter, M., Herbst, G. (2002). Wahrnehmungspsychologie (2. deutsche Auflage). Spektrum Lehrbuch. Heidelberg: Spektrum Akad. Verl.
- [47] Goss, M. E. (1990). A real time particle system for display of ship wakes. IEEE Computer Graphics and Applications, 10(3), 30–35. <https://doi.org/10.1109/38.55150>
- [48] Greiser, S., Lantzsch, R., Wolfram, J., Wartmann, J., Müllhäuser, M., Lüken, T., Peinecke, N. (2015). Results of the pilot assistance system “Assisted Low-Level Flight and Landing on Unprepared Landing Sites” obtained with the ACT/FHS research rotorcraft. Aerospace Science and Technology, 45, 215–227. <https://doi.org/10.1016/j.ast.2015.05.017>
- [49] Gundelsweiler, F., Memmel, T., Reiterer, H. (2004). Agile Usability Engineering. In R. Keil-Slawik, H. Selke, & G. Szwillus (Eds.), Mensch and Computer 2004: Allgegenwärtige Interaktion. München Wien: De Gruyter. <https://doi.org/10.1524/9783486598773.33>
- [50] Halbe, O., Hajek, M.: A Methodology towards Rotorcraft Piloting Autonomy for Approach on Moving Offshore Platforms, American Helicopter Society 74th Annual Forum, Phoenix, AZ, 2018. [\[Link\]](#)
- [51] Halbe, O., Hajek, M. (01062020). Robust Helicopter Sliding Mode Control for Enhanced Handling and Trajectory Following. In AIAA Scitech 2020 Forum (p. 574). Reston, Virginia: American Institute of Aeronautics and Astronautics. <https://doi.org/10.2514/6.2020-1828>
- [52] Halbe, O., Mehling, T., Hajek, M., Vrdoljak, M., “Synthesis and Piloted Evaluation of Advanced Response-Types Based on Robust Sliding Mode Control,” AHS Journal, July 2021. [\[Link\]](#)

- [53] Halbe, O., Mehling, T., Vrdoljak, M., Hajek, M., "Synthesis and Piloted Evaluation of Advanced Response-Types Based on Robust Sliding Mode Control," In: AHS International Forum 77: AHS International. [\[Link\]](#)
- [54] Harding, T. H., Rash, C. E. (2017). Daylight luminance requirements for full-color, see-through, helmet-mounted display systems. *Optical Engineering*, 56(5), 51404. <https://doi.org/10.1117/1.OE.56.5.051404>
- [55] Hardy, G. J., Foote, B. (2015). Flight evaluation of an ISIE-11 based digital night vision goggle prototype. In J. Sanders-Reed & J. J. Arthur (Eds.), *SPIE Proceedings, Degraded Visual Environments: Enhanced, Synthetic, and External Vision Solutions 2015* (p. 947102). SPIE. <https://doi.org/10.1117/12.2180251>
- [56] Hart, S. G., "Nasa-Task Load Index (NASA-TLX); 20 Years Later," 2016; *Proceedings of the Human Factors and Ergonomics Society Annual Meeting*, 50(9), 904-908. [doi: 10.1177/154193120605000909](https://doi.org/10.1177/154193120605000909).
- [57] HELIOP - Lehrstuhl für Hubschraubertechnologie (2020, March 28). Retrieved from <https://www.lrq.tum.de/ht/forschungsprojekte/heliop/>
- [58] Henry, D. (2018). On three-dimensional Gerstner-like equatorial water waves. *Philosophical Transactions. Series A, Mathematical, Physical, and Engineering Sciences*, 376(2111). <https://doi.org/10.1098/rsta.2017.0088>
- [59] Hensoldt (2020). SFERION Pilot Assistance during the entire mission under all conditions. Retrieved from https://www.hensoldt.net/fileadmin/hensoldt/Solutions/Air/Situational_Awareness/0361_17_Sferion_brochure_E_intranet.pdf, 29.03.2020.
- [60] Hess, R. A., "Flight simulator fidelity assessment in a rotorcraft lateral translation maneuver," *Guidance, Navigation and Control Conference, Guidance, Navigation and Control Conference*, Hilton Head Island, SC, U.S.A, 10 August 1992 - 12 August 1992, American Institute of Aeronautics and Astronautics, Reston, Virginia, 08101992. [doi: 10.2514/6.1992-4424](https://doi.org/10.2514/6.1992-4424).
- [61] Hess, R. A., Zeyada, Y., and Heffley, R. K., "Modeling and Simulation for Helicopter Task Analysis," *Journal of the American Helicopter Society*; Vol. 47, No. 4, 2002, p. 243. [doi: 10.4050/JAHS.47.243](https://doi.org/10.4050/JAHS.47.243).
- [62] Hess, R. A., "Simplified approach for modelling pilot pursuit control behaviour in multi-loop flight control tasks," *Proceedings of the Institution of Mechanical Engineers, Part G: Journal of Aerospace Engineering*; Vol. 220, No. 2, 2006, pp. 85–102. [doi: 10.1243/09544100JAERO33](https://doi.org/10.1243/09544100JAERO33).
- [63] Hess, R. A., "Obtaining multi-loop pursuit-control pilot models from computer simulation," *Proceedings of the Institution of Mechanical Engineers, Part G: Journal*

- of Aerospace Engineering; Vol. 222, No. 2, 2008, pp. 189–199. [doi: 10.1243/09544100JAERO260](https://doi.org/10.1243/09544100JAERO260).
- [64] Hilderman, V. (2014, November - 2014, November). Understanding DO-178C Software Certification: Benefits Versus Costs. In Software Reliability Engineering Workshops (ISSREW), 2014 IEEE International Symposium on (p. 114). IEEE. <https://doi.org/10.1109/ISSREW.2014.118>
- [65] Hinterstoisser, S., Lepetit, V., Ilic, S., Holzer, S., Konolige, K., Bradski, G., Navab, N. (2012). Technical Demonstration on Model Based Training, Detection and Pose Estimation of Texture-Less 3D Objects in Heavily Cluttered Scenes. In A. Fusiello, V. Murino, & R. Cucchiara (Eds.), LNCS sublibrary. SL 6, Image processing, computer vision, pattern recognition, and graphics: Vol. 7585. Computer vision--ECCV 2012. Workshops and demonstrations: Florence, Italy, October 7-13, 2012, Proceedings. Part III (Vol. 7585, pp. 593–596). Berlin, New York: Springer. https://doi.org/10.1007/978-3-642-33885-4_60
- [66] Hodge, S. J., Forrest, J. S., Padfield, G. d., Owen, I. (2012). Simulating the environment at the helicopter-ship dynamic interface: research, development and application. The Aeronautical Journal, 116(1185), 1155–1184. <https://doi.org/10.1017/S0001924000007545>
- [67] Horn, J. F., Yang, J., He, C., Lee, D., Tritschler, J. K. (2015). Autonomous ship approach and landing using dynamic inversion control with deck motion prediction. In *41st European Rotorcraft Forum 2015, ERF 2015* (pp. 864-877). (41st European Rotorcraft Forum 2015, ERF 2015; Vol. 2). Deutsche Gesellschaft fuer Luft und Raumfahrt (DGLR). [ISBN: 9781510819832](https://doi.org/10.1017/S0001924000007545).
- [68] Inside BAE's Striker II – The most advanced fighter pilot helmet ever made (2020, May 15). Retrieved from <http://home.bt.com/tech-gadgets/future-tech/inside-baes-striker-ii-the-most-advanced-fighter-pilot-helmet-ever-made-11364174261792>
- [69] jdupuy/whitecaps (2020, April 10). Retrieved from <https://github.com/jdupuy/whitecaps>
- [70] Jedeye - Elbit Systems (2020, May 15.000Z). Retrieved from <https://elbitsystems.com/pdf/jedeye-2/>
- [71] Johnson, W., “A History of Rotorcraft Comprehensive Analyses,” NASA/TP-2012-216012, Ames Research Center, California, 2012. https://rotorcraft.arc.nasa.gov/Publications/files/TP-2012-216012_Johnson_final.pdf
- [72] Kahana, A. (2015). Obstacle-Avoidance Displays for Helicopter Operations: Spatial Versus Guidance Symbolologies. Journal of Aerospace Information Systems, 12(7), 455–466. <https://doi.org/10.2514/1.1010306>

- [73] Kennedy, R. S., Lane, N. E., Berbaum, K. S., and Lilienthal, M. G., "Simulator Sickness Questionnaire: An Enhanced Method for Quantifying Simulator Sickness," *The International Journal of Aviation Psychology*; Vol.3, No.3, 1993, pp. 203–220. [doi: 10.1207/s15327108ijap0303_3](https://doi.org/10.1207/s15327108ijap0303_3).
- [74] Klein, O., Doehler, H.-U., Trousil, T., Peleg-Marzan, R. (2012). Use of 3D conformal symbology on HMD for a safer flight in degraded visual environment. In *SPIE Proceedings, Airborne Intelligence, Surveillance, Reconnaissance (ISR) Systems and Applications IX (83600Q)*. SPIE. <https://doi.org/10.1117/12.918871>
- [75] Knabl, P. M., Döhler, H., Schmerwitz, S., Biella, M. (2012). Integration of a helmet-mounted display for helicopter operations in degraded visual environment: a human factors perspective. Retrieved from <https://elib.dlr.de/76069/>
- [76] Knabl, P. M., & Peinecke, N. (2013). Designing an obstacle display for helicopter operations in degraded visual environment. In B. E. Rogowitz, T. N. Pappas, & H. de Ridder (Eds.), *SPIE Proceedings, Human Vision and Electronic Imaging XVIII* (p. 865111). SPIE. <https://doi.org/10.1117/12.2004143>
- [77] Knabl, P., Schmerwitz, S., Doehler, H.-U. (2015). Target Detection with Helmet-mounted Displays in Low Visibility Helicopter Operations. *Procedia Manufacturing*, 3, 2558–2565. <https://doi.org/10.1016/j.promfg.2015.07.558>
- [78] Konishi, Y., Hattori, K., Hashimoto, M. (2019, November - 2019, November). Real-Time 6D Object Pose Estimation on CPU. In *2019 IEEE/RSJ International Conference on Intelligent Robots and Systems (IROS)* (pp. 3451–3458). IEEE. <https://doi.org/10.1109/IROS40897.2019.8967967>
- [79] Lampton, A., Klyde, D. H., "Power Frequency: A Metric for Analyzing Pilot-in-the-Loop Flying Tasks," *Journal of Guidance, Control, and Dynamics*; Vol. 35, No. 5, 2012, pp. 1526–1537. <https://doi.org/10.2514/1.55549>.
- [80] Lantzsich, R., Greiser, S., Wolfram, J., Wartmann, J., Müllhäuser, M., Lueken, T., Döhler, H., Peinecke, N. (2012). ALLFLIGHT: HELICOPTER PILOT ASSISTANCE IN ALL PHASES OF FLIGHT. Retrieved from https://dspace-erf.nlr.nl/xmlui/bitstream/handle/20.500.11881/660/ERF2012_023.pdf?sequence=1
- [81] Lehmann, P. H., Jones, M., and Höfinger, M., "Impact of turbulence and degraded visual environment on pilot workload," *CEAS Aeronautical Journal*; Vol. 8, No. 3, 2017, pp. 413–428. [doi: 10.1007/s13272-017-0246-3](https://doi.org/10.1007/s13272-017-0246-3).
- [82] Lemoine, O., François, J.-M., Point, P. (2013). Contribution of TopOwl head mounted display system in degraded visual environments. In K. L. Bernier & J. J. Güell (Eds.), *SPIE Proceedings, Degraded Visual Environments: Enhanced, Synthetic, and External Vision Solutions 2013 (87370B)*. SPIE. <https://doi.org/10.1117/12.2015824>

- [83] Lemoussu, S., Chaudemar, J. C., Vingerhoeds R. A. (2018). Systems Engineering And Project Management Process Modeling In The Aeronautics Context: Case Study Of Smes. <https://doi.org/10.5281/ZENODO.1315743>
- [84] Lenhart, P. M., Räumliche Darstellung von Flugführungsinformationen in Head-Mounted Displays, Ergonomia-Verl., Stuttgart, 2006. [ISBN: 978-3-935089-88-3](https://doi.org/10.1007/s11263-008-0152-6)
- [85] Lepetit, V., Moreno-Noguer, F., & Fua, P. (2009). EPnP: An Accurate O(n) Solution to the PnP Problem. International Journal of Computer Vision, 81(2), 155–166. <https://doi.org/10.1007/s11263-008-0152-6>
- [86] Lüken, T., Schmerwitz, S., Halbe, O., Hamers, M., Roland, B., Ganille, T. (2019) Flight Evaluation of Advanced SBAS Poin-in-Space Helicopter Procedures Facilitating IFR Access in Difficult Terrain and Dense Airspaces, 45th European Rotorcraft Forum, Warschau, Polen. [\[Link\]](#)
- [87] Lumsden, R. B., Padfield, G. D., Braby-Deighton, C. D. (1999). Human Factors Challenges at the Helicopter-Ship Dynamic Interface. In SAE Technical Paper Series, SAE Technical Paper Series. SAE International400 Commonwealth Drive, Warrendale, PA, United States. <https://doi.org/10.4271/1999-01-5607>
- [88] Lynx Helicopter amazing ship landing - YouTube (2020, April 17). Retrieved from <https://www.youtube.com/watch?v=iAdHsW7u0Q4>
- [89] Ma, T., Huang, J., Zhang, Q. (2013). Ship wakes 3D simulation based on OSG. In IEEE TENCON 2013: October 22-25, 2013: Xi'an, China: 2013 IEEE International Conference of IEEE Region 10 (TENCON 2013) : Shaanxi Guesthouse, Xi'an, Shaanxi, China : October 22-25, 2013 (pp. 1–3). IEEE. <https://doi.org/10.1109/TENCON.2013.6719053>
- [90] Maibach, M., Jones, M., Walko, Ch. (2020): Using Augmented Reality to Reduce Workload in Offshore Environments. In: AHS International Forum 76: AHS International.
- [91] Mastin, G., Watterberg, P., Mareda, J. (1987). Fourier Synthesis of Ocean Scenes. IEEE Computer Graphics and Applications, 7(3), 16–23. <https://doi.org/10.1109/MCG.1987.276961>
- [92] Mehling, T., Paul, T., Puchan J. (2015), “Anforderungsanalyse zur Steuerung eines Unmanned Aerial Vehicle (UAV) aus einem Hubschrauber mit Hilfe eines Tablet Computers,” Bachelor Thesis at University of Applied Sciences Munich, Munich, Germany.
- [93] Mehling, T., Eichhorn, Ch., Yixuan, L., Klinker, G., Hajek, M., (2021) “Ship Detection and Visual Augmentation during Helicopter Ship Deck Operations,” AIAA Aviation Forum 2021, Washington, D.C., USA. [\[Link\]](#)

- [94] Mehling, T., Halbe, O., Gasparac, T., Vrdoljak, M., and Hajek, M., “Piloted Simulation of Helicopter Shipboard Recovery with Visual and Control Augmentation,” AIAA Scitech 2021 Forum, American Institute of Aeronautics and Astronautics, Reston, Virginia, 01112021. <https://doi.org/10.2514/6.2021-1136>
- [95] Mehling, T., Halbe, O., Vrdoljak, M., Hajek, M., “Visual and Control Augmentation Techniques for Pilot Assistance During Helicopter Shipboard Recovery,” published in Journal of AHS American Helicopter Society. [DOI: 10.4050/JAHS.67.042004](https://doi.org/10.4050/JAHS.67.042004)
- [96] Miller, J.D., Goodfrey-Cooper, M. (2019): Augmented-Reality Multimodal Cueing for Obstacle Awareness: Towards a New Topology for Threat-Level Presentation. In: AHS International Forum 75: AHS International. [\[Link\]](#)
- [97] Minotra, D., Feigh, K., “Studying Pilot Cognition in Ship-Based Helicopter Landing Maneuvers,” *AHS International 74th Annual Forum & Technology Display*, Phoenix, Arizona, USA, May 14 – May 17, 2018. [\[Link\]](#)
- [98] Misra, G., Gao, T., Bai, X. (01072019). Modeling and Simulation of UAV Carrier Landings. In AIAA Scitech 2019 Forum (p. 7345056). Reston, Virginia: American Institute of Aeronautics and Astronautics. <https://doi.org/10.2514/6.2019-1981>
- [99] Moon, J., Domercant, J. C., Mavris, D. (2015). A simplified approach to assessment of mission success for helicopter landing on a ship. *International Journal of Control, Automation and Systems*, 13(3), 680–688. <https://doi.org/10.1007/s12555-013-0092-y>
- [100] Morland, A. B., Jones, S. R., Finlay, A. L., Deyzac, E., Lê, S., Kemp, S. (1999). Visual perception of motion, luminance and colour in a human hemianope. *Brain : A Journal of Neurology*, 122 (Pt 6), 1183–1198. <https://doi.org/10.1093/brain/122.6.1183>
- [101] Moy, Y., Ledinot, E., Delseny, H., Wiels, V., Monate, B. (2013). Testing or Formal Verification: DO-178C Alternatives and Industrial Experience. *IEEE Software*, 30(3), 50–57. <https://doi.org/10.1109/MS.2013.43>
- [102] Münsterer, T., Völschow, P., Singer, B., Strobel, M., Kramper, P. (2015). DVE flight test results of a sensor enhanced 3D conformal pilot support system. In J. Sanders-Reed & J. J. Arthur (Eds.), *SPIE Proceedings, Degraded Visual Environments: Enhanced, Synthetic, and External Vision Solutions 2015* (p. 947106). SPIE. <https://doi.org/10.1117/12.2180634>
- [103] Münsterer, T., Schafhitzel, T., Strobel, M., Völschow, P., Klasen, S., Eisenkeil, F. (2014). Sensor-enhanced 3D conformal cueing for safe and reliable HC operation in DVE in all flight phases. In J. J. Güell & J. Sanders-Reed (Eds.), *SPIE Proceedings, Degraded Visual Environments: Enhanced, Synthetic, and External Vision Solutions 2014* (90870I). SPIE. <https://doi.org/10.1117/12.2050377>

- [104] Nascimento, F. A. C., Majumdar, A., Jarvis, S. (2012). Nighttime approaches to offshore installations in Brazil: Safety shortcomings experienced by helicopter pilots. *Accident; Analysis and Prevention*, 47, 64–74. <https://doi.org/10.1016/j.aap.2012.01.014>
- [105] NATO STANDARDIZATION OFFICE. (2017). MPP-02(H)(1), Vol I, Helicopter Operations from Ships other than Aircraft Carriers (HOSTAC). *EDITION (H) VERSION (1)*. Retrieved from <https://www.japcc.org/wp-content/uploads/MPP-02-VOL-I-EDH-V1-E.pdf>, 30.05.2019.
- [106] Newman, R. L., Greeley, K. W. (1997). *Helmet-Mounted Display Design Guide*. Retrieved from <https://ntrs.nasa.gov/archive/nasa/casi.ntrs.nasa.gov/19980018292.pdf>
- [107] O'Brien, P., Baughman, D. C., Wallace, H. B. (2013). Helicopter synthetic vision based DVE processing for all phases of flight. In K. L. Bernier & J. J. Güell (Eds.), *SPIE Proceedings, Degraded Visual Environments: Enhanced, Synthetic, and External Vision Solutions 2013* (p. 873706). SPIE. <https://doi.org/10.1117/12.2016555>
- [108] Ockier, C. J., Gollnick, V., “ADS-33 Flight Testing—Lessons Learned,” *AGARD Conference Proceedings 592: Advances in Rotorcraft Technology*, Canada Communication Group, Hull (Quebec), Canada, 1996, pp. 10.1–10.12.
- [109] Owen, I., White, M., Padfield, G.D., Hodge, S. J. (2017). A virtual engineering approach to the ship-helicopter dynamic interface – a decade of modelling and simulation research at the University of Liverpool. *The Aeronautical Journal*, 121(1246), 1833–1857. <https://doi.org/10.1017/aer.2017.102>
- [110] Padfield, G.D., Charlton, M., Kimberley, A. (1992). *Helicopter Flying Qualities in Critical MTEs; initial experience with the DRA (Bedford) Large Motion Simulator*. Retrieved from <https://dspace-erf.nlr.nl/xmlui/bitstream/handle/20.500.11881/2452/ERF%201992-Vol2-F2.pdf?sequence=1&isAllowed=y>
- [111] Padfield, G.D., *Controlling the Tension Between Performance and Safety in Helicopter Operations. A Perspective on Flying Qualities*, Proceedings of the 24th European Rotorcraft Forum, Marseilles, France, September 1998. <https://doi.org/10.4050/JAHS.58.011001>.
- [112] Palmer, S. E. (2002). *Vision science: Photons to phenomenology* (3. printing). A Bradford book. Cambridge, Mass.: MIT Press. Retrieved from https://www.researchgate.net/publication/224282145_Vision_Science_From_Photos_to_Phenomenology

- [113] Peinecke, N., Schmerwitz, S., Döhler, H.-U., Lüken, T. (2017). Review of conformal displays: more than a highway in the sky. *Optical Engineering*, 56(5), 51406. <https://doi.org/10.1117/1.OE.56.5.051406>
- [114] Peng, S., Liu, Y., Huang, Q., Bao, H., Zhou, X. (2018). PVNet: Pixel-wise Voting Network for 6DoF Pose Estimation. Retrieved from <https://arxiv.org/pdf/1812.11788>
- [115] Perfect, P., White, M., Padfield, G.D., Gubbels, A. W. (2013). Rotorcraft simulation fidelity: new methods for quantification and assessment. *The Aeronautical Journal*, 117(1189), 235–282. <https://doi.org/10.1017/S0001924000007983>
- [116] Pfanmüller, L., Bengler, K. (2017). Anzeigekonzepte für ein kontaktanaloges Head-up Display. Dissertation at TUM Technical University of Munich. <https://mediatum.ub.tum.de/node?id=1314300>
- [117] Priot, A.-E., Vacher, A., Vienne, C., Neveu, P., Roumes, C. (2018). The initial effects of hyperstereopsis on visual perception in helicopter pilots flying with see-through helmet-mounted displays. *Displays*, 51, 1–8. <https://doi.org/10.1016/j.displa.2017.11.002>
- [118] Radford, R. C., Andrisani, D., “An experimental investigation of VTOL flying qualities requirements in shipboard landings,” *Journal of Aircraft*; Vol. 21, No. 6, 1984, pp. 371–379. <https://doi.org/10.2514/3.44975>
- [119] Schmerwitz, S., Knabl, P. M., Lueken, T., Doehler, H.-U. (2015). Drift indication for helicopter approach and landing. In J. Sanders-Reed & J. J. Arthur (Eds.), *SPIE Proceedings, Degraded Visual Environments: Enhanced, Synthetic, and External Vision Solutions 2015 (94710D)*. SPIE. <https://doi.org/10.1117/12.2177816>
- [120] Schmerwitz, S., Lueken, T., Doehler, H.-U., Peinecke, N., Ernst, J. M., da Silva Rosa, D. L. (2017). Conformal displays: human factor analysis of innovative landing aids. *Optical Engineering*, 56(5), 51407. <https://doi.org/10.1117/1.OE.56.5.051407>
- [121] Scott, P., Kelly, M., White, Owen, L. (2017). Using piloted simulation to measure pilot workload of landing a helicopter on a small ship. Retrieved from <https://livrepository.liverpool.ac.uk/3009013/1/ERF%202017%20size%20paper%20final.pdf>
- [122] SHOLDS | Aeronautical & General Instruments (AGI) Ltd (2020, May 22.000Z). Retrieved from <https://www.agild.co.uk/naval-products/ship-navigation/operational-limits/>.
- [123] Sicherer Hubschraubereinsatz bei schlechter Sicht (2020, May 22.000Z). Retrieved from https://www.dlr.de/content/de/artikel/news/2017/20170711_sicherer-hubschraubereinsatz-bei-schlechter-sicht_23205.html
- [124] Singh, A. (2011). RtcA DO-178B (EUROCAE ED-12B). from <https://doi.org/10.13140/RG.2.2.14788.42886>, 20.03.2020.

- [125] Sonesson, G. L., Horn, J. F., Zheng, A. (2016). Simulation Testing of Advanced Response Types for Ship-Based Rotorcraft. *Journal of the American Helicopter Society*, 61(3), 1–13. <https://doi.org/10.4050/JAHS.61.032011>
- [126] STANAG Nr. 1154.- NATO Qualifikations for Helicopter Controllers - Deutsche Digitale Bibliothek. Retrieved from <https://www.deutsche-digitale-bibliothek.de/item/MVAPZ44YUJPRQAXMYPLZAKCISZFAXMLR>, 31.05.2019.
- [127] Stanton, N. A., Roberts, A. P., Plant, K. L., Allison, C. K., Harvey, C. (2018). Head-up displays assist helicopter pilots landing in degraded visual environments. *Theoretical Issues in Ergonomics Science*, 19(5), 513–529. <https://doi.org/10.1080/1463922X.2017.1394506>
- [128] Stanton, N. A., Plant, K. L., Roberts, A. P., Allison, C. K., Harvey, C. (2018). The virtual landing pad: facilitating rotary-wing landing operations in degraded visual environments. *Cognition, Technology & Work*, 20(2), 219–232. <https://doi.org/10.1007/s10111-018-0467-1>
- [129] Stelmash, S., Münsterer, T., Kramper, P., Samuelis, C., Bühler, D., Wegner, M., Sheth, S. (2015). Flight test results of ladar brownout look-through capability. In J. Sanders-Reed & J. J. Arthur (Eds.), *SPIE Proceedings, Degraded Visual Environments: Enhanced, Synthetic, and External Vision Solutions 2015* (p. 947105). SPIE. <https://doi.org/10.1117/12.2180629>
- [130] Striker® II Digital Helmet-Mounted Display (2020, May 15). Retrieved from <https://www.baesystems.com/en-uk/product/striker-ii-digital-helmet-mounted-display>
- [131] Sugihara, Y., Ohga, K., Funabiki, K., Tawada, K. (01062020). GPV: HMD Symbology for Terrain Following in DVE. In *AIAA Scitech 2020 Forum*. Reston, Virginia: American Institute of Aeronautics and Astronautics. <https://doi.org/10.2514/6.2020-0666>
- [132] System Engineering Life-Cycle Building Blocks. Retrieved from <http://sidsoft.in/SELifeCycleBuildingBlocks.aspx>, 20.03.2020.
- [133] Swan, J. E., Jones, A., Kolstad, E., Livingston, M. A., Smallman, H. S. (2007). Egocentric depth judgments in optical, see-through augmented reality. *IEEE Transactions on Visualization and Computer Graphics*, 13(3), 429–442. <https://doi.org/10.1109/TVCG.2007.1035>
- [134] Szoboszlay, Z., Davis, B., Fujizawa, B., Minor, J., Osmon, M., Morford, Z., “Degraded Visual Environment Mitigation (DVE-M) Program, Yuma 2016 Flight Trials in Brownout,” *American Helicopter Society 57th Annual Forum Proceedings*, Washington, D.C., May 9-11, 2017. [\[Link\]](#)

- [135] Tchou, J. L., Barnidge, T. J. (2015). Review of the evolution of display technologies for next-generation aircraft. In (94700F). International Society for Optics and Photonics. <https://doi.org/10.1117/12.2181092>
- [136] Tekin, B., Sinha, S. N., Fua, P. (2017). Real-Time Seamless Single Shot 6D Object Pose Prediction. Retrieved from <https://arxiv.org/pdf/1711.08848>
- [137] Tessendorf - 2001 - Simulating Ocean Water. Retrieved from <http://citeseerx.ist.psu.edu/viewdoc/download?doi=10.1.1.161.9102&rep=rep1&type=pdf>
- [138] TopOwl, Helmet-mounted Sight & Display for Helicopters (2020, May 22.000Z). Retrieved from <https://www.thalesgroup.com/en/markets/aerospace/vision-systems/topowl-helmet-mounted-sight-display-helicopters>
- [139] TopOwl, Helmet-mounted Sight & Display for Helicopters (2020, May 22.000Z). Retrieved from <https://www.thalesgroup.com/en/markets/aerospace/flight-deck-avionics-equipment-functions/topowl-helmet-mounted-sight-display>
- [140] TSO (The Stationery Office) on behalf of the UK Civil Aviation Authority. (2010). CAA PAPER 2010/01 - The SBAS Offshore Approach Procedure (SOAP). (2020, May 22.000Z). Retrieved from <https://publicapps.caa.co.uk/docs/33/2010001.pdf>.
- [141] Viertler, F., Hajek, M. (2015). Dynamic registration of an optical see-through HMD into a wide field-of-view rotorcraft flight simulation environment. In D. D. Desjardins, K. R. Sarma, P. L. Marasco, & P. R. Havig (Eds.), SPIE Proceedings, Display Technologies and Applications for Defense, Security, and Avionics IX; and Head-and Helmet-Mounted Displays XX (94700Y). SPIE. <https://doi.org/10.1117/12.2176190>
- [142] Viertler, F., Hajek, M. (2017). Evaluation of Visual Augmentation Methods for Rotorcraft Pilots in Degraded Visual Environments. Journal of the American Helicopter Society, 62(1), 1–11. <https://doi.org/10.4050/JAHS.62.012005>
- [143] Viertler, F., Hajek, M. (2015). Requirements and Design Challenges in Rotorcraft Flight Simulations for Research Applications. In AIAA SciTech: AIAA Modeling and Simulation Technologies Conference. <https://doi.org/10.2514/6.2015-1808>
- [144] Viertler, F., Hajek, M. (2017). Visual Augmentation for Rotorcraft Pilots in Degraded Visual Environments. Dissertation at TUM Technical University of Munich. <http://nbn-resolving.de/urn/resolver.pl?urn:nbn:de:bvb:91-diss-20170421-1335668-1-9>
- [145] Vitale, A., Bianco, D., Corrado, G., Martone, A., Corrado, F., Giuliano, A., Arcadipane, A. (2018). Simulation Environment for Development of Unmanned Helicopter Automatic Take-off and Landing on Ship Deck. In Linköping Electronic Conference Proceedings, Proceedings of The 9th EUROSIM Congress on Modelling and

- Simulation, EUROSIM 2016, The 57th SIMS Conference on Simulation and Modelling SIMS 2016 (pp. 228–234). Linköping University Electronic Press. <https://doi.org/10.3384/ecp17142228>
- [146] Walters, R., McCandless, J., Feigh, K. M. (01062020). Pilot Cueing for Rotorcraft Shipboard Landings. In AIAA Scitech 2020 Forum. Reston, Virginia: American Institute of Aeronautics and Astronautics. <https://doi.org/10.2514/6.2020-0056>
- [147] Wang, Y., White, M., Owen, I., Hodge, S., Barakos, G., “Effects of visual and motion cues in flight simulation of ship-borne helicopter operations,” CEAS Aeronautical Journal; Vol. 4, No. 4, 2013, pp. 385–396. [doi: 10.1007/s13272-013-0085-9](https://doi.org/10.1007/s13272-013-0085-9).
- [148] Wang, C., Xu, D., Zhu, Y., Martín-Martín, R., Lu, C., Fei-Fei, L., Savarese, S. (2019). DenseFusion: 6D Object Pose Estimation by Iterative Dense Fusion. Retrieved from <https://arxiv.org/pdf/1901.04780>
- [149] Wartmann, J., Zimmermann, M., Lüken, T. (2015) Abschlussbericht LuFo IV-Projekt HELIcopter Situation Awareness für eXtreme Missionsanforderungen (HELI-X). DLR-Interner Bericht, Projektbericht. DLR-IB 111-2015/12, 81 S. <http://www.gbv.de/dms/tib-ub-hannover/828630119.pdf>
- [150] Watson, N.; Owen, I.; White, M. (2020): Piloted Flight Simulation of Helicopter Recovery to the Queen Elizabeth Class Aircraft Carrier. In: Journal of Aircraft 57 (4), S. 742–760. [DOI: 10.2514/1.C035733](https://doi.org/10.2514/1.C035733).
- [151] Wickens, C. D., Goh, J., Helleberg, J., Horrey, W. J., Talleur, D. A. (2003). Attentional models of multitask pilot performance using advanced display technology. Human Factors, 45(3), 360–380. <https://doi.org/10.1518/hfes.45.3.360.27250>
- [152] Wickens, C. D. (2008). Multiple resources and mental workload. Human Factors, 50(3), 449–455. <https://doi.org/10.1518/001872008X288394>
- [153] Wickens, C. D., Alexander, A. L. (2009). Attentional Tunneling and Task Management in Synthetic Vision Displays. The International Journal of Aviation Psychology, 19(2), 182–199. <https://doi.org/10.1080/10508410902766549>
- [154] WIKING Helikopter Service GmbH, Peter Schweer (2020, May 22.000Z). Standorte. Retrieved from <http://www.wiking-helikopter.de/standorte.html>.
- [155] Wilkonson, C. H., Roscoe, M. F., Determining Fidelity Standards for the Shipboard Launch and Recovery Task, AIAA Paper No. 2001-4062, AIAA Modeling and Simulation Technologies Conference, Montreal, Canada, August 2001. <https://doi.org/10.2514/6.2001-4062>
- [156] Winner, H. (Ed.) (2015). ATZ/MTZ-Fachbuch. Handbuch Fahrerassistenzsysteme: Grundlagen, Komponenten und Systeme für aktive Sicherheit und Komfort. Wiesbaden: Springer Verlag. <https://doi.org/10.1007/978-3-658-05734-3>

- [157] Xiang, Y., Schmidt, T., Narayanan, V., Fox, D. (2017). PoseCNN: A Convolutional Neural Network for 6D Object Pose Estimation in Cluttered Scenes. Retrieved from <https://arxiv.org/pdf/1711.00199>
- [158] Zan, S. J. (2005). On Aerodynamic Modelling and Simulation of the Dynamic Interface. Proceedings of the Institution of Mechanical Engineers, Part G: Journal of Aerospace Engineering, 219(5), 393–410. <https://doi.org/10.1243/095441005X30315>
- [159] Zhang, W., Zhang, J., Zhang, T. (2017). Fast Simulation Method for Ocean Wave Base on Ocean Wave Spectrum and Improved Gerstner Model with GPU. Journal of Physics: Conference Series, 787, 12027. <https://doi.org/10.1088/1742-6596/787/1/012027>
- [160] Zhao, D., Krishnamurthi, J., Gandhi, F., Mishra, S. (2018). Differential flatness-based trajectory generation for time-optimal helicopter shipboard landing. In A. A. C. Conference (Ed.), *2018 Annual American Control Conference (ACC): June 27-29, 2018, Wisconsin Center, Milwaukee, USA* (pp. 2243–2250). [Piscataway, NJ]: IEEE. <https://doi.org/10.23919/ACC.2018.8430942>
- [161] Zimmermann, M., Gestwa, M., König, C., Wolfram, J., Klasen, S., Lederle, A. (2019). First results of LiDAR-aided helicopter approaches during NATO DVE-mitigation trials. CEAS Aeronautical Journal, 10(3), 859–874. <https://doi.org/10.1007/s13272-018-0354-8>
- [162] Zimmermann, M. (2016) Sensor-based Online Path Planning for Rotorcraft Landing. Deutscher Luft- und Raumfahrtkongress, 13.-15. September 2016, Braunschweig. <https://elib.dlr.de/109821/>
- [163] Zimmermann, M. (2016). Flight test results of helicopter approaches with trajectory guidance based on in-flight acquired LIDAR data. In J. Sanders-Reed & J. J. Arthur (Eds.), SPIE Proceedings, Degraded Visual Environments: Enhanced, Synthetic, and External Vision Solutions 2016 (p. 983902). SPIE. <https://doi.org/10.1117/12.2225054>

Appendix

A.1. Rating Scales

Rating scales of proceeded simulator flight tests included assessments of pilot workload and its weighting, handling qualities on the basic and advanced flight control modes, and a visual cue rating focusing on HMD symbology layout. Ratings were proceeded along ADS-33 PRF [2] standards and include corresponding offshore procedures [105] [140].

Pilot workload was assessed during all experiments using Bedford workload rating scale [121], see Figure A- 1, and DIPES [109], see Figure A- 2. Both rating scales start at the lower left corner. Upcoming questions as defined within the scaling were asked to the pilots resulting to sideline in one branch. Afterwards, all rating definitions of the resulting branch were read to the pilot, so a final rating between 1 and 10 with Bedford workload rating scale, and a final rating between 1 and 5 with DIPES were achieved.

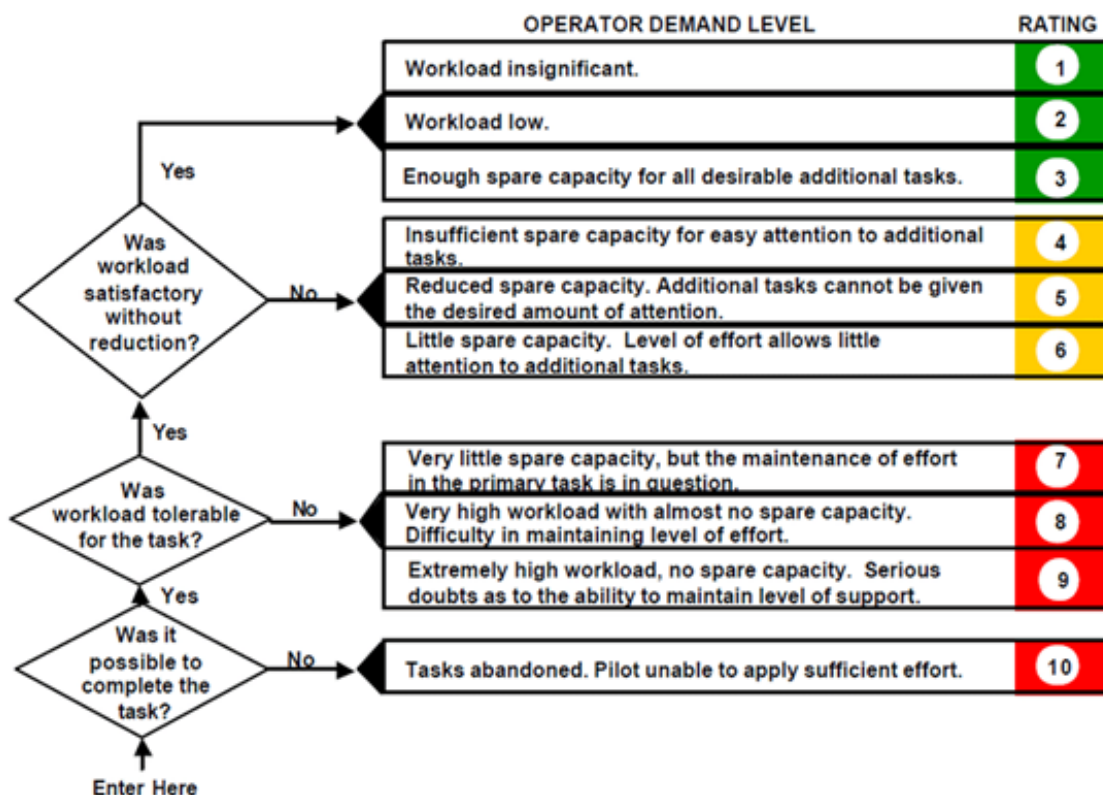


Figure A- 1 Bedford workload rating [121]

Bedford workload rating scale as well as DIPES are designed for helicopter shipboard - and onshore flight test proceedings. Ratings were given for all flights broken down into its MTEs.

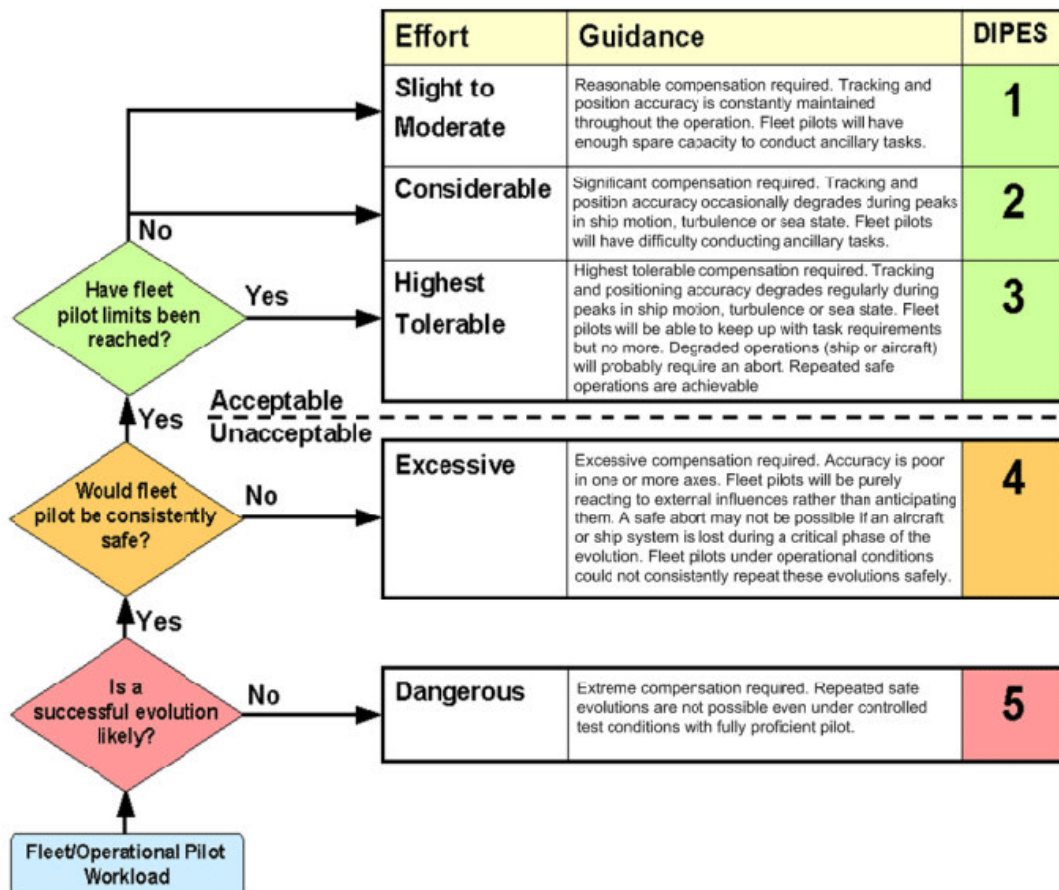


Figure A- 2 Deck interface pilot effort scale [109]

Both rating scales can be used for test pilot and fleet pilot ratings. The corresponding Cooper-Harper rating based on ADS-33 PRF [2] analyzing HQs is detailed below.

HQR, as given in Figure A- 3, was proceeded in the same manner as Bedford workload rating and DIPES. The result was an HQR rating between 1 and 10 for each MTE during each flight.

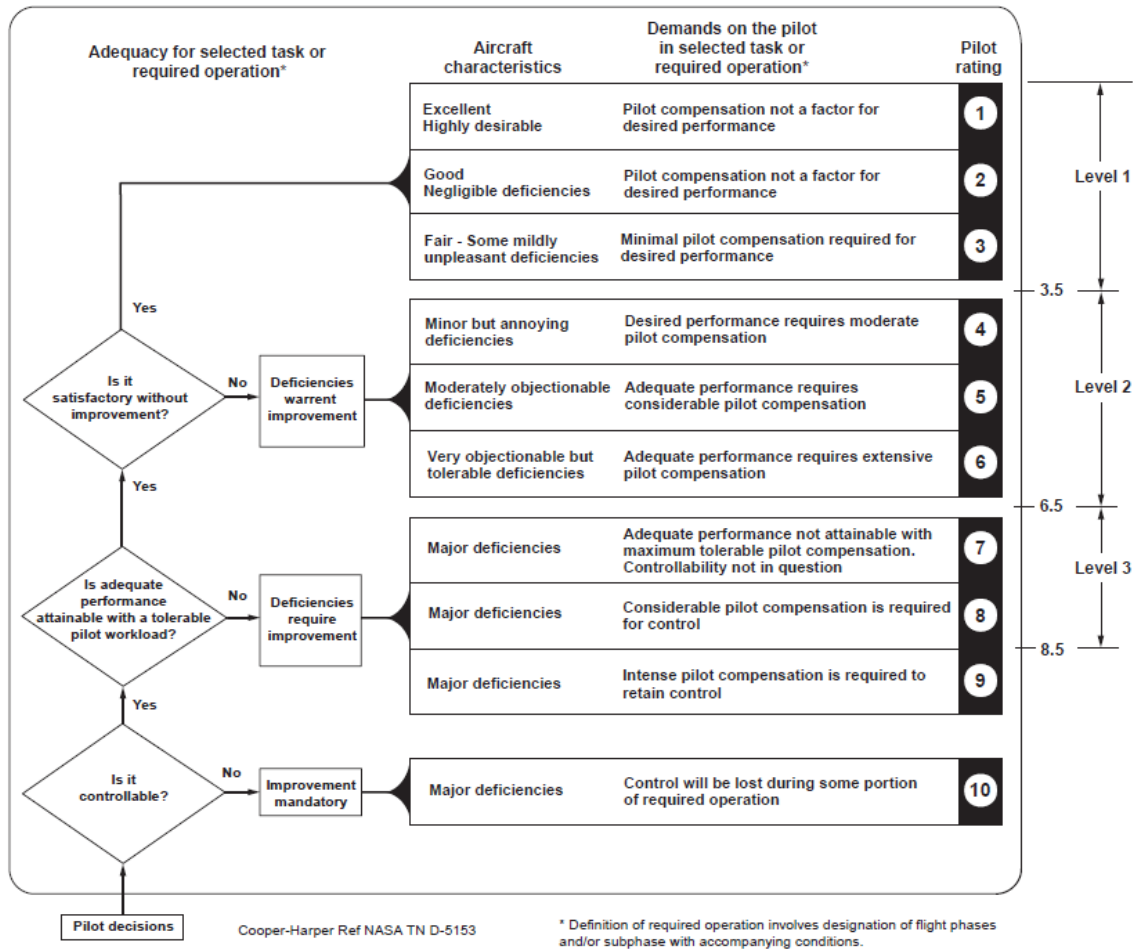
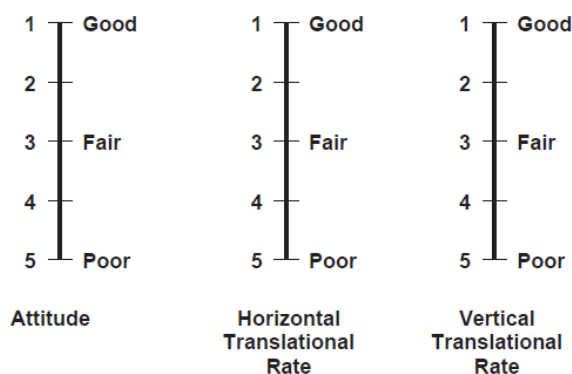


Figure A-3 Cooper- Harper handling qualities rating [2]

In sum, all flights detailed down to MTE level were assessed by all pilots with a Bedford workload and DIPES rating focusing on pilot's effort to fulfill all tasks. Additionally, basic, and advanced flight control modes were rated via the HQR.

For investigations of the HMD symbology concept, the visual cue rating [2] as shown in Figure A- 4 gave insights into pilots benefit of synthetic visual cues. The VCR were given by the pilots for each MTE during each flight in three categories: Attitude, horizontal translational rate, and vertical translational rate. Definitions of ratings were introduced to the pilots, resulting in one number between 1 and 5 for each axis. Hence, three ratings were given by the pilots for each MTE during each flight.



Pitch, roll and yaw attitude, and lateral-longitudinal, and vertical translational rates shall be evaluated for stabilization effectiveness according to the following definitions:

- Good :** Can make aggressive and precise corrections with confidence and precision is good.
- Fair :** Can make limited corrections with confidence and precision is only fair.
- Poor:** Only small and gentle corrections are possible, and consistent precision is not attainable.

Figure A- 4 Visual cue rating scale [2]

Finally, for deeper analysis of pilot workload and its weighting during all flights, the NASA-TLX rating scale [56], as shown in Figure A- 5, were proceeded. Each MTE during each flight was rated to the six categories of NASA-TLX: Mental demand, physical demand, temporal demand, performance, effort, and frustration. Descriptions were read to the pilots before flights and pilots were given a staggered rating in steps of ten between 0% (low) and 100% (high), see Figure A- 6.

TITLE	ENDPOINTS	DESCRIPTIONS
MENTAL DEMAND	Low/High	How much mental and perceptual activity was required (e.g. thinking, deciding, calculating, remembering, looking, searching, etc.)? Was the task easy or demanding, simple or complex, exacting or forgiving?
PHYSICAL DEMAND	Low/High	How much physical activity was required (e.g. pushing, pulling, turning, controlling, activating, etc.)? Was the task easy or demanding, slow or brisk, slack or strenuous, restful or laborious?
TEMPORAL DEMAND	Low/High	How much time pressure did you feel due to the rate or pace at which the task or task elements occurred? Was the pace slow and leisurely or rapid and frantic?
PERFORMANCE	Good/Poor	How successful do you think you were in accomplishing the goals of the task set by the experimenter? How satisfied were you with your performance in accomplishing these goals?
EFFORT	Low/High	How hard did you have to work (mentally and physically) to accomplish your level of performance?
FRUSTRATION LEVEL	Low/High	How insecure, discouraged, irritated, stressed, and annoyed versus secure, gratified, content, relaxed, and complacent did you feel during the task?

Figure A- 5 NASA TLX six dimensions definitions [56]

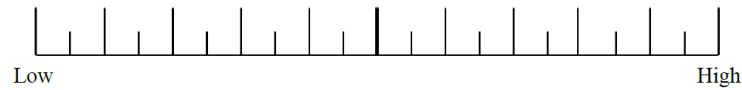


Figure A- 6 NASA TLX rating scale definition [56]

A.2. Simulator Sickness Pilot Ratings

Figure A-6 shows the given pilot ratings on SSQ with in sum none up to slight effects. Slight effects of general discomfort (Mean 0.25, SD 0.46), fatigue (Mean 0.5, SD 0.53), headache (Mean 0.38, SD 0.74), eye strain (Mean 0.25, SD 0.46), difficulty in focusing (Mean 0.25, SD 0.46), sweating (Mean 0.13, SD 0.53), and difficulty in concentrating (Mean 0.13, SD 0.53) had been overserved after proceeding simulated flights.

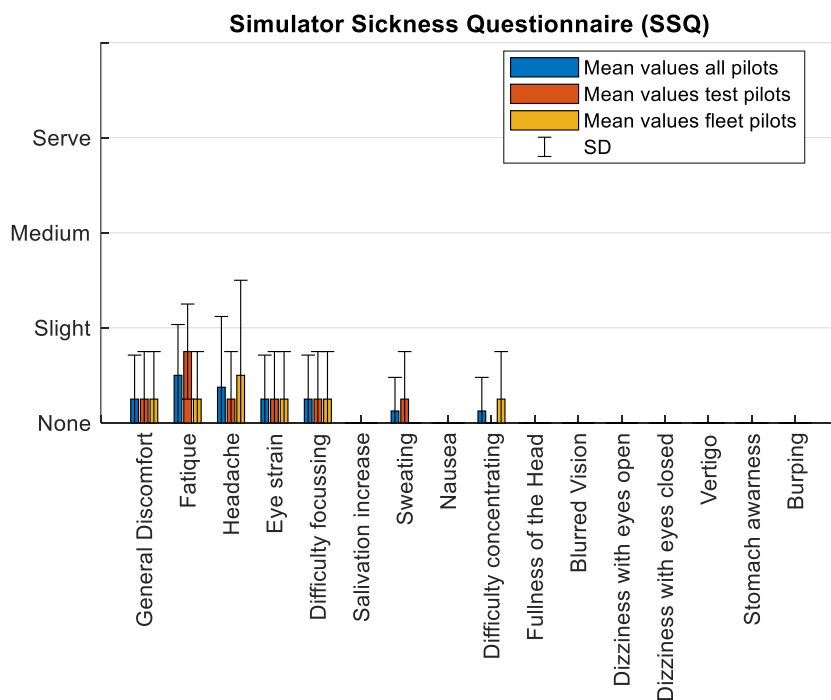


Figure A- 7 SSQ HELIOP 2, N=8

These none to slight effects within the realistic experimental helicopter ship setup were underlined by most of the participating pilots as follows:

- None of the pilots observed effects of dizziness with eyes open or closed, as enough short and long breaks were conducted during the experiments.
- Pilots showed no indication of vertigo in the dynamic environment, although the simulator is a fixed-based simulation. Here, pilots were offered to stop or to halt the experiment at any time. However, no abortion or interrupt of an experiment had been done during the experiments.
- The high conformity of HMD visual augmentation and the projected outside scenery allowed to operate the helicopter without any issues, such as eye strain or blurred vision.

A.3. Helicopter performance results

In the following, figures show complementing results for the helicopter ship approach and landing maneuvers. Side views of fleet and test pilots' approaches in degrading visibility conditions are given, as well as corresponding mean values of helicopter speeds and control inputs aggressiveness during operation. Moreover, a representative example is illustrated for scalograms of a maritime helicopter test pilot (PID5) and a helicopter fleet pilot (PID6) on given control inputs while proceeding the approach and landing mission until the final touchdown.

All pilots were able to successfully fulfill all helicopter ship approach and landing maneuvers in different and demanding weather conditions of degraded visibility, as given in Figure A-8. Moreover, participating test pilots as well as fleet pilots could achieve good results to stay within the virtual glidepath of HMD ESAS symbology, and even to the ideal flight path visualized via the HMD SAS symbology.

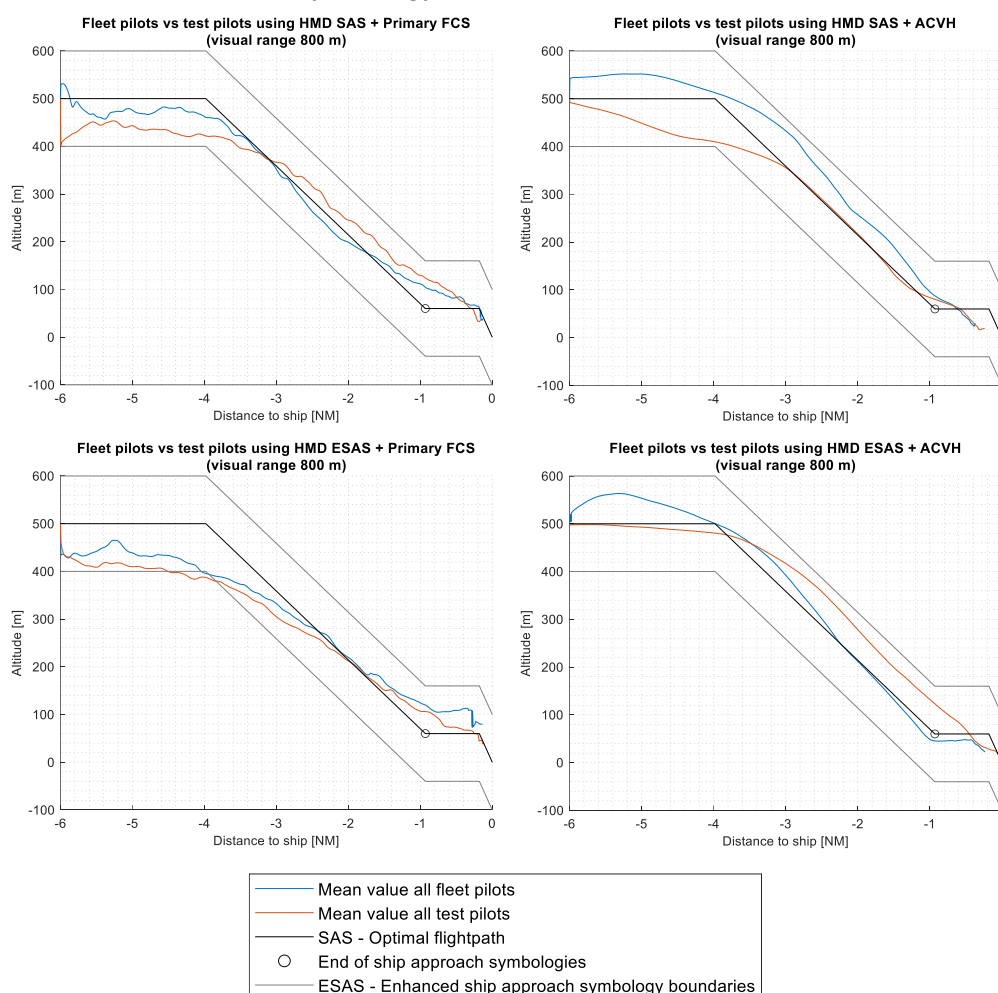


Figure A-8 Side view of helicopter ship approaches in degraded visibility of 800m, N=8

While the maritime test pilots showed a tendency to fly at lower altitude, as given in Figure A-8 and Figure A-9, maritime fleet pilots operated the helicopter higher in comparison to the test pilots. This effect could be argued by the effect that test pilots are trained to fly the

helicopter at the safe limits, while fleet pilots are educated to operate the helicopter along the safe optimal values.

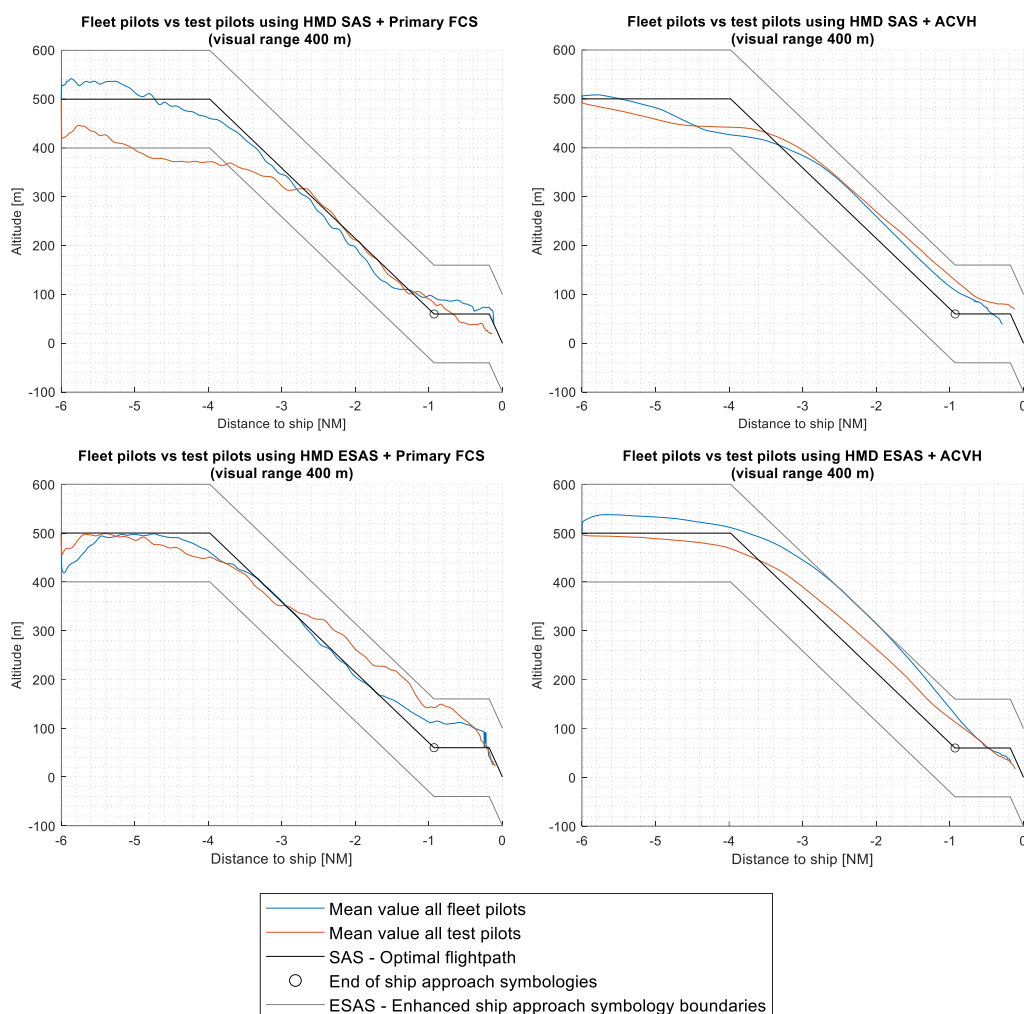


Figure A-9 Side view of helicopter ship approaches in degraded visibility of 400m, N=8

Best results were achieved by the participating pilots when control augmentation had been activated on top to the HMD visual augmentation. However, HMD SAS as well as HMD ESAS showed similar good results.

The overall good performance by reaching optimal flight parameters also for the predefined approach speed of 90 KIAS, as given in Figure A-10, substantiate those good results independent from the degrading visibility were achieved with visual augmentation and as visual and control augmentation being activated.

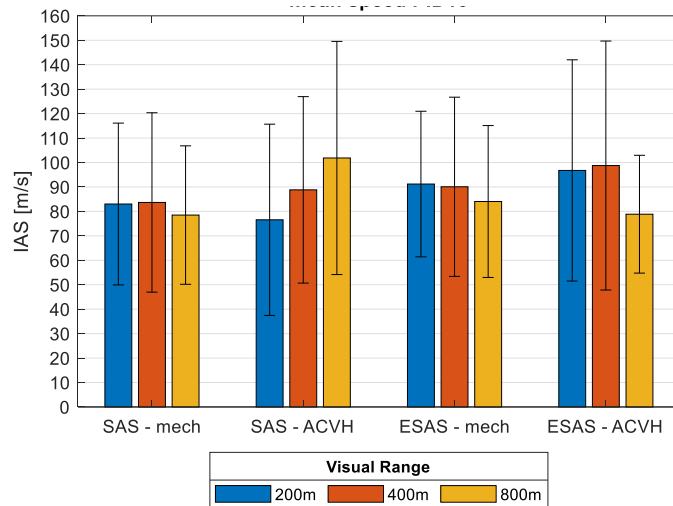


Figure A- 10 Helicopter mean speeds during ship approach, N=8

The comparison of fleet and test pilots cyclic control inputs aggressiveness, see Figure A-11, go along with the previously described achieved approach speeds degrading visibility ranges. Here, control inputs aggressiveness is at low level, again even when DVE conditions constantly increased over the different flights.

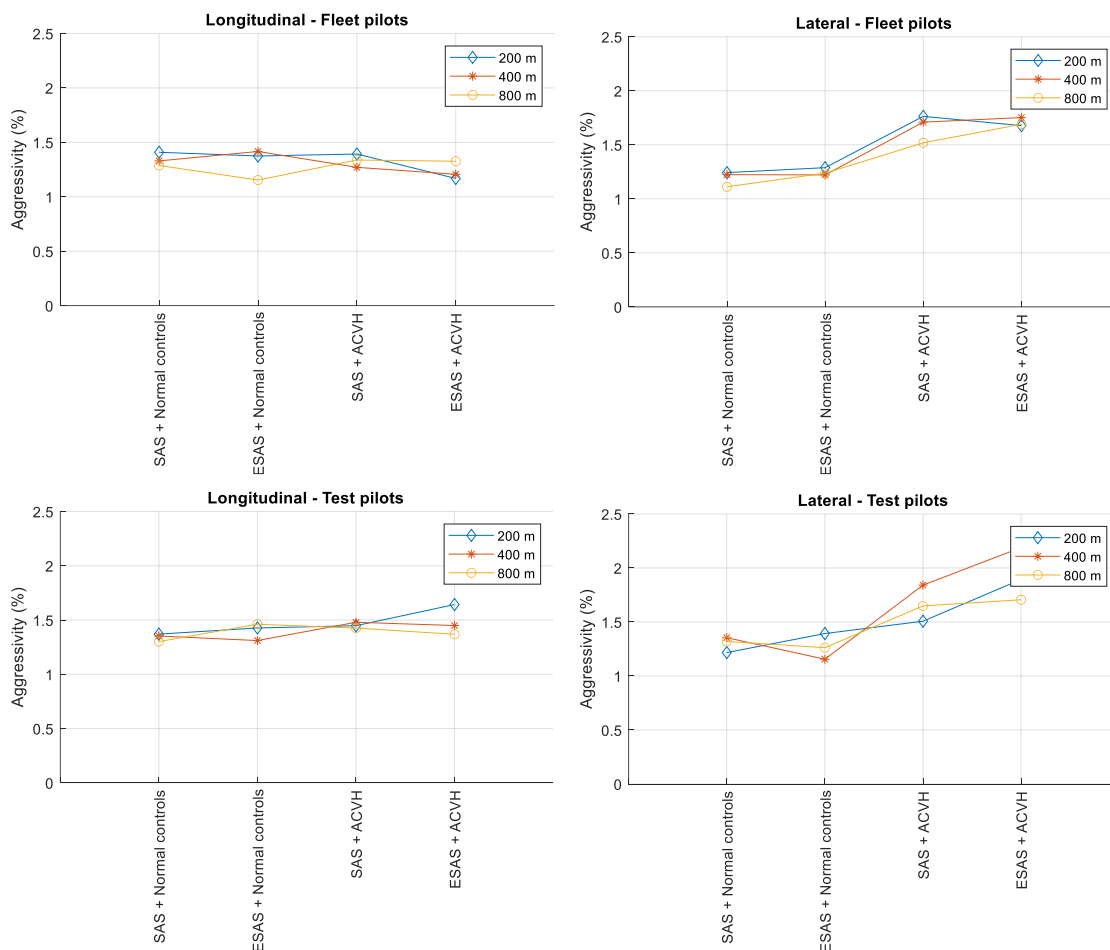


Figure A- 11 Comparison of fleet vs test pilot controls inputs aggressiveness, N=8

Additionally, the pilots control cyclic inputs in roll and pitch axis had been investigated for the whole mission endurance. The 2D and 3D scalograms of a representative maritime test

(PID5) and fleet pilot (PID6) complement the observations as given in chapter 7.3.1 for the pilots' inputs of cyclic control roll axis. Here, the scalograms of the cyclic pitch axis indicate expected results: At the beginning of the flight, pilots tried to approximate the helicopter to an ideal approach glide path in altitude. During the last phase of the flight, pilots had to challenge the final recovery of the helicopter, besides and over the landing deck, to keep a safe distance in longitudinal axis during the sidestep maneuver, and to avoid the rear deck wall right in front of the landing place of the moving ship.

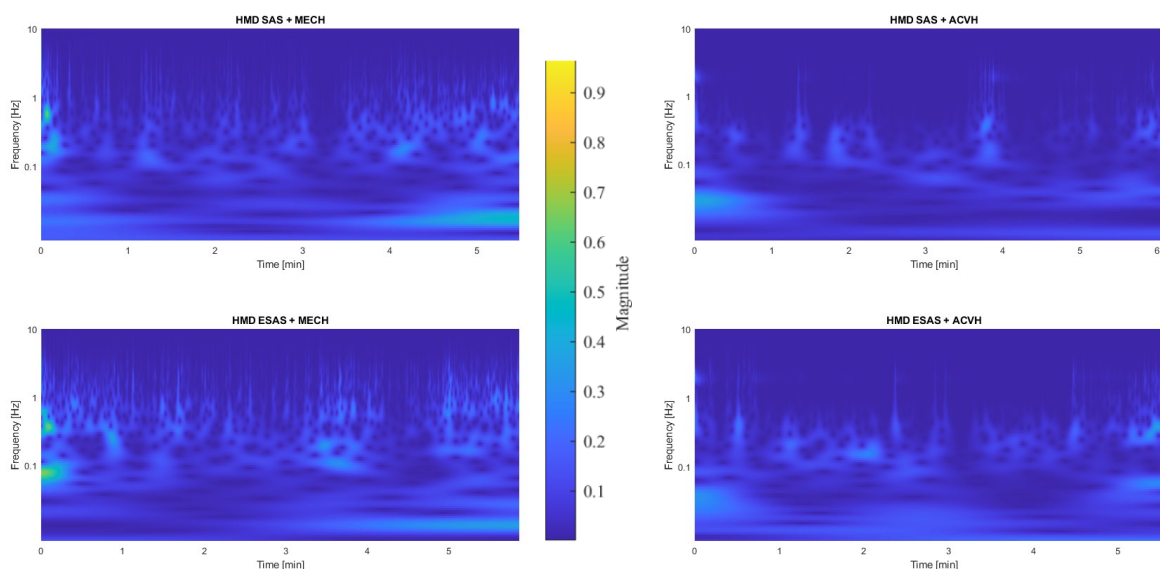


Figure A- 12 PID5 Test pilot cyclic control pitch axis scalograms during DVE flights

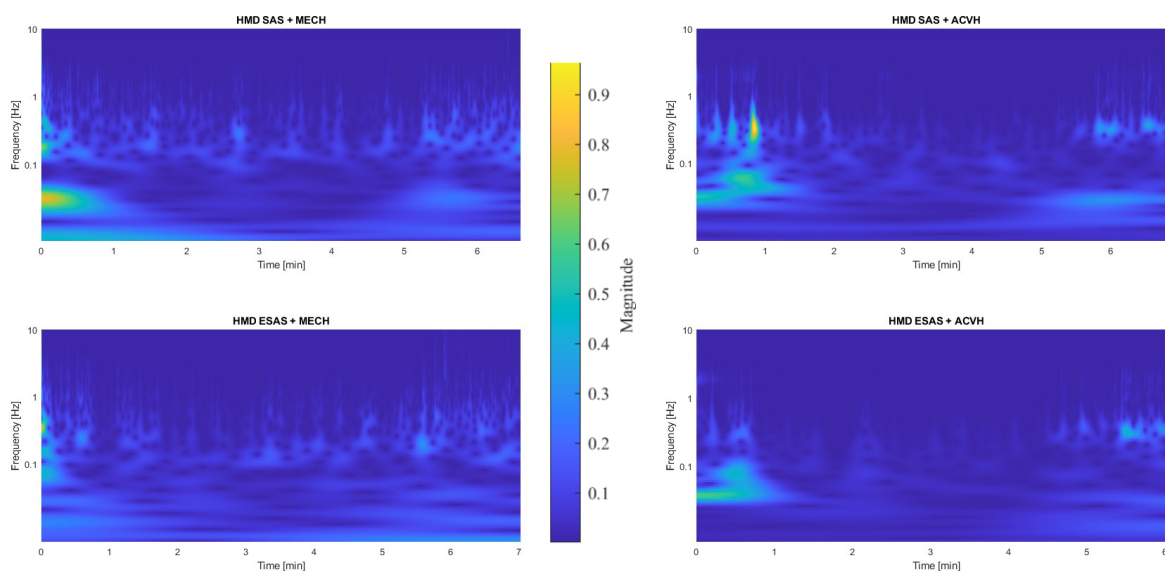


Figure A- 13 PID6 Fleet pilot cyclic control pitch axis scalograms during DVE flights

The activation of the control augmentation lowered the amount and intensity of pilots cyclic control inputs to an acceptable level, reflecting a lower pilot workload during the critical final recovery. Moreover, the pilots were able to operate the helicopter at low control inputs during the approach flying the helicopter with the activated control augmentation, resulting in an increased SA.

However, it might be discussed, that fleet pilots control inputs had been at a higher magnitude than control inputs of test pilots. A comparison of a representative maritime test (PID5) and fleet pilot (PID6), as given in Figure A-14 and Figure A-15, indicated that test pilots cyclic control inputs were at lower magnitude in general. However, the segments of higher control inputs with respect to the frequency and the mission sequence obtained to be comparable: The MTEs of which highest pilots cyclic pitch control inputs had been observed were during the beginning of the mission, and during the final helicopter ship recovery, when the helicopter initialized the sidestep maneuver.

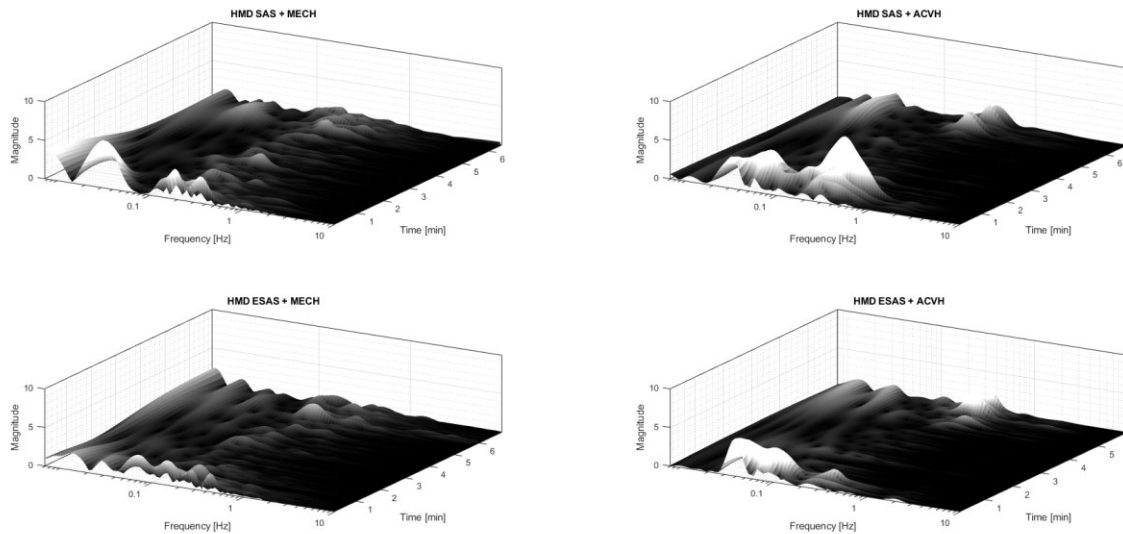


Figure A- 14 PID5 Test pilot cyclic control pitch axis scalograms during DVE flights

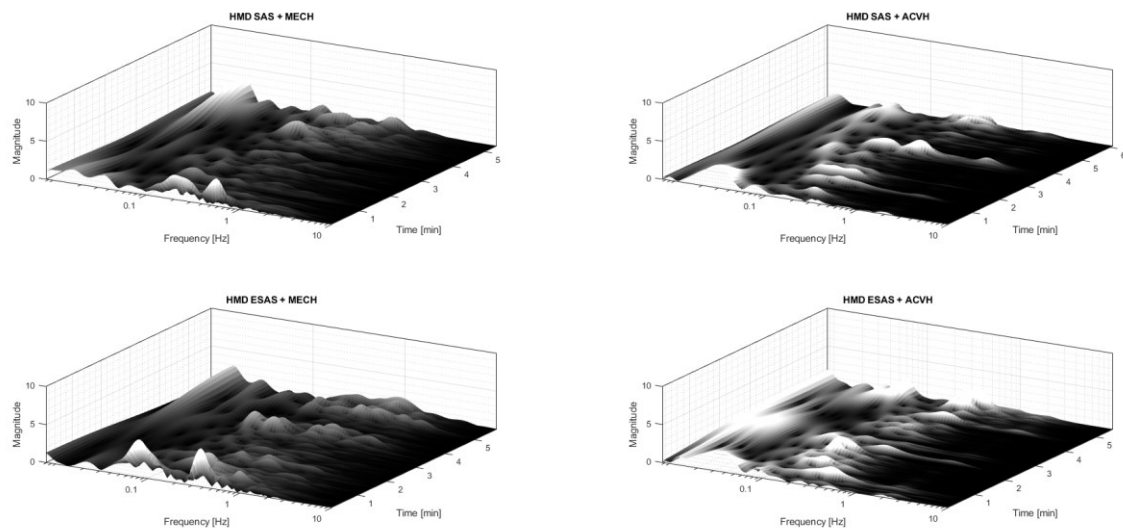


Figure A- 15 PID6 Fleet pilot cyclic control pitch axis scalograms during DVE flights